LIPID EXTRACTION FROM THERMAL FENTON REACTION IN HYBRID LIQUID BIPHASIC SYSTEM FOR BIOFUEL AND RUBBER BIO-ADDITIVE COMPOUNDS

YEW GUO YONG, BEng.

Thesis submitted to the University of Nottingham

For the degree of Doctor of Philosophy

MARCH 2021

Abstract

This thesis is focusing on utilization of lipid compound and exploring the extraction method for producing lipid compound in which could be used in biofuel and synthetic rubber polymer. The existing extraction technology which is energy intensive, high investment cost on equipment and multistep procedure in which reduced the efficiency of the overall production process. Besides, the cultivation process incorporating artificial intelligent for rapid detection and used of sustainable medium from waste materials (waste molasses) and less depend on chemical based of salt. The *chlorella sp.* of microalgae has been selected with high lipid contain (*Chlorella sorokiniana CY-1*) and rough survivability strain (*Chlorella vulgaris FSP-E*). The objective of the study is to develop a sustainable system for large scale production of lipid compound from microalgae and exploring the application from the lipid derived of fatty acids compound. Hybrid liquid biphasic system (HLBS) has been developed from this study for suiting in large scale of lipid production in 83.5% of lipid recovery from microalgae biomass. The HLBS has included the disruptive and extractive properties in a single system, where it has been reduced the overall process duration more than 30%. Furthermore, the system has been exploring for biofuel production and combining with a non-catalytic transesterification method. The yield of F.A.M.E C4, C6, and C10 at 8.2 mg/g, 0.33 mg/g and 0.24 mg/g respectively, the duration of the transesterification for biofuel production at 4 min for a batch with lipid to methanol ratio 1:6 pulse at 0.8 in a single step

process. The analysis of the cultivation medium for microalgae has been incorporated by artificial intelligent (K-NN algorithm) from photo-to-properties by using waste molasses as medium with 1206.43 mg/L of dry cell weight, protein content improved for 20.6%, while the Ai algorithm assisted to reduce the dependency of analysis from spectrophotometer. In conjunction, the lipid compound was found to be incorporated with metal ions as promising cross-linking compound for synthetic polymer - carboxylated nitrile butadiene rubber, (XNBR) improved stability of the sulphur-less linker compound L-MBL at 10.85% and raise the tensile strength 8.71% (27.55 MPa) higher than Sulphur based of linker. Last but not least, the content has been highlighted the research achievement and future opportunities from current techniques and technology that developed.

Acknowledgement

I would like to take this chance to express my gratitude to my parents (Yew Thean Lye, Lai Moi) and family members (Shwu Fen, Shwu Lih, Shwu Min and their love ones) for their care and love during my progression. A big thanks to Prof. Ir. Ts. Dr. Show Pau Loke for giving me the opportunity to pursue my PhD and for showing the path for me during my ups and downs. My appreciation goes to Dr Ho Yeek-Chia for her support, and also to Prof. Ir. Dr. Law Chung Lim for his support as my co-supervisor. I am thankful to Dr Chew Kit Wayne for his guidance and all his care towards achieving my goals. Furthermore, to all my colleagues and friends (Dr. Eddie Puah, Peter Chia, Eddie Liu, Mrs Ain, Say Ling, Yuen Sean, Dr. Chia Shir Reen, Dr. Isabelle Leong, Dr. Apurav, Dr. Jerry Khoo, Doris Tang, Kathlyne Chia, Dr. Tham, and Dr. Tan Chung Hong), I thank you all and I am blessed to share this important fate between us, that has allowed us to meet for these occasions. I truly appreciate all their motivation and all the time that we have spent together for joy and distress. All those moments have created a wonderful period in my postgraduate study. I may have left out some who are not in the list, hereby I express my greatest gratitude to them.

List of Publications

1) **Guo Yong Yew**, Thing Chai Tham, Chung Lim Law, Dinh-Toi Chu, Chiaki Ogino, Pau Loke Show. Emerging crosslinking techniques for glove manufacturers with improved nitrile glove properties and reduced allergic risks (Published in, Materials Today Communications, 19, 39-50) [Accepted 18 Dec 2018; IF 2.678 (2018)]

2) **Guo Yong Yew**, Sze Ying Lee, Pau Loke Show, Yang Tao, Chung Lim Law, Thi Trung Chinh Nguyen, Jo-Shu Chang. Recent advances in algae biodiesel production: From upstream cultivation to downstream processing (Published in, Bioresource Technology Reports, 7, 100227) [Accepted 7 May 2019; IF 1.7(2018)]

3) **Guo Yong Yew**, Kit Wayne Chew, Marlinda Abdul Malek, Yeek-Chia Ho, Wei-Hsin Chen, Tau Chuan Ling, Pau Loke Show*. (2019) "Hybrid liquid biphasic system for cell disruption and simultaneous lipid extraction from microalgae *Chlorella sorokiniana CY-1* for biofuel production" Biotechnology for biofuels, 12(1), pp. 1-12. [Accepted 12 October 2019; IF: 5.452 (2018)]

4) **Guo Yong Yew**, Thing Chai Tham, Pau-Loke Show*, Yeek-Chia Ho, Siew Kooi Ong, Chung Lim Law, Changnian Song, Jo-Shu Chang*. (2020). "Unlocking the Secret of Bio-additive Components in Rubber Compounding in Processing Quality Nitrile Glove" Applied biochemistry and biotechnology, 1-28. [Accepted 5 December 2019; IF: 2.140(2018)]

5) **Guo Yong Yew**, Boon Keat Puah, Kit Wayne Chew, Sin Yong Teng, Pau Loke Show*, The Hong Phong Nguyen*. (2020). "*Chlorella vulgaris FSP-E* cultivation in waste molasses: Photo-to-property estimation by artificial intelligence" Chemical Engineering Journal, 126230. [Accepted 7 July 2020; IF: 10.652(2019)]

5) **Guo Yong Yew**, Kuan Shiong Khoo, Wen Yi Chia, Yeek-Chia Ho, Chung Lim Law, Hui Yi Leong, Pau Loke Show*. (2020). "A novel lipids recovery strategy for biofuels generation on microalgae *Chlorella* cultivation with waste molasses" Journal of Water Process Engineering, 38, 101665. [Accepted 8 September 2020; IF: 3.465(2019)]

7) **Guo Yong Yew**, Xuefei Tan, Kit Wayne Chew, Jo-Shu Chang, Yang Tao, Ning Jiang, Pau Loke Show*.(2020). "Thermal-Fenton mechanism with sonoprocessing for rapid non-catalytic transesterification of microalgal to biofuel production" Chemical Engineering Journal, 127264. [Accepted 2 Oct 2020; IF: 10.652(2019)]

8) Toan Nguyen-Sy, **Guo Yong Yew**, Kit Wayne Chew, Thi Dong Phuong Nguyen*, Thi Ngoc Thu Tran, Thi Dieu Huong Le, Chau Tuan Vo, Hoang Kim Pham Tran, Muhammad Mubashir*, Pau Loke Show*. (2020). "Potential Cultivation of Lactobacillus pentosus from Human Breastmilk with Rapid Monitoring through the Spectrophotometer Method" Processes, 8(8), 902. [Accepted 15 July 2020; IF: 2.753(2019)]

9) Doris Ying Ying Tang, **Guo Yong Yew**, Apurav Krishna Koyande, Kit Wayne Chew, Dai-Viet N Vo, Pau Loke Show*. (2020). "Green technology for the industrial production of biofuels and bioproducts from microalgae: a review" Environmental Chemistry Letters, 1-19. [Accepted 7 August 2020; IF: 5.922(2019)]

10) Sin Yong Teng, **Guo Yong Yew**, Kateřina Sukačová, Pau Loke Show*, Vítězslav Máša*, Jo-Shu Chang. (2020). "Microalgae with artificial intelligence: A digitalized perspective on genetics, systems and products" Biotechnology Advances, 107631. [Accepted 8 September 2020; IF: 10.744(2019)]

Conference presentation and showcase:

1. **Yew, G.Y.,** Show, P. L., Law, C. L., 2019. The study of nanosize surfactant enhancing the stability of the carboxylated acrylonitrile butadiene rubber for lightlycrosslinked products. 5th Postgraduate Colloquium of Environmental Research (POCER). Putrajaya, Malaysia

2. **Yew, G.Y.,** Chew, K.W., Law, C. L., Show, P. L., 2019. Hybrid liquid biphasic system cell disruption with simultaneous lipid extraction for biofuel application. FOSE Postgraduate Research Showcase (PGRs). Selangor, Malaysia

3. **Yew, G.Y.,** Show, P. L., 2019. The stability enhancement of cross-linked carboxylated acrylonitrile butadiene rubber (XNBR) using nano-size surfactant. International Conference on Enviromental and Energy Engineering 2019. Holiday Inn, Kuala Lumpur, Malaysia.

4. **Yew, G.Y.,** Law, C. L., Show, P. L., 2018. Emerging crosslinking technique on carboxylated acrylonitrile butadiene rubber glove. Asean Emerging Researcher Conference. Sunway University, Malaysia.

Book chapters:

1. **Guo Yong Yew**, Kai Xin Kow, Kit Wayne Chew, Pau Loke Show, 2020. Microwave-assisted liquid biphasic system. Liquid biphasic system 1st edition, fundamental and application in bioseparation technology. Elsevier.

2. **Guo Yong Yew**, Chor Hoong Cheah, Kit Wayne Chew, Pau Loke Show., 2020. Extractive technologies in LBS: Extractive cell disruption. Liquid biphasic system 1st edition, fundamental and application in bioseparation technology. Elsevier.

3. Yee Ho Chai, **Guo Yong Yew**, Suzana Yusup, Pau Loke Show., 2021. State-of-the-art technologies. Industry 5.0. Taylor & Francis.

Table of Contents:

Abstract 2

Acknowledgement 4

List of Publications 5

List of Figures 20

List of Tables 29

List of Abbreviation and Acronyms 32

Chapter 1. Introduction 34

1.1 Background 34

1.2 Problem Statement 37

1.3 Research Objective 39

1.4 Research Scopes 40

Chapter 2. Literature Review 44

2.1 Biofuels 45

2.2 Upstream Processing of Microalgae 48

2.3 Downstream processing 56

2.3.1 Dewatering and drying 57

2.3.2 Pre-treatment 58

2.3.3 Lipid extraction 60

2.3.4 Product fractionation 66

2.3.5 Transesterification 67

2.4 Emerging crosslinking technique and bio-additive in rubber polymer 69

2.5 Organic oil for rubber polymerization production..... 73

Chapter 3. Hybrid liquid biphasic system for cell disruption and simultaneous lipid extraction from microalgae *Chlorella vulgaris CY-1* for biofuel production..... 78

3.1 Introduction..... 80

3.2 Materials and methods..... 84

3.2.1 Microalgae biomass cultivation..... 84

3.2.2 Determination of nitrate content and microalgae cell concentration..... 85

3.2.3 Hybrid liquid biphasic system with radical cell disruption properties 86

3.2.4 Total lipid analysis..... 88

3.2.5 Determination of recovery yield and enhancement value 88

3.2.6 Chemical reaction chains of radical formation..... 89

3.3 Result and discussion..... 94

3.3.1 Effect of concentration of hydrogen peroxide toward lipid extraction.... 94

3.3.2 Effect of solvent concentrations 99

3.3.3 Effect of different ratio (H_2O_2: Hexane)..... 103

3.3.4 Effect of volume differences 105

3.3.5 Effect of contact time..... 108

3.3.6 Effect of biomass amount with solvent ratio and GC-FID lipid profile 111

3.4 Conclusion 114

Chapter 4. A Novel Lipids Recovery Strategy for Biofuels Generation on Microalgae Chlorella Cultivation with Waste Molasses 115

4.1 Introduction..... 117

4.2 Materials and methods..... 121

4.2.1. Materials 121H

4.2.2. Pre-treatment of waste molasses with Fenton reaction..... 121

4.2.3. Microalgae cultivation and medium composition 122

4.2.4. Determination of biomass and dry cell weight (DCW)..... 124

4.2.5 Medium data analysis 125

4.2.6. Acids assisted HLBS and direct transesterification for F.A.M.E..... 126

4.2.7. Total lipids in microalgae biomass analysis 129

4.2.8. Determination of lipids recovery yield and cell disruption enhancement in fold value 129

4.2.9. FESEM visualisation and EDX analysis on cell wall..... 130

4.2.10. Statistical analysis..... 132

4.3. Results and discussion 133

4.3.1. Characterisation of acid-treated microalgae biomass 133

4.3.2. Microbial growth and nutrient removal 135

4.3.2. Lipids extraction and optimisation study 140

4.3.2.1. The effect of sulphuric acid concentration 140

4.3.2.2. The effect of nitric acid concentration 143

4.3.2.3. The effect of volume ratio of solvents 145

4.3.2.4. The effect of the amount of microalgae biomass 147

4.3.2.5. The effect of temperature 149

4.3.3. GC profile of F.A.M.E and EDX analysis 153

4.4. Conclusions 157

5. Thermal-Fenton mechanism with sonoprocessing for rapid non-catalytic transesterification of microalgal to biofuel production 158

5.1 Introduction 160

5.2 Materials and methods 164

5.2.1. Materials 164

5.2.2. Microalgae biomass cultivation and medium composition 164

5.2.3. Determination of biomass and nitrate concentration 165

5.2.4. Fenton reaction for HLBS and oil/lipid determination 165

5.2.5. Total lipid analysis 168

5.2.6. Determination of recovery yield and ratio in weight 168

5.2.7. Numerical studies of lipid extraction from microalgae biomass 169

5.2.8. Non-catalytic transesterification 173

5.2.9. Statistical analysis 174

5.3. Results and discussion 175

5.3.1. Optimization study of Fenton reaction in HLBS 175

5.3.1.1. Effect of temperature contact in HLBS 175

5.3.1.2. Effect of $FeCl_2$ concentration on H_2O_2 in HLBS 178

5.3.1.3. Effect of ratio solvents in HLBS 180

5.3.1.4. Effect of dosage for 5% $FeCl_2$ in HLBS 181

5.3.1.5. Effect of time of contact in HLBS 182

5.3.1.6. Effect of biomass amount in HLBS 184

5.3.1.7. Numerical studies and mathematical model simulation for optimized lipid extract 187

5.3.1.8. Effect of co-optimization of temperature and concentration for Fenton reaction 190

5.3.2 Optimization study for ultrasound in non-catalytic transesterification . 196

5.3.2.1. Effect of methanol ratio for ultrasound in non-catalytic transesterification..... 198

5.3.2.2. Effect of duration for ultrasound in non-catalytic transesterification 199

5.3.2.3. Effect of pulse for ultrasound in non-catalytic transesterification..... 201

5.3.3. Characterization of transesterification of microalgae oil molecule bonding 203

5.4. Conclusions 206

Chapter 6. *Chlorella vulgaris FSP-E* cultivation in waste molasses: Photo-to-property estimation by artificial intelligence..... 207

6.1 Introduction..... 209

6.2 Materials and Methods 213

6.2.1 Microalgae strain and medium compositions..... 213

6.2.2 Pretreatment of waste molasses..... 214

6.2.3 Determination of microalgae cell concentration..... 214

6.2.4 Quantification of nitrate content in medium..... 215

6.2.5 Microalgae lipid extraction..... 216

6.2.6 Protein extraction and quantification..... 216

6.2.7 Determination of carbohydrate content 217

6.2.8 Photo-to-Property Estimation Method..... 218

6.2.9 Preparation of Data 219

6.3 Result and discussion 220

6.3.1 The effect of molasses nutrients on concentration of biomass 220

6.3.2 Nutrient removal from molasses by C. Vulgaris FSP-E 226

6.3.3 The variation of pH value correlate to biomass growth 231

6.3.4 Biochemical composition 233

6.3.4.1 The total lipid content 233

6.3.4.2 The protein content 236

6.3.4.3 The Carbohydrate content 238

6.3.5 Predicting in K-Nearest Neighbor algorithm for biomass, nitrate content, and pH 240

6.4 Conclusion 246

Chapter 7: Stability Enhancement of Synthetic Rubber (XNBR) with Microalgae Based Fatty Acids Incorporated Zirconium Metal Ion 247

7.1 Introduction 249

7.2 Materials and Methods 252

7.2.1 Metal incorporated bio-linker (MBL) as ligand from microalgae *Chlorella sorokiniana CY-1* 252

7.2.2 Preparation of vulcanised XNBR latex film 254

7.2.3 Preparation of latex films 257

7.2.4 Colloidal stability test 257

7.2.5 Swelling measurement (crosslink density) 258

7.2.6 Tensile testing 259

7.2.7 Aging testing 259

7.2.8 FTIR analysis 259

7.2.9 Statistical analysis 260

7.3 Results and discussion 260

7.3.1 Characterization of the functional groups of compounded polymer 260

7.3.2 Effect of lipid with metal on XNBR for the resultant tensile properties 262

7.3.3 Effect of MBL on the elongation properties 264

7.3.4 Effect of crosslink density from metal lipid linker (MBL) on XNBR .. 266

7.3.5 Effect of tensile force at 300% and 500% on specific elongation 268

7.3.6 Effect of aging for different types of linkers on XNBR film 269

7.3.7 Effect on the stability of compounded polymer samples 271

7.4 Conclusion 273

Chapter 8. Conclusions and Future Plans 275

8.1 Conclusions 275

8.2 Limitation, recommendations and future works 278

References..... 282

List of Figures

Figure 1-1: Research scope involvment of exploring the industry application

Figure 2-1: Process flow diagram for algae biodiesel

Figure 2-2: Microalgae lipid extraction

Figure 3-1: Concentration of Peroxide with hexane effect for the extract lipid productivity for recovery yield and enhancement comparison toward water-organic solvent biphasic system from C. vulgaris CY-1. Other operating condition fix at 3ml of 85% concentration of organic solvent (hexane), contact time at 1 min, biomass 20 mg (± 1 mg), and at room temperature 25°C

Figure 3-2: Concentration of peroxide with chloroform effect for the extract lipid productivity for recovery yield and enhancement comparison toward water-organic solvent biphasic system from C. vulgaris CY-1. Other operating condition fix at 3ml of 85% concentration of organic solvent (chloroform), contact time at 1 min, biomass 20 mg (± 1 mg), and at room temperature 25°C.

Figure 3-3: Concentration of organic solvent (hexane) effect for the extract lipid productivity for recovery yield and enhancement comparison toward water-organic solvent biphasic system from C. vulgaris CY-1. Other operating condition fix at 3ml of 30% concentration of hydrogen peroxide, contact time at 1 min, biomass 20 mg (± 1 mg), and at room temperature 25ºC.

Figure 3-4: Concentration of organic solvent (chloroform) effect for the extract lipid productivity for recovery yield and enhancement comparison toward water-organic solvent biphasic system from C. vulgaris CY-1. Other operating condition fix at 3ml of 30% concentration of hydrogen peroxide, contact time at 1 min, biomass 20 mg (± 1 mg), and at room temperature 25°C.

Figure 3-5: Ratio of (H_2O_2: Hexane) effect for the extract lipid productivity for recovery yield and enhancement comparison toward water-organic solvent biphasic system from C. vulgaris CY-1. Other operating condition fix at 30% concentration of hydrogen peroxide, pure analytical grade of organic solvent (hexane), contact time at 1 min, biomass 20 mg (± 1 mg), and at room temperature 25°C.

Figure 3-6: Volume of hydrogen peroxide (H_2O_2) effect for the extract lipid productivity for recovery yield and enhancement comparison toward water-organic solvent biphasic system from C. vulgaris CY-1. Other operating condition fix at 30% concentration of hydrogen peroxide, pure analytical grade of organic solvent 85% (hexane) at volume 3ml, contact time at 1 min, biomass 20 mg (± 1 mg), and at room temperature 25°C.

Figure 3-7: Volume of organic solvent (hexane) effect for the extract lipid productivity for recovery yield and enhancement comparison toward water-organic solvent biphasic system from C. vulgaris CY-1. Other operating condition fix at 30% concentration of hydrogen peroxide at volume 3ml, pure

analytical grade of organic solvent 85% (hexane), contact time at 1 min, biomass 20 mg (± 1 mg), and at room temperature 25°C

Figure 3-8: The graph of concentration for H_2O_2 and hydroxyl radical formation against time simulate by MATLAB 2018a. The concentration of hydrogen peroxide 30% in 2mL, in room temperature condition 25°C, with the presence of florescent lamp at intensity 8 μmol $m^{-2}s^{-1}$.

Figure 3-9: Time of contact effect for the extract lipid productivity for recovery yield and enhancement comparison toward water-organic solvent biphasic system from C. vulgaris CY-1. Other operating condition fix at 30% concentration of hydrogen peroxide, pure analytical grade of organic solvent 85% (hexane), biomass 20 mg (± 3 mg), and at room temperature 25°C.

Figure 4-1: Microscopic view of FESEM capture for *C. sorokiniana CY-1* biomass. High vacuum mode of multi-cellular biomass in (a) 10000, (b) 5000 and (c) 6000 magnification. ESEM mode of 15% nitric acid-treated multi-cellular biomass in (d) 12000 and (e) 5000 magnification. (f) High vacuum mode of 15% nitric acid-treated multi-cellular biomass in 6000 magnification. The orange circle and arrow indicate the disrupted cell.

Figure 4-2: (a) Biomass concentration and (b) nitrite concentration in different molasses concentrations medium of 140 mg/L, 145 mg/L, 150 mg/L, 155 mg/L and 160 mg/L for 14 days. (c) COD, Sucrose and TSS reduction between 1st and 14th days.

Figure 4-3: (a) The effect of *C. sorokiniana CY-1* biomass amount on single-step lipids recovery yield and enhancement in HLBS; Operating conditions: concentration of 15% of HNO3, 98% organic hexane (analytical grade), ratio 1:3 (acids:hexane) and time of contact = 3 min. (b) The effect of temperature of the water bath on single-step lipids recovery yield and enhancement in HLBS; Operating conditions: concentration of 15% of HNO3, 98% organic hexane (analytical grade), ratio 1:3 (acids: hexane), time of contact = 3 min, biomass weight of 50 mg. (c) The effect of time of contact on single-step lipids recovery yield and enhancement in HLBS; Operating conditions: concentration of 15% of HNO3, 98% organic hexane (analytical grade), ratio 1:3 (acids:hexane), water bath at 80 oC and the biomass weight of 50 mg.

Figure 4-4: (a) The effect of *C. sorokiniana CY-1* biomass amount on single-step lipids recovery yield and enhancement in HLBS; Operating conditions: concentration of 15% of HNO3, 98% organic hexane (analytical grade), ratio 1:3 (acids:hexane) and time of contact = 3 min. (b) The effect of temperature of the water bath on single-step lipids recovery yield and enhancement in HLBS; Operating conditions: concentration of 15% of HNO3, 98% organic hexane (analytical grade), ratio 1:3 (acids: hexane), time of contact = 3 min, biomass weight of 50 mg. (c) The effect of time of contact on single-step lipids recovery yield and enhancement in HLBS; Operating conditions: concentration of 15% of

HNO3, 98% organic hexane (analytical grade), ratio 1:3 (acids:hexane), water bath at 80 oC and the biomass weight of 50 mg.

Figure 4-5: (a) GC profile of F.A.M.E from *C. sorokiniana CY-1* lipids sample (1 = C11:0; 2 = C12:0 (internal standard); 3 = C16:0; 4 = C16:1(n-9); 5 = C21:0; 6 = C22:0(n-5); 7 = C22:4). (b) EDX analysis on biomass for all elements on *C. sorokiniana CY-1*. (c) EDX analysis on acid-treated biomass for all elements on *C. sorokiniana CY-1.*

Figure 5-1: The non-catalytic transesterification of microalgae lipid through thermal Fenton reaction in HLBS.

Figure 5-2: (a) Effect of various temperature (25.5 °C, 30.5 °C, 32.5 °C, 34.5 °C, 36.5 °C, 38.5 °C, 40.5 °C, 42.5 °C) of disruptive solvent (H2O2) for the study of lipid recovered and concentration of lipid from *C. sorokiniana CY-1* . Other operating conditions: concentration of H2O2 of 30% w/w, organic solvent hexane 85%, volume ratio of solvent 3 mL:3 mL, contact time 3 min, and biomass amount at 30 mg. (b) Effect of various concentration of FeCl2 (1% - 9%) on disruptive solvent (H2O2) for the study of lipid recovered and concentration of lipid from *C. sorokiniana CY-1*. Other operating conditions: concentration of H2O2 of 30% w/w, organic solvent hexane 85%, volume ratio of solvent 3 mL: 3 mL, contact time 3 min, 5 μL/g FeCl2, and biomass amount at 30 mg. (c) Effect of various ratio of solvent with average for 1=1mL, 3mL (disruptive:organic solvent) for the study of lipid recovered and concentration of

lipid from *C. sorokiniana CY-1* . Other operating conditions: concentration of H2O2 of 30% w/w, organic solvent hexane 85%, contact time 3 min, 5% of FeCl2, 5 µL/g FeCl2, and biomass amount at 30mg. (d) Effect of dosage with 5% FeCl2 on disruptive solvent (H2O2) for study of the lipid recovered and concentration of lipid recovered from *C. sorokiniana CY-1*. Other operating conditions: concentration of H2O2 of 30% w/w, organic solvent hexane 85%, contact time 3 min, ratio 1:1.33, and biomass amount at 30 mg. (e) Effect of time of contact on disruptive solvent (H2O2) for the study of lipid recovered and concentration of lipid from C. *sorokiniana CY-1.* Other operating conditions: concentration of H2O2 of 30% w/w, organic solvent hexane 85%, ratio 1:1.33, 4 µL/g 5 % FeCl2, and biomass amount at 30mg. (f) Effect of biomass amount on disruptive solvent (H2O2) for the study of lipid recovered and concentration of lipid from *C. sorokiniana CY-1*. Other operating conditions: concentration of H2O2 of 30% w/w, organic solvent hexane 85%, ratio 1:1.33, time of contact 4 min, and 4 µL/g of 5 % FeCl2.

Figure 5-3: Optimized lipid extraction data co-relate to time with predicted values of lipid extraction using hexane. The lines representing the diffusion model.

Figure 5-4: Distribution of lipid content within biomass powders during extraction using the numerical simulation results.

Figure 5-5: Effect of different concentration of FeCl2 with varies temperature in disruptive solvent (H2O2) for the study of a) concentration of lipid (mg/g) from *C. sorokiniana CY-1*. Other operating conditions: concentration of H2O2 of 30% w/w, organic solvent hexane 85%, ratio 1:1.33, time of contact 4 min, 4 µL/g of FeCl2, and biomass amount at 10 mg. b) lipid recovered % from *C. Sorokiniana CY-1*. Other operating conditions: Concentration concentration of H2O2 of 30% w/w, organic solvent hexane 85%, ratio 1:1.33, time of contact 4 minutes, 4 µL/g of varies FeCl2 and, and biomass amount at 10 mg.

Figure 5-6: The kinetic study of hydroxyl radical's illustration between gaseous and liquid phase generated from the cavitation bubbles

Figure 5-7: (a) Effect of methanol volume ratio for non-catalytic transesterification from ultrasound Hielsher, UP400S. Other operating conditions: amplitude 35%, pulse: 0.4 pulse (cycles), 6 mins, system volume at 7 mL, and 25 ^{o}C room temperature condition. (b) Effect of duration for non-catalytic transesterification by ultrasound. Other operating conditions: amplitude 35%, 0.4 cycles, oil: methanol volume ratio 1:0.17, system volume at 7 mL and 25 ^{o}C room temperature condition. (c) Effect of pulse (cycles) for non-catalytic transesterification by ultrasound Hielsher, UP400S. Other operating conditions: amplitude 35%, duration of 4 min, oil: methanol volume ratio 1:0.17, system volume 7 mL and 25 ^{o}C room temperature condition.

Figure 5-8: The overall absorbance spectra for microalgae oil and lipid via rapid transesterification reaction by ultrasound observed at wavelength range 400-4000 cm-1

Figure 6-1: 5 selected pictures from the pool of microalgae image data for the purpose of illustration.

Figure 6-2: Biomass concentration shown in the growth of *C. vulgaris FSP-E* in BG-11 and various molasses mediums combination in without additional of CO2 condition

Figure 6-3: Nitrate content shown in the growth of *C. vulgaris FSP-E* in BG-11 and various molasses mediums combination in without additional of CO2 condition

Figure 6-4: Sucrose content shown in different cultivation days for *C. Vulgaris FSP-E* in control BG-11 and various molasses concentration mediums without additional of CO2 condition

Figure 6-5: pH of the medium shown in different cultivation days for *C. Vulgaris FSP-E* in control BG-11 and various molasses concentration mediums without additional of CO2 condition

Figure 6-6: Comparison of different K-value by predicting and actual data using normalise Root Mean Square Error (nRMSE) in (a) biomass, (b) nitrate and (c) pH value.

Figure 6-7: The comparison of prediction data by k=4 with actual set of biomass, nitrate, and pH value using k-NN algorithm

Figure 7-1: Zirconium based molecules, sodium dodecyl sulphate (SDS), and lipids that have been shown as potential linker compounds for binding.

Figure 7-2: Metal incorporated bio-linker (MBL) compounded with XNBR polymer demonstrates potential coordination linking.

Figure 7-3: FTIR scanning in the range of 400-4000 cm-1 (a) compounded XNBR after 24 h of maturation (b) vulcanization of the compounded XNBR.

Figure 7-4: a) Comparison of the tensile strength (MPa) and force at break (N) of various latex formulation samples. b) Comparison of elongation in percentage (%) and crosslink density (mol·g-1) of various latex formulation samples.

Figure 7-5: a) Comparison of specific elongation, 300% and 500% in tensile strength (MPa) and force at break (N). b) Comparison of aging profile in tensile strength (MPa) and force at break (N).

Figure 7-6: Compounded XNBR polymer (a) Zeta potential (b) Polydispersity index (PDI).

List of Tables

Table 2-1: Species and pH toleration

Table 2-2: Culture medium composition

Table 2-3: Solvent extraction methods

Table 3-1: Operating parameter and conditions

Table 3-2: Model parameter for estimating the time of hydroxyl radical formation.

Table 3-3: Rate constant and reaction equation

Table 3-4: Comparison of lipid profile using GC-FID.

Table 3-5: The effect of biomass with different ratio for the extraction of lipid for recovery yield and enhancement comparison toward water-organic solvent biphasic system from *C. vulgaris CY-1*. Other operating condition fix at 30% concentration of hydrogen peroxide, pure analytical grade of organic solvent 85% (hexane), and at room temperature 25°C.

Table 4-1: BG-11 medium compositions.

Table 4-2: Operating parameters and conditions of HLBS

Table 4-3: Microalgae polysaccharides

Table 4-4: Growth profile for different concentrations of molasses

Table 4-5: The fatty acids methyl ester (F.A.M.E) weight profile from GC-FID

Table 5-1: Operating parameters and conditions

Table 5-2: The diffusion of lipid extraction data and accuracy of the mathematical modelled

Table 5-3: Comparison on the list of strains and extraction methods with lipid recovered

Table 5-4: Energy profit ratio (EPR) based on energy input and output from microalgae lipid contain.

Table 5-5: Comparison of the catalytic and non-catalytic process specification

Table 5-6: Show compounds yield of saturated or polyunsaturated fatty acids from non-catalytic transesterification (HLBS/U.S.), dissolved of F.A.M.E in chloroform, catalytic transesterification (HLBS/Catalyst-sulphuric)

Table 6-1: Comparison and indication of with and without CO_2 in biomass productivity, specific growth rate and percentage difference between both methods.

Table 6-2: The Bio-composition from different mediums of molasses and control BG-11 in without addition of CO_2 condition.

Table 7-1: Compounding of XNBR sample formulations

List of Abbreviation and Acronyms

k-NN	k-Nearest Neighbor
PBR	Photo-bioreactor
G3P	Glyceraldehyde-3-phosphate
DCW	Dry Cell Weight of microalgae
Pb	Productivity of biomass
μ	Specific growth rate
DW	Dry Weight of microalgae
AMPK	Adenosine Monophosphate-activated Protein Kinase
AMP	Adenosine Monophosphate-activated Protein
CoA	Coenzyme A
ACCase	Acetyl-CoA carboxylase
TAG	Triglyceride
RGB	Red, green, and blue
OD	Optical density (wavelength for UV-Vis spectrophotometer)
nRMSE	Normalise root mean square error
AOP	Advance oxidation process
EPR	Energy profit ratio
FFA	Free fatty acid
F.A.M.E	Fatty acid methyl ester
HLBS	Hybrid liquid biphasic system
MJ	Mega joule (energy)
OH	Hydroxyl
PBR	Photo-Bioreactor
PUFAs	Polyunsaturated fatty acids

ROS	Reactive oxygen species
ROO	Peroxyl radicals
W	Watt
XNBR	Carboxylated nitrile butadiene rubber
LAT	Latex
MBL	Metal incorporated bio-linker

Chapter 1. Introduction

1.1 Background

Microalgae is an abundant and biodiversified species with a potential prospective in utilizing the cellular component for various applications as bio-based products. This study is focusing on lipid for industry application. There are around 150,000 kinds of microalgae species in the world and not every single species has been studied from [1]. Microalgae is categorised as microscopic aquatic plants, which could perform photosynthesis reaction through chlorophyll molecules, while macro-algae are usually referred as seaweeds and as primitive photosynthetic plants. They are capable of utilizing carbon dioxide from the atmosphere and convert into source of energy for their growth. The objective of this project study is to focus on microalgae as raw material for industrial application such as biofuel and bio-additive to polymer material (e.g. plastic, rubber). Furthermore, area of cultivation space for producing the amount of oil per acre of land is potentially higher compare to palm oil, soy bean oil, and sun flower oil. Microalgae unlike common plants, they are plants which do not contain any root, stem, or vascular tissue to produce flower. The microalgae-derived products in the world are anticipated to reach USD 1143 million by 2024 [2]. Future market of algae for biofuels and other applications is the main motivation for conducting this project studies. Since, microalgae resources gaining momentum in the resources market as third generation of biofuels. The

research on biofuel from microalgae plants is mostly on laboratory scale, the current extraction technique required multiple steps and takes time to complete the whole lipid extraction process. The main issue is the costing for the microalgae derived biofuel production with high equipment cost. In which, investor have lost the interest for investing money for developing this potential raw material in the nation. Moreover, certain microalgae species, such as *Botryococcus braunii* and *Chlorella vulgaris*, have been reported to contain more than 50 % of lipids, which has ascertained their potentials to produce biodiesels [3]. Besides, many high-value products can be extracted from algae for the applications in pharmaceutical, nutraceutical, and cosmetic industries [4].

There are eight types of algae species such as *Euglenophyta, Chrysophyta, Pyrrophyta, Chlorophyta, Rhodophyta, Phaeophyta, Xanthophyte,* and *Diatom*. Some algae species are suitable to be used for food supplement applications while some consisting of high content of lipids are appropriate to be made biofuels [5]. To further assess the usefulness of varied algae species, highlights main biochemical compositions of algae, including proteins, carbohydrates and lipids. Moreover, the selection of extraction methods is crucial to obtain maximum amount of products from algae for the subsequent applications. Combinations of traditional and advanced extraction techniques might be adopted to maximize the extraction efficiency of the target products from algae. The conventional extraction methods include liquid-liquid extraction, solid-liquid phase extraction and solid phase micro-extraction. On the

other hand, modern extraction methods usually refer to the cavitation technology, pressurized process, aqueous biphasic separation, critical liquid, microwave membrane disruption, instant pressure drop, and temperature alternation methods [6-8]. The current trend of the research is lacking of combination of disruptive extraction technique where fusion two different types properties of solvent in a system for separating the microalgae components.

The extraction of biological compounds and their addition to the polymer bring a new trend in multinational company where they are heading towards environmental friendly properties of disposable glove products. Bayer Company introduced the first bio-based cross linker for polyurethane products during the European Coating Show 2015. The bio-based crosslinker (Pentamethylene diisocyanate, PDI) contains 70% of the molecular carbon content from the biomass materials, as the world is gearing towards green environment and renewable energy to meet the 3 pillars of sustainability i.e., to harmonize the social requirements, economy feasibility and reducing the environmental carbon footprint. bio-based cross linkers are poly (y-glutamic acid) PGA, a polymer produced by microorganisms i.e. Bacillus subtilis F-2-01 and Bacillus subtilis IFO3335 [9-11]. There are several applications for PGA such as esterification, y-irradiation, and as an additive for crosslinking [12]. Their studies showed that PGA could induce different cross-linked density on the polyurethane, hence improving the strength of the product in terms of performance including tensile strength, durability, etc. A recent finding discussed the crosslinking of PGA with

saccharides (i.e. chitosan) through esterification in the presence of water-soluble carbodiimide (WSC) in dimethyl sulfoxide DMSO [9, 13, 14].

The application of microalgae extract components is very promising product for utilizing in industrial application. The focus of lipid study in which will be a gratifying project for biofuel or bio-additive in the rubber polymer industry. The lipid compound from the microalgae in which have a great potential to replace the current petroleum based of crude oil where microalgae biofuel (F.A.M.E) appears to be more environmental friendly and could be accepted by various exporting standard body (e.g. ASTM, EN). With the preservation and caring the environmental as objective, integrated microalgae cellular components may suit for various industrial application with the selected strain of microalgae species in which may provide the suitable components as additive and consumer products.

1.2 Problem Statement

Microalgae is found abundant based on its high growth rate and high adaptive properties, it has been categoried as photosynthetic eukaryote cells with the ability for mitigating carbon dioxide during the process of photosynthesis. The abundances of microalgae have cause eutrophication in lake or any large body of the water. The dense growth of the microalgae plant life in the water may cause starvation of oxygen beneath the surface of water for others aquatic life such as fish. Therefore, the topic for microalgae research has been intensively

discussed especially in the aspect of carbon capture through cultivation, nutrient extraction, and emerging sustainable energy in recent decade [15-17]. However, some limitations, obstacles and challenges still on the subject in research mind endeavor for improvement.

One of the main limitations for microalgae to be commercialized into the market which is feasibility on large scale and high energy consumption [18, 19]. The microalgae cell mostly consists of cell wall where nutrient compound is embedded inside the cell. Pretreatment a step which is common procedure for penetrating the layer of cell wall to release the nutrient. The pretreatment method which is based on mechanical, physico-chemical adverse properties in high energy (benchmark temperature around 650^{o}C) [20, 21], supercritical CO_2 high in operating cost (extraction fluid maintain at 150 bar for operation,50 bar for liquid storage) [22], bead milling low yield (<16%, various by cell wall thickness) [23] , hydrodynamic cavitation high energy consumtion in creating the pressure (~1000 bar) [24, 25], ammonia fiber explosion (AFEX) needs long duration of drying time at vacuum oven 40^{o}C (24 hrs) [26] and enzymatic pretreatment which is relatively high in energy consumption consists of biological instability concern and subsequently raises in capital cost during start-up of a project.

Despite the availability of variety nutrient extraction method of lipid from microalgae biomass has been introduced from worldwide research groups, company and institution. There is still a gap to be filled with practical study

together a clear clarification for a single system that can involve of pretreatment method combined with extraction properties. Besides, the parameters that may affect the single system such as types of solvents, pH value, volume ratio, contact temperature, $FeCl_2$ concentration, contact time, biomass amount and duration which are the main focuses in this study that may affect the yield of extract.

1.3 Research Objective

The aim of current research study is to assess of microalgae lipid and develop an extraction method which is efficient, productive, sustainable and with enhancement properties of the extraction method to be applicable for industrial application. The focus is to extract the lipid content in the cellular membrane of microalgae for biofuel and bio-additive in rubber industry especially lightly cross-linked products. The reason for developing this method is due to low operating cost and step reduction for the overall lipid extraction process. Thus, the overall microalgae based biofuel production cost can be reduced for commercialized. Hence, the application may apply in industrial application, developed, and optimized to achieve higher efficiency and productivity.

The specific objectives of the research study include:

1. To develop a disruptive extraction method based on chemical for disrupting microalgae biomass cell wall with simultaneous extraction properties.

2. To optimise the disruptive extraction method and explore the cultivation medium through waste compound to study the microalgae cell growth behaviour.
3. To make lipid compound into industrial application with novel rapid and high production method for high output.

This report outline included of literature review for microalgae compound specifically on lipid compound, the upstream cultivation processing and downstream processing for biofuel production with a section on bio-additive where possible utilize in rubber polymer. In upstream production have explained the important parameter for cultivate lipid rich microalgae species, such as effect of temperature, pH, salt concentration, light intensity, and nutrient medium. On the others hand, downstream process has included for dewatering, drying, pre-treatment, lipid extraction, product fractionation, and transesterification process.

1.4 Research Scopes

The research scope as explain in **Figure 1-1** which is involment of planned and system with fabricating a simultaneous extraction system specifically for lipid extract followed by application for the lipid. The system should be in rapid production and simple procedure in which suitable to be used with minimum supervision upon date of commission into the plant. Besides, the following scope involve of exploring the application for large scale obtained from the extract.

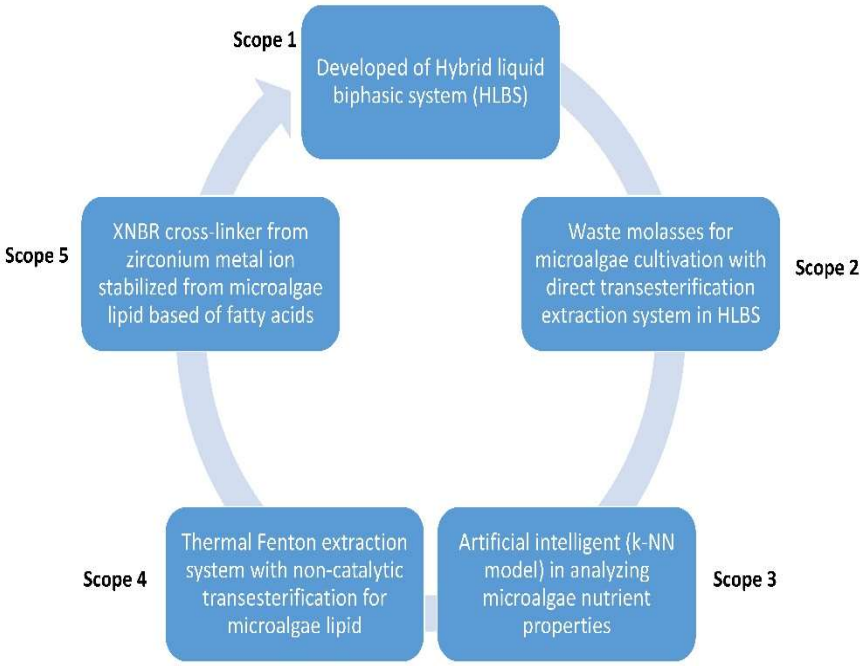


Figure 1-1: Research scope involvment of exploring industry application

i. **Exploring the potential from liquid biphasic system (LBS) modify into a simultaneous two-phases system specifically for lipid extract.**

The liquid biphasic system (LBS) conventionally is used for extraction of bioactive compounds e.g. protein, chlorophyll, and lipase. The LBS is claimed by several researchers from local and international as low cost, energy saving, and relatively mild separation technique compare to others extraction system, where may highest chances retain the originality form of the extract.

ii. **Assessment on the possibility for cultivating microalgae using waste compound as medium with different properties phase of the developed hybrid liquid biphasic system (HLBS) in lipid extraction.**

The cultivation of the microalgae cell contains of 3 basic of needs which are nutrients, carbon dioxide, and intensity of light. The early proposed is use of waste compounds to replace salts medium (BG-11) and reduce the dependence on concentrated carbon dioxide. Further investigate the HLBS for the feasibility for biofuel production.

iii. **Investigation the potential of the non-catalytic transesterification of the microalgae lipid derived from the HLBS system using sono-processes**

The HLBS system have feature the potential of triglyceride, di-glyceride, and mono-glyceride conversion to fatty acids. The investigation would be involving of sono-processes for assisting the non-catalytic transesterification. The enhancement of the existing HLBS system and followed by the affecting parameter for the sono-processes in non-catalytic transesterification toward formation of the fatty acids methyl ester (F.A.M.E).

iv. **The selection of waste molasses as the cultivation medium incorporate with the artificial intelligent (Ai) for assisting to analysis of the growth properties.**

The cultivation of the microalgae cell has to conduct laboratory analysis for understanding the growth properties, the procedure which is time taken and consist of multiple procedure. The incorporation of the photo-to-properties through (Ai) algorithm is potential for a rapid analysis by in-situ technique. The methodology is shown in the chapter below.

v. **Metal incorporated with microalgae derived fatty acids compound into synthetic polymer to enhanced the physical properties.**

The metal ions as one of the emerging cross-linking compound for rubber, however, due to the negative impact of metal ion molecules alone easily cause agglomeration during rubber compounding. The incorporation with fatty acids targeted the charges from the metal ions to resolve the stability issue toward establishing covalent or hydrogen bond.

Chapter 2. Literature Review

This chapter will first introduce microalgae cultivation, then pre-treatment methods, follow-by extraction techniques, and lastly potential product application. Malaysia has been focusing on the research and development for a worth of RM 5 billion global market value a year of microalgae products reported in 2018 [27]. In which, every microalgae cell is able to convert salt medium, carbon dioxide, and light into nutrient and high value bioactive compounds. The application for microalgae from mitigating excess carbon dioxide, wastewater treatment, biofuel, pharmaceutical, food supplement, and bio-molecules for industry purposes. Microalgae is diverse and contain numerous of unique characteristic in both freshwater and saltwater environments. The different types of microalgae strains contain of different properties such as Cynobacteria able to do nitrogen fixation, Rhodophytes with presence of red pigments, Dinoflagellates are class of unicellular with grow-in-the-dark properties and also common strain for wastewater treatment and Xanthophyte with yellow-green color potential used for colour pigment. The natural strain is common to go through genetic modification for high growth rate and high content of the nutrient compound followed by performing in-house cultivation such as open pond, raceway, cascade and photo-bioreactor for mass production of the microalgae biomass. The application of the microalgae which

is separated into upstream and downstream process, in brief the biomass nutrient is never a part from the process of cultivation, pre-treatment, extraction, purification and drying before converted into the products. The gene of the strain plays the fundamental role for the content of nutrient in each microalgae biomass, subsequently the cultivation parameters that may optimize to sustain the nutrient content from each of the microalgae cell. The highly controlled photo-bioreactor has contributed a major portion for the capital and operating cost. Current study is focusing in lipid compound from *Chlorella* species of microalgae to be exploring the used for industry application. The potential market in Malaysia is bio-molecules substitution for rubber compounding industry and lipid compound for the production of biofuel, which is a great market to be explored from the microalgae biomass.

2.1 Biofuels

This section will include of introduction for the microalgae prospective in biofuels sector, explained about third generation of biofuel and comparison for different generation of biofuel. The current commercial and non-renewable fuels such as coal, petroleum, and natural gas contribute about 85% of total energy consumption in 2007 as reported by United State Energy Source [28]. The United Nation, however, has concerns with regard to the climate change policy stated in Paris Agreement 2018 [29] that will intrinsically affect the exploration of fossil fuels. The first-generation biofuels are associated with the

conversion of edible food crops cultivated in the farm for the energy source. The examples are wheat, soybean, sugar, starch and vegetable oil [30]. The next generation biofuels, after the use of edible crops plants in first-generation biofuels, are derived from non-food wastes and lignocellulosic biomass that are generated as agriculture and forestry by-products. The process of converting lignocellulosic biomass to biofuels requires the separation of xylose and lignin from the crystalline cellulose [31]. The second-generation biofuels derived from lignocellulosic biomass are cost intensive and require pre-treatment process that consumes large amount of energy, especially in the process of scarification and steam explosion [32]. In addition, high cost of enzymes that used in the process is the main challenge for the commercialization of second-generation of biofuels [33].

The emerging third-generation biofuels, namely algae oils, are emerging in the market as fuel source. Algae biofuels have been laboratory tested, and extraction methods using various organic solvents have been introduced namely chloroform, hexane, and heptane for dissolving the lipids compound in the membrane cell [34, 35]. The combustion and exhaust emission performances of the diesel engine fuels supplied by algae biodiesels have demonstrated competitive results when compared to conventional fuels [36]. It was reported that the compress injection engine that uses the blend of algae oils and conventional diesels showed a reduction of nitrogen oxide production of 27.98% and improve optimization of the incomplete combustion rate by 30% [37].

Although algae biofuels have demonstrated promising performance as transportation fuels when compared to conventional fuels, the unit price of algae fuels (estimated to be reached USD 2.0 to 2.8 per liter) is remarkably higher than that of fossil fuels (estimated to be approximately USD 1 per liter). Nevertheless, it is expected that algae biofuels will dominate the fuel market by establishing a market share of 75% in the coming decade, with reference to the ongoing sustainable development trend [34, 38, 39].

The first-generation biofuels are disputable due to usage of edible plants and food crops (i.e. sugarcane, corn, whey, barley, potato, and sugar beets) as raw materials to produce fuels. The common products of first-generation biofuels are bioethanol's and biodiesels. From the financial perspective, first-generation biofuels are relatively high cost compared to the third-generation biofuels, since the edible plants that serve for fuel production might trigger a food supply crisis. On the other hand, the raw materials used for second-generation biofuels are lignocellulosic biomass. The examples are wood chips (with price ranging from USD 100 to USD 120 per tonnes) and forest residues (with price ranging between USD 60 to USD 80 per tonnes), which are relatively cheaper than the raw materials used to produce first-generation biofuels [40]. The processes involved in the production of second-generation biofuels include material allocation, pyrolysis, gasification and enzyme hydrolysis to break down the waste biomass to produce biofuels. Second-generation biofuels require additional extraction step before proceeding to fermentation or

transesterification processes. In addition, the municipal waste might need to be sorted out before sending for further treatment.

To sum up the above, the availability of the food crops and lignocellulosic biomass might heavily depend on the economy, climate change, land and water availability, and fertilizer to support the growth of the said crops into a matured stage to supply for biofuel production [41]. The production of algae biofuels in volume per hectare of land is equivalent to 9 times more than palm oil, 41 times more than castor crops, and 241 times more than corn crops [3, 42, 43]. Nevertheless, the high production cost remains the major obstacle to restraint the third-generation biofuels from being commercially viable. Therefore, the development of sustainable and viable technologies for algal cultivation, algal oil extraction, and biodiesel conversion is of upmost important to commercialize of the algal biofuels.

2.2 Upstream Processing of Microalgae

2.2.0 Algae cultivation

Several algae species with relatively high lipid content that are suitable for biofuel production have been identified, including *Nannochloropsis oculate, B. braunii,* and *C. vulgaris* [44]. Apart from the selection of microalgae species, the cultivation conditions, namely temperature, pH, light intensity and nutrient

availability, might stimulate the accumulation of specific valuable components in microalgae cells. The cultivation method is always closely related to the type of microalgae strain [5]. The algae cultivation can be conducted in a closed system such as photobioreactor, in which the algae are grown in a transparent tube with the supply of carbon dioxide and nutrients medium. Besides, the algae culture can also be performed in open circular or raceway ponds with a lower capital and operation cost, but the production stability and quality control of the algal biomass might be more difficult to maintain.

Microalgae can be cultivated in wastewater since the main nutrients in municipal wastewater system such as nitrate and phosphate can act as the supplement intake for microalgae to produce lipids [45]. Besides, acetate is found abundant in wastewater and can be utilized as one of the carbon source supplies for algae cultivation [46]. Besides, microalgae cultivation can be coupled with the treatment of flue gas, whereby the flue gas from power plants (mainly from the combustion chamber) can be channelled to supply carbon dioxide to support the microalgae growth [47]. However, the flue gas from the power plant should be pre-treated to filter harmful impurities including heavy metals before feeding into the photobioreactor for algae cultivation.

2.2.1 Effect of the temperature

Temperature is an important factor to support the growth of any plant organism, since it affects the cellular biochemical composition. The variation of

temperature affects the nutrient uptake, carbon dioxide adsorption capacity, and photon capture ability. The increase of temperature might promote the growth of algae, but the growth rate will deteriorate after it reaches the optimum level, and it might eventually affect the cellular biochemical compositions [48] . Compared to the closed system, open cultivation system usually experiences large temperature fluctuation. The relation between growth rate and optimum temperature has been investigated through a modelling study using Arrhenius equation [49]. It was reported that 25^{o}C is the optimum temperature for most of algae species [49]. N. oculate, and C. vulgaris can achieve maximum lipid content when they are cultivated at temperatures between 20 and 25^{o}C. The increment of temperature from 25 to 30^{o}C might lead to a sharp decrease in the lipid contents of C. vulgaris from 14.71 to 5.9 % [50, 51]. However, another heavy-duty microalgae species, namely *Scenedesmus*, can survive in a wide range of temperature from 10 to 40^{o}C.

2.2.2 Effect of the pH and salt concentration

Acidity or basicity of a culture medium might affect the growth and distribution of algae species [52]. In marine system, pH value can be correlated to the temperature and dissolved oxygen, and it influences the algal growth. **Table 2-1** presents the tolerable limit of pH for different algae species, and the suggested salts for the pH adjustment. Most of the phytoplankton grows optimally at pH 7.0 to 9.4 [53]. The alternation of pH in the culture medium

might affect photosynthesis rate and enzyme activity in algae cell which will then have impact on the lipid accumulation rate in cells [54]. Beside of pH, salt concentration in the culture medium might affect the growth of microalgae. For instances, the increment of salt concentration from 0.4 to 4 M could result in an increase in the yields of both saturated and monounsaturated fatty acids obtained from Dunaliella sp. but lead to a decrease in the collection of unsaturated fatty acids [55]. Besides, it was reported that the salinity stress exerted by the salt concentration can lead to a significant increase in the accumulation of lipids in cells of Chlamydomonas sp. [56].

Table 2-1: Species and pH toleration

Algae	Tolerate pH	Suggesting salt for pH adjustment	References
Phaeodactylum tricornutum	pH > 10, continuous monoculture	NaCl, $MgCl_2$, $CaCl_2$, KCl	[57]
Dunaliella tertiolecta	pH < 9.4	NaCl, KNO_3	[55]
B. braunii	pH 6 - 8.5	$NaNO_3$, KNO_3, NaCl	[58] [59]

C. vulgaris	pH 6.9 - 8	NaCl, KCl	[60] [61]

2.2.3 Effect of the light intensity

The light intensity provided for microalgae cultivation might have impact on the cell growth rate, since sunlight is the major energy source to drive the photosynthesis reaction. C. littorale demonstrated optimum growth rate when it was cultured at a light intensity of 170 μ $mol \cdot m^{-2}s^{-1}$ and temperature of 22ºC [62]. Green microalgae such as Dunaliella salina are able to grow in both dark and light environments, however their cellular compositions increase when they are grown under light illumination [63]. Nevertheless, excess light intensity might cause the damage of cells and chlorophylls, since chlorophylls absorb energy between wavelength of 700 nm to 680 nm [64].

Besides, some microalgae species are cultivated under a sequence of light and dark environments for certain periods. B. braunii can be grown under photoautotrophic conditions with a light:dark period of 16:8 h, whereas *Spirogyra, Chlorella and Picochlorum* are preferably growing under light:dark period of 12:12 h, 14:10 h, and 14:10 [58, 65, 66]. There might be a decrease of biomass growth when the cultivation is conducted under dark period [67]. Despite the species variety, the average biomass loss during the dark incubation

period was 6.8 %. This might be attributed to the decrease in temperature when there is absence of light radiation [66]. Besides, the absence of light reduces the photosynthesis rate and thus reduces the conversion of solar energy to chemical energy compounds such as adenosine triphosphate (ATP) and nicotinamide adenide dinucleotide phosphate (NADPH) to support for the cell growth [68].

2.2.4 Effect of the nutrient medium

Different microalgae strains might require different culture medium compositions to support for their optimum growth. Nutrient medium, such as bold basal medium (BBM), is suitable for freshwater algae. However, bold basal medium with ammonium carbonate (BBMa), which contains the formulations of BBM but with added ammonium carbonate that serves as a source for nitrate and inorganic carbon, can be used for algae cultivation when the nitrogen and carbon sources are insufficient. Another culture medium, namely Chu's modified nutrient medium, is usually used to cultivate Nannochloropsis sp. for enhanced oil yields [69]. Likewise, blue-green medium (BG11) has proven to increase the lipid productivity for B. braunii [58, 70]. The compositions of these culture medium are summarized in **Table 2-2**. A suitable culture medium definitely helps to maximize the nutrient intake for each microalgae species, and if it is coupled appropriately with other process parameters, such as temperature, pH and light intensity, the microalgae growth can be optimized [71].

Table 2-2: Culture medium composition modiefied from source [72]

Salt	Modified CHU 13 (g / L)					BG11	BBM	BBMa
	0.25X[1]	0.5X[2]	0.75X[3]	X	2X[4]			
KNO_3	0.05	0.1	0.15	0.2	0.4	-	-	-
$NaNO_3$	-	-	-	-	-	1.5	0.25	-
K_2HPO_4	0.01	0.02	0.03	0.04	0.08	0.04	0.074	0.074
KH_2PO_4	-	-	-	-	-	-	0.0175	0.0175
$CaCl_2.2H_2O$	0.02	0.04	0.06	0.08	0.16	0.036	0.024	0.024
$MgSO_4.7H_2O$	0.025	0.05	0.075	0.1	0.2	0.075	0.073	0.073
Na_2CO_3	-	-	-	-	-	0.02	-	-
NaCl	-	-	-	-	-	-	0.025	0.025
$FeSO_4$	-	-	-	-	-	-	0.005	0.005

EDTA	-	-	-	-	-	0.001	0.045	0.045
Citric acid	0.025	0.05	0.075	0.1	0.2	0.006	-	-
Ferric ammonium citrate	-	-	-	-	-	0.006	-	-
Ferric citrate	0.0025	0.005	0.0075	0.01	0.02	-	-	-
Ammonium carbonate	-	-	-	-	-	-	-	0.157

[1] Factor of 0.25 for salt compositions from original Chu 13 (1X).
[2] Factor of 0.5 for salt compositions from original Chu 13 (1X).
[3] Factor of 0.75 for salt compositions from original Chu 13 (1X).
[4] Factor of 2 for salt compositions from original Chu 13 (1X).

2.3 Downstream processing

Downstream processing of microalgae comprises of multiple sequential processes involving harvesting, product extraction, purification, and product finishing. Downstream processing for algae-based biodiesels accommodates 60 % of the total biodiesel production cost [73]. The downstream processing will depend on the cell wall nature of the microalgal strains [74]. For instances, Cyanidioschyzon merolae, which is a type of red-algae without complex cell wall structure normally are found in hot spring with acidic sulfur and metal-rich condition, requires least effort for cell disruption in order to proceed for cell component extraction purposes [75]. **Figure 2-1** illustrates the overview of downstream processing, and each stage is described in detail in the following sections.

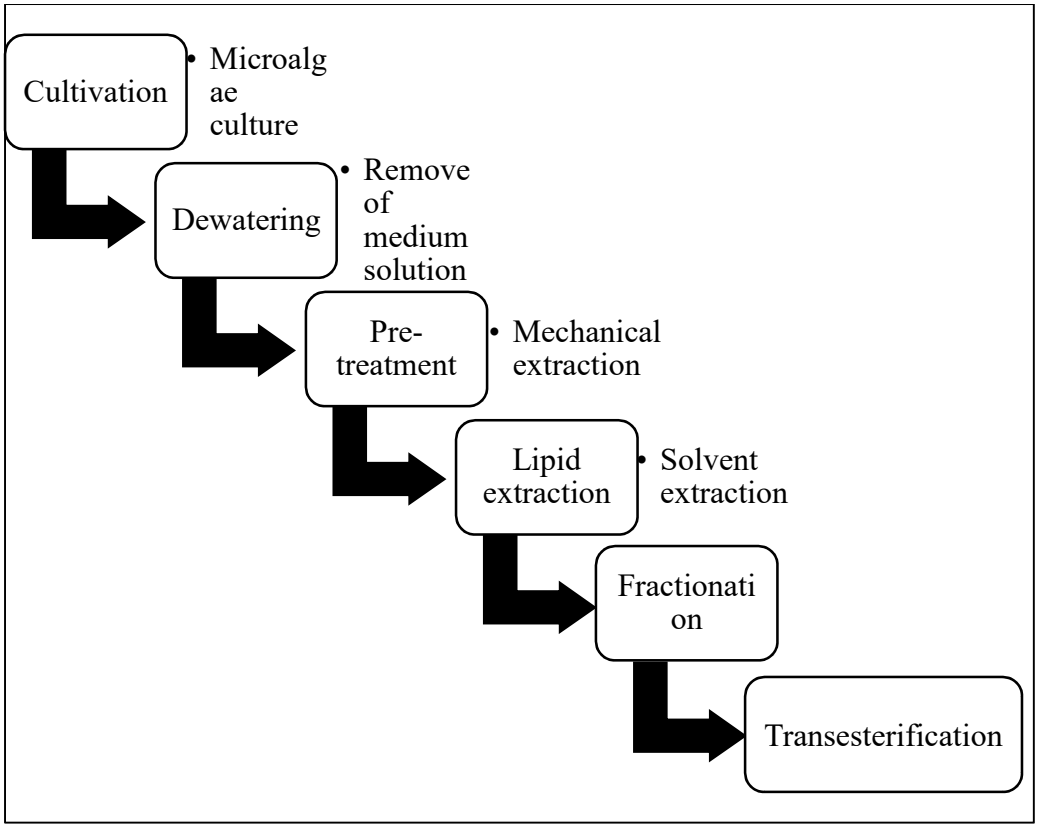


Figure 2-1: Process flow diagram for algae biodiesel

2.3.1 Dewatering and drying

Dewatering is an important process in biofuel production, in which water is removed from the depleted cell culture to obtain biomass paste. Forward osmosis (FO) can be used to separate water and biomass using low energy membrane separation process [76]. It was reported that polyethersulfone membrane achieved water removal efficiency of 81 % when it was used for algae dewatering [77]. Also, natural drying by sunlight is often conducted for drying of algae biomass [78]. Despite its low operation cost, the dewatering efficiency of natural drying is usually low and unstable due to the change of climate.

Drying is the application of moisture removal with mechanism of providing heat energy or vapour transport for the drying process. Air-drying is one of the methods for vapour transport where vapor generated in the heating of product or substances interior of the material eventually will be removed by the force in term of air, which the moisture will be evaporated [79]. After microalgae dewatering process, the biomass slurry will be subjected to drying process such as spray drying, solar drying, convective drying, and freeze-drying. Convective drying is one of the conventional processes for dehydration for microalgae where hot air will be introduced for the drying in the oven. The example temperature for air-drying Spirulina sp. is 40 ^{o}C – 55 ^{o}C [80]. Spray drying is for high value microalgae product to retain nutrient and less influence on lipolysis [81]. Solar drying is the lowest cost technique and requires longer drying time compared to the others and a wider drying surface, but this method could be affected by weather condition. One of the widely used drying methods is lyophilisation (or freeze drying), where ice crystal formed during the lyophilisation process may lead to disruption of the cell wall. It is known that lyophilisation could retain most cellular proteins when compared to the above-mentioned drying methods [82].

2.3.2 Pre-treatment

Pre-treatment plays an important role in downstream processing, since the output of the pre-treatment process will affect the following downstream

processing and product conversion. The pre-treatment process can be categorized into thermal, mechanical, chemical and biological methods [83]. The selection of pre-treatment methods is depending on the types of microalgae species. Some algae species, such as Scenedesmus sp., contain multilayer cell wall structure that has high resistance to chemical and biological disruption [84]. On the other hand, Dunaliella sp. and Pavlova sp. are the species without cell wall, therefore they are being more prone to chemical and biological attacks [85]. The examples of the mechanical methods are the homogenization of the cells using blender, glass beads, sonication, ultrasonic wave, microwave, and the electricity [86]. However, single pre-treatment method such as acid treatment to dissolve cell membrane or cellulose may require the use of concentrate acid under pressurized condition to achieve higher treatment efficiency [32].

Therefore, combinations of different pre-treatment methods are used to improve the cell disruption level. Different combinations of mechanical, thermal, and chemical methods have been investigated and examined for their performance in cell disruption [87]. For an example, the combination of thermal and mechanical methods is efficient to disrupt complex cell walls [88]. Another example is the combination of chemical and mechanical methods. The biomass was first acid- or alkaline-treated to disturb cell wall, and the cells were then further lysed using mechanical method using homogenizer, as described in **Figure 2-2**.

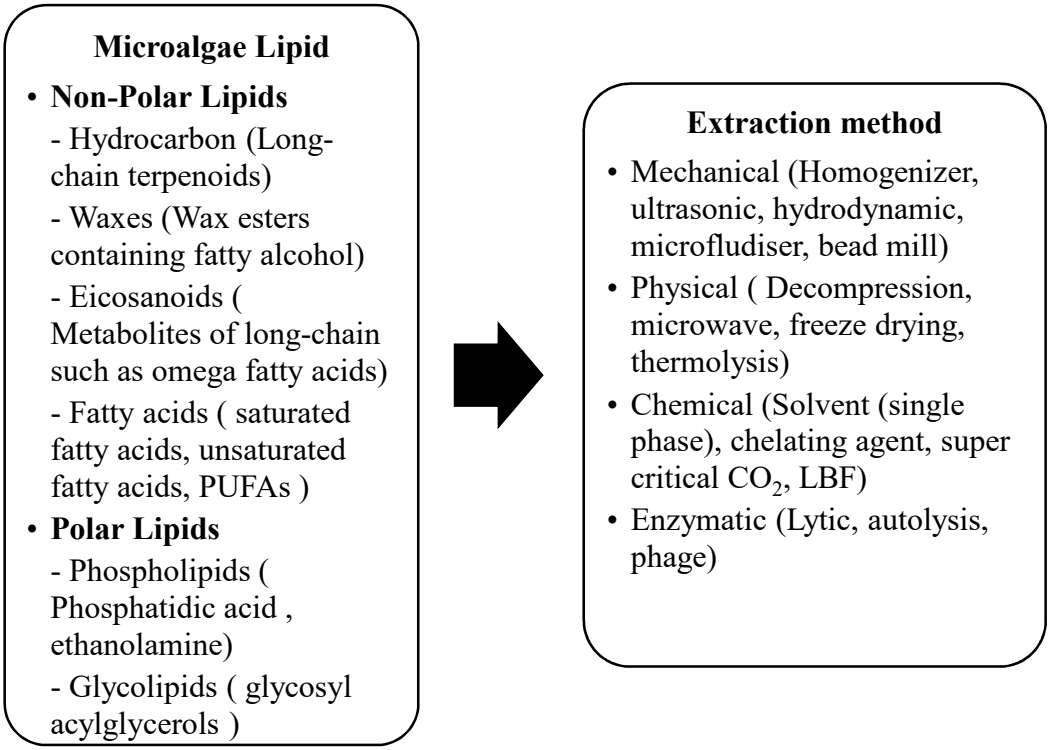


Figure 2-2. Microalgae pre-treatment method

2.3.3 Lipid extraction

Lipid extraction is the core process in the production of biofuels from microalgae. **Table 2-3** summarizes the techniques adopted for lipid extraction. There are two widely used conventional solvent extraction methods, namely, Folch method, and Bligh and Dyer method. Folch method applies the use of chloroform-methanol (in volume ratio of 2:1) for the extraction of lipids from the organism cell, and this method needs to equilibrate the homogenized cells

with one-fourth volume of saline solution [89]. On the other hand, Bligh and Dyer method is conducted using 1:2 (v/v) chloroform and methanol [90]. The Bligh and Dyer extraction method has been conducted in large scale processes which enable lipid extraction [91]

Table 2-3: Solvent extraction methods

Name of the method or developer	Solvent used	Technique	Reference (s)
Folch / Bligh and Dyer method	Chloroform: Methanol: Water	4 h of agitation	[89, 90]
Cequier-Sánchez method developer	Dichloromethane: methanol	2 h of agitation, and then filtration, subsequently 1.25 ml of KCl aqueous solution was added into filtrate, and followed by centrifugation at 1500 g at 4ºC for 5 min.	[92]
Schlechtriem method developer	Propan-2-ol: cyclohexane: water	Solution was vortexed for 30 s, followed by ultrasonication at 60ºC for 30 min. 5.5ml of water was added to the solution, and the mixture was vortexed for 30 s and centrifuged at 1800 g for 10 min. The organic	[93]

		phase was transferred to new test tube and 5ml of propan-2-ol and cyclohexane was added.	
Saponification method	Ethanol: KOH	15.2 ml of 3mM KOH and 96 % ethanol were added into test tube, and the mixture was vortex in 60^{o}C for 60 min. Biomass was washed with 4 ml of ethanol and alcohol solution, and next 4 ml of water was added.	[94]
Liquid biphasic flotation (LBF)	Ethanol: K_2HPO_4 (alcohol:salt)	Solution was mixed with 20 ml of K_2HPO_4 solution, and then 10ml ethanol. Air flotation rate was controlled at 15 min and 20-30 cc/min.	[7, 95, 96]

In recent, high voltage electric discharge (HVED) has been applied for the disruption of cells and simultaneously assists the extraction of intracellular bioactive compounds and lipids [97]. The technique applies electrical voltage charge to destruct cellular structure and thus allows the liberation of the cellular compounds. Besides, mechanical-assisted extraction method applies mechanical equipment for cell disruption to facilitate the release of extracted compounds into the solution. For instances, homogenizer is an equipment rotating in high speed typically up to 35,000 rpms with addition of pressure and thermal treatment [98] . The high rotational speed of homogenizer can disrupt the cell wall membrane and release cellular components into the solvent.

Moreover, hydrodynamic cavitation is a type of mechanical extraction, in which the microalgae culture solution is continuously fed into a device for cell wall rupture and simultaneous microalgae oil extraction. The adaption of magnetic impulse with hydrodynamic cavitation has provided uniform cavitation distribution over the flow from a chamber of hydrodynamic cavitation processing device, which may generate the liquid in a turbulent flow through bubbling as driving force. The collapse of cavitation bubble at the boundary phase leads to the separation of the liquid-solid particles. In the case of algae extraction, the pressure of cavity bubbles could reach 150,000 psi and shock waves may occur at the point of the collapsed cavitation bubble [99].

Another physical extraction method, namely decompression, has been studied to identify the effect of pressure, processing time and number of decompressions on the extraction efficiency [100]. Furthermore, thermolysis that applies the localized heat without catalyst is one of the thermal methods for cell lysis. Thermolysis reactor comprises mechanical arms to break deposition in the reactor and reduce thermal resistance from the reactant for better heating surface contact for the product extraction from microalgae [101].

The solvent extraction is often combined with different types of physical and mechanical treatment to enhance the performance of oil extraction. Algae oil is often extracted by hexane owing to its low cost. Pure algae oil can be obtained by extraction through repeated washing or percolation [99]. On the other hand, supercritical fluid extraction is often carried out for lipid extraction from algae biomass. It is operated using liquefied carbon dioxide as the solvent for the extraction. Supercritical fluid can be removed easily, leaving solvent-free extracts through simple depressurising. Therefore, supercritical fluid extraction seems to be a right candidate for the extraction of a variety of natural products from biomass [102]. On the other hand, enzyme-assisted extraction has been studied by adding hydrolytic enzymes to degrade the cell walls [103]. The common enzymes used are cellulose, α-amylase, β-glucosidase, β-glucanase, pectinase, viscozyme L, pectinex, and lallzyme beta [104] . The lysis enzymes can digest the cell wall components through hydrolysis reaction, and eventually rupture the cell wall.

The extraction method is not comprehensive with separated step for conducting the cell disruption and extraction process. The proposed idea for combining both steps is given in 3.3.2 pre-treatment and 3.3.3 extraction as single step. This would reduce the equipment cost, operating cost and duration of the overall process as well.

2.3.4 Product fractionation

Fractionation is a process to separate the desired product from pools of impurities. It works based on the principles of product size, solubility, ionic strength and volatility [105]. The products in microalgae extracts which are to be separated in downstream processing are proteins, chlorophylls, carotenes, non-acylglycerols, and neutral lipids [104, 106-108]. There is possibility of fractionating protein through factors such as concentration of polarisation, molecular weight distribution, and membrane pore-size distribution [109]. Separation from using the technique of altering concentration and polarization as the molecules fractioning through different geometrical orientation during rotating as a mixture solution. Molecular weight distribution which could be fractioned by layer, one of the methods is through ionic liquid for attracting polar or charges molecules before separation from the bulk solution [95]. Efficient membrane separation for specific compound may be done through varying the permeate flux rate and membrane pore size which could be used to manipulate

the fractionating process of desired compound according to their molecular size diameter.

2.3.5 Transesterification

During transesterification process, 3 moles of triglycerides from algae oil react with alcohol, either methanol or ethanol, to yield one mole of glycerol and three moles of fatty acid methyl ester (F.A.M.E) or fatty acid ethyl ester (FAEE). The selection of alcohol type will determine the products are either methyl esters or ethyl esters. The transesterification process is often boosted by acidic or alkaline catalyst to reduce the reaction time. The reaction occurs at atmospheric pressure and temperature of 60 ºC to 70 ºC with excess of methanol [110]. The wastes generated from the biodiesel synthesis during purification (e.g., alkaline/mineral oxide catalyst, free fatty acids, alcohol) are not environmentally friendly. Conventionally, sodium hydroxide was used as catalyst whereas sulphuric acids might be an option to replace alkaline catalyst, where the main concept is to break the glycerol part in the triglyceride to obtain the fatty acids to react with alcohol [111]. Supercritical transesterification method seems to be another option since it does not require the use of catalysts and could also avoid the occurrence of soap formation or saponification reaction [112]. Nonetheless, the biodiesel production using supercritical transesterification method still needs to be further investigated.

2.3.6 Combination of bioremediation and biofuel production with microalgae

Bioremediation for treating industrial or municipal waste through microalgae is viable in reducing the biological oxygen demand (BOD) and nutrients level in wastewater [113]. Microalgae have been tested to assist in the remediation of domestic municipal wastewater. The growth rates of both C. vulgaris and S. quadricauda were enhanced when they were grown in the domestic wastewater system [114] .The removal of nitrate and chemical oxygen demand (COD) was mainly contributed by C. vulgaris, while S. quadricauda exhibited positive effects on the reduction of BOD and phosphate [114]. The survival of microalgae in wastewater treatment plant depends on the pH level, temperature, as well as the levels of phosphate, nitrate, BOD, and COD. The domestic or municipal wastewater contains a high nutrient level for the cultivation of microalgae. The microalgae cells can utilize nutrients from wastewater, such as nitrate and phosphate, as primary food source for conducting photosynthesis reaction for accumulation of lipids and other functional compounds. If the level of nutrients or organic wastes is too high, the growth of algae will be inhibited.

The combination of wastewater treatment and biofuel feedstock generation is beneficial several microalgae species such as B. braunii, C. vulgaris, Dunliella sp., Nannochloropsis sp., E. gracilis and P. tricornutum are identified as potential species. These microalgae potentially contain non-polar

long-chain lipids, but they might need genetic modification to improve their adaptation ability to grow in the wastewater [115]. Nevertheless, some wild-type strains, such as *Chlorella sorokiniana* and *S. obliquus*, are able to grow under the physiological stress arising from the composition of wastewater and are capable to accumulate high lipids content through the intake of nutrients from the wastewater [116]. Therefore, the microalgae that are capable to grow under stress conditions of wastewater have high potential for simultaneous wastewater treatment and biofuels production.

Besides, the high rate algae ponds (HRAPs) that use wastewater as culture medium consist of a shallow raceway with single or multiple loops connecting to paddlewheel vane pumps aiming to create turbulence flow continuously for mixing the algae cultures. The blending of bacteria and algae in the wastewater in HRAPs improves the efficiency of the waste removal rate. The comparison of mixed and unmixed processes shows that the biomass production in the mixed ponds is higher due to high rate mixing, which promotes the growth of the microalgae cells in the ponds [117]. Therefore, the operating cost of HRAPs is relatively low when compare to the cultivation of microalgae in the photobioreactors [118].

2.4 Emerging crosslinking technique and bio-additive in rubber polymer

The long revolution of nitrile rubber in the rubber industries, especially for lightly cross-linked products has been reviewed in this paper. The advancement

is remarkable from the first invention of acrylonitrile butadiene rubber and till date, the physical and chemical properties were elevated. Recent rubber chemists are mainly focus in modifying the nature of the synthetic latex based on butadiene and cross-linker to enhance the perform ability for rubber product to be used in broad range of applications [119-122]. Besides, the different types of rubber had contributed to different sectors of usage due to their speciality properties. All belong to the effort of various types of cross-linking methods which making the liquid latex to suit in plenty of applications and usage from space shuttle (O-ring) to food hawker hygiene gloves [11, 123]. Natural rubber is a superior latex glove which show high elasticity and tactility however not suitable for medical usage due to its protein allergic issues. Moreover, current development of natural rubber by synthesis through, in vitro and in vivo method, with the aim to produce equivalent properties of rubber product with lower materials cost [11, 120, 124]. In fact, the glove manufacturing process have various parameters to monitor to produce an accepted quality of gloves. A quality of nitrile glove may need to pay close attention on latex compounding formulation and the choice of the value-added process options.

The establishment of biological systems (i.e. algae, fungal, etc) could be helpful for industrial applications such as cosmetics, pharmaceuticals, industrial chemicals, nutrient recovery for fertilizers, bio-remediation of wastewater treatment, biofuel and biodegradable additives [50, 125-127]. The idea of using biological extract as chemical additives to promote the quality of rubber glove

in which is beneficial to the industry. Biological additives are sustainable with lower toxicity than their chemical alternatives, and the release of chemical additives end up in a landfill with further environmental leaching. The experimental method for biological cross linker from starch with sucrose reinforced with cellulose nano-fibrils (CNFs) has been studied. The outcome is positive with good performance in mechanical strength, high flexibility and barrier properties [128]. The study from Balakrishanan et al, [128] mainly focused on food packaging, but it may be applied to different fields as well. Due to, biological extract products as intermediate in manufacturing or packaging industry is a contemporary application.

Furthermore, Zhang and Sun, [129] have introduced the use of bean dreg and crab shell powder for their physio-chemical and microbiological properties in composting of any organic waste product, where the added product may accelerate the composting period based on few parameters [129]. Optimization of composting conditions like temperature, microorganism loading, enzyme loading and phytotoxicity could accelerate the composting process. The introduction of apple pomace, citric acid, element sulphur, sulphuric acid, magnesium hydrogen phosphate and calcium superphosphate showed promising results for the composability [130]. These bio-additives are able to retain the nitrogen in the soil and reduce the greenhouse gases emission during the composting period. Mechanism of nitrogen preservation is by eliminating the NH_3 volatilization during landfill or condition composting method. Therefore,

the use of bio-additives may be viable for application in rubber polymer industry for controlled bond formation and reduction in adhesiveness [11]. Besides, the bio-additive may cause reduction the usage of existing chemical such as pigment, sulphur, and the bioactive compound with potential to influence the biodegradability of the latex glove, condom, and balloon. Later, in composting, the bacteria-based enzymes and oxidants could bring about the decomposition if nitrogen and carbon present in the rubber glove [131].

There are others example of bio-based compounds like polylactic acid and starch-based cross-linker to be added in the compounding process to produce thermoset product. Thermoset or thermosetting or better known as plastics which are synthetic materials can be cross-linked by divinylbenzene and the product could not be remoulded or processed further after initial heat forming. One of the researches showed that thermosetting polymer can be produced by acrylate epoxidized soybean oil and tung oil through free radical polymerization method. This technique uses bio-based and renewable materials with inherent of biodegradability and low toxicity for polymer synthesis. The embedded crosslinking component in the tung oil is triglyceride (consists of three fatty acids chains and glycerol by an ester linkage) to induce the crosslink reaction [132]. Triglyceride is composed mainly of alpha-elaeostearic acid (cis-9, trans-11, trans-13-octadecatrienoic acid) with high unsaturation and conjugation of carbon-carbon double bond [133]. Tung oil and soybean oil are both bio-based raw materials for polymeric synthesis and has been thoroughly researched for

different polymer products, including the high-density crosslinking behaviour and the properties of the product [134]. The soybean oil-based thermoset product possesses equivalent physical properties (tough and rigid plastic formed) and is biodegradable in ambient environmental conditions.

2.5 Organic oil for rubber polymerization production

Polymerization of tung oil must be carried out at high temperatures (100 ^{o}C – 200 ^{o}C), and the physical properties could be elevated by the copolymerization of tung oil and divinylbenzene initiated by boron trifluoride diethyl etherate [133]. In polymer production, the raw materials of crude oil could be replaced by renewable materials (i.e. Tung oil, soy oil, canola oil, etc) with bio-based linker for inducing crosslinking process (i.e. polyactic acid, elaeostearic acid, etc). The processes are tested and are viable in laboratory scale [133, 135]. The production of bio-based compounds would uplift the image for green environment and zero carbon footprint. Life cycle assessment (LCA) reports shows that bio-based polymer products promote the cradle to cradle concept, while non-bio-based polymer will be cradle to grave generating huge amounts of waste. It was also mentioned that the bio-based polymer should be composted at industrial facilities for degradation under appropriate conditions [136, 137]. The typical ‘backyard’ compost pile cannot meet the requirements for the degradation of bio-based polymers. The current sustainable research on bio-degradable product still depends on several aspects for composting such as

aeration rate and mode, temperature, turning frequency, carbon nitrogen content, pH and more [138]. The carbon chains are sourced from petroleum or fossil fuels for most polymer products (i.e. plastic, rubber polymer, etc) leading to environmental persistence and non-biodegradability by microbes. Replacement of petroleum and fossil carbon to biogenic carbon could turn every product towards high biodegrading possibility [139]. However, installation cost is needed for constructing the composting facilities. Bio-based polymer technology is still under intensive research and it is not on par with petroleum-based polymer product. The future technology, economy and environmental trend would favour renewable resources and biodegradable materials [140, 141]. The bio-based crosslinker are being used currently in several companies such as Bayer, Royal Cosun, and BASF for few different types of polymeric products. Nitrile rubber can be a platform for this kind of bio-based crosslinker to produce biodegradable product where the used glove can be decomposed in atmospheric conditions. The bio-based cross linker could promote environmental friendliness of the product, and the life cycle of the product will have a lower carbon footprint. Bio-based crosslinker will assist in composting of polymer products, where the molecular and structural features will be disintegrated and transported across microbial cell membrane for assimilation. Thus, the yearly rubber glove waste from the hospital can be reduced based on the bio-based crosslinker and the rubber compound formulation.

Rubber product biodegradability under atmospheric condition has not been commercialized yet. The experimental method for degrading natural rubber with di-cumyl peroxide (DCP) with Pseudomonas sp. and Gordonia sp. is viable in atmospheric condition [142]. Polyhydroxyalkanoates (PHA) is a class of plastic which is bio-based and biodegradable. PHA blended nitrile rubber and natural rubber have shown biodegradable properties and reduction in manufacturing cost [143].

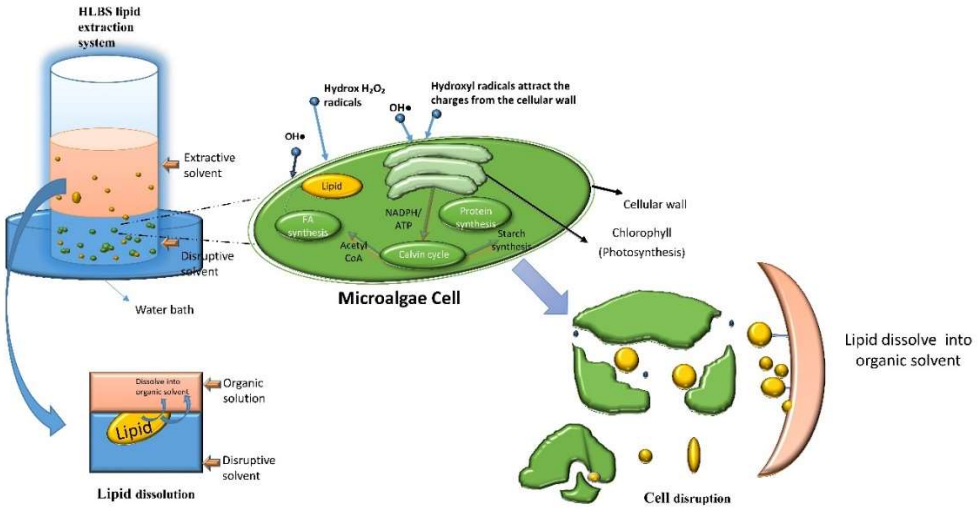
The nitrile synthetic rubber is the major demand as disposable glove especially in medical sectors, the coumpound for synthetic polymer is contain of chemicals based of linker and substances to improve the physical properties. The compounding formulation have been focusing in sulphur based of chemical for crosslinking purposes in rubber thin film. However, the sulphur based of linker is potentially caused for agglomeration during compounding and affect yellowish for the rubber film [11]. Besides, sulphur based of linker together with accelerator are trigering for dermatitis issues for skin health. Therefore, this have leading to be one of the thesis objective toward exploring emerging crosslinking system with bio-based of fatty acids to improve the stability properties of the rubber compound.

This project would be involved of upstream and downstream of the experiments included for cultivation, pre-treatment, lipid extraction techniques, transesterification methods, and potential applications for rubber compounding in which it will include of bio-additive from microalgae biomass. The potential compounds for introducing into the rubber compound formulation from the microalgae such as lipid-derived triglyceride as cross-linker and bioactive compound as pigments. Therefore, an effective extraction method has to be selected for extracting the compound in microalgae. Objective of the project is to reduce the step in the overall process especially from the pre-treatment and extraction process in the experiment. The pre-treatment for treating microalgae biomass mostly utilizing mechanical methods. Selection for combining the both pre-treatment and extraction process could be skipping a step and at the same time could be conducting for a simultaneous extraction process.

The process would be conducting in laboratory scale, as the experiment would be needed for an organic solvent phase such as chloroform, hexane, acetonitrile for assisting in the extraction process and hydrogen peroxide as the disruption phase of the solvent for propagating the cell wall breaking mechanism. The variation of the parameters will be involved of ratio from the solvent (organic solvent and disruptive solvent), concentration of disruption solvent and organic solvent, contact time, contact temperature, ultrasound frequency, ultrasound time, ferric (II) chloride concentration, biomass amount and linker amount in (phr) as the experiment main objective. These parameters will be optimized for

the highest lipid yield. The related work to the rubber compounding, where microalgae compound such as pigment as colour additive and functionalized lipid as crosslinking agents. The industry may reduce the consumption of the existing chemical additive in the manufacturing process and introduce bio-additive compound into the compound formulation.

Chapter 3. Hybrid liquid biphasic system for cell disruption and simultaneous lipid extraction from microalgae *Chlorella vulgaris CY-1* for biofuel production



This chapter covers the establishment and development of hybrid liquid biphasic system (HLBS) from the liquid biphasic system (LBS). The system of HLBS is potential for cell disruption and extraction procedure happened in a single system. Idea of developed this system to replace the famous Bligh and Dyer, or Folch methods are due to the system utilization of cell disruption solvent in the system which is promote the duration of lipid extraction process. The effect of various disruptive solvent and organic solvent parameters were evaluated to obtain the optimum types and amount of lipid from the microalgae biomass. This chapter consists of thesis-version of the manuscript published in Biotechnology for biofuels journal (Yew G. Y. et al., 2019, Biotechnology Biofuels, 12, 252).

Abstract

The extraction of lipids from microalgae requires a pretreatment to break the cell wall and subsequent extraction processes to obtain the lipids for biofuels production. The multistep operation tends to incur high costs and are energy intensive due to longer process operations. This research work applies the combination of radicals from hydrogen peroxide with an organic solvent as a chemical pretreatment method for disrupting the cell wall of microalgae and simultaneously extracting lipids from the biomass in a one-step biphasic solution. Several parameters which can affect the biphasic system were analyzed: contact time, volume of solvent, volume ratio, type of organic solvent, biomass amount and concentration of solvents, to extract the highest amount of lipids from microalgae. The results were optimized and up to 83.5% of lipid recovery yield and 94.6% of enhancement was successfully achieved. The result proven by GC-FID with percentage of error less than 1% comparison with lipid standard of triglyceride. The profound hybrid biphasic system shows great potential to radically disrupt the cell wall of microalgae and instantaneously extract lipids in a single step approach. The lipids extracted were tested to for its comparability to biodiesel performance.

Keywords: radical; lipid; microalgae; biofuel; extraction

3.1 Introduction

Microalgae consists of high lipid content and is very potential as a sustainable feedstock for commercial biofuel production. The lipid content in microalgae constitutes of more than 50% of the total composition in the biomass [50, 144]. They are listed as a third-generation of biofuel which can convert carbon dioxide into lipids and biofuel compound through transesterification process. The productivity of microalgae oil in liters per hectare of land is higher compared to palm oil and sunflower oil by more than 16-fold [145, 146]. Furthermore, microalgae can grow in abundance and emerge as a potential source for lipid extraction for biofuel generation to replace petroleum fuel [147]. Lipids are a class of organic compounds which comprises of fatty acids and glycerol in its natural form, commonly known as triglyceride. The microalgae cell contains various types of lipid, however, the lipid favored for biofuel production is neutral lipids. Phospholipids and glycolipids are polar lipids which belong to the category of structural lipids mainly use for constructing of cell wall membranes, such as being integrated with fiber and polysaccharide in the raw molecular compound in the cell wall membrane [148]. The extraction technique for lipid extraction commonly involves the use of organic solvents to dissolve lipids and further purification of the lipid content by evaporating the solvents [149]. The crude oil from microalgae could be processed to produce cosmetic products, biofuel, nutraceuticals, and synthetic polymer [50, 150-152].

The conventional solvent extraction technique using alcohol and organic solvents by Folch method or Blight and Dyer method is a common practice for lipid extraction in a laboratory scale [89, 90]. The alcohol solvent is prone to attracting polar compounds as it contains hydroxyl group molecules (OH), while organic solvent is categorized as non-polar solvent which can dissolve lipids in the solution. The molecular structure of every alcohol contains similar carbon chain with non-polar characteristic due to the carbon and hydrogen both consisting of low electronegativity difference, and OH group with polar properties attached at the tail of the chains [153, 154]. Thus, alcohol has been categorized as a polar group of solvent due to the presence of hydroxyl functional group in the chains. Typical solvent extraction is a separation process for different type of solvents in the immiscible phase, where the distribution of ions and particle may occur according to the compatibility of the types of solvent to attract or release reaction in the solution [155]. The conventional alcohol and organic solvent extraction does not create a significant cell disruption mechanism for the microalgae biomass. Pre-treatment processes such as mechanical or chemical method are needed for inducing the cell wall membrane disruption before the lipid compound may be released and readily dissolve into the organic solvent [156].

Current technologies used for mechanical pre-treatments in microalgae cell disruption includes bead milling, high-pressure homogenization, ultrasonication, microwave, pulse electric field, cavitation and thermal

disruption methods [157]. These cell disruption techniques are reviewed intensively for the industrial algae biorefinery processing. The efficiency of mechanical cell disruption methods is based on energy input and duration of the process, where most of these techniques are highly energy intensive and require costly equipment [158, 159]. On the others hand, cell wall could be disrupted by chemical treatments such as acids, alkaline, and surfactants [160]. Chemical treatments are often associated with concerns on contamination and product quality compromise which is observed for food products extraction such as protein, antioxidant, and others nutrient supplements. The use of chemical treatments provides greater contact surface for liquid cell disruption compared to mechanical methods as the mechanical pretreatments rely on the contact orientation and is mobility restraint. The introduction of peroxyl cell disruption as a chemical treatment layer for enhancing extractability of microalgae lipids can be considered through the possibility of radical formation including peroxidation for the lipids. The biofuel production performance from biomass has also been reported to improve through applying radical cell disruption methods [161].

The oxygen-oxygen bond homolyzes in hydrogen peroxide (HOOH) form a radical pair, in which the separation of the two hydroxyl radicals (OH) are in symmetrical and there are more than 10 kJ/mol of energy needed. The difference of heterolysis and homolyzes of the dissociation components from the molecules are between ions and radicals. Heterolysis is a process of cleaving or

loosening of electrons from the original bonded pair of the elements to form ions charge in the solution [162]. The transfer of ion occurs by breaking itself from a neutral molecule and subsequently made into a form of cation and anion from their parent compounds. Homolyzes is a process where the mechanism of radical forming in which the chemical bond dissociates from a molecule and form radical pairs [161, 163]. Each of the fragments obtain equal quantity of the original bonded electron. There is a possibility that applying heat or light source such as UV-ray to the bonds from the solution can trigger the homolytic and heterolytic cleavage process and generate radicals and ions [164].

In this work, a simple extractive method with radical cell disruption properties for lipids extraction purpose was performed. This hybrid method involves the cell disruption of microalgae using a chemical base liquid mixture with an organic solvent for dissolving the lipids. The mixture of two types of liquids will form a biphasic system and the organic phase containing the lipid was characterized for the lipid concentration obtained. Process parameters such as the concentration of the hydrogen peroxide disruption solvent, type of organic solvent, concentration of the organic solvent, ratio alternation, biomass variation, and volume of solvent, was optimized throughout the experiment to obtain the maximum recovery of lipid from microalgae biomass.

3.2 Materials and methods

Hydrogen peroxide (H_2O_2), hexane (C_6H_{14}), chloroform ($CHCl_3$), acetone (C_3H_6O), methanol (CH_3OH), and sodium chloride (NaCl) were purchased from R&M chemicals (Malaysia). Triglyceride lipids standard mixture were purchased from Sigma Aldrich (USA). All chemicals and solvents used were of analytical grade.

3.2.1 Microalgae biomass cultivation

Chlorella vulgaris CY-1 strain has been selected in this study due to its high lipid content and the strain was provided by the National Cheng Kung University, Taiwan. C. vulgaris CY-1 was cultivated in a laboratory scale vertical photobioreactor (PBR) as [165] using BG-11 medium containing (g/L): $NaNO_3$, 1.5; K_2HPO_4, 0.03; $MgSO_4.7H_2O$, 0.075; citric acid, 0.006; Na_2CO_3, 2.0; $CaCl_2.2H_2O$, 3.6; Ferric ammonium nitrate, 0.6, EDTA, 0.1; H_3BO_3, 2.86; $MnCl_2.4H_2O$, 1.81; $ZnSO_4.7H_2O$,0.222; $Na_2MoO_4.2H_2O$, 0.39; $CuSO_4.5H_2O$, 0.079; $Co(NO_3).6H_2O$, 0.049. The pre-culture and batch culture were both conducted in an indoor PBR system consisting of a 1 L glass vessel. The PBR was aerated with compressed air and an additional 5% of CO_2 from a tank. The aerated air is filtered through a 0.45 μm air filter before entering the PBR. The photobioreactor was illuminated by external LED light sources with a light intensity of 200 μmol/m^2/s on both sides of the vessel. The light intensity was

determined by using LI-190SA pyranometer sensor (LI-COR, Lincoln USA). The operating temperature was in room condition around 25 – 27 °C with agitation speed of 300 rpm. Adequate biomass content was cultivated for the whole experiment.

3.2.2 Determination of nitrate content and microalgae cell concentration

Nitrate content and microalgae cell concentration was measured by spectrophotometric method as mentioned in a previous research [166]. For nitrate content, the supernatant fluid after centrifugation of the microalgae samples was obtained and diluted with deionized water. The nitrate content was measured at optical density of 220 nm using UV-Vis spectrophotometer (UV-1800, Shimadzu). While for microalgae cell concentration, the microalgae samples were measured directly at an optical density 680 nm. Harvesting of microalgae was conducted when the biomass and nitrate level reached a constant value. The approximation of harvesting period was around 14 – 16 days, where the microalgae culture broth harvested was centrifuged at 7000 rpm for 5 mins. The microalgae biomass was freeze dried for 24 hr and the resulting microalgae powder was used for experimental extraction studies.

3.2.3 Hybrid liquid biphasic system with radical cell disruption properties

The hybrid liquid biphasic system (HLBS) was generated by initially adding functionalized hydrogen peroxide (functionalized by exposing hydrogen peroxide to the florescent lamp at intensity of 8 μmol $m^{-2}s^{-1}$ for initiating the radical propagation) to 20 mg of biomass, followed by the addition of organic solvent for dissolving lipid in a 1:1 volume ratio of mixture. The solution was vortexed for 10 seconds and left for 1 min to allow the contact of the liquid mixture. Two phases were formed where the upper phase was hexane and lower phase was hydrogen peroxide disruption solvent. The organic solvent phase was separated using a pipette and analyzed for lipids concentration. Lipid triglyceride concentration was optimized at every parameter by utilizing the UV-Vis spectrometer at range of 220 nm – 290 nm, in which the exact value for lipid content in hexane and chloroform are at 239 and 223.5 nm, respectively [167-169]. The final optimized lipid was tested through Perkin Elmer GC-FID. The column used was Perkin Elmer Elite-5 (30 m × 0.32 mm × id 0.25 μm) with helium 1.0 mL/min, column oven temperature held at 35°C for 3 mins, increasing to 200°C with increment of 20°C/min. The split ratio was 15:1. The concentration of organic solvent 20% pure of the organic solvent, by diluting through acetone formed a homogeneous phase of solvent. Acetone is one of the stable with oxidant solvent and mixed well with chloroform and hexane (ECHA, 2019). The operating condition as shown in **Table 3-1** with initial condition and variables.

Table 3-1: Operating parameter and conditions

No	Operating parameter	Initial condition	Variables	Unit
1	Concentration of hydrogen peroxide	5	5, 10, 15, 20, 25, 30	%w/w
2	Type of solvents and concentration	Hexane, 20	Hexane: 20, 40, 60, 80, ~85(Max) Chloroform: 20, 40, 60, 80, ~99.5(Max)	%w/w
3	Contact time	1 min	1, 2, 3, 4	min
4	Biomass amounts	20	20, 30, 40, 50	mg
5	Ratio of solvents - Cell disruption solvent (hydrogen peroxide) : Organic solvent (hexane)	1:1	1:1, 1:2, 1:3, 2:1, 2:3, 3:1, 3:2	-
6	Volume - Hydrogen Peroxide (X), Organic Solvent (Y)	X : 1, Y : 3	Hydrogen Peroxide (X): 1, 2, 3, 4 Organic Solvent (Y): 3, 4, 5, 6	mL

3.2.4 Total lipid analysis

Total lipid content in the microalgae biomass was determined using the following methods [89, 170]. Approximately 20 mg (± 0.3 mg) of microalgae biomass powder was filled into a 10 mL centrifuge tube. 3 mL of the solvent mixture, chloroform: methanol (2:1, v/v) was added. The contact duration for microalgae biomass in the solution was set at 30 mins to allow the biomass to settle down and particulate in the solution. The supernatant lipid mixture was extracted using micropipette and transferred to a separate tube. The solution was heated 60°C for 1 hr, then washed with 0.9% NaCl solution by 20% volume of the solution mixture. After vortexed, the mixture and the solution will form two phases, where the upper phase will be siphoned out and the lower phase containing lipids was dried by evaporation in a fume hood at room temperature condition for 3 hrs [171, 172]. The total weight of lipid extract remaining after evaporation was measured.

3.2.5 Determination of recovery yield and enhancement value

The recovery yield (R, %) of lipids from the total lipid content was represented by Eqn 1 below:

$$\text{Recovery yield, R (\%)} = \frac{\text{Total lipid recovered in organic solvent phase}}{\text{Total lipid content in microalgae biomass}} \times 100\% \quad (3\text{-}1)$$

The comparison percentage of using organic solvent biphasic compared to using water (without cell disruption solvent) is known as the enhancement value (E, %). For the non-disruptive solvent extraction, the microalgae biomass was dissolved in distilled water in room temperature followed by the addition of organic solvent. The contact time duration was set as 1 min.

$$\text{Enhancement, E}\ (\%) = \frac{A_i - H_{ref}}{A_i} \times 100\% \quad (3\text{-}2)$$

Where A_i stands for optimized concentration of lipids, and H_{ref} stands for H_2O with organic solvent (biphasic system without cell disrupt properties). The results were analyzed for three repetitive individual samples.

3.2.6 Chemical reaction chains of radical formation

The potential of using radicals generated by the Fenton reaction to promote cell disruption for microalgae was experimentally tested [161]. Hydrogen peroxide was used without introducing Ferric ion to initiate the radical in the presence of conventional room fluorescent lamp condition. The reaction ID R3 – R4 is the lumped reaction with rate constant k_d and k_{Lp} respectively, as shown in **Table 3-2**.

In **Table 3-2**, the model parameters for estimating OH* radical concentration were shown. The lipid yield coefficient $Y_{L/X}$ (mg $_{lip}$/ mg $_{biomass}$) mentioned in [173] was used to anticipate the capability of oxidizing organic compounds in the solution, while the yield coefficient $Y_{OH/X}$ depicts the amount of OH* radical

needed for rupturing cell wall of microalgae. k_d is the rate constant for Eqn (3) and k_{Lp} is the rate constant for Eqn (4) as well as shown in **Table 3-2**.

Table 3-2: Model parameter for estimating the time of hydroxyl radical formation.

Symbol	Value	Units	References
k_d	5.00×10^8	L mol^{-1} s^{-1}	[174]
k_{Lp}	5.44×10^7	L mol^{-1} s^{-1}	Concas et al., 2015)
$Y_{L/X}$	0.596	-	Experimental value
$Y_{OH/X}$	2.27×10^4	-	Concas et al., 2015)

The OH* radical produced by hydrogen peroxide may react with several compounds released from microalgae. Thus, the cell wall may cause degradation and consequent disruption on the protective cell layer. These reactions are known as a lumped reaction scheme to describe the overall disruption process [161]. The key radical formation steps as reported in **Table 3-3**.

Cell disrupted scheme

$Y_{OH/X}$ OH● + X → $Y_{L/X}$LH + DX (rate constant = k_d) (3-3)

OH● + LH → L● + H_2O (rate constant = k_{Lp}) (3-4)

Where

$Y_{OH/X}$ is the OH* needed to disrupt 1 mol of biomass

$Y_{L/X}$ is the coefficient for amount (mol) of lipid released when 1 mole of biomass cell has been disrupted (amount of lipid peroxidation)

DX is the disrupted cell

LH is the unsaturated lipid

X is the microalgae cells (biomass)

Table 3-3: Rate constant and reaction equation.

Reaction ID	Reaction symbol and equation	K-Value	Units	Reference
R5	H_2O_2 → 2 OH* (presence of UV)	10^9 - 10^{10}	L mol^{-1} s^{-1}	[175]
R6	OH* + H_2O_2 → H_2O + HO_2*	3.2 x 10^7	L mol^{-1} s^{-1}	[176]
R7	L* + O_2 → LO_2*	3.0 – 4.6 x 10^8	L mol^{-1} s^{-1}	[161]

R8	LO_2^* + LH → LO_2H + L*	1.9 x 10	L mol^{-1} s^{-1}
R9	L* + L* → NRS_1	6.6 x 10^4	L mol^{-1} s^{-1}
R10	L* + LO_2^* → NRS_2	1.0 x 10^5	L mol^{-1} s^{-1}
R11	LO_2^* + LO_2^* → NRS_3	6.6 x 10^4	L mol^{-1} s^{-1}

The radical reaction chain and peroxidation of lipid molecules were performed according to the initial, propagation and termination steps. The rate constants for the reaction steps are found in **Table 3-3** and the reaction chain was described for the key reactions in the cell disruption from the interaction of radical species and lipid molecules.

Initiation (Homolytic Reaction)

$H_2O_2 \rightarrow 2OH\bullet$ (3-5)

Propagation

$H_2O_2 + OH\bullet \rightarrow HO_2\bullet + H_2O$ (3-6)

$L\bullet + O_2 \rightarrow LOO\bullet$ (lipid peroxyl radical) (3-7)

$LOO\bullet + LH \rightarrow LOOH + L\bullet$ (3-8)

Termination

$L\bullet + L\bullet \rightarrow NRS_1$ (3-9)

$LOO\bullet + L\bullet \rightarrow NRS_2$ (3-10)

$LO_2\bullet + LO_2\bullet \rightarrow NRS_3$ (3-11)

The hydroxyl radical OH* is highly reactive of free radical with short life span, therefore, the steady state of the concentration value for hydroxyl radical could be ignored. The concentration of the OH radical could be integrated through Eqn (12). Besides, the initial formation of hydroxyl could be described from Eqn (13) for the evolution of time and the effect of concentration of OH radical from the UV radiation from florescent lamp in normal room condition with intensity 8 μmol $m^{-2}s^{-1}$.

$$[OH*] = \frac{k_5[H_2O_2]}{k_5[H_2O_2] + y_{OH/X}k_d[x] + k_{Lp}[LH]} \quad (3\text{-}12)$$

$$\frac{1}{2}\frac{d[H_2O_2]}{dt} = -k_4[OH*] \quad (3\text{-}13)$$

$$\frac{d[H_2O_2]}{dt} = -k_5[OH*][H_2O_2] \quad (3\text{-}14)$$

The formation of hydroxyl radical could be estimated from differentiating equation from Eqn (14) through ordinary differential equation (ODE) from Matlab2018a to express the radical formation time taken and concentration. Initial condition [x] = 0.8229 mol L^{-1} (experimental value for 20 mg of biomass

for conversion), $[H_2O_2]$ = 0.03837 mol L^{-1}, [LH] = 0.03837 mol L^{-1} (assumption value for every H_2O_2 reacted with lipid and formed lipid hydroxide).

3.3 Result and discussion

3.3.1 Effect of concentration of hydrogen peroxide toward lipid extraction

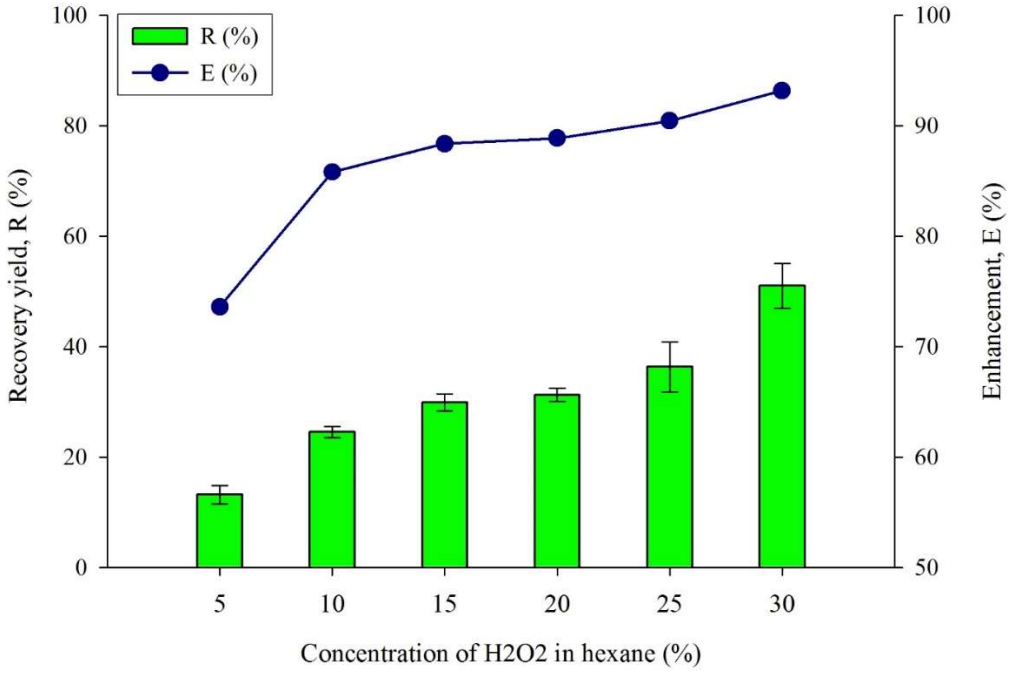


Figure 3-8: Concentration of Peroxide with hexane effect for the extract lipid productivity for recovery yield and enhancement comparison toward water-organic solvent biphasic system from C. vulgaris CY-1. Other operating condition fix at 3ml of 85% concentration of organic solvent (hexane), contact time at 1 min, biomass 20 mg (± 1 mg), and at room temperature 25°C.

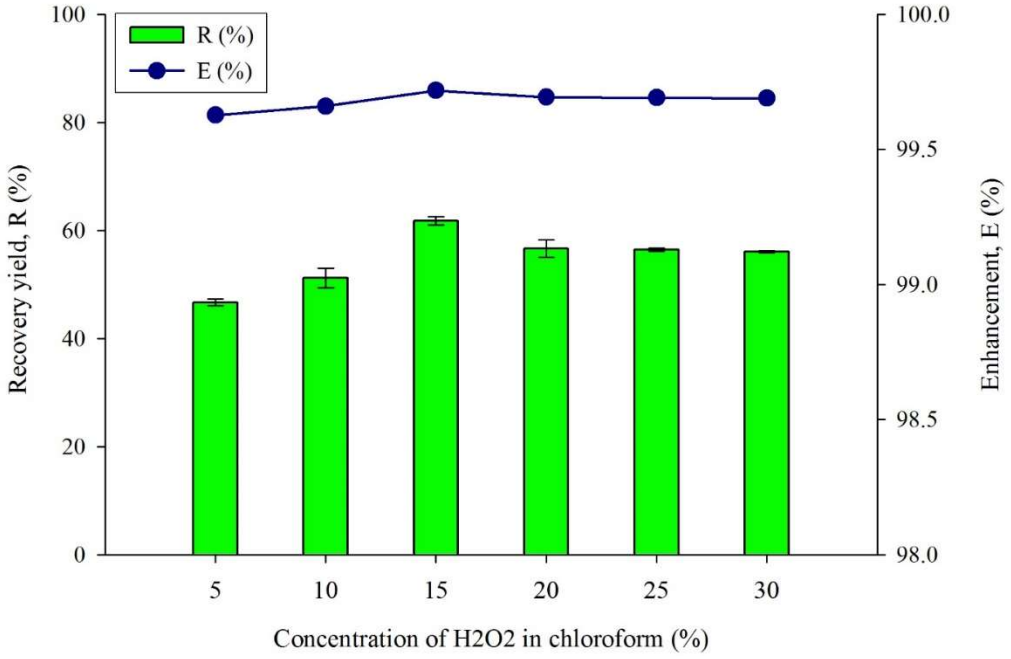


Figure 3-9: Concentration of peroxide with chloroform effect for the extract lipid productivity for recovery yield and enhancement comparison toward water-organic solvent biphasic system from C. vulgaris CY-1. Other operating condition fix at 3ml of 85% concentration of organic solvent (chloroform), contact time at 1 min, biomass 20 mg (± 1 mg), and at room temperature 25°C.

The concentration of hydrogen peroxide in the hybrid liquid biphasic system (HLBS) will directly affect the yield of lipids. Formation of hydroxyl or peroxyl is through homolytic reaction, where the bond breaking from the molecules causes abnormal valency that causes the radicals to seek for electrons to substitute the valency [177]. The radical molecules may attract the electron from

the cell wall surface of the microalgae biomass to form new bonds out of the cellular wall. The rapid radical formation through Fenton reaction is potential in causing disruption to the cell wall membrane of microalgae which leads to the release of nutrient compounds including lipids, making these compounds dissolve in the organic solvent phase [161]. The current method is suitable for extracting compounds in industrial applications and will not pose concerns of the radical degrading the extracted compound and causing peroxidation for lipid. This will avoid the lipid peroxidation chain reactions that leads to the formation of highly reactive electrophilic aldehydes, and hinder its negative effect for human internal organs [178, 179]. The radical formation is supported by florescent UV in open space condition with intensity of 8 μmol $m^{-2}s^{-1}$ without any external equipment for further enhancing the homolytic reaction.

Figure 3-1 shows the effect of hydrogen peroxide concentration on the lipid recovery yield and enhancement of the process. The highest recovery of lipid was observed at 30% concentration of hydrogen peroxide solution which yielded 50.9% lipid. The results show an increasing trend from the lowest hydrogen peroxide concentration, from 5% up to 30%. The maximum purity of hydrogen peroxide used in this work was limited to 30%, while for the purity of hydrogen peroxide, values higher than 30% would result in a highly oxidizing agent with strong oxidative properties that is usually used in the aerospace propulsive system as a hypergolic propellant thruster, also known as propulsion grade of reagent [180]. Therefore, the maximum concentration of the hydrogen

peroxide does not exceed 30% in this experiment. Hydrogen peroxide is a polar solvent that attracts polar compound, while organic solvent tends to dissolve neutral or non-polar lipids [181]. Polar lipid consisting of glycolipid and phospholipid as the major components will affect the biofuel properties and conversion rate [182].

Chloroform compared with hexane as the organic solvent, have higher density at 1.49 g/cm^3 compared to the density of hexane (0.65 g/cm^3) and hydrogen peroxide (1.45 g/cm^3). Thus, chloroform will settle to the bottom of the solution along with the biomass. Additional steps such as centrifugation were needed to fully separate the biomass and the organic solvent. Moreover, chloroform will not clearly separate the polar lipid into the surface of the solution, where it dissolves both polar lipid and non-polar lipid into the solvent. The HCl molecules may also convert the chloroform into carbon dioxide which will bring negative impacts to the atmosphere. **Figure 3-2** shows the lipid recovery and enhancement using chloroform as an organic solvent with varying concentration of radical solvent for lipid extraction. The highest enhancement (99.7%) and recovery yield (61.7%) for lipid was found at 15% H_2O_2 in chloroform. Comparing similar concentrations at 30%, the use of chloroform combination showed about 5% higher in recovery yield compared to the hexane combination.

The hydrogen peroxide concentration in chloroform at 5% have lowest recovery yield of 46.65% and enhancement of 99.63%, while the highest lipid

recovery yield and enhancement is 61.8% and 99.7%, respectively at 15% concentration of hydrogen peroxide in chloroform. The overall chloroform mixture results for recovery yield is higher than hexane as chloroform dissolves both polar and non-polar lipids in the solvent, where it will add salt solution in the solvent for washing and purification purposes [170]. The suitable type of lipid-based biofuel conversion utilizes neutral lipid which can perform better during the conversion into biofuel. Chloroform is tautomeric in-equilibrium where there is common relocation of the proton in the molecules. During light beam lighting on electrons, the tautomeric effect causes absence of energy returning electron back to the ground state, therefore no energy dissipation may create unstable measurements in the UV-vis for chloroform [183]. Due to the characteristic of chloroform which dissolves both the polar and non-polar lipids, these lipids are not favorable to be used as biofuels because polar lipid from phosphorous and glycolipid affects the combustion and causes environmental issues. Furthermore, tautomeric and aprotic effect not contribute to any advantages for the stability of the biofuel however, may disturb the spectroscopic analysis performance. Therefore, hexane was selected as the better solvent of the two for lipid extraction.

3.3.2 Effect of solvent concentrations

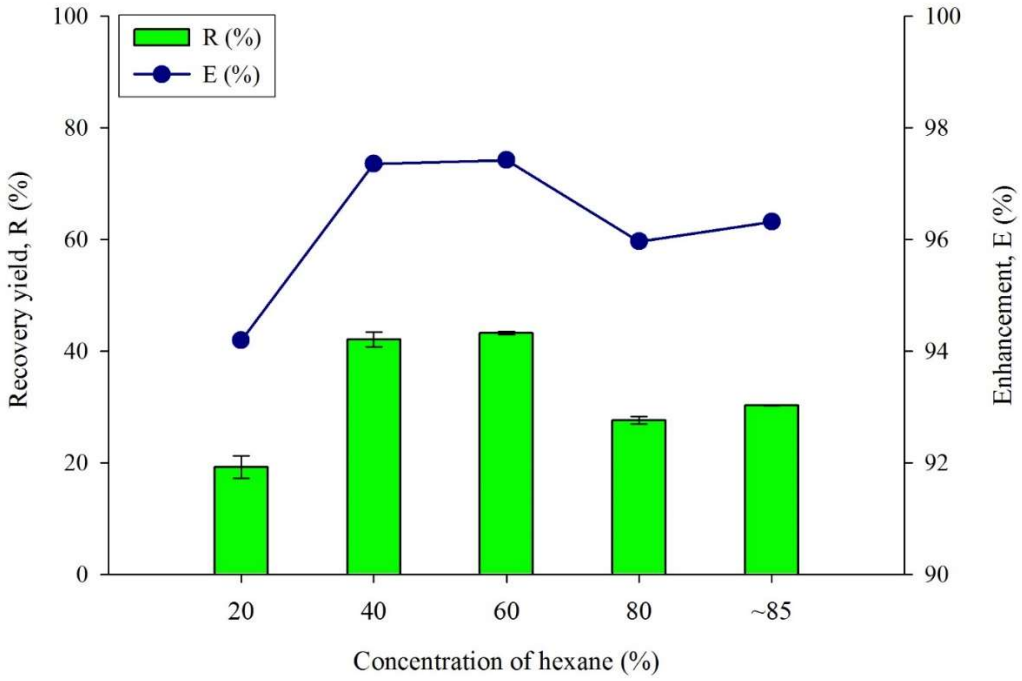


Figure 3-10 Concentration of organic solvent (hexane) effect for the extract lipid productivity for recovery yield and enhancement comparison toward water-organic solvent biphasic system from C. vulgaris CY-1. Other operating condition fix at 3ml of 30% concentration of hydrogen peroxide, contact time at 1 min, biomass 20 mg (± 1 mg), and at room temperature 25ºC.

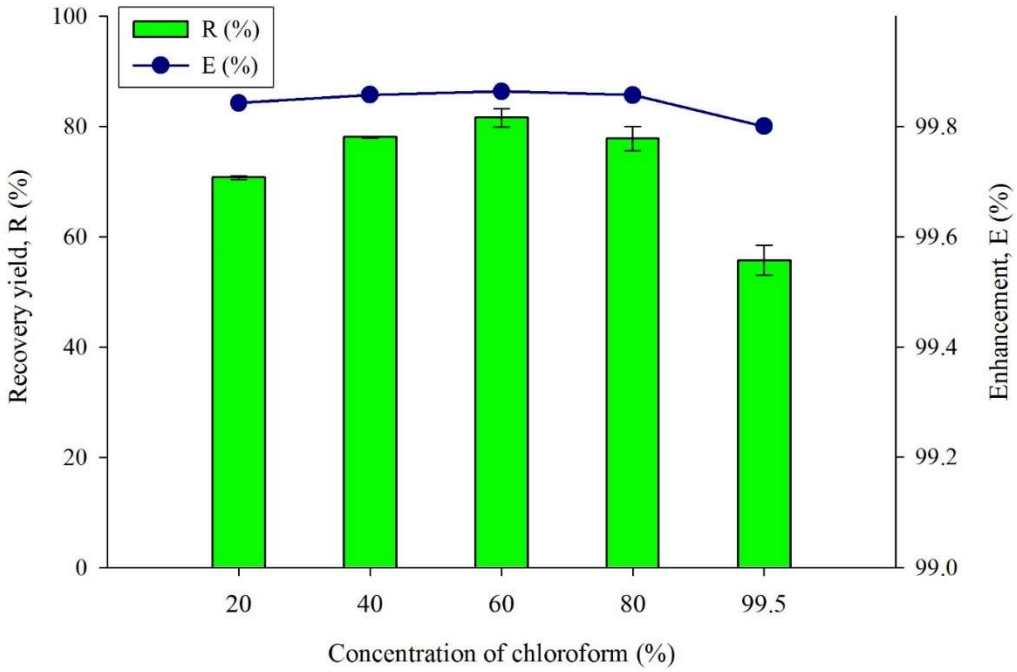


Figure 3-11: Concentration of organic solvent (chloroform) effect for the extract lipid productivity for recovery yield and enhancement comparison toward water-organic solvent biphasic system from C. vulgaris CY-1. Other operating condition fix at 3ml of 30% concentration of hydrogen peroxide, contact time at 1 min, biomass 20 mg (± 1 mg), and at room temperature 25°C.

Organic solvents play a vital role for lipid extraction due to its capability of dissolving lipids. The concentration for organic solvents in the HLBS has been altered to observe the effect towards recovery yield and enhancement. The concentration of organic solvent was investigated in the range of 20 - 85%. From **Figure 3-3**, the optimum concentration for hexane is 60% for R and E value

which is 43.2% and 97.42% respectively. The dilution of hexane is done with acetone which is nonreactive, non-metabolized, low viscosity and able to mixed well with most organic solvent [184]. The least recovered yield of lipid is at 20% concentration of hexane at 19.17%. The highest purity 85% of hexane showed reduced recovery yield at 30.2% and the enhancement at 96.3% compare to 60% concentration of hexane dilution with 40% of acetone. The highest recovery yield and enhancement for hexane dilution is at 60% where 97.4% of enhancement and 43.2% of recovery yield was achieved. Acetone can dissolve in polar and non-polar solvents, it consists of non-polar methyl groups and polar carbonyl (C=O) groups that allows it to dissolve in most polar and non-polar solvent types. Acetone is also an aprotic solvent with polar features and is prone to attract polar compound such as phospholipid and glycolipid [185]. Hence, acetone was selected as the suitable choice for its capability to dissolve in most types of non-polar solvent including chloroform and hexane without forming two different phases.

The concentration varying for chloroform for extracting lipid was shown in **Figure 3-4**, the optimum concentration for chloroform is at 60% and the enhancement is at 99.8% while recovery yield is 81.5%. The pure chloroform shown 99.8% enhancement and 55.7% recovery yield which is significantly lower for by 25.8% compare to 60% concentration of chloroform, this indicates that too high chloroform concentration will greatly reduce the lipid recovery

yield. The optimum result for dilution of organic solvent for lipid extraction was selected to be 60% dilution of chloroform solvent with 40% of acetone.

Comparing with hexane dilution parameter, both the enhancement and recovery yield of using chloroform are higher. However, chloroform and acetone dilution for optimizing the lipid content is unstable due to the aprotic and tautomeric effect. According to the eluotropic series, taking silica as stationary medium indicates that hexane is a non-polar solvent with low detecting value in UV-Vis compared to chloroform [186, 187]. This means that the minimum detecting value for hexane is lower compare to most organic solvent including chloroform, acetone and toluene. Moreover, hexane is a more favorable choice for solvent as it has higher stability and is more accurate for the parameter determination. It is reported that there are more monounsaturated fatty acids than polyunsaturated fatty acids in extraction processes using hexane derived solvents [188]. The monounsaturated fatty acids are preferred as the quality components for biodiesel properties in terms of low temperature fluidity and oxidative stability [189]. Therefore, hexane of 60% is been selected as the choice of organic solvent with 43.2% of lipid recovered yield.

3.3.3 Effect of different ratio (H_2O_2: Hexane)

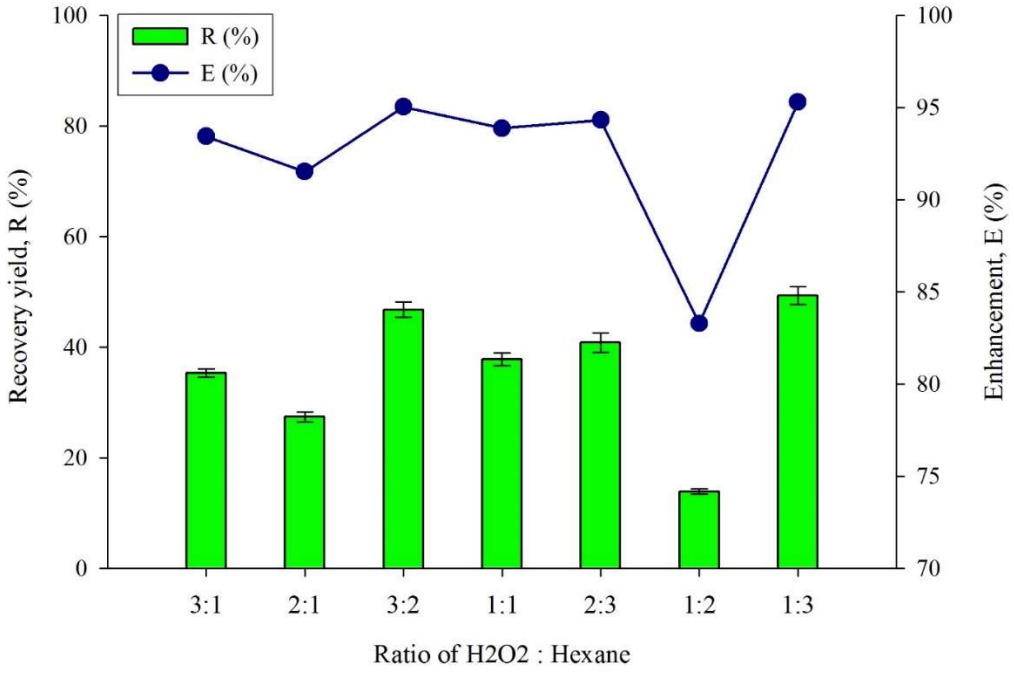


Figure 3-12: Ratio of (H_2O_2: Hexane) effect for the extract lipid productivity for recovery yield and enhancement comparison toward water-organic solvent biphasic system from C. vulgaris CY-1. Other operating condition fix at 30% concentration of hydrogen peroxide, pure analytical grade of organic solvent (hexane), contact time at 1 min, biomass 20 mg (± 1 mg), and at room temperature 25°C.

Due to tautomeric effect and aprotic solvent distraction, pure hexane is chosen for optimizing this parameter for enhancing the lipid extraction for HLBS system. In **Figure 3-5,** cell disruption and organic solvent extraction ratio in the

system was altered for the lipid productivity of microalgae biomass. In the HLBS, the bottom aqueous layer consists of solvent for cell disruption of the biomass and the top organic layer contains hexane as the solvent for dissolving lipids. The ratio for both solvents is studied to evaluate the effect for alternating the ratio of the solutions on the enhancement and recovery rate. The optimum ratio for lipid extraction is 1:3 where the E and R value are at 95.3% and 49.3% respectively. By increasing the cell disruption layer phase, the recovery yield does not increase proportionally, as the recovery yield for ratio 1:1, 2:1 and 3:1 showed 37.8%, 27.4% and 35.3%, respectively. Whereas by adjusting the ratio for cell disruption and organic phase layer will lead to a significant increase in recovery by about 3.5-fold when compared between the ratio 1:2 and 1:3. For a constant H_2O_2 amount, adding more organic solvent will assist in dissolving more lipid from the biomass.

H_2O_2 ratio in the default time of contact within 1 min accumulated more lipid from biomass compare to 1:2 (H_2O_2 : Hexane). This may be due to more peroxyl and hydroxyl radical from the H_2O_2 assisting in the cell disruption once the H_2O_2 ratio has increased. The introduction of H_2O_2 assures the presence of peroxyl and hydroxyl radical in the solvent to cause disruption of the cell membrane and allow lipid molecules to dissolve into the organic solvent. The contact time represents the cycle of radical propagation frequency of the biomass in HLBS system, which plays a major role for preventing further disruption of the lipid compounds [190]. This parameter evaluation has indicated that the

higher organic solvent with a same disruptive solvent amount will result in higher recovery of lipid as there will be more available volume for the lipids to dissolve into the system.

3.3.4 Effect of volume differences

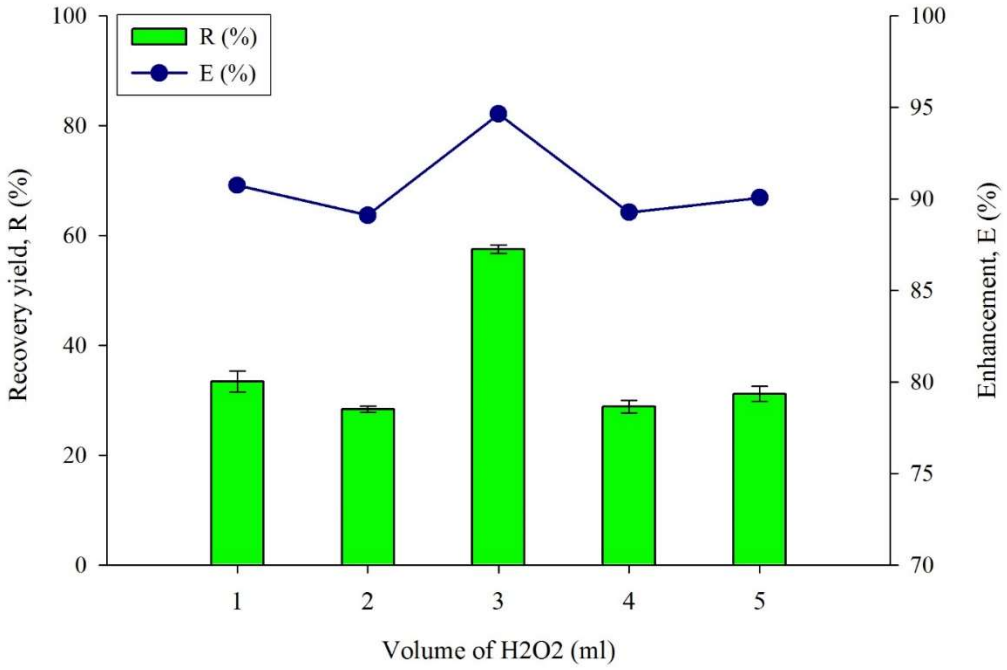


Figure 3-13: Volume of hydrogen peroxide (H_2O_2) effect for the extract lipid productivity for recovery yield and enhancement comparison toward water-organic solvent biphasic system from C. vulgaris CY-1. Other operating condition fix at 30% concentration of hydrogen peroxide, pure analytical grade of organic solvent 85% (hexane) at volume 3ml, contact time at 1 min, biomass 20 mg (± 1 mg), and at room temperature 25°C.

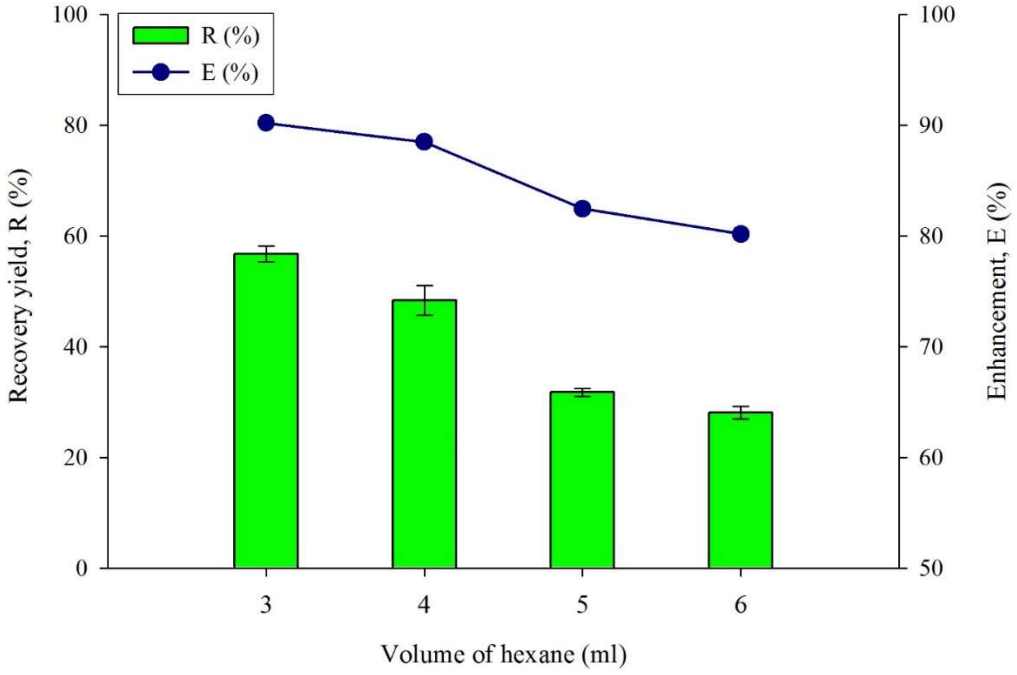


Figure 3-14: Volume of organic solvent (hexane) effect for the extract lipid productivity for recovery yield and enhancement comparison toward water-organic solvent biphasic system from C. vulgaris CY-1. Other operating condition fix at 30% concentration of hydrogen peroxide at volume 3ml, pure analytical grade of organic solvent 85% (hexane), contact time at 1 min, biomass 20 mg (± 1 mg), and at room temperature 25°C

The difference in volume for the hydrogen peroxide cell disruption layer was studied and its effect on the lipid recovery yield and enhancement is shown in **Figure 3-6**. The highest extracted lipid is with 3ml of volume, obtaining 94.6% enhancement and 57.5% of recovery yield of lipid. The addition of more

hydrogen peroxide volume into the HLBS system may tend to induce more hydroxyl and peroxyl radical which should increase the cell disruption rate [191], however, the results shows an inconsistent trend. External factors may have induced the radicals in the cell disruption solvent phase, causing the radical disruption cycle to be affected by an increase in the volume. The least recovery and enhancement is in 2ml of hydrogen peroxide, which is at 28.37% and 89.1% respectively. The increasing cell disruption layer phase volume in general does not contribute to a significant recovery yield of lipid. This is due to the cell membrane properties which needs more radical propagation cycles to disrupt the cell membrane of microalgae. The optimum volume amount is 3ml as it achieved the highest yield in this experimental parameter.

The volume difference of organic solvent in the HLBS system was also studied and the results of lipid recovery and enhancement are shown in **Figure 3-7**. The highest extracted lipid amount is at 3ml of hexane and 1 ml of hydrogen peroxide in the HLBS system, achieving an enhancement of 90.2% and recovery yield of 56.7%. A decreasing trend was observed by adding more volume of organic solvent (hexane) into the HLBS system. Hexane has a delta value of 14.9 δ for total and partial solubility value after propane in the non-polar fluids categories, indicating the solubility value for oil and lipid [192]. Thus, by adding more solvents of the same solubility into the HLBS system will not enhance the extraction capability but may dilute the solution for analysis of lipid compound. The enhancement in Figure 3-7 shows a decrement by more than 10% as more

hexane were added in the system. The optimum volume for HLBS is 3ml in this experimental parameter.

3.3.5 Effect of contact time

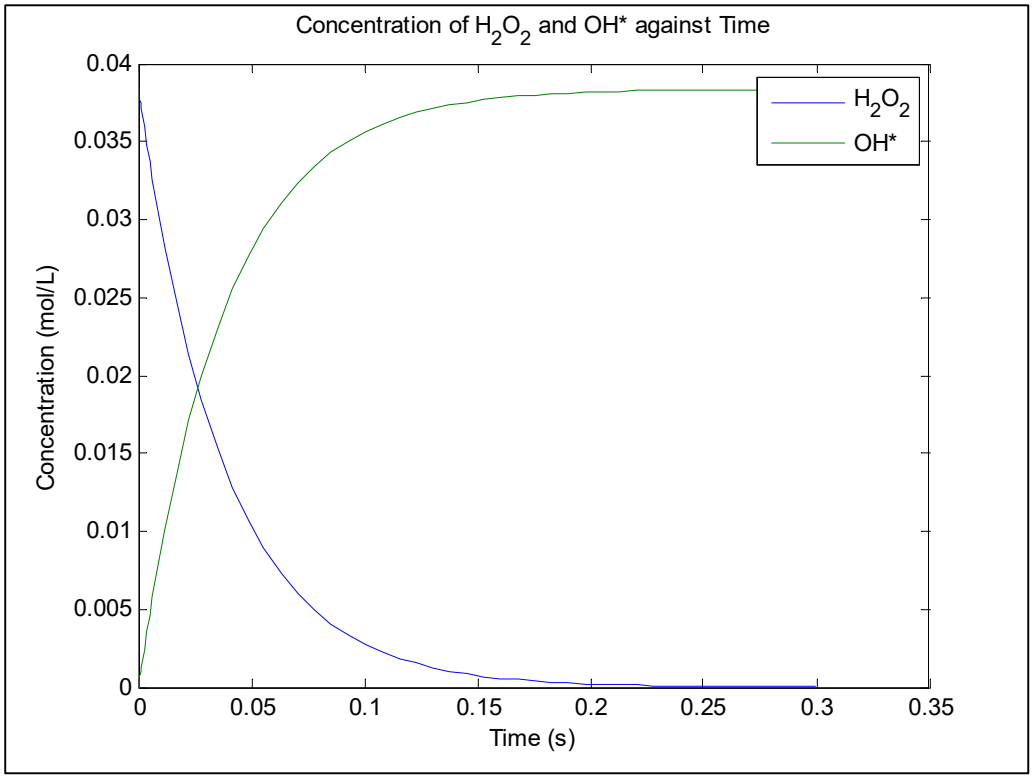


Figure 3-8: The graph of concentration for H_2O_2 and hydroxyl radical formation against time simulate by MATLAB 2018a. The concentration of hydrogen peroxide 30% in 2mL, in room temperature condition 25°C, with the presence of florescent lamp at intensity 8 μmol $m^{-2}s^{-1}$.

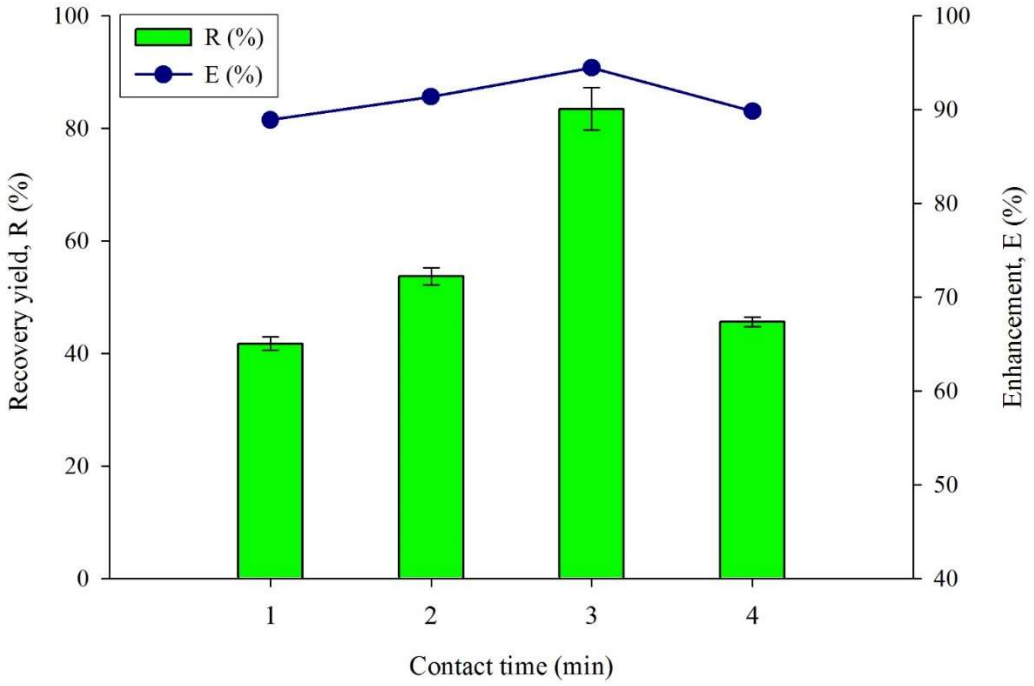


Figure 3-9: Time of contact effect for the extract lipid productivity for recovery yield and enhancement comparison toward water-organic solvent biphasic system from C. vulgaris CY-1. Other operating condition fix at 30% concentration of hydrogen peroxide, pure analytical grade of organic solvent 85% (hexane), biomass 20 mg (± 3 mg), and at room temperature 25°C.

The concentration of hydrogen peroxide and hydroxyl radical formation against time was simulated by using the mathematical modelling, where the time of hydroxyl radical formation was completed within 0.35 seconds. The estimated concentration was at 0.035 mol/L for the hydroxyl radical (**Figure 3-8**). The optimized time may enhance the lipid extraction into the organic solvent. This

parameter may affect the degradation rate of the cell membrane with the initial reasoning that longer contact time of the cell disruption phase layer could improve the productivity of lipid extraction. The highest lipid recovery yield and enhancement is with 3 mins contact time at 83.5% and 94.4% respectively (**Figure 3-9**). The least enhancement and recover yield are found within 1 min of contact time at 88.9% and 41.7% respectively. According to the study by Concas et al. (2015), the peak value of time contact exceeding 3 mins will reduce lipid production and our results are in accordance with their work [161]. The recovery yield and enhancement of lipid extraction reached the peak at 3 mins and started fall at 4 mins. The time of contact may increase the cell disruption and lipid will be released more efficiently in the organic solvent, resulting in more lipids accumulation in the solvent. The radical cell disruption method has also been reported to enhance the quality of biodiesel, as the characteristic of biodiesel produced with radical disruption method are more stable with reduction of undesired polyunsaturated fatty acid, such as linolenic acids (C18:3), from the lipid molecular structure [193]. Furthermore, the lipids produced may be used as industrial intermediate products for polymer crosslinking products, since the lipid compounds extracted have been radically treated and retain a partially functionalized form of the unsaturated chains from the hydrocarbon molecules [11]. The contact time of 3 mins showed the best R and E and hence it was selected as the optimum value for this experimental parameter.

3.3.6 Effect of biomass amount with solvent ratio and GC-FID lipid profile

Table 3-4: Comparison of lipid profile using GC-FID.

Peak	HLBS (mins)	Pure triglyceride mixture (mins)	Area of graph for HLBS	Percentage of error (%)
1	1.663	1.664	42.94	0.06
2	1.859	1.861	28.62	0.11
3	2.097	2.1	23.4	0.14
4	2.411	2.416	5.04	0.21

Table 3-5: The effect of biomass with different ratio for the extraction of lipid for recovery yield and enhancement comparison toward water-organic solvent biphasic system from C. vulgaris CY-1. Other operating condition fix at 30% concentration of hydrogen peroxide, pure analytical grade of organic solvent 85% (hexane), and at room temperature 25°C.

Ratio	**1:3**		**2:3**		**3:4**		**3:3**	
Amount (mg)	E%	R%	E%	R%	E%	R%	E%	R%
20	93.8	37.4	89.4	21.9	87.6	18.7	88.7	20.7
30	93.0	33.2	93.1	33.6	88.7	20.6	89.7	22.5
40	93.5	35.5	95.7	53.9	93.4	35.5	91.3	26.8
50	95.8	54.6	95.8	55.1	93.6	36.4	94.8	45.4

The retention time for the lipid profile comparison in **Table 3-4** has shown that the percentage error for peak 1, 2, 3, and 4 are less than 1%. The similarity of the lipid profile through GC-FID results for these 4 peak components in Figure 3-10 is apparent and observed with the lipid extraction in the optimized HLBS solution mixture. The results from GC-FID indicates that the lipids extracted are comparable to that of commercial triglyceride and the HLBS process used is very potential in recovering the lipids efficiently. In chromatography, the detect signal for the analyte is directly proportional to the concentration of the component in the solution against functional of time (Pierce and Synovec, 2012). These components of fatty acids are the potential tail which are attached to the glycerol to form triglycerides in lipids.

The effect of biomass amount correlates with the ratio of solvent in HLBS for improving the lipid productivity. Increase in biomass amount will increase the lipid output from the final extraction process, but it will not directly

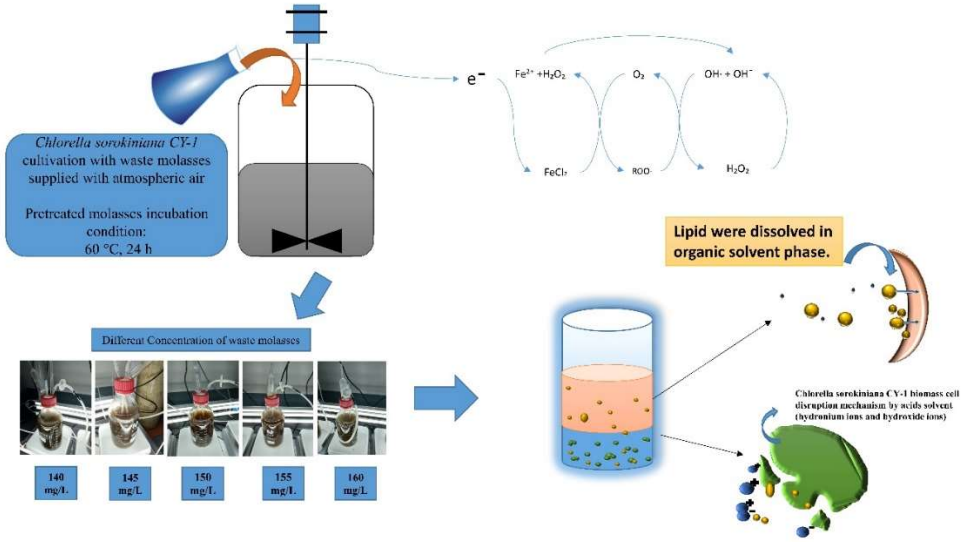
improve the lipid recovery yield and enhancement value (**Table 3-5**). The optimum ratio for 20 mg of biomass was found at 1:3 (H_2O_2: Hexane solvent ratio), where the values E and R achieved 93.8% and 37.4% respectively. In 30 mg of biomass, the 2:3 solvent ratio is best where the E and R values achieved 93.1% and 33.6% respectively. The value for 40 mg of biomass achieved higher productivity at 2:3 ratios, where the recovery is 53.9% and enhancement is 95.7%. While for 50 mg of biomass, 2:3 was the optimum ratio for extraction as the R and E values reported were the highest. The addition of more biomass does not assist in lipid recovery, but it demonstrates a relationship between varying biomass weight with ratio which will affect the lipid recovery and enhancement value. This is due to more contact surface area for cell disruption when more biomass is added within the same amount of solvent. Ratio of 1:3 showed higher lipid recovery yield at 54.6% with 50 mg of biomass and enhancement value of 95.8%. Besides, for ratio 2:3 the highest lipid recovery and enhancement is at 55.1% and 95.8%, respectively, which showed improvements of 1.2% for R and 0.09% for E value compare to 40 mg with the same ratio. The ratio for 3:3 have the highest E and R value at 50 mg which are 94.9% and 45.4% respectively, while the value is higher than 3:4 ratio with the same amount of biomass at 50 mg with an increment of 1.26% in E and 9% in R value. Ratio 2:3 (H_2O_2 : Hexane) is the most versatile ratio to various biomass amount in this experimental parameter. It is deduced that a suitable ratio of the solvents will

assist in optimizing the extraction through reducing chemical solvent consumption as well as lowering the material costs needed.

3.4 Conclusion

The hybrid liquid biphasic system (HLBS) in a single solution with two different phases in the system is viable for efficient extraction of lipid from microalgae. The combination of cell disruption pre-treatment along with simultaneous extraction process will contribute to cost and energy saving by reducing the multistep procedure to a single step extraction technique. Furthermore, this HLBS method could be applied in producing biofuel with enhanced properties through treatment in the hybrid system. Both the extraction and cell disruption will be formed in two immiscible phases for ease of separation which is sustainable as there is potential to recycle of the solvents in large scale applications. More than 80% of lipids were successfully recovered from microalgae biomass and the extraction enhancement compare to water biphasic system achieved was higher than 90%. This hybrid biphasic system is potential to be applied in various types of lipid extraction involving biomass with cell wall membrane, especially for commercial biofuel production which requires biofuels of enhanced quality performance.

Chapter 4. A Novel Lipids Recovery Strategy for Biofuels Generation on Microalgae *Chlorella* Cultivation with Waste Molasses



This chapter covers the utilization of waste molasses from sugar mills as alternative source for the inorganic medium for microalgae cultivation and tested of HLBS for lipid extraction and transesterification in a single system. The potential of the acids based of the hybrid liquid biphasic system without using of catalyst for direct conversion of biofuel from the microalgae lipid compounds. The effect of the types of acids for the properties of cell disruption as well as free the fatty acids chain from the glycerol and dissolve in the organic solvents phase in the system have been evaluated. This chapter consist of a thesis version of the manuscript published in Journal of Water Process Engineering (Yew G. Y. et al., 2020, Journal of Water Process Engineering, 38, 101665).

Abstract

This study demonstrated a novel approach of lipids extraction with simultaneous biofuels conversion on microalgae *Chlorella sorokiniana CY-1* cultivation using waste molasses as culture medium. The lipid extraction process was based on a hybrid liquid biphasic system (HLBS) which comprises of disruptive and extractive solvents in a single system. The microalgae cultivation with waste molasses showed a reduction in the chemical oxygen demand (COD), total suspended solid (TSS) and nitrate content on the waste medium (61.48%, 63.94% and 63.79%, respectively). Additionally, a prompt lipids extraction with a recovery of 92.84% and a cell disruption enhancement of 8.3-fold in the organic solvent phase was attained. The acid-treated *C. sorokiniana CY-1* biomass showed a composition of carbon at 61.3%, oxygen at 33.2%, nitrogen at 5.5% and potassium at 0.12%. Sulphur content was not detected in the microalgae biomass and this had aided the production of fatty acids methyl ester (F.A.M.E) which was observed by a gas chromatographic-flame ionisation detector (GC-FID) profile. A disruptive-extraction method using acid assisted phase on HLBS showed potential for direct conversion of lipids into F.A.M.E to produce biofuels for engine combustion.

Keywords: Biofuels; Cell wall; Microalgae; Acid disruption; Lipids recovery

4.1 Introduction

Microalgae are one of the promising source of renewable energy which can be found on freshwater and oceanic water systems. According to International Energy Agency (IEA), the consumption of fossil fuels increased to 81 Mtoe in 2018 and more than 300GW of new electric generator running on fossil fuels was constructed between 2008-2019 [194-196]. The sustainable source of microalgae is emerging as a promising alternative raw material to power-up electric generators. One of the important factors on microalgae growth is the culture medium which serve as the main nutrients supply for photosynthesis reaction within the cell cytoplasm to accumulate lipids and other high value compounds. The nutrients' composition could be enhanced by various organic-rich components for the cultivation medium to improve the properties of the biomass as raw material for biofuels, pharmaceuticals, cosmetics and nutraceuticals production [197-199]. Waste molasses is one of the most abundant by-products from the sugar mills factory which is suitable for microalgae cultivation for biofuels production [200]. The utilisation of waste molasses as the microalgae culture medium can reduce the cultivation cost besides of representing a cheap carbon source for bio-oils generation. The sugar content of the molasses is more than 40% and it represents a rich-source of nutrients such as micro-minerals (e.g., Mg^{2+}, K^{+}, Fe^{2+}), carbohydrates (hemicellulose, cellulose) and urea [200, 201]. According to Satyawali and

Balakrishnan [202], the molasses-based waste liquor produced from the sugar mills industry has created a large volume of nutrients rich wastewater which contributed to the growth of fungi, bacteria and algae that can pollute the drinking water source.

Hybrid liquid biphasic system (HLBS) consists of two solvents with different properties in a single system using liquid-liquid extraction mechanism employed as a disruptive-extraction method for lipid compounds from the microalgae cell [203, 204]. The intracellular bio-compounds (i.e., lipids, proteins and carotenoids) of microalgae can be extracted from penetrating the cell wall using both solvent phases of HLBS in a disruptive-extraction manner. The acid phase in the system initially disrupts the cell wall (as disruptive phase) and this is followed by the extraction using organic phase. Acid and organic solvent will form an immiscible two-phase system. The acids based disruptive solvent will break the cell walls by dehydrating the polysaccharide molecules with hydrolysis reaction [205]. Besides, the acids solvent in the disruptive phase tend to remove glycerol or free fatty acids into diglyceride and monoglyceride from the lipid compound through hydrolysis [206, 207]. The lipids will be released into the aqueous phase of the system and eventually dissolved into the organic solvent phase. The organic solvent can dissolve water-insoluble materials such as fats, oils, waxes, resins, plastic material and rubber. Lipids are classified into polar and non-polar category; as for biofuels application, both polar and non-polar lipids can be used in the conversion process as it will increase the yield of the

biofuels production [19]. The HLBS shows a liquid-liquid interface where two layers of liquid will come into contact with each other at phase boundary layer. The lipid compound tends to dissolve into the organic solvent phase once the cellular wall has been penetrated or disrupted.

Usually, cell disruption techniques are based on mechanical and electrical methods such as bead milling, thermolysis, steam explosion, ultrasonication, pulsed electric field treatment, high-pressure homogenisation and supercritical carbon dioxide (SC-CO_2) which is based on high pressure of CO_2 used during the extraction process as part of the mechanical disruption method [197, 204]. However, the operation of these techniques involves high electric power, high-end equipment and exhaustive operation process which will increased the process cost and is currently not feasible for large scale production compared to HLBS method [208, 209]. Acid treatment which based on the hydrolysis reaction can disrupt the cell wall and other major cell wall contents like fibrous polysaccharides, glycoproteins and polar lipids. The acid-treated microalgae biomass causes disruption on the polysaccharides compounds in the microscopic chain of the biomass; the polysaccharides are around 13% - 19% found as the microalgae structure in the cell wall [210, 211]. The HLBS represents a low cost, sustainable and highly efficient method of chemical cell disruption treatment compared to the mechanical methods. The tensile strength of microalgae cell wall is around 9.5 MPa which is similar to bacteria and yeast, and it is known to have the highest tensile strength of the cellular wall compared

to other plant cells such as carrot [88, 212, 213]. Therefore, this work aims to utilise a chemical cell disruption treatment owing to its higher surface coverage. Also, it could be integrated with extraction as a single processing step in order to achieve a better yield.

This research investigated the use of waste molasses to cultivate microalgae *Chlorella sorokiniana CY-1.* The growth properties and waste reduction such as chemical oxygen demand (COD) and total suspended solid (TSS) are being monitored. In addition, the lipids recovery and enhancement on the *C. sorokiniana CY-1* culture for biofuels production using a HLBS as a disruptive-extraction approach are analysed and optimised. The acid solvent will be used as the bottom phase while the organic solvent appears to be the top phase of the biphasic system to induce the cell disruption for the microalgae cell wall and direct conversion of lipids into fatty acids methyl ester (F.A.M.E). The effects on various types and concentrations of acids, volume ratio, biomass concentration, temperature and contact time are being optimised. The characterisation of the optimised lipids extract are evaluated using a gas chromatography equipped with a flame ioniser detector (GC-FID), an energy-dispersive X-ray spectroscopy (EDX) and a field emission scanning electron microscopy (FESEM).

4.2 Materials and methods

4.2.1. Materials

The waste molasses was obtained from Shinko Sugar Mills Co. Ltd., Japan, and contained 83° brix polysaccharides (30.4%) and inverted sugar (disaccharides and monosaccharides) (9.79%) as well as pH of 5.83. Sulphuric acid (H_2SO_4), nitric acid (HNO_3), hexane (H_6H_{14}), chloroform ($CHCl_3$), methanol (CH_3OH) and sodium chloride (NaCl) were of analytical grade obtained from R&M Chemicals (Malaysia). The mixture of the triglyceride in lipids standard and F.A.M.E (C4-C24) mixture in individual packages were purchased from Sigma Aldrich (USA).

4.2.2. Pre-treatment of waste molasses with Fenton reaction

According to Yu et al. and Bhange et al. [199, 214], a Fenton oxidation reaction was used for the saccharification for high degree of polysaccharide chains. The raw material information from the waste molasses of COD (12587 mg/L), TSS (15024.9 mg/L), and phosphorus (79.2 mg/L). The waste molasses was adjusted to pH 4 which is the optimum pH range [215] for Fenton reaction and added with HNO_3 for saccharification of the concentrated waste molasses with Fenton reagent solution. The solution was mixed with 1 mL of 4% (w/w) of $FeCl_2$ into 30% concentration of H_2O_2 in a ratio of 1:1 to the concentrated waste molasses followed by incubation at 60 °C for 24 h. The mixture was neutralized with 5% of NaOH to pH 7.3 to meet the optimal pH range at 6.5-7.5 for sustainable pH

growth of *C. sorokiniana CY-1* species. The Fenton reaction in the waste molasses converts a major portion of polysaccharides into monosaccharides. The selected concentrations of molasses cultivation medium used was based on previous studies with modified pre-treatment method for improvingd biomass productivity and the concentrations tested are 140 mg/L, 145 mg/L, 150 mg/L, 155 mg/L and 160 mg/L, where the remaining medium was filled with deionised water up to a total of 1 L.

4.2.3. Microalgae cultivation and medium composition

The microalgal *C. sorokiniana CY-1* was used in this study as it exhibits a high lipids content [213]. The pre-culture of microalgae was performed for seven days by using molasses medium as mentioned in section 2.2 and consistently supplied with atmospheric air. The batch culture was conducted in an indoor photo-bioreactor (PBR) after the maturation of the pre-culture sample by transferring the inoculum into 1 L culture using BG-11 medium (refer to **Table 4-1**) for 14 days. Each PBR was aerated with compressed air and illuminated by external LED lighting source with light intensity of 180 μmol/m^2.s^{-1} in parallel of the vessel, the lighting intensity was measured by LI-250 light meter with LI-190SA pyrometer sensor (LI-COR, Inc., Lincoln, USA). The cultivation was conducted at room temperature with an agitation speed of 300 rpm for continuously stirred the aqueous medium. Air was filtered using a filter with a pore size of 0.45μm for the culture. The air was aerated at the rate of 0.2 vvm (volume gas per

working volume per min). The microalgae batch cultures were cultivated until sufficient biomass was obtained.

Table 4-1: BG-11 medium compositions.

Components	**Concentration (g L^{-1})**
$NaNO_3$	1.5
K_2HPO_4	0.03
$MgSO_4.7H_2O$	0.075
Citric acid anhydrous	0.006
Na_2CO_3	0.02
$CaCl_2.2H_2O$	0.036
Ammonium iron (III) citrate	0.006
EDTA.2Na	0.001
H_3BO_3	0.00286
$MnCl_2.4H_2O$	0.00181
$ZnSO_4.7H_2O$	0.000222
$Na_2MoO_4.2H_2O$	0.00039
$CuSO_4.5H_2O$	0.000079
$Co(NO_3)_2.6H_2O$	0.000049

4.2.4. Determination of biomass and dry cell weight (DCW)

The biomass concentration in the medium was determined by the spectrophotometric method as described in a previous work [204]. The microalgae dry weight from the blank filter was subtracted from the loading filter to obtain the microalgae dry cell weight (DCW). The microalgae biomass was measured at OD 680 and converted to biomass concentration by calibration between OD 680 and DCW. The harvesting period was determined by nitrate and biomass concentration. The dry cell weight of microalgae biomass was measured through filtered 5 mL of aliquots through a 0.45 µm pore size of the glass-fibre filter paper (Whatman, USA). After filtered, the papers were dried through hot air oven at 120 °C for 12 h and the difference between the initial (W_i) and final (W_f) weight was calculated by gravimetric method. The difference of the initial and final weight from the filter paper used to calculate DCW for the biomass. The harvesting period was around 14-16 days and harvested microalgae were centrifuged at 7500 × g for 5 min, and the clear supernatant was removed. The resulting wet biomass was placed in the freezer at -20 °C for 24 h before the extraction has been studied. The microalgae growth rate was calculated according to [166, 216] for biomass productivity (P_b)(mg/L/day) as in Eq. 1 and specific growth rate (µ)(day^{-1}) as in Eq. 4-2.

$$P_b\ (mg\ L^{-1}\ d^{-1}) = \frac{(DW_2 - DW_1)}{(t_2 - t_1)} \qquad (4\text{-}1)$$

$$\mu\ (d^{-1}) = \frac{\ln(\frac{DW_2}{DW_1})}{t_2 - t_1} \qquad (4\text{-}2)$$

The DW_1 and DW_2 represent DCW (g/L) at time t_1 and t_2, respectively.

4.2.5 Medium data analysis

The microalgae samples were centrifuged and conducted a series dilution with deionised water, then measured at OD 220 for nitrate content using a UV-Vis spectrophotometer (UV-1800, Shimadzu, Japan) to determine the maturation stage of the microalgae cell. Chemical oxygen demand (COD) was using high range of digester 20 – 1500 mg/L (Hach,USA) tested by taking from day 1 as initial sample and day 14 as final day sample through homogenized the sample and further diluted for 8-fold from each waste molasses concentration medium. Subsequently, pipet 2.0 mL of sample into the Hach digestor vial followed by inverted gently for well mixing and inserted into preheated DRB200 (Hach, USA) reactor for 2 hours. The spectrophotometer DR1900 (Hach, USA) was selected for its high range (program 821) for reading the COD in mg/L. The total suspended solid (TSS) was done by filtering 100 mL of sample from each concentration medium by pre-weight 0.45 μm pore size of the glass-fibre filter paper (Whatman,USA). Then, the filtered paper was placed in the oven at 110 °C for 1 hour, the final weight was obtained after cooling the filter paper for 1 hour. The brix content was measured by refractometer calibrated by pure sucrose in 1g per 100mL of deionised water for 1° brix. The experiment was conducted in triplicate and the data were reported in mean with standard deviation [198, 217]. The COD, TSS and brix reduction were determined according to Eq. 3.

$$\text{Reduction } (\%) = [(C_i - C_f)/C_i] \times 100 \qquad (4\text{-}3)$$

Where C_i and $C_{f\ refer}$ to initial and final value of COD, TSS and brix concentration, respectively.

4.2.6. Acids assisted HLBS and direct transesterification for F.A.M.E

The acid assisted HLBS was performed in two different sections of the experiment as mentioned in Yew et al [204]. The instantaneous lipids extraction contained aqueous phase (acids) and organic phase (hexane). Organic phase has been extracted subsequently the transesterification is using methanol and chloroform without catalyst during the reaction. The effect of temperature parameter was conducted through immersing the system (borosilicate tube) in water bath where maintained for initially 1 min and allowed to cool in distilled water at room temperature for 1 min. After that, the organic solvent was added for instantaneous lipids extraction. The F.A.M.E method was modified according to Indarti et al [218] for a direct transesterification. The lipids extracted (±20 mg) were weighed in a clean 10 mL of screwed bottle containing 4 mL of the mixture comprised of analytical grade of methanol and chloroform (1.7:2.0, v/v). The bottle was closed tightly and heated in 90 °C for 40 min. 1 mL of the deionised water was then added and vortexed for 1 min. Two phases will be formed and 1 µL of methyl dodecanoate (C12:0) was diluted in a ratio of 1:499 (v/v) was added as an internal standard into 0.5 mL of the solution. The internal standard was chosen due to the test run methyl dodecanoate (C12:0) was

not detected. The samples were tested by gas chromatography (Perkin Elmer Clarus 690 GC, USA) with a flame ionisation detector (GC-FID). The samples were injected into an Agilent Technologies analytical laboratory instrument column (30 m × 0.25 mm × id 0.25 μm) with helium at 1.0 mL/min, column oven temperature at 35 °C for 3 min, then increased to 220 °C with an increment of 4 °C/min and held at 220 °C for 35 min, injector and detector temperature were set at 250 °C and 260 °C, respectively. The split ratio was 15:1, carrier gas (helium) was controlled at 103.4 kPa. **Table 4-2** shows the operating parameters and conditions of the HLBS in this experiment.

Table 4-2: Operating parameters and conditions of HLBS

No.	Operating parameter	Initial condition	Variables	Unit
1	Time of contact	1	1, 2, 3, 4, 5	min
2	Biomass amount	20	20, 30, 40, 50	mg
3	Ratio of solvents – Cell disruption solvent : Organic solvent	1:3	1:1, 1:3, 2:3, 4:3, 3:4, 3:5	-
4	Concentration of diprotic acid (H_2SO_4)	5	5, 10, 15, 20, 25, 30	% (w/w)
5	Concentration of aprotic acid (HNO_3)	5	5, 10, 15, 20, 25, 30	% (w/w)
6	Temperature	25	25, 40, 60, 80	°C

4.2.7. Total lipids in microalgae biomass analysis

The total lipid contents analysis of the microalgae biomass was carried out according to methods [89, 219]. The biomass weight of 20 mg (± 0.3 mg) was transferred into a 10 mL centrifuge tube containing 3 mL of the solvent mixture in a chloroform: methanol ratio of 2:1 (v/v). The contact time for the microalgae biomass was set at 5 min and allowed to particulate in the solution. The supernatant lipids mixture was transferred by micropipette into a separate tube. The solution was heated to 60 °C for 1 h, followed by the addition of 0.9% NaCl solution in 20% volume of the solution mixture and placed into oven at 50°C for 5 min. The solution was then vortexed and a biphasic layer was formed. The upper phase was pipetted out and the lower phase which contains lipids was dried by using nitrogen gas. The total weight of the lipids extract was measured.

4.2.8. Determination of lipids recovery yield and cell disruption enhancement in fold value

The lipids recovery yield in organic solvent phase from total lipid contents in the biomass was represented by Eq. 4-4.

$$\text{Recovery yield, R (\%)} = \frac{\text{Total lipids recovered in organic solvent phase}}{\text{Total lipid contents in microalgae biomass}} \times 100 \quad (4\text{-}4)$$

The cell disruption enhancement (Fold) was evaluated by comparing the disruptive solvents with neutral solvent H_2O (deionised water) in the biphasic system as in Eq. 4-5.

$$\text{Cell disruption enhancement} = \frac{A_i}{H_{ref}} \text{ fold} \quad (4\text{-}5)$$

where A_i represents the optimised concentration of lipids from disruptive solvents with organic solvents in the biphsic system, while $H_{ref\ represents}$ by lipid dissolved in deionised water H_2O with organic solvent in the biphasic system. The tests were analysed for three repetitive individual samples with *C. sorokiniana CY-1* biomass.

4.2.9. FESEM visualisation and EDX analysis on cell wall

The microalgae cell wall after subjected to varying concentrations of acid in the system was observed by Field Emission Scanning Electron Microscope (FESEM, Quanta 400F) (FEI, USA) and the composition analysis of the biomass was evaluated by Energy-dispersive X-ray (EDX) spectroscopy (Oxford-Instruments INCA 400 with X-Max Detector). Two types of samples consisting of biomass with acid-treated and dry biomass in powder form were evaluated. SEM characterisation was performed to observe the cellular wall and potential fibrous polysaccharides. Previous studies and investigation of polysaccharides in *Chlorella sp.* as the main component of structural in the eurkaryotic cellular wall are presented in **Table 4-3.**

Table 4-3: Microalgae polysaccharides

Chlorella sp.	**Polysaccharides Composition**	**Polysacharides disruption techniques**	**Reference**
Chlorella pyrenoidosa	Glucose, mannose and tri-O-methylhexose (24 wt%, 8 wt%, 8 wt%)	Size exclusion chromatography and anion exchange chromatography	[217]
Chlorella vulgaris	Rhamnose, arabinose, mannose, Galactose, Di-O-methylrhamnose, tri-O-methylrhamnose (67 wt%, 6.1 wt%, 4.6 wt%, 2.6 wt%, 10.5 wt%, 5.6 wt%, 3.2 wt%)	Benzene ethanol with hot water (80-85 ^{o}C, 2h)	[214]
Chlorella kessleri	Galactose A, arabinose, galactose, fucose (41 wt%, 34 wt%, 20 wt%, 5 wt%)	Precipitation (water and methanol)	[199]
Chlorella sp.	Rhamnose, arabinose, xylose, mannose, galactose, glucose (5.3 %, 8.5 %, 8.4 %, 8.0 %, 53.7 %, 16.2%)	Alkaline solution with 1% H_2O_2)	[213, 220]

4.2.10. Statistical analysis

The statistical analysis of the experimental data was performed by taking the average of triplicate readings and the standard error was calculated based on the values. Datas were subjected to one-way factor ANOVA using Microsoft Excel to determine the significant difference where ($p \leq 0.05$).

4.3. Results and discussion

4.3.1. Characterisation of acid-treated microalgae biomass

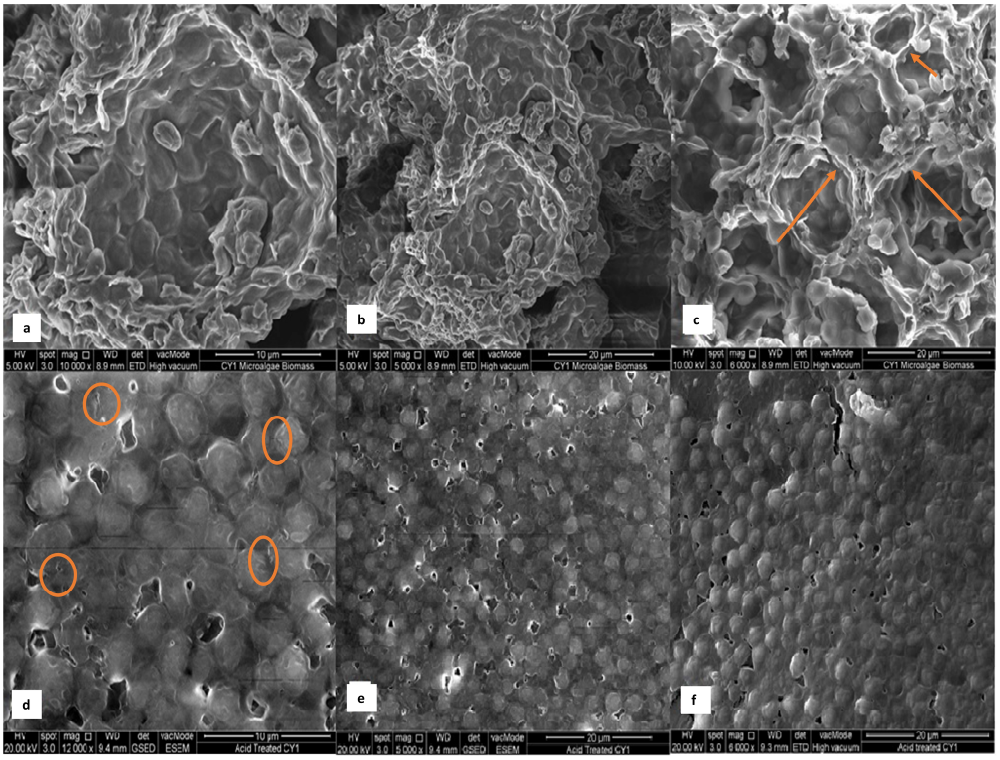


Figure 4-1: Microscopic view of FESEM capture for *C. sorokiniana CY-1* biomass. High vacuum mode of multi-cellular biomass in (**a**) 10000, (**b**) 5000 and (**c**) 6000 magnification. ESEM mode of 15% nitric acid-treated multi-cellular biomass in (**d**) 12000 and (**e**) 5000 magnification. (**f**) High vacuum mode of 15% nitric acid-treated multi-cellular biomass in 6000 magnification. The orange circle and arrow indicate the disrupted cell.

Figure 4-1 shows the FESEM image of *C. sorokiniana CY-1* biomass in high vacuum mode and under ESEM (Environmental Scanning Electron Microscope). The images for the microalgae biomass before and after the acid treament in HLBS were observed. Cell wall was structured by polysacharides compounds as stated in **Table 4-3** on *Chlorella sp.* for clarifying the common types of polyssacharide composition in the cell wallasshown in **Figure 4-1a** that shown a denser multi-cellular biomass, where the microalgae cell was observed through the hyperbolic curvature on the surface and the lipid compound exist underneath the hyperbolic surface. In **Figure 4-1b**, each microalgae cell wall was interconnected to form a large network supporting each other. The disruption of the cell wall appearance as shown in **Figure 4-1c** which were indicated by the arrow pointing on the sample holding up by tensile interaction. **Figure 4-1d** observes the disrupted cell wall as the circumference of the biomass that was not joined completely. **Figure 4-1e** and **4-1f** display the biomass that was treated with acid in HLBS and can be seen clearly the pin holes spreaded around the center. The disruption of the cell was caused by acid treatment, in which causes the disruption of the structural form of microalgae cell. **Figure 4-1f** uses a high vacuum mode in enhancing the image stability to observe the tearing on the connection between the cells.

4.3.2. Microbial growth and nutrient removal

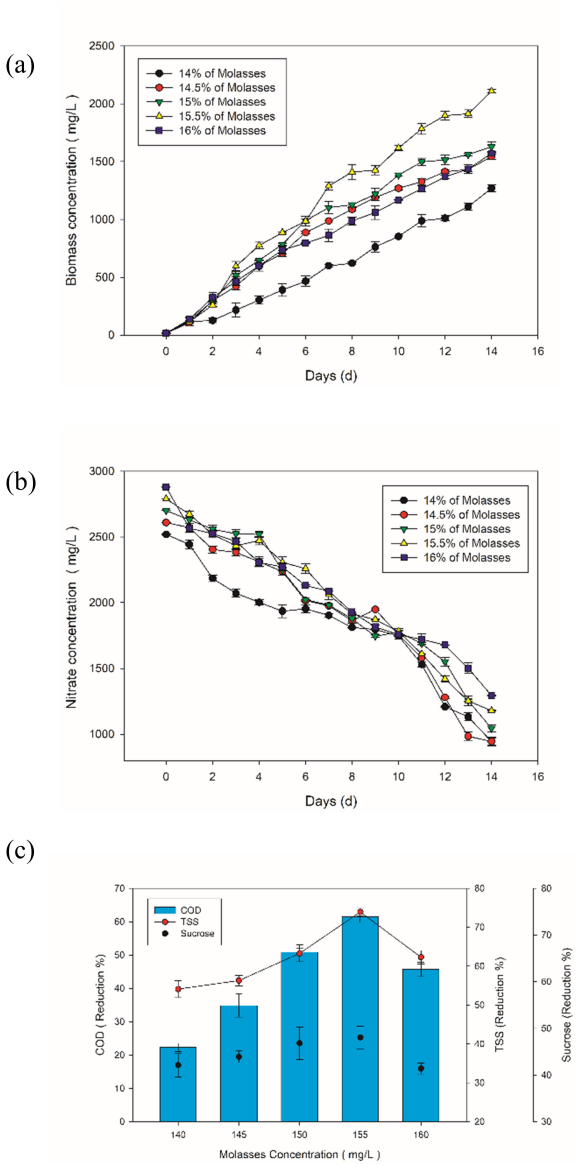


Figure 4-2: (**a**) Biomass concentration and (**b**) nitrite concentration in different molasses concentrations medium of 140 mg/L, 145 mg/L, 150 mg/L, 155 mg/L and 160 mg/L for 14 days. (**c**) COD, Sucrose and TSS reduction between 1st and 14th days.

Table 4-4: Growth profile for different concentrations of molasses

Concentration of molasses (mg/L)	**140**	**145**	**150**	**155**	**160**
Biomass productivity (mg/L/d)	96.34 ± 2.08	117.5 ± 1.72	124.03 ± 0.70	160.89 ± 0.96	119.66 ± 0.58
Specific growth (d^{-1})	0.33 ± 0.02	0.35 ± 0.04	0.35 ± 0.16	0.37 ± 0.1	0.35 ± 0.01
DCW (mg/L)	641.83 ± 0.12	877.51 ± 0.24	985.64 ± 1.21	2001.12 ± 0.87	2123.45 ± 1.63

Figure 4-2a shows the biomass cell growth based in different molasses concentrations in medium (140 mg/L, 145 mg/L, 150 mg/L, 155 mg/L and 160 mg/L). This study has found the optimum range of molasses concentration to be 14%-16% and a Fenton reaction was utilized for saccharification to treat the polysaccharide chains [221]. The highest accumulated biomass was observed at 155 mg/L of molasses concentration with a value of 2108.32 ± 14.56 mg. The DCW, biomass productivity and specific growth rate at day 14th were 2001.12 ± 0.87 mg/L, 160.89 ± 0.96 mg/L/d and 0.37 ± 0.1 d^{-1}, respectively. The biomass produced from optimum concentration of molasses (155 mg/L) showed an improvement of 89.83% and 45.95% for biomass productivity and specific growth rate, respectively based on the control parameters from the studied.

According to Yu et al. [199], Fenton reaction had resulted in a higher yield of monosaccharides in corn stalks. Also, the use of Fenton reaction which is similar to fungi will naturally degrade the polysaccharide chains and improve the cellulose accessibility by cellulose during the composting [220]. The lowest biomass (1268.74 ± 28.2 mg), biomass productivity (96.34 ± 2.08 mg/L/d) and specific growth rate (0.33 ± 0.02 d^{-1}) were observed at 140 mg/L of molasses concentration. Referring to **Table 4-4**, the specific growth rate for all the molasses concentrations were not high with statistical analysis ($p \leq 0.05$). The low biomass growth rate might due to the quality of light adsorption for the microalgae cell as the high colour intensity from the medium inhibits light penetration. Therefore, it could affect the Calvin Cycle and subsequently influence the cell growth and nutrients consumption. 16% of molasses decreased in trend due to the higher amount of molasses concentration that limits the light penetration by the color intensity from the molasses medium. This finding corresponds to the previous studies where higher concentration of molasses will reduce the biomass productivity. The overall trend has indicated the microalgae is consuming the nutrient from the molasses and optimum biomass was found from 155 mg/L of molasses concentration.

As shown in **Figure 4-2b**, the highest nitrate removal (63.79%) was noted at 145 mg/L of molasess concentration and followed by 62.53% at 140 mg/L of molasess concentration in day 14th. In contrast, the lowest reduction of nitrate was observed at 160 mg/L of molasses concentration which is decreased from

2880.36 ± 1.31 mg/L on the first day to 1293.73 ± 2.21 mg/L on the day of 14th of the cultivation period. Nitrate is found in most plants and eurkaryotic cell to perform important molecules signal for transcriptional and post-translational regulation as well as involve in nitrogen cycle [209, 213]. The lowest nitrate removal was found in 160 mg/L of molasses concentration with 55.08% and followed by 155 mg/L molasses concentration at 57.72% of reduction percentage. The biomass productivity dependson several intrinsic cell growth qualities such as the light absorbing intensity of chlorophyll, cell metabolite, kinases transferase and each cell gene sequence. The reducing trend of the nitrate showed for the removal value was insignificant ($p \leq 0.05$) and indicate microalgae as one of the choice for reducing the nitrate from molasses waste and converting it into useful nutrients for microalgae cell. The absence of nitrate in stagnant water may cause eutrophication and cover the surface of the water for preventing sunlight penetrate for oxygenators plant such as water hyacinth, water lettuce, and duckweed.

The COD of waste molasess after the pretreatment of saccharification by Fenton reaction was 12,587 mg/L (**Figure 4-2c**). The concentrated waste molasses was then separated into various molasses concentrations as culture medium with different COD values. The COD on day 14th for molasses concentration at 140 mg/L, 145 mg/L, 150 mg/L, 155 mg/L and 160 mg/L were 1412.8 ± 2.56 mg/L, 1770.4 ± 3.48 mg/L, 1728.0 ± 1.37 mg/L, 1685.6 ± 3.65 mg/L and 2643.2 ± 0.78 mg/L, respectively. The highest COD reduction was 61.5% at 155 mg/L of

molasses concentration of molasses value while the lowest COD reduction was 22.2% at 140 mg/L of molasses concentration at day 14th. The highest (63.94%) and lowest (54.17%) TSS reduction were observed at 155 mg/L and 140 mg/L of molasses concentration, respectively. Similarly, the Brix ° or sucrose reduction followed the same trend; the highest reduction of 48.08% and the lowest reduction of 42.11% were noted at 155 mg/L and 144 mg/L of molasses concentration at day 14th, respectively. The results have indicated the culture of microalgae have caused the reduction of COD and sucrose value raised from the origin content of the waste molasses, the microalgae cell will consume the micronutrient and subsequently convert into biomass. This has indicated the potential of microalgae cell for treating waste from sugar mills industry and using the waste as an additive to enhance the growth of the cell. The statistical analysis showed that the COD value is insignificant affected ($p \leq 0.05$) by variation of the molasses concentration. Aqueous waste molasses mainly comprised of mineral and chemical substances that will elevate the level for the COD, the reduction of the value during the cultivation was due to the cell from microalgae may consume the nitrate, phosphate, potassium and other micro-minerals as nutrient for the growth.

4.3.2. Lipids extraction and optimisation study

4.3.2.1. The effect of sulphuric acid concentration

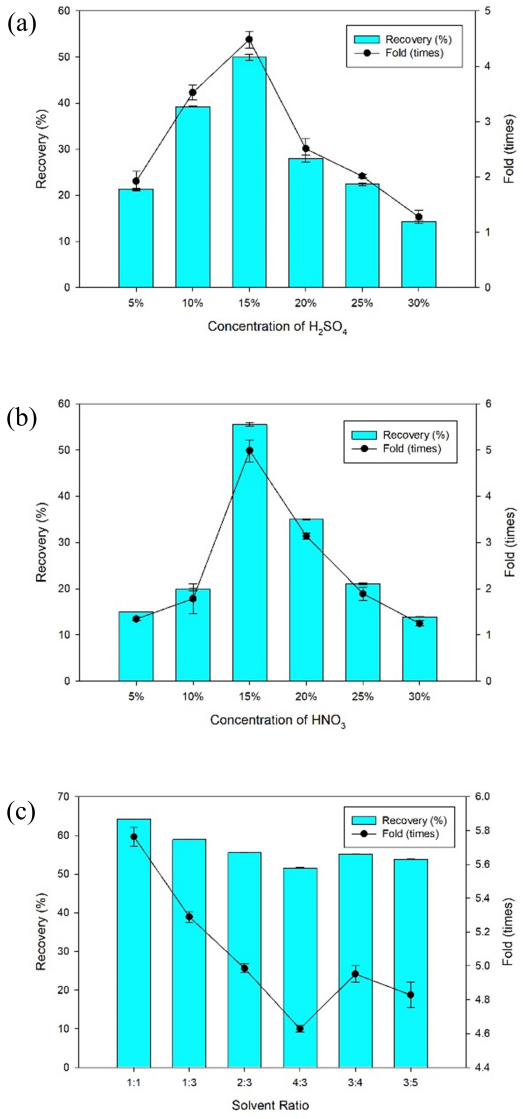


Figure 4-3: (**a**) The effect of *C. sorokiniana CY-1* biomass amount on single-step lipids recovery yield and enhancement in HLBS; Operating conditions: concentration of 15% of HNO_3, 98% organic hexane (analytical grade), ratio 1:3

(acids:hexane) and time of contact = 3 min. (**b**) The effect of temperature of the water bath on single-step lipids recovery yield and enhancement in HLBS; Operating conditions: concentration of 15% of HNO_3, 98% organic hexane (analytical grade), ratio 1:3 (acids: hexane), time of contact = 3 min, biomass weight of 50 mg. (**c**) The effect of time of contact on single-step lipids recovery yield and enhancement in HLBS; Operating conditions: concentration of 15% of HNO_3, 98% organic hexane (analytical grade), ratio 1:3 (acids:hexane), water bath at 80 ºC and the biomass weight of 50 mg.

According to **Figure 4-3a**, the highest lipids recovery and cell disruption enhancement were observed at 15% concentration of sulphuric acid (H_2SO_4) in HLBS, with a value of 49.92% and 4.5-fold, respectively. Strong acid solvents are likely to donate protons to solutes through hydrogen bonding [222]. H_2SO_4 is known as a diprotic acid containing two hydrogen ions (H^+) which is a stronger acid. The highest concentration of H_2SO_4 (30%) in HLBS did not provide an optimum lipid yield, and could be explained by the H^+ particles that were not fully hydrolysed at this concentration and thus only partially released to react with the cell wall. The 15% concentration of the H_2SO_4 showed the optimum reaction in the given experimental conditions while simultaneously dissolving the lipids into the organic solvent phase. Lipids production from microalgae in HLBS has various merits, the supportive mechanism from the disruptive phase of the system mainly targets the penetration of the cell wall of microorganism,

causing it to release the nutrient compound from the cell. The key reason for conventional lipids extraction technique being unable to be commercialised is due to the extraction technology which is costly and mainly dependent on mechanical pre-treatment methods which are energy intensive [34]. Owing to thick and multiple layers of microalgae cell wall, the use of acid solvents for cell disruption creates more surface of contact for each molecule of the microalgae biomass as compared to mechanical method to penetrate into the aqueous compound in the biomass [223]. This experiment shows a similar result in accordance with the study conducted by Harun and Danquah, which uses sulphuric acid for acid treatment in biomass where the lipids yield decreased gradually towards using a higher concentration of sulphuric acid [224]. The statistical analysis showed the concentration of H_2SO_4 significantly affected the lipids recovery ($p \leq 0.05$). Since 15% concentration of H_2SO_4 showed optimum results, it was then chosen to further compared with aprotic acid in the following parameters in HLBS.

4.3.2.2. The effect of nitric acid concentration

Nitric acid (HNO_3) was used to investigate the optimum concentration of microalgae biomass in disrupting the cell wall for lipids extraction in HLBS. The lipid compound tends to dissolve into non-polar organic solvents such as hexane from the cell cytoplasm. The 15% concentration of HNO_3 showed the highest lipids recovery yield (55.54%) and cell disruption enhancement (5-fold) (**Figure 4-3b**). The value of lipids recovery yield in this case was slightly higher of 5.62% compared to that of H_2SO_4. HNO_3 contains only one H^+ and is less likely to donate protons for the hydrogen bonding interaction [225]. Thus, acids with higher hydronium ion will have more protons readily to react with basic species and the pK_a value would be very low in the HLBS. Moreover, HNO_3 does not contain any sulphur element compared to H_2SO_4. The sulphur element may dissolve in the organic solvent and aid the conversion of biofuels in the transesterification reaction. The addition of sulphur in the aliphatic chain is not favourable for the engine combustion system and the environment [226].

As previously mentioned, H_2SO_4 has a higher hydronium value than HNO_3 with two positive charges in the same mole of solvents, therefore the electronegativity for H_2SO_4 is slightly higher than HNO_3 and it may disrupt the structure of mono-, di- and triglyceride [227]. The HNO_3 has a single positive charge at the nitrogen atom and when the acid dissociates in the water it will form hydrogen ions in the aqueous solution. In this case, H_2SO_4 will release more hydrogen ions compared to nitric acid. Moreover, aprotic acids like HNO_3 behave less aggressive

compared to H_2SO_4 in terms of amount for the hydrogen ions contained in each molecule, where it may reduce the potential of lipid peroxidation. The peak of lipids recovery yield was noted at 15% of HNO_3 concentration and the value dropped gradually from 15% to 30% in HLBS. While enhancement value from 15% to 30% was in a decreasing manner, i.e, from 5.0 to 1.2-fold. The European Standards for Biofuels (EN ISO 20846, EN ISO 20884) states that the sulphur content should not exceed 10 mg/kg for the purpose of being used as a heating fuel, therefore HNO_3 appears as a better choice. Besides, sulphur compound is avoided in the combustion engine due to easily releases to the atmosphere and cause acid rain. Nitric acid in n ignition engine may react rapidly with H and OH radicles to form N_2 avoided for the formation of nitrogen oxide (NOx). Nitrogen N_2 is relatively stable and less harmful compared with sulphuric acids, however in near future it may be tested on acetic acids and carbonic acids. The lipids recovery and enhancement in fold were significantly affected by varying the concentration of aprotic acid-like solvent ($p \leq 0.05$). Considering the environmental aspect as a priority for both acids, HNO_3 of 15% concentration will be the choice for optimising as it does not contain sulphur in the molecular structure and can avoid the production of sulphuric gases during the process.

4.3.2.3. The effect of volume ratio of solvents

The ratio of extractive and disruptive properties of the acid-assisted HLBS affected the lipids recovery yield and enhancement value as shown in **Figure 4-3c**. The peak value of lipids recovery yield (64.19%) and enhancement (5.8-fold) were showed at ratio of 1:1. The increasing ratio of cell disruption solvent did not directly affect the lipids recovery yield and cell disruption enhancement. The lowest lipids recovery yield and enhancement were observed at volume ratio of 4:3 (51.56% and 4.6-fold, respectively). The surface of contact and interaction of the acid with the biomass was optimised at a volume ratio of 1:3. The solvent-accessible surface area for the bottom layer of HNO_3 is well in contact with the biomass and causes the structural cell wall to be disrupted efficiently. Thus, the lipids have more accessibility to dissolve into the organic solvent. The fluctuating trend of 4:3, 3:4 and 3:5, where the lipids recovery values are at 51.56%, 55.17% and 53.79% respectively. This result could be explained theoretically using Derjagin-Landau-Verwey-Overbeek (DLVOD), where liquid as a medium for hydronium ion and the ions tends to be unevenly distributed due to the aggregation of aqueous dispersion on the surfaces of microalgae biomass. Hence, the disproportional force of interaction between the cell wall with the dispersion of acid molecules presently assists the disruption mechanism [228]. Cell wall disruption enhancement of 4:3, 3:4 and 3:5 were 4.6-fold, 5.0-fold and 4.8-fold, respectively. In ratio 2:3, the lipids recovery was 58.93% while in 3:3 it was 55.54%. The lipid dissolves into the organic solvent

from the disruption cell wall when the attraction from the van der Waals forces and electrostatic repulsion happen on the biomass surface area, affecting the enhancement fold value in the HLBS. The reason is due to sum of the energy of interaction between both biomass and acid solvent interfacial boundaries which would eventually contribute to the acids molecules disruptive level for each of the microalgae biomass cell walls, hence the lipids recovery is being affected [229]. The increase in organic solvent in the HLBS had significantly assisted in the lipids recovery yield and the increment of lipid recovered is less than 10%. The statistical analysis shows that the volume ratio of solvents was significantly affected the lipids recovery yield and enhancement ($p \leq 0.05$). Overall, the HLBS with a volume ratio of 1:3 was opted for further optimisation study.

4.3.2.4. The effect of the amount of microalgae biomass

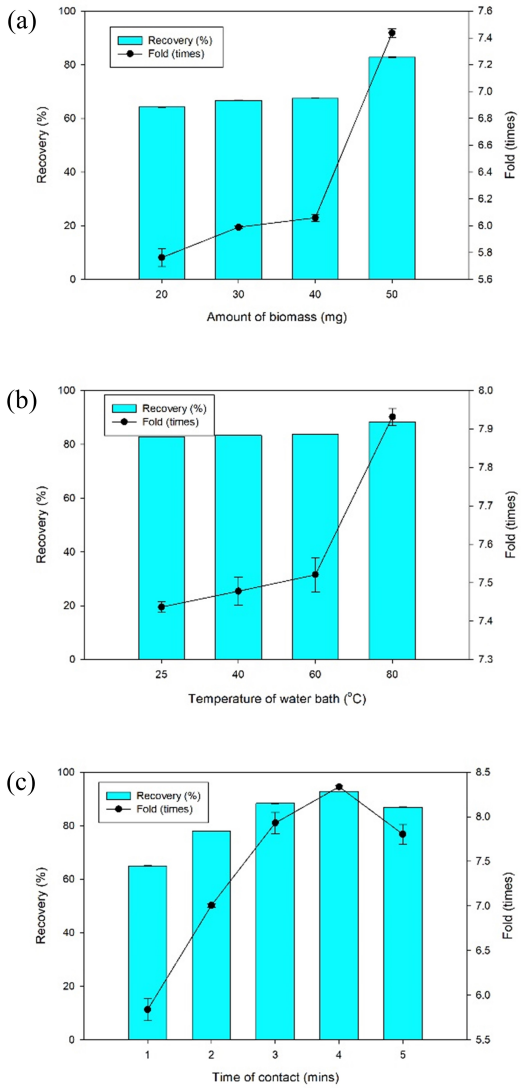


Figure 4-4: (**a**) The effect of *C. sorokiniana CY-1* biomass amount on single-step lipids recovery yield and enhancement in HLBS; Operating conditions: concentration of 15% of HNO_3, 98% organic hexane (analytical grade), ratio 1:3 (acids:hexane) and time of contact = 3 min. (**b**) The effect of temperature of the

water bath on single-step lipids recovery yield and enhancement in HLBS; Operating conditions: concentration of 15% of HNO_3, 98% organic hexane (analytical grade), ratio 1:3 (acids: hexane), time of contact = 3 min, biomass weight of 50 mg. (**c**) The effect of time of contact on single-step lipids recovery yield and enhancement in HLBS; Operating conditions: concentration of 15% of HNO_3, 98% organic hexane (analytical grade), ratio 1:3 (acids:hexane), water bath at 80 ^oC and the biomass weight of 50 mg.

The amount of biomass added in the HLBS will affect the lipids recovery yield as it influences the viscosity of the extracting solvent in the system [197, 214]. Therefore, HLBS may pose difficulty in disruption and separation process for the biomass compounds. Based on **Figure 4-4a**, the cell disruption enhancement was slightly higher at 30 mg of biomass (6-fold) compared to that at 20 mg of biomass (5.8-fold). The cell disruption enhancement increases as the biomass concentration increases in the HLBS. This was likely due to the lower concentration of biomass which contains lesser total lipids, resulting in a low lipids content to be dissolved into the organic solvents. For 40 mg of biomass, the enhancement was 6.1-fold and lipids recovery increased to 67.49%. The enhancement and lipids recovery at 30 mg were 6.0-fold and 66.70%, respectively. The increment of the lipids recovery yield and the enhancement value was apparent in higher concentrations of biomass in HLBS and disrupting solvent that contacts the surface of the cell wall to release the lipids. In 50 mg of biomass, the enhancement was 7.4-fold and lipids recovery yield was 82.83%.

The differences between the enhancement and lipids recovery value for 40 mg and 50 mg are 1.4-fold and 15.34%, respectively. Biomass in lower concentrations between 20 mg and 30 mg showed the differences for enhancement and lipids recovery value at 0.22-fold and 2.5%, respectively. The statistical analysis indicated that the biomass amount significantly affected lipids recovery yield and enhancement value ($p \leq 0.05$). The biomass content in HLBS will influence the surface of contact for the disruption phase of the solvent, and hence, it is necessary to add an optimum amount of 50 mg of the biomass into the system with proper solvent ratio.

4.3.2.5. The effect of temperature

The effect of temperature was conducted to evaluate the thermal effect for maximising the lipids to be recovered through HLBS in disruptive solvent phasein a temperature water bath. The use of the water bath is to transmit the heat energy without directly heating on the solvent in the system. In order to avoid the evaporation of all the organic solvent, it was added after the disruption phase of solvent immersed in the water bath with the time of contact of the extract at 4 min. The highest enhancement and lipids recovery value were at 80 °C of the water bath, with values of 7.9-fold and 88.35%, respectively (**Figure 4-4b**). The disruption of the microalgae cell wall can be accelerated by using acid solvents with thermal assistance to increase the rate of hydrolysis reaction at outer boundary layer of the cell in HLBS [230]. Acid is a proton donor that

increases the temperature and affects the dissociation rate of the hydrogen ions into the aqueous solution [231, 232]. At the ambient temperature of 25 °C, the enhancement and lipids recovery were 7.4-fold and 82.83%, respectively, whereas at 40 °C, the enhancement and lipids recovery value were 7.5-fold and 83.29%, respectively. The heat energy affected the dissociation rate of hydrogen ion from the nitric acid in HLBS, where the pH dropped to 3.12. Hydrogen ion will be concentrated in the solution and further disrupted the biomass cell wall by withdrawing the electron from the cell wall layer. Besides, the effect of temperature will enhance the dissociation rate of the hydrogen ion from the nitric acid [233]. Lipids were recovered by 6.6% when the temperature of the water bath increased from 25 ºC to 80 ºC, intrinsically the water bath introduces the thermal energy in which it would enhance the lipid extraction into the organic solvents in HLBS. The statistical analysis showed that the temperature contact significantly affected the lipid recovery yield and enhancement value ($p \leq 0.05$). The water bath temperature at 80°C was chosen to be further studied.

4.3.2.6. The effect of time of contact

Figure 4-4c shows the effect of contact time on lipids recovery yield and enhancement value for extraction of *C. Sorokiniana CY-1* using HLBS. The contact time at 4 min successfully achieved the highest lipids recovery yield and enhancement at 92.84% and 8.3-fold, respectively. The 15% concentration of nitric acid has a pH of 4.32, where the acidic property may gradually break down the cell wall structure during the contact time. The high pH value of the solvent

may hydrate the cell wall and further disrupt the cell wall with a high content of polysaccharides structure [234]. Microalgae or any plants have a cell wall that shows mechanical strength to withstand the tensile and compressive force in nature to protect against the external factor to disrupt the cell wall compound. The conventional mechanical cell disruption method using bead milling applies a mechanical shear force to disrupt the cellular wall and tensile strength among polysaccharide through grinding with rotating shaft. The efficiency of bead milling depends on several parameters such as agitation geometry, biomass concentration, bead type and speed of agitation. This is energy-intensive compared to the acid assisted method to disrupt the tensile strength within the plant cell wall as the mechanical method mostly required electrical motors to power-up the agitator in transferring the shear force to induce the disruption mechanism to the microalgae cell wall. The chemical method in time of contact parameter intended to study the microalgae biomass cellular wall compounds interaction with acids derived hydrogen ions in HLBS. The contact time from 1 mins to 5 min of the recovery value have an increasing trend at 65.02%, 78.04%, 88.35%, 92.84% and 86.92%, respectively. Enhancement value increased from 1 mins to 4 min from 5.8-, 7.0-, 7.9- and 8.3-fold, respectively, and then the value dropped to 7.8-fold at 5 min. This might cause by the possibility in which the cellular wall exceeds the optimum time of contact causes the occurrence of lipid peroxidation reaction. After the peak lipids recovery at the contact time of 5 min, where the reduction for enhancement and recovery value have dropped

the value at 0.5-fold and 5.92%, respectively. The peak reduction could mainly due to the time factor where affects the disruption quality of the cellular wall and lipid compound from the microalgae biomass. The disruption quality may further affect the dissolving ability of the lipid into the organic solvent, disruption mechanism from acid solvent through hydrolysis to break up the major polysaccharide components from the cellular wall into monomeric constituents where allow the lipid release from the cell and further dissolved into the organic solvent [235]. The optimum duration for this experiment parameter studied was at 4 min with ($p \leq 0.05$) for HLBS the recovery of lipids and has the highest enhancement in fold. The acids solvent after recovery may left as major challenge at industry level. For HLBS system the aqueous phase (acids) will be at the bottom, treated microalgae biomass will be sink to the bottom due to density of the biomass in the aqueous phase after vortexed. As long as the acidity is below pH 5, it is recommended to funnel out the biomass and reused the solvent. Once the acidity level is raised above pH 5, the solution may neutralize by salt solution and discarded.

4.3.3. GC profile of F.A.M.E and EDX analysis

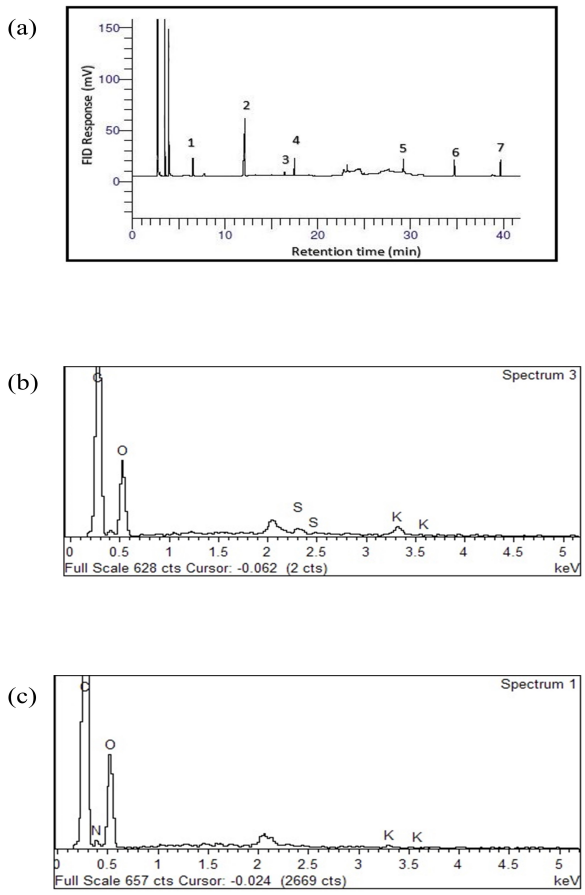


Figure 4-5: (**a**) GC profile of F.A.M.E from *C. sorokiniana CY-1* lipids sample (1 = C11:0; 2 = C12:0 (internal standard); 3 = C16:0; 4 = C16:1(n-9); 5 = C21:0; 6 = C22:0(n-5); 7 = C22:4). (**b**) EDX analysis on biomass for all elements on *C. sorokiniana CY-1*. (**c**) EDX analysis on acid-treated biomass for all elements on *C. sorokiniana CY-1.*

Table 4-5: The fatty acids methyl ester (F.A.M.E) weight profile from GC-FID

Fatty Acids	**C11:0**	**C16:0**	**C16:1(n-9)**	**C21:0**	**C22:0(n-5)**	**C22:4**
(mg/g)	0.714	0.357	0.786	0.536	0.571	0.607

A direct transesterification method for lipid compounds using methanol successfully obtained F.A.M.E and was characterised by gas chromatography to display the F.A.M.E profile as shown in **Figure 4-4a.** The composition of the fatty acids methyl ester from the selected acids and others optimum parameters in the lipid extract is shown in **Figure 4-4** and data as describe **Table 4-5** from the GC-FID profile, the middle chains allocated as C11:0, C16:0, C16:1(n-9) and long chains C21:0, C22:0(n-5) and C22:4. As shown in **Tables 4-5**, the highest weight found in C16:1 (n-9) in 0.786 mg/g, while the lowest in C16:0 for 0.357 mg/g. The HLBS with acid solvent as the disruptive phase is partially acted as a catalyst in assiting the transesterification process. This is due to the acid phase in the HLBS releases the glycerol molecules from the triglycerides before the transesterification process. The addition of methyl ester molecules as tails into the bio-oil hydrocarbon chain will increase the combustion properties for the molecules, however, it is susceptible to oxidation for the overall biofuels production [236]. The stability depends on the unsaturated content in biofuels and a higher stability will prolong storage which improves the combustion

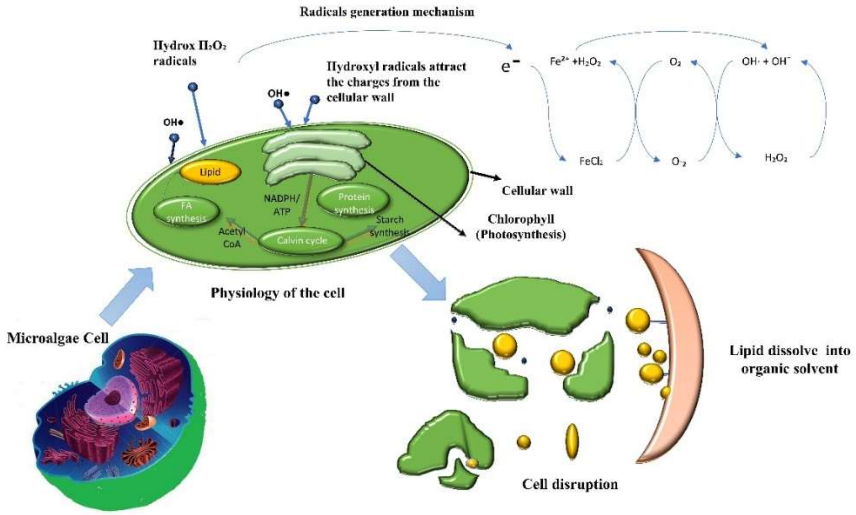
engine in terms of performance and emission [237]. The degradation of biofuels normally caused by oxidation, thermal oxidation at high-temperature conditions, hydrolysis with moisture from air and biological factors degradation due to microbial, bacteria and fungi [238]. The fatty acid chain length is one of the factors that could affect the ignition delay, shorter chains result in a shorter time of the ignition where ignition delay issues will be resolved [239].

In **Figure 4-4b**, the EDX analysis of *C. sorokiniana CY-1* biomass showed four major elements in the non-acid treated biomass. The four major compositions were carbon (66.5%), oxygen (32.5%), potassium (0.62%) and sulphur (0.39%). The carbon content may comprise of hydrocarbon from the polysacharide chains as the EDX analysis showed that the surface of the biomass was mainly comprise of organic compounds. Besides, the presence of sulphur content in the biomass although in low amount, it did not favour the biofuels production due to the residue of sulphur affects in the combustion process and contributes to environmental pollution during the internal engine ignition [240]. On the other hand, **Figure 4-4c** reveals the EDX analysis on acid-treated microalgae biomass collected from HLBS. The sulphur content had been eliminated in the biomass as there was no detection. The acid treatment on microalgae biomass was aided in removing the sulphur and displaced them in the acids assisted disruptive solvent phase during the hybrid biphasic extraction system. The EDX analysis of the microalgae biomass characterised the elemental composition from the acid-treated biomass: carbon content of 61.3%, oxygen content of 33.2%, nitrogen content of 5.5% and potassium content of 0.12%. The sulphur content was not detected while the nitrogen was appeared as one of the majot constituents.

4.4. Conclusions

In summary, 155 mg/L of molasses concentration medium obtained the highest biomass rate. The COD, TSS and brix reduction were 61.48%, 63.94% and 48.08%, respectively. Subsequently, an acid-assisted HLBS approach was used in extracting lipids from microalgae *C. sorokiniana CY-1* biomass in this study. This novel extraction strategy showed potential to significantly reduce or eliminate sulphur content and effectively disrupt the polysaccharides in the microalgae biomass. The optimised conditions of the HLBS resulted in 92.84% lipids recovery yield; with 15% nitric acid (aprotic), disruptive solvent to organic solvent ratio of 1:3, thermal condition of 80 °C and contact time of 4 min. This study contributes to the prospects of HLBS as a rapid and cost-effective separation method for biofuels production.

5. Thermal-Fenton mechanism with sonoprocessing for rapid non-catalytic transesterification of microalgal to biofuel production



This chapter has been covered the high intensity of cell disruption method with rapid transesterification process from the microalgae biomass. The procedure is potential replacing the conventional biofuel conversion from the lipid compounds by ultra-sonication. The effect of various parameter for study the hydrocarbon chains of fatty acids methyl ester has been verified through gas chromatography (GC) flame ionization detector (FID) mainly to replace for the catalyst based of transesterification substances. This chapter consists of the thesis-version of the manuscript published in the Chemical Engineering Journal (Yew G. Y. et al., 2020, Chemical Engineering Journal, 127264).

Abstract

This study has investigated on two objectives which are enhancing the microalgae *Chlorella sorokiniana CY-1* cell disruption mechanism using thermal Fenton reaction and performing non-catalytic transesterification by ultra-sonication method. Radicles generated by Fenton reaction are rapid, dynamic, and the reaction was assisted by thermal heating to optimize the kinetic of the radical generation by obtained the lipid recovery at 53.3% and 977.41 mg/g at 36.5 ºC with 4 min of contact time. The conversion of lipid into fatty acid methyl esters (F.A.M.E) through rapid non-catalytic transesterification using ultrasound was also performed. The significant parameters were done by varying the ratio of methanol to lipid, duration and pulse mode of sonication, to optimize the bonding reaction with methyl ester compound to free fatty acids. The formed of hydrocarbon chains with C4, C6, and C10 at 8.20 mg/g, 0.33 mg/g, and 0.24 mg/g respectively. This is a promising method as it is marketable and can be conducted in large scale with substantial improvement on the process yield of F.A.M.E in a rapid manner.

Keywords: Rapid processing, Non-catalytic Transesterification, Biofuel, *Chlorella sorokiniana*

5.1 Introduction

Microalgae are known as third generation of biofuel as promising green and sustainable fuel supply for mitigating environmental pollution and crude oil depletion issues [39, 50]. In general, it is part of the carbon neutral fuel that can be categorized into four different generations, where microalgae as the third generation biofuel has one of the most intensive research organism in lipid extraction for biofuel applications [19]. The steps for pre-treatment of microalgae through cell disruption depends on the cellular membrane structure, moisture content, and amount of biomass. Chemical pretreatment such as Fenton reaction method that utilizes solvent has a great advantage of high surface contact compared to mechanical methods like bead milling, centrifugation and homogenization in microalgae biofuel-related industry.

Fenton reaction is an effective chemical solvent reaction involving ferric (II) ion and radicles suitable for microalgae lipid extraction in large scale [18, 193, 241]. The primary intention is to utilize ferric ion and H_2O_2 to generate hydroxyl and peroxyl radicals for an effective disruption of microalgae cell wall to release the lipid compounds [242]. Thermal Fenton reaction in the process involves the application of heat energy for homolysis molecule bond that promotes radical's generation in the solution as the temperature rises [243]. The H_2O_2 contact with temperature assists the reaction by enhancing the kinetic for homolysis dissociation reaction of radicles propagation especially for forming

of OH radicles within the duration period. According to Igor et al., [244] temperature may contribute to reduce the half-life of the H_2O_2 by at least 8.5 folds, where this enhances the homolytic cleavage rate causing the Fenton reaction to release radicles such as hydroxyls ($OH^{\cdot}$) and peroxyls ($OO^{\cdot}$) compound in a shorter time and significantly contributing to the rapid extraction process.

The primary research involves the introduction of thermal Fenton reaction in hybrid liquid biphasic system (HLBS) as a cell disruption phase for microalgae *Chlorella sorokiniana CY-1*. Thermal energy will raise the temperature of the disruptive solution containing Ferric ion, Fenton reaction is Fe^{2+} with H_2O_2 where the ferric ion would rapidly expand with heat energy assisted causing the homolytic reaction to occur [245, 246]. The equation of Fenton system depends on the ferrous ions react with hydrogen peroxide (reagents) which will produce hydroxyl radicals with powerful oxidizing features to disrupt microalgae cell wall as shown in Eqs. (5-1 to 5-5)

$$H_2O_2 + Fe^{2+} \rightarrow OH^{\cdot} + OH^{-} + Fe^{3+} \quad (5\text{-}1)$$

$$OH^{\cdot} + RH \rightarrow R^{\cdot} + H_2O \quad (5\text{-}2)$$

$$R^{\cdot} + 2H_2O \rightarrow ROO^{\cdot} + H_2 \quad (5\text{-}3)$$

$$ROO^{\cdot} + Fe^{3+} \rightarrow R^{+} + Fe^{2+} + O_2 \quad (5\text{-}4)$$

$$Fe^{2+} + OH^{\cdot} \rightarrow Fe^{3+} + OH^{-} \quad (5\text{-}5)$$

The HLBS in this experiment involves thermochemical methods where the combination of two different phases properties of solvent with thermal assisted in a single system is applied [18]. The extraction phase uses non-polar organic solvent with high hydrophobicity to dissolve the oil/lipid from the microalgae biomass. The contribution of organic solvent and radicles which is able to dissolve lipid and organic based compound, followed by saponification, transesterification or esterification process with the acid or alkaline substances added as catalyst for conventional biofuel production [247, 248]. The role of catalyst is to accelerate the overall biofuel production by breaking triglyceride chains of hydrocarbon from the glycerol molecules [249]. However, the challenges that are encountered by the catalytic process includes high cost of the catalyst, chemical properties tend to easily change, molecules stability, difficulties in separation and purification of the end product of biodiesel, with these issues the research direction have diverted the focus on the application of non-catalytic method [250-252].

Another part of this research is the introduction of the non-catalytic transesterification reaction that does not involve any catalyst in the biofuel conversion process from lipid into biofuel. This reaction can reduce the energy usage, unstable activity and multiplex ties of the separation process [253]. The utilization of ultrasound as a non-catalytic transesterification equipment involves high frequency waves for replacing organic alkyl group from the microalgae lipid with methyl alcohol [254, 255]. This saves the cost for the catalyst material

and purification process which is one of the most energy intensive procedure. Besides, the biofuel products from non-catalytic process can neglect the impurities that would otherwise be contaminated from the catalyst materials [254, 256, 257]. It also helps save time and cost for the overall lipid conversion to fatty acids methyl ester (F.A.M.E) in the biofuel production process. In this study, there are two innovations which is thermal Fenton reaction to enhance the lipid production and extraction duration where may effectively applicable in large scale of HLBS. Subsequently, non-catalytic transesterification for converting lipid into biofuel.

The disruptive phase in HLBS by thermal Fenton reaction optimizing as followed: various contact temperature in disruptive phase with only H_2O_2, concentration of $FeCl_2$ for Fenton reaction at room temperature, ratio of disruptive phase and extractive phase in HLBS, dosage of $FeCl_2$, various contact time, various amount of biomass, and co-optimizing concentration of $FeCl_2$ with various temperature. Subsequent objective is to study the non-catalytic transesterification via ultra-sonication technique through ratio of methanol, duration, and pulse of ultrasound transmitter.

5.2 Materials and methods

5.2.1. Materials

Ferric (II) chloride ($FeCl_2$), hydrogen peroxide (H_2O_2), hexane (C_6H_{14}), methanol (CH_3OH), sodium hydroxide (NaOH), and methyl non-decanoate were purchased from R&M chemicals (Malaysia). The triglyceride mixture for lipid standard and fatty acid methyl ester (F.A.M.E) (C4-C24) neat form were purchased from Sigma Aldrich (USA). All chemicals and solvents used were analytical grade.

5.2.2. Microalgae biomass cultivation and medium composition

The microalgae strain *C. sorokiniana CY-1* biomass was used in this work due to high lipid content. Stock culture was prepared using BG-11 medium which contains $NaNO_3$ 1.5 mg/mL; K_2HPO_4 0.03 mg/mL; $MgSO_4 \cdot 7H_2O$ 0.075 mg/mL; citric acid 0.006 mg/mL; $NaCO_3$ 2.0 mg/mL; $CaCl_2 \cdot 2H_2O$ 3.6 mg/mL; Ferric ammonium nitrate 0.6 mg/mL; EDTA·2Na 0.1 mg/mL; H_3BO_3 2.86 mg/mL; $MnCl_2 \cdot 4H_2O$ 1.81 mg/mL; $ZnSO_4 \cdot 7H_2O$ 0.222 mg/mL; $Na_2MoO_4 \cdot 2H2O$ 0.39 mg/mL; $CuSO_4 \cdot 5H_2O$ 0.079 mg/mL; $Co(NO_3)_2 \cdot 6H_2O$ 0.049 mg/mL. The pre- and batch culturing were conducted using an indoor photobioreactor (PBR) as reported in a previous work [197], consisting of 250 mL bottle and 1 L glass vessel respectively. The PBR was aerated by air compressor with additional of 4% of compressed CO_2 purchased from Linde (Malaysia) through filtered air (0.45 µm air filter). The PBR was illuminated with external LED light sources

with a light intensity of 220 μmol/m^2/s on parallel sides of the glass vessel. Light intensities were measured by LI-250 light meter with LI-190SA pyrometer sensor (LI-COR, INC., Lincoln, USA). The rotational magnetic stirrer was agitated with a speed of 300 rpm. The culture broth was aerated at a rate of 0.5 vvm (volume gas per working volume per min). The microalgae biomass obtained from these cultivation condition fulfills all experimental needs.

5.2.3. Determination of biomass and nitrate concentration

The microalgae biomass cell and nitrate content in the medium were detected as previous works [18, 258]. The microalgae biomass was measured at optical density of 680 nm, the days for harvested was approximately 7-14 days to reach a constant level. The harvested microalgae culture broth was then centrifuged at 7000 rpm for 15 min and the clear supernatant was discarded. The wet biomass was used for conducting the extraction studies. The samples were then further diluted with deionized water and determination of nitrate content was conducted using UV-vis spectrophotometer (UV-1800, Shimadzu) at the optical density of 220 nm. The microalgae biomass was then stored in the freezer at -20 °C for 24 h before conducted the experiment.

5.2.4. Fenton reaction for HLBS and oil/lipid determination

The overall mechanism of thermal Fenton HLBS was generated by adding microalgae *C. sorokiniana CY-1* biomass followed by H_2O_2 with $FeCl_2$ to create

a Fenton reaction for cell disruption in a minimum of 1 min time of contact exposed to low lighting environment condition at 5 μmol/m^2/s by florescent light. Subsequently, organic solvent of hexane was added to dissolve the lipid in set ratio as extractive solvents. The amount of lipid triglyceride was optimized through UV-vis spectrophotometer at 225 nm with pre-calibrated plot at OD_{225} [18]. The samples were analyzed by gas chromatography (Perkin Elmer Clarus 690 GC) with flame ionization detector (GC-FID). The samples were injected with helium 3.0 mL/min into Agilent Technologies analytical laboratory instrument column (30 m × 0.25 mm × id 0.25 μm), column oven temperature at 35 ˚C for 3 min, then increased to 220 ˚C with increment of 4 ˚C/min and held at 220 ˚C for 35 min, injector and detector temperature were set at 250 ˚C and 260 ˚C respectively. The flowrate at continuous mode with carrier gas (helium) was controlled at 103.4 kPa. **Table 5-1** shows the operating parameter and conditions throughout the experiment.

Table 5-1: Operating parameters and conditions

No.	Operating parameter	Initial condition	Variables	Unit
1	Contact temperature	25.5	25.5, 30.5, 32.5, 34.5, 36.5, 38.5, 40.5, 42.5	˚C
2	$FeCl_2$ concentration	1	1, 2, 3, 4, 5, 6, 7, 8, 9	%
3	Ratio of solvents – Cell disruption solvent: Organic solvent (with solvent volume of 3 mL and 1 mL)	1:0.33	1:0.33, 1:0.6, 1:0.67, 1:0.75, 1:1, 1:1.33, 1:1.67	-
4	Dosage of 5% $FeCl_2$	1	1, 2, 3, 4, 5, 6	µL/g
5	Contact time	1	1, 2, 3, 4, 5, 6	min
6	Biomass amount	10	10, 20, 30, 40	mg
7	Temperature and concentration of the disruptive phase solvent	25.5/1	25.5, 30.5, 32.5, 34.5, 36.5 and 1, 2, 3, 4, 5, 6	˚C/%
8	Methanol volume	1:0.5	1:0.5, 1:0.25, 1:0.17, 1:0.125	mL
9	Duration	2	2, 4, 6, 8, 10	min
10	Cycle of the ultrasound emission rate (per 1 min)	0.4	0.4, 0.6, 0.8, 1 (continuous)	-

5.2.5. Total lipid analysis

The total lipid content in the microalgae biomass was determined using established methods [219, 259]. The microalgae biomass 20 mg (± 0.3 mg) was shifted into a 10 mL centrifuged tube. A total of 3 mL of the solvent mixture, chloroform:methanol (2:1, v/v) was added. The solution was heated to 60 ˚C for 1 h, followed by addition of 0.9% NaCl solution in 20% volume of the solution. The mixture was vortexed and a biphasic layer will form. The upper phase was pipetted out while the lower phase which contains lipids was dried by a mild stream of nitrogen gas. The total weight of the lipid extract was measured.

5.2.6. Determination of recovery yield and ratio in weight

The lipid recovery yield (R) from the total lipid content was represented by Eqn 5-6 as below:

$$\text{Recovery yield, R (\%)} = \frac{\text{Total lipid recovered in organic solvent pha}}{\text{Total lipid content in microalgae biomass}} \times 100\% \quad (5\text{-}6)$$

The non-disruptive biphasic system was completed by dissolving the biomass with the distilled water at room temperature condition and added organic solvent for extraction.

$$\text{Ratio in weight, (mg/g)} = \frac{\text{Weight of fatty acids (mg)}}{\text{Weight of microalgae biomass (g)}} \quad (5\text{-}7)$$

where weight of fatty acids from extracted lipid in (mg) through non-catalytic transesterification method represent the optimized experiment of lipids and weight of biomass (g). Each test was analyzed for three repetitive individual samples of *C. sorokiniana CY-1*.

5.2.7. Numerical studies of lipid extraction from microalgae biomass

The extraction solvent was perfectly agitated, the major mass resistance during the extraction process was the internal diffusion of the lipid within the microalgae biomass [256]. In this case, the extraction process was modelled according to the Fick's second law of diffusion. There are several assumptions taken prior in the simulation [260].

a. Microalgae biomass powder were regarded as spherical geometry and lipids were homogeneous distributed. The radius of the microalgae biomass was 50 μm.
b. The diffusion coefficient of the lipid consistence throughout the extraction process. While the lipid content in the biomass changed with time and position.
c. No external mass resistance was taken into consideration due to external agitation.

The diffusion equation for spherical geometry is written as:

$$\frac{\partial C_S}{\partial t} = D_e \left(\frac{1}{x^2} \frac{\partial}{\partial x} \left(x^2 \frac{\partial C_S}{\partial x} \right) \right) \quad (5\text{-}8)$$

where C_s is lipid concentration within the particle (g/m^3), De is effective diffusion coefficient for lipid (m^2/s), x is radial distance in the diffusion direction (m), and t is time (s).

The initial conditions are $C_s = C_{s,0}$ lipid in solid phase without dissolve in the solution and $C_L=0$ in liquid phase. $C_{S,0}$ is the initial concentration of the lipid in microalgae biomass (g/m^3) and C_L is the concentration of lipid in solvent (g/m^3).

The boundary conditions for Eq. as below [260]:

$$\left(\frac{\partial C_S}{\partial x} \right)_{x=0} = 0 \quad (5\text{-}9)$$

$$-D_e A \left[\frac{\partial C_S(x,t)}{\partial x} \right]_{x=r} = V \frac{dC_L(t)}{dt} \quad (5\text{-}10)$$

Where A is the surface area of biomass (m^2), V refer to solvent volume used during extraction process (m^3), r is radius of microalgae biomass (m).

The model was solved using 1-D parabolic and elliptic PDEs (pdepe) function in Matlab, R2010a (The Mathworks, Inc., MA, USA) aforementioned as parabolic partial differential equation [261]. The original differential equation (Eq.5-8) were integrated in time and solved using pdepe solver to discretized spatially of the lipid in the biomass. The D_c value was adjusted iteratively to fit

the actual experimental data, hence root mean square error (RMSE) as followed for validate the estimation.

$$\mathrm{RMSE}(\mathrm{g/m^3}) = \sqrt{\frac{1}{n}\sum_{i=1}^{n}\left[C_{S,p}(t) - C_{S,e}(t)\right]^2} \qquad (5\text{-}11)$$

Where $C_{S,e}$ and $C_{S,p}$ are the experiment and estimation value respectively for lipid content in the microalgae biomass (g/m^3), n is number of experimental samples value.

The optimized D_c value was obtained for 3 statistical indicators including R^2 for coefficient of determination, RMSE and absolute average deviation (AAD) were calculated based on the experimental data and predictive data of the extracted lipid from Fenton hybrid liquid biphasic system for validation.

$$R^2 = 1 - \frac{\sum_{i=1}^{n}(Y_e - Y_p)^2}{\sum_{i=1}^{n}(Y_e - Y_m)^2} \qquad (5\text{-}12)$$

$$\mathrm{RMSE}(\mathrm{mg/g\ DM}) = \sqrt{\frac{1}{n}\sum_{i=1}^{n}\left[Y_p(t) - Y_e(t)\right]^2} \qquad (5\text{-}13)$$

$$\mathrm{AAD}(\%) = \left[\frac{\sum_{i=1}^{n}(|Y_e - Y_p|)/Y_{S,e}}{n}\right] \times 100 \qquad (5\text{-}14)$$

The Y_e, Y_p, Y_m refer to prediction value based on actual data of the lipid extraction yield respectively (mg/g DM). Y_m is the mean value for lipid extract (mg/g DM). Following the numerical simulation results, the lipid extract is within the microalgae biomass at various stage of diffusion visualized through Matlab.

The basic kinetic energy analysis on the HLBS system based on the hydroxyl radicles created by Fenton reaction as Eq. (5-15) assumption constant acceleration from mass of radicles from rest to final velocity. Formation of cavitation (effervescent) and within the cavitation bubble contain low pressure, high velocity state of particles where generated through Fenton reaction. According to Sergey et al., [262], OH radical emission may not be populated but based on the kinetic theory it may raise of the rate of collision as the thermal energy increases proportionally.

$$v = \sqrt{\frac{3kT}{m}} \qquad (5\text{-}15)$$

The k_B, as the Boltzmann constant 1.38×10^{-23} m^2 kg s^{-2} K^{-1}, T, as the temperature in Kelvin, m, as kg mass of hydroxyl radicles (·OH), v, as velocity of cleavage uncharged particles or atom.

5.2.8. Non-catalytic transesterification

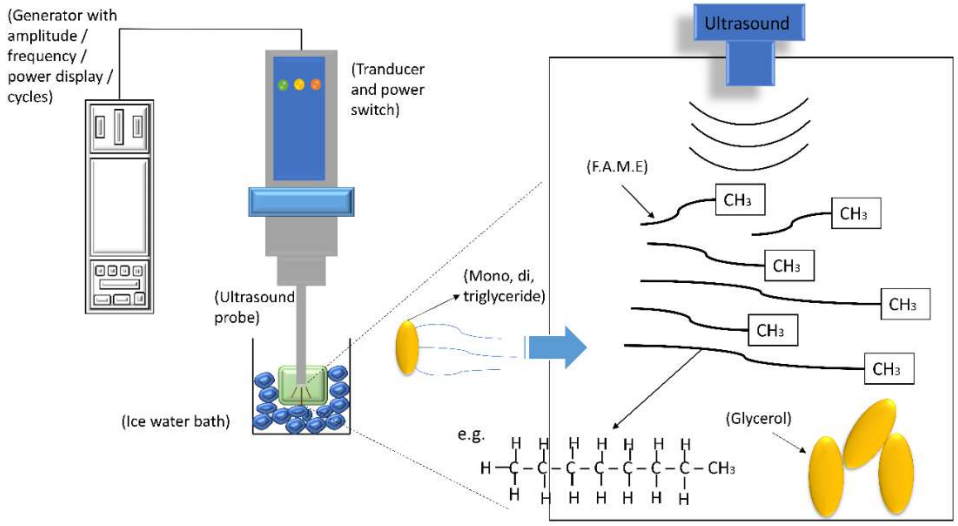


Figure 5-15: The non-catalytic transesterification of microalgae lipid through thermal Fenton reaction in HLBS.

A ratio of 1:6 of lipid/oil to methanol (1 mL:6 mL) mixture was transferred into the 50 mL beaker. The ultrasonic processor (Hielsher, UP400S) with a standard sonotrodes H22D was used and set as **Figure 5-1**, the processor operated at an initial power of 400 W, 25 kHz in a 0.4 cycle. The operation was conducted at batch mode in room temperature and atmospheric pressure condition.

5.2.9. Statistical analysis

The statistical analysis of the experimental data was presented the average of triplicate readings. Data was subjected to one-way factor ANOVA using SPSS to determine the significant differences where ($p \leq 0.05$). The standard error was calculated for the experimental data with three times of repeated experiment cycle.

5.3. Results and discussion

5.3.1. Optimization study of Fenton reaction in HLBS

5.3.1.1. Effect of temperature contact in HLBS

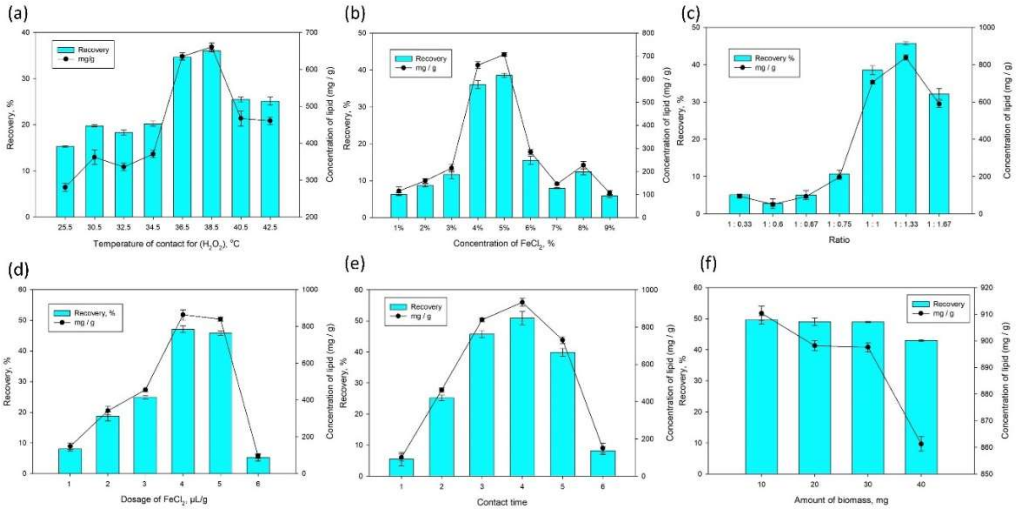


Figure 5-16: **(a)** Effect of various temperature (25.5 °C, 30.5 °C, 32.5 °C, 34.5 °C, 36.5 °C, 38.5 °C, 40.5 °C, 42.5 °C) of disruptive solvent (H_2O_2) for the study of lipid recovered and concentration of lipid from *C. sorokiniana CY-1* . Other operating conditions: concentration of H_2O_2 of 30% w/w, organic solvent hexane 85%, volume ratio of solvent 3 mL:3 mL, contact time 3 min, and biomass amount at 30 mg. **(b)** Effect of various concentration of $FeCl_2$ (1% - 9%) on disruptive solvent (H_2O_2) for the study of lipid recovered and concentration of lipid from *C. sorokiniana CY-1*. Other operating conditions: concentration of H_2O_2 of 30% w/w, organic solvent hexane 85%, volume ratio of solvent 3 mL: 3 mL, contact time 3 min, 5 µL/g $FeCl_2$, and biomass amount at 30 mg. **(c)** Effect

of various ratio of solvent with average for 1=1mL, 3mL (disruptive: organic solvent) for the study of lipid recovered and concentration of lipid from *C. sorokiniana CY-1* . Other operating conditions: concentration of H_2O_2 of 30% w/w, organic solvent hexane 85%, contact time 3 min, 5% of $FeCl_2$, 5 µL/g $FeCl_2$, and biomass amount at 30mg. **(d)** Effect of dosage with 5% $FeCl_2$ on disruptive solvent (H2O2) for study of the lipid recovered and concentration of lipid recovered from *C. sorokiniana CY-1*. Other operating conditions: concentration of H_2O_2 of 30% w/w, organic solvent hexane 85%, contact time 3 min, ratio 1:1.33, and biomass amount at 30 mg. **(e)** Effect of time of contact on disruptive solvent (H_2O_2) for the study of lipid recovered and concentration of lipid from *C. sorokiniana CY-1*. Other operating conditions: concentration of H_2O_2 of 30% w/w, organic solvent hexane 85%, ratio 1:1.33, 4 µL/g 5 % $FeCl_2$, and biomass amount at 30mg. **(f)** Effect of biomass amount on disruptive solvent (H_2O_2) for the study of lipid recovered and concentration of lipid from *C. sorokiniana CY-1*. Other operating conditions: concentration of H_2O_2 of 30% w/w, organic solvent hexane 85%, ratio 1:1.33, time of contact 4 min, and 4 µL/g of 5 % $FeCl_2$.

The range of the temperature contact for the disruptive solvent H_2O_2 from room temperature 25.5 °C to 42.5 °C have found the lipid recovery value a leap started at 30.5 °C, therefore with an interval of 2 °C were studied for the lipid recovery yield. The disruptive solvent (H_2O_2) at the bottom phase for variation contact of temperature had enhanced the reaction on the system for optimizing the cell disruptiveness mechanism. The recovery yield and concentration of the lipid

from biomass in the system is shown in **Figure 5-2(a)**. The highest recovery value was perceived at 38.5 °C with 36.04% of lipid recovered. This was followed by the temperature 36.5 °C and 40.5 °C, both temperatures obtained slightly lower recovery with H_2O_2, as the recovery of lipid at 34.63% and 25.47% respectively. The concentration of lipid from 38.5 °C in the disruptive solvent was appeared to be higher compared to 36.5 °C and 40.5 °C, while the highest concentration of lipid for 38.5°C was 660.67 mg/g. The temperature raises influenced the kinetic of the disruptive solvent of H_2O_2 for the radical propagation to generate hydroxyl radical within 3 min, in which it will interact on the microalgae cell wall and subsequently caused disruption to release the lipid compound [263]. Hydroxyl radicals may disrupt the cellular wall mainly the structure of polysaccharides. The polysaccharides are part of the compound found in cell wall also with the purpose of contributing the energy storage for sustaining the cell [210]. The lower temperature range may affect for the radical's disruptive performance as the lipid recovery yield was not higher than 30% for 25.5 °C, 30.5 °C, 32.5°C, and 34.5 °C. The rate of reaction for H_2O_2 will reduce the effectiveness for disruption in 30% of concentration. In lower temperature in terms of thermal energy where it affect the radical generation and propagation rate which is relatively lower compared to higher temperature of contact [264]. Higher temperature as 40.5 °C and 42.5 °C, shown lipid recovery yield dropped to 25.47% and 25.12%, respectively. This may cause peroxidation of the lipid compound by over generating the radical from the disruptive solvent

and also the thermal effect degrades the lipid compound that would cause for the reduction for the lipid recovered value. The temperature is selected based on the highest lipid yield as the room temperature condition is 57.5% lower than the temperature in 38.5° C. The statistical analysis shows the effect of temperature on H_2O_2 was significantly affected for the lipid recovery and concentration of lipid ($p \leq 0.05$). Overall, the selected temperature for pure H_2O_2 is at 38.5 °C, the subsequent parameter is to study the addition of $FeCl_2$ for induce the Fenton reactions for radical generation.

5.3.1.2. Effect of $FeCl_2$ concentration on H_2O_2 in HLBS

The addition of $FeCl_2$ into the disruptive solvent of H_2O_2 is a vital parameter for Fenton reaction to enhance cell disruption in microalgae. $FeCl_2$ concentration reacts in the H_2O_2 for releasing lipid from the cell membrane. The range of $FeCl_2$ concentration range from 1% - 9% was investigated as shown in the **Figure 5-2(b)** for different lipid recovered and concentration of lipid. The highest lipid recovered and concentration of lipid were achieved at 5% with the value 38.55% and 706.73 mg/g respectively. The recovered of lipid reaches the peak at 5% where 1% to 4% are gradually increases until the peak before the yield dropped. There is fluctuation from the concentration of $FeCl_2$ at 6% to 8% depending on the external factors such as, photometric value from the environment affecting the radical's interaction of the reaction. Less amount of $FeCl_2$ may cause less aggressiveness of the radical propagating and causes the reaction to disrupt the

biomass, while overly adding of the $FeCl_2$ may cause degradation of the lipid compounds. The recovery of lipid showed a difference of 32.71% comparing the highest recovery yield at 5% and the lowest at 9%. Moreover, the lipid recovery yield improvement is at 2.51% compared from 38.5 °C for non-additive of $FeCl_2$ in the solution. The cell disruption of microalgae cells through reacting of Fe^{2+} ions with H_2O_2 to produce reactive oxygen species (ROS) OH^* to react with the cell wall mostly comprise of polysaccharides, cellulose, glycoproteins, glycolipid and phospholipids [193, 265]. Hence, the studies of different concentrations of $FeCl_2$ for disrupting cell wall through advance oxidation process (AOP) by Fenton reaction may assist in disruption and enhanced the lipid recovery [266], particularly for contributing in lipid extraction for the HLBS. The advance oxidation process has minimum toxicity from the reaction process, less residues and conditions are easy to accomplish [267, 268]. However, excessive of the concentration for $FeCl_2$ may propagate excess Fe^{2+} radicals which will degrade the lipid compounds, causing fluctuations of lipid recovered. The statistical analysis shows that the concentration of $FeCl_2$ was significantly affected the concentration of lipid recovery and concentration of lipid value ($p \leq 0.05$). The optimum concentration of $FeCl_2$ is at 5%, the subsequent parameter to be tested will be the ratio of the solvents.

5.3.1.3. Effect of ratio solvents in HLBS

The solvents for both organic solutions have very low miscible rate where both mixtures will not form a homogeneous solution in different proportions. However, lipid will tend to rise in the upper surface of the disruptive solvent due to density difference and further dissolve into the solution. There are experiments on the biphasic system for water-immiscible organic solvent for extracting furfural with optimum aqueous-to-organic phase ratio to enhance the extraction [269]. The effect of solvents ratio shown in **Figure 5-2(c)** was studied for the range 1:0.33, 1:0.6, 1:0.67, 1:0.75, 1:1, 1:1.33 and 1:1.67 for ratio of disruptive solvents to organic solvent recovery of lipid from *C. sorokiniana CY-1*. The recovery yield of lipid was found as the highest at the ratio of 1:1.33, the recovery yield and concentration of lipid at 45.76% and 839.05 mg/g. At ratio of 1:0.6, the recovery found to be the lowest at 2.73 % and 50.05 mg/g, this indicated the increases of the disruptive solvent or organic solvent did not improve the lipid content but the optimum amount will extract the highest lipid compound from the biomass. The different between highest and lowest lipid recovery yield at 43.04%, where the concentration of lipid at 839.05 mg/g. The HLBS contains two different properties of solvents, disruptive solvent will be at the bottom phase for disruption mechanism to be occurred. The disruptive solvent will interact with the microalgae biomass to release the lipid compound through Fenton reaction to propagate the radicals to oxidize the wall membrane molecule e.g. polysaccharide [270]. The hydroxyl radicals ·OH produced by the

Fenton reaction will attract the polysaccharides based from the cell wall and release the compound in heterogeneous mixture into the solution. Furthermore, hexane is a non-polar solvent with high hydrophobicity, high interfacial tension, low viscosity, high selectivity toward lipid, and economical viable for large scale which is idea solvent choice for microalgae lipid extraction [271, 272]. The statistical analysis shows the various ratio of solvent was significantly affected the parameter lipid recovery and concentration of lipid ($p \leq 0.05$) The ratio of disruptive solvent and organic solvent are important in optimizing the lipid extraction from the HLBS, for ratio 1:1.33 has been selected as optimum ratio for further optimization in the subsequent parameters.

5.3.1.4. Effect of dosage for 5% $FeCl_2$ in HLBS

The addition of 5% $FeCl_2$ in the H_2O_2 for Fenton reaction in the solution to propagate radical to oxidize microalgae cellular wall molecule. The optimization was done in the range from 1 µL/g to 6 µL/g of $FeCl_2$ to recover the highest amount of lipid compound at the optimized concentration. Introducing higher volume µL of the $FeCl_2$ in a fixed concentration may lead to the increment of the amount for Fe^{2+} ion, and the previous parameter (ratio) have to be performed to alternate the volume of H_2O_2 in disruptive phase to propagate higher amount of hydroxyl radicals. Therefore, adjusting the reagent in µL/g is to refine the optimum radicals to be generated for the disrupting reaction. Dosage of the $FeCl_2$ result for lipid recovery yield and lipid concentration was shown in **Figure 5-**

2(d). The highest recovery and concentration of lipid at 4 µL/g where the value at 47.03 % and 862.29 mg/g respectively. The recovered of the lipid reduces when the dosage of $FeCl_2$ at 5 µL/g and 6 µL/g where the recovery drops to 45.77 % and 5.21 %. The low volume of $FeCl_2$ range from 1 µL/g to 3 µL/g shown lower lipid recovery and concentration of lipid. The hydroxyl radical which is an effective method to cause disruption for the polysaccharides and productivity for oil/lipid extraction [273]. The Fenton reaction is promoted by the amount of ions in deionized water from the metal compound. Radicals are the species contain at least one unpaired electron and appear as independent existence in the solution as an example for oxygen radical (OO^-), hydroxyl (OH^-), and peroxyl radical (ROO^-). The half-life for hydroxyl radical is 10^{-10} seconds, peroxyl radical 17 seconds, and hydroperoxyl radical (HO_2) 30 seconds where may form during the radical propagation in H_2O_2 reaction, it easily enter to the phospholipid bilayer [274]. The statistical analysis shows a significantly affected for the dosage of $FeCl_2$ in lipid recovery and concentration of lipid ($p \leq 0.05$) The dosage of 4 µL/g of 5% $FeCl_2$ been selected as the optimum lipid recovery for subsequent parameter.

5.3.1.5. Effect of time of contact in HLBS

The contact time for the microalgae biomass and disruptive solution is one of the important parameters that may affect the overall lipid recovered in terms of energy usage, yield, quality of the lipid extracted. Contact time of the phases

with Fenton reaction occurring in the solution may affect the disruptiveness as well as the lipid quality. **Figure 5-2(e)** shows the time of contact from 1 to 6 min. The highest lipid recovered yield and concentration of lipid at 4 min for 48.96% and 897.61 mg/g respectively. At 1 min the lipid recovered yield at 5.46% and 100.07 mg/g, which is the lowest value for both lipid recovery yield and concentration of lipid compared among the range of contact time. The concentration of lipid for time of contact at 1 min to 3 min are increasing until the peak at 4 min, after that the value significantly dropped. This indicate the optimum contact time may assist for effective cell disruption to release lipid compounds without degrading the molecular structure. The degradation of lipid products will turn them into lipid peroxides where it affects the stability of the biofuel as the lipid peroxide which is an unstable chemical compound may further trigger the radical chain reaction or cause NOx formation [275]. According to Steriti et al., the contact time at 3 min had recovered the cumulative data for the sum of monosaturated and unsaturated of lipid compound, in which had improved from the previous extracted lipids for single extraction at 17.4% [193]. The HLBS with simultaneous extraction method have assisted in recovering the optimum amount of lipid in the shortest amount of time with high lipid recovered. The pretreatment of cell disruption section has been attached with the extraction process, the forming of two different phase in the solution have reduce the tendency of lipid lost during the transferring procedure. The lipids dissolve in the organic solvent at the top phase of the system due to the

characteristic of non-polar organic solvent with low interfacial tension which is able to dissolve oil and lipid. Compared to the Soxhlet extraction method, the duration of time needed is about 2.5 to 14 h, while for hybrid biphasic extraction method has found to be relatively faster for lipid recovery [276, 277]. In engineering applicability aspect, it has reduced the process duration and the energy usage is lower compared to the method. The statistical analysis shows the time of contact have significantly affected for lipid recovery and concentration of lipid ($p \leq 0.05$). The time of contact is selected at 4 min to be optimized for next parameter.

5.3.1.6. Effect of biomass amount in HLBS

The HLBS could be affected by the biomass amount, as different amount of the microalgae biomass may disrupt the lipid recovery yields and concentration of lipid. In this parameter, the concentration for both organic solvents for hexane and disruptive solvent for H_2O_2 was fixed with constant amount of $FeCl_2$ for propagating the radical's reaction. The results shown in **Figure 5-2(f)** indicates different amount of microalgae biomass from *C. sorokiniana CY-1* in optimizing the parameters of the experiment. The highest lipid recovery yield was found at 10 mg where the lipid recovered at 49.66% while the concentration of lipid at 910.36 mg/g. The subsequent lipid recovered was found at 20 mg of biomass in the system where lipid recovered at 49.03% while concentration of lipid at 898.19 mg/g. According to Pinelo et al., [278], the extract recovered value can

be enhanced by the optimum solvent-to-solid ratio by 15%. The biomass in 30 mg and 40 mg cause the lipid recovery to reduce to 48.96% and 42.97%, respectively. The concentration of lipid from the amount of biomass obtained the highest for 10 mg at 910.36 mg/g and the lowest at 40 mg at 861.27 mg/g, the different amount of biomass for the highest and the lowest lipid recover yield showed a difference of 6.68%. Based on the study from Efthymiopoulos et al. [277], higher biomass or raw materials value conventionally will provide higher value for lipid or oil recovery through a maximum extraction duration. In HLBS, the condition of the experiment depends on the size of the system, an optimum amount of biomass will contribute to the effective cell disruption to release lipid compounds. However, according to Zhang et al. [252], too high ratio will cause excess of solvent and require a longer duration of extraction. The insufficient disruption of the cell wall will retain the lipid compound in the cells. Compared to the Soxhlet extraction method, the amount of biomass is manipulated by the reflux duration and cycles to obtain the equal amount of free fatty acids and triglycerides molecules [244, 276]. The scale-up of HLBS taken the consideration on the effect of different biomass amount and volume of the $FeCl_2$ to appropriate estimate of the production. The statistical analysis shows the amount of biomass loading have significantly affected lipid recovery and concentration of lipid. ($p \leq 0.05$). The difference of biomass amount been reported in Chew et al. [197], the extraction process will be affected by the quantity of the biomass amount and eventually lower the biomass quality

through the amount of free fatty acids (FFA). The hydrocarbon chain found in biofuel either long chain or short chain in which short chain of fatty acids may found lighter in density while longer chain have higher density [279]. The variation of the biomass amount would increase for the productivity of hydrocarbon chains, however with Fenton reaction the disruptiveness may affect the lipid hydrocarbon majorly in short to medium chains [280]. Hence, the amount of 10 mg has been selected as the amount.

5.3.1.7. Numerical studies and mathematical model simulation for optimized lipid extract

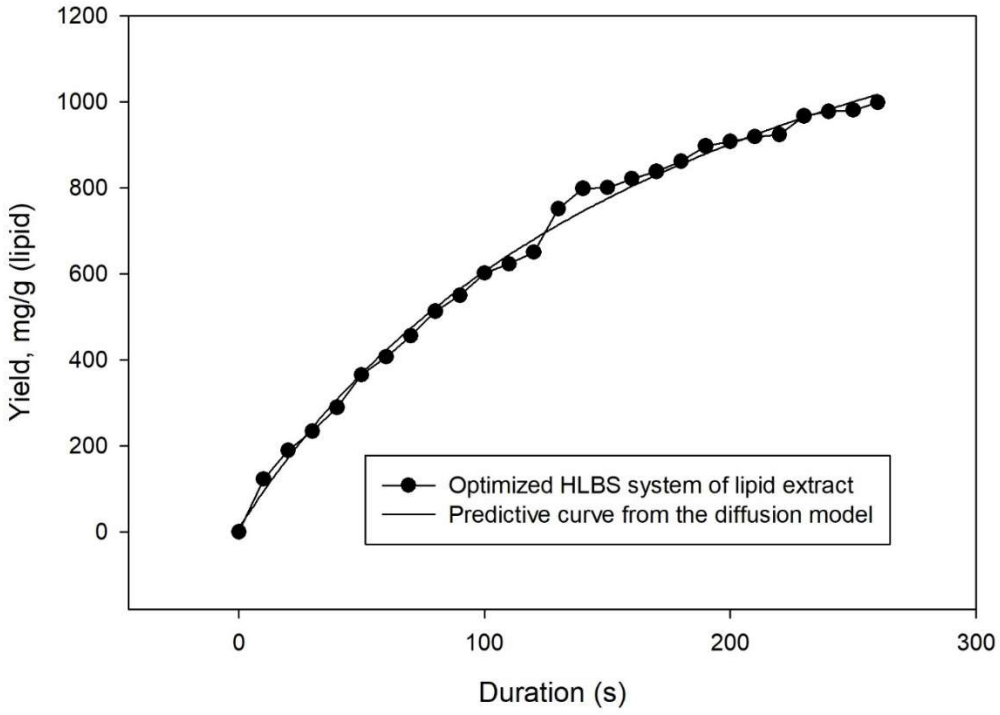


Figure 5-3: Optimized lipid extraction data co-relate to time with predicted values of lipid extraction using hexane. The lines representing the diffusion model.

Table 5-2: The diffusion of lipid extraction data and accuracy of the mathematical modelled

Solvent	De (m^2/s)	R^2	nRMSE (mg/g DM)	AAD (%)
hexane	2.58×10^{-6}	0.995	0.03	3.586

The experiment and model simulation result from the lipid extract kinetic are illustrated as in **Figure 5-3**. As the diffusion model has generated a high accuracy prediction model according to extraction process. Although there were divergences in some duration especially in the middle of the extraction period between 140 s to 180 s. Meanwhile the R^2 values is exceeded 0.96 and AAD values were relatively low as shown in **Table 5-2**. The optimum point from the predictive data is located at 260 seconds or 4 min 18 second where has been verified by the experiment data at 998.13 mg/g. According to the diffusion model was qualified to fit as a model for the extraction process and investigate the lipid yield mechanism at particular time duration for estimating the lipid yield amount.

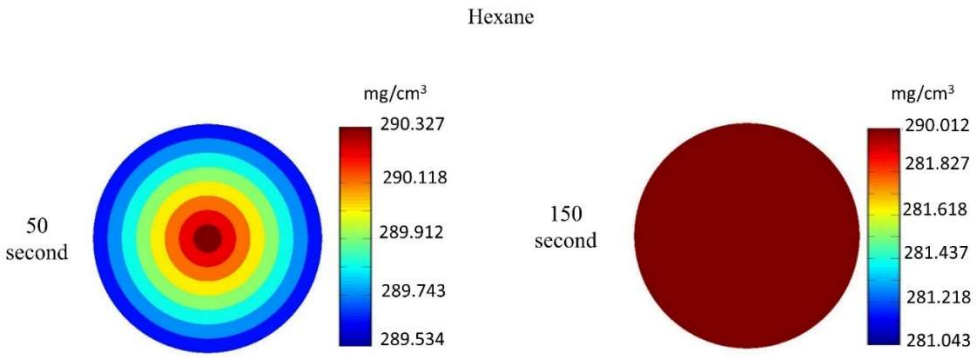


Figure 5-4: Distribution of lipid content within biomass powders during extraction using the numerical simulation results.

The distribution of the lipid content at the extraction duration 50 s, and 150 s were visualized in **Figure 5-4**. As the illustration shown relatively high concentration of gradient for microalgae lipid distribution within the biomass at 50 s from the extraction process using hexane as solvent. The extraction time and lipid concentration of gradient was increased according to time, once reached 150 second the diffusion is more than 290.012 mg/cm^3.

5.3.1.8. Effect of co-optimization of temperature and concentration for Fenton reaction

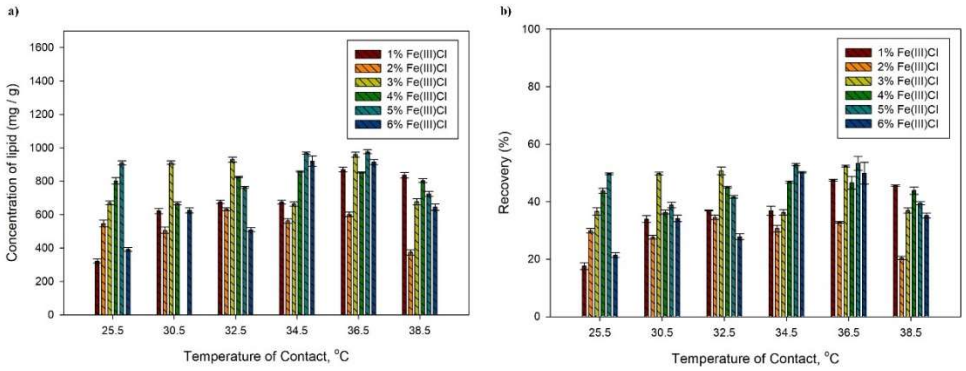


Figure 5-5: Effect of different concentration of $FeCl_2$ with varies temperature in disruptive solvent (H_2O_2) for the study of **a)** concentration of lipid (mg/g) from *C. sorokiniana CY-1*. Other operating conditions: concentration of H_2O_2 of 30% w/w, organic solvent hexane 85%, ratio 1:1.33, time of contact 4 min, 4 µL/g of $FeCl_2$, and biomass amount at 10 mg. **b)** lipid recovered % from *C. Sorokiniana CY-1*. Other operating conditions: Concentration concentration of H2O2 of 30% w/w, organic solvent hexane 85%, ratio 1:1.33, time of contact 4 minutes, 4 µL/g of varies FeCl2 and, and biomass amount at 10 mg.

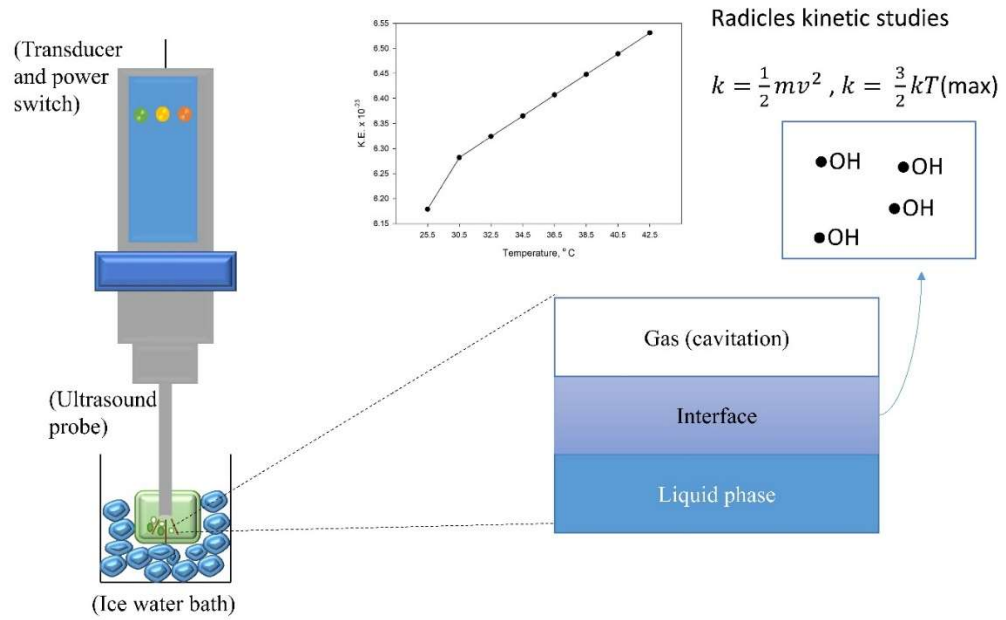


Figure 5-6: The kinetic study of hydroxyl radical's illustration between gaseous and liquid phase generated from the cavitation bubbles

The **Figures 5-5** showed the concentration of lipid in mg/g and lipid recovered in percentage for different concentration of $FeCl_2$ range from 1% to 6% in the H_2O_2 solution and variation of temperature for propagating the radical's generation. The thermal effect was created by soaking the biphasic system in a heated water bath to increase the reacting temperature. The radical generation rate is affected by temperature where higher temperature will generate more radicals [281, 282]. Temperature affects the chemistry of polymerization by controlling the chains stability of the unsaturated bond for formation of the

molecule network system. In the case of cell disruption from hydroxyl and peroxyl radical's reaction on the cell wall, the radical is initiating the disruptive mechanism. The highest concentration of lipid effect from **Figure 5-5(a)** shown 5% of $FeCl_2$ at 36.5 ^oC for 977.41 mg/g. The **Figure 5-5** indicate the higher the temperature and $FeCl_2$ concentration will increase the kinetic of the Fenton reaction. The kinetic will shorten the period of the radicles generation caused an effective disruptiveness in shorter time and releases the lipid compound into the solvents. In **Figure 5-5(b)**, the highest lipid recovered at 5% of $FeCl_2$ at 36.5 ^oC for 53.31 % of lipid recovered. The concentration and reacting temperature in the solution increase proportionally with the disruptive ability until the peak concentration at 5% in 36.5 ^oC. The higher radical's concentration in the solution compound may degrade or destroy the compound in the organic solvent. This indicates the concentration of $FeCl_2$ and temperature will increase the effective of the disruptiveness for the microalgae cells at the same time it will affect the lipid recovery. The free radicals generated from hemolytic reaction will produce scavenging activity that attracts the electron for bonding, this is further affected by the high temperature condition [283]. Electron from the cellular walled will be tearing or attracted by the radicals to form a stable molecule while the walled membrane will be disengaged from the walled membrane chains. As showed in **Figure 5-6**, the kinetic studies from the co-optimization parameters indicated thermal energy as one of the causes for altering atomic velocity from an uncharged atom or particles, based on the calculation from 25.5 $^{\circ}C$ to 38.5 °C

the velocity of an uncharged atom increased 2.70×10^{-11} ms^{-1} to $2.75 \times^{-11}$ ms^{-1} while kinetic energy raises from 6.18×10^{-21} joules to 6.45×10^{-21} joules, hence the raises of the kinetic would elevate the collision rate of the uncharged atom or radicals. The macroscopic observation from the effervescence reaction from the solution consists of the interface phase where radicals emerging in between liquid and gaseous state of the solution. The statistical analysis shows varies concentration of $FeCl_2$ with different temperature from the water bath have a significantly affected for lipid recovery and concentration of lipid ($p \leq 0.05$). Hence, the Fenton reaction is applicable as a disruption process for any microalgae species or microorganism with cellular wall membrane.

Table 5-3: Comparison on the list of strains and extraction methods with lipid recovered

Strain	**Methods**	**Lipid content % w/w**	**Conditions**	**References**
C. sorokiniana IAM-212	Carbonization and solvent extraction	19%	24 h, room temp.	[278]
C. vulgaris	Aqueous enzyme extraction	48%	1 h, 37 °C	[252]
C. zofingiensis	Folch method with acid tranesterification	51%	24 h, 50 °C	[255]
C. vulgaris	Soxhlet extraction	18%	14 h	[244]
C. vulgaris	Supercritical CO_2	17.70%	3h, 60 °C, 7000 psi	
Botryococus sp.	Microwave oven	32%	5 min, 100 °C	[284]
C. Sorokiniana CY-1	HLBS (thermal Fenton reaction)	53.31%	4 min, 36.5°C	This study

According to **Table 5-3**, in this study, the lipid recovered was 53.31% using 4 min of processing time at 36.5 °C, it is a relatively shorter duration with higher yield compared to aqueous enzyme extraction or Folch method. The Soxhlet extraction method used 14 h which is much longer in duration and yielded a lower lipid content compared to this study. Besides, the set-up for HLBS is simple and the operating equipment involved can be obtained and fabricated with ease compared to supercritical CO_2 and carbonization with solvent extraction processes. The operating temperature is also lower compared to microwave oven and other methods utilizing heat as well. In **Table 5-4,** the total energy input is 77.07 MJ where the cultivation was based on 14-day continuous cultivation followed by centrifugation, then extraction by thermal Fenton reaction with non-catalytic transesterification. Energy output based on the microalgae species with 29-55% of lipid content, producing 5,779.10 MJ of energy in 1% w/v of harvested biomass concentration [255]. This process energy profit ratio is 1.5 based on the energy output over input, hence, the ERP value of more than 1 signifies that the operation process is indeed profitable. Therefore, the economical aspect, based on the ERP value showed this laboratory scale is having a positive growth and it is a potential for the technique to be used in to industrial application.

Table 5-4: Energy profit ratio (EPR) based on energy input and output from microalgae lipid contain.

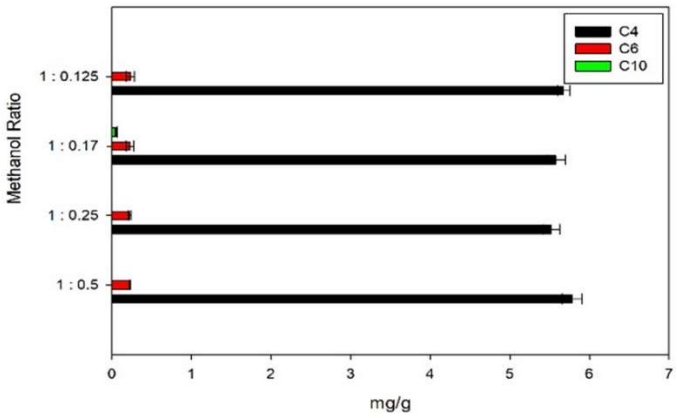
Energy Input			
Type	Watt (W)	Time (h)	Energy (MJ)
Fluorescence lamp	40.00	336.00	48.38
Air pump	20.00	336.00	24.19
Centrifuged,7500 x g, 10 min	180.00	0.17	0.11
Freezer	35.00	24.00	3.02
Ultrasound, 10 L , 4 min	70.00	0.07	0.02
Heater, 10 L, to 36.5 C	1,500.00	0.25	1.35
Total (Obtained)	1,845.00	696.48	77.07
Energy output			
Energy produced (MJ), 1% biomass	5,779.10		
Current biomass yield, %(w/v)	0.02		
[1]Total of 1 L biomass with 0.02%	115.58		
[2]Energy profit ratio (EPR)	1.50		

[1] Energy produced 1% biomass multiply by current biomass yield.

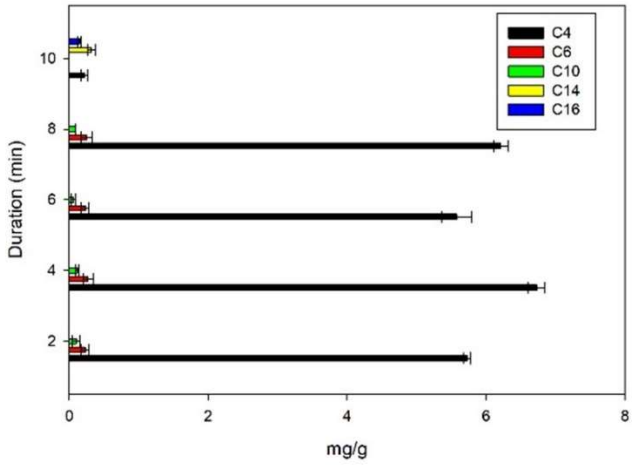
[2] Energy produced divided by energy obtained.

5.3.2 Optimization study for ultrasound in non-catalytic transesterification

(a)



(b)



(c)

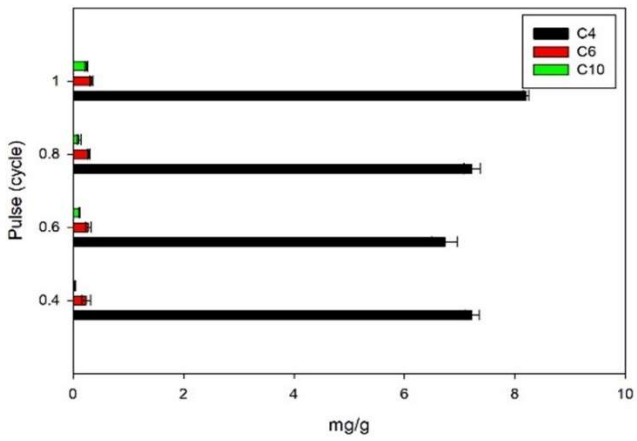


Figure 5-7: **(a)** Effect of methanol volume ratio for non-catalytic transesterification from ultrasound Hielsher, UP400S. Other operating conditions: amplitude 35%, pulse: 0.4 pulse (cycles), 6 mins, system volume at 7 mL, and 25 ^{o}C room temperature condition. **(b)** Effect of duration for non-catalytic transesterification by ultrasound. Other operating conditions: amplitude 35%, 0.4 cycles, oil: methanol volume ratio 1:0.17, system volume at 7 mL and 25 ^{o}C room temperature condition. **(c)** Effect of pulse (cycles) for non-catalytic transesterification by ultrasound Hielsher, UP400S. Other operating conditions: amplitude 35%, duration of 4 min, oil: methanol volume ratio 1:0.17, system volume 7 mL and 25 ^{o}C room temperature condition.

Table 5-5: Comparison of the catalytic and non-catalytic process specification

Types	Duration	Temperature	Yield	Ratio (Methanol : Lipid)	Reference
Catalytic (Zirconia-alumina/sulphated tin oxide)	20 h	200 -300 °C	90	40:1	[285]
Catalytic (La/Zeolite beta)	4 h	200 -300 °C	48.9	14.5	[286]
Catalytic (Ma-Al-CO3 HT)	12 h	180-210 °C	87	6:01	[287]
Lipase (7%, P.cepacia lipase)	18 h	37 °C	40.3 %	5:1	[288]
Non-catalytic Supercritical	5-10 min	~ 350 °C (43 Mpa)	50-95%	42:1	[289]
Non-catalytic Microwave	20 min	265 °C, 80 bar, 500W	27-95%	12:1	[290]
This study	2-10 min	25 °C, 24kHz, Continuous cycle	85.7 - 92.9 %	6:1	

5.3.2.1. Effect of methanol ratio for ultrasound in non-catalytic transesterification

The volume ratio plays a major role for the microalgae lipid converted into biofuel by using ultra-sonication as non-catalytic transesterification process. As shown in **Figure 5-7(a)**, the yield for F.A.M.E was found significantly for methyl compound such as methyl butyrate ($C_5H_{10}O_2$), methyl hexanoate ($C_7H_{14}O_2$), and methyl decanoate ($C_{12}H_{24}O_2$). Methanol is the primary solvent used in producing methyl ester compound and bond with the free fatty acid during the methylation reaction. The yield of F.A.M.E in ratio 1:0.17, in which is 6 mL of methanol to 1 mL of lipid, where methyl butyrate ($C_5H_{10}O_2$), methyl hexanoate ($C_7H_{14}O_2$), and methyl decanoate ($C_{12}H_{24}O_2$) at 5.58 mg/g, 0.23 mg/g and 0.057 mg/g respectively. The lowest yield of F.A.M.E found in ratio 1:0.25, oil to methanol ratio 1:4, C4 and C6 at 5.52 mg/g and 0.22 mg/g respectively. Molar ratio of alcohol to oil is one of the significant factors affecting the conversion yield of biofuels and production efficiency [284, 291]. According to Barakos et al., mentioned the higher methanol in the stoichiometric value would lead to more methyl ester formation [292]. The optimum amount of methanol volume ratio will reduce the waste or excess of methanol solvent in reaction from the oil compound, until a saturation point where optimum amount of free fatty acids formed of the methyl ester in the solution. Moreover, for triglyceride molecules with three major fatty acid chains, if the methanol solvent is less than 3 for stoichiometric ratio, it will not be optimum consuming the lipid or oil to

react towards the product side in the stoichiometric equation. According to Le Chatelier's principle, the range of molar ratio should be higher than the stoichiometric ratio of the reacting species in order to shift the reaction towards the product side [293]. **Figure 5-7(a)** shows that the higher methanol volume in the ultra-sonication based on non-catalytic transesterification method at 6 mL where it will increase the yield of medium-chain F.A.M.E. The increase in ratio of alcohol to oil affected the shift of the reaction toward yield of the F.A.M.E, this experimental finding matches with the reported information from [291] on ratio of oil to methanol of 1:0.17, which could make higher yield for the medium and a shorter chain of the hydrocarbon compared to the rest of the ratio. The volume ratio of the methanol of 1: 0.17 for methanol which has been chosen for subsequent test of the parameter for reaction duration.

5.3.2.2. Effect of duration for ultrasound in non-catalytic transesterification

The effect of different duration (min) indicates different yield for the non-catalytic transesterification by ultrasonic. The range of duration performed for the non-catalytic transesterification by 35% amplitude from the ultrasound probe are 2 min to 8 min in the system as shown in **Figure 5-7(b)**. The duration range within 8 min with the consideration of the polymerization of the lipid/oil compound during the reaction process as aromatic ring is one of the most common structure molecule in polymers will be generated if the duration

increased [294]. The highest amount of chains of F.A.M.E was found in duration of 4 min for C4, C6, and C10, where the weights found are 6.73 mg/g, 0.27 mg/g and 0.11 mg/g, respectively. On the other hand, the lowest yield was at duration of 6 min, there are C4 and C6, and C10 at 5.58 mg/g, 0.23 mg/g and 0.057 mg/g respectively. The detection of short chain for the F.A.M.E was found significantly in rapid transesterification by ultra-sonication method. The duration of the ultra-sonication for the solution have caused breakage in the chain of C-C bond from the long chains of hydrocarbon from lipid and oil, where they have the tendency to reform or rearrange from the unstable oxidized products [295]. The C6 and C10 are medium chains while C4 belong to short chains of the hydrocarbon. The total of medium chain hydrocarbon of the F.A.M.E (C6 and C10) yield is favorable as lighter hydrocarbon fuel such as jet fuel. The duration of the reaction at 10 min could yield long chains of the F.A.M.E for the microalgae lipid /oil in the methanol solution by ultrasonic non-catalytic transesterification method C4, C14 and C16 at 0.2 mg/g, 0.32 mg/g and 0.146 mg/g respectively. The intention of this work is to target medium and short chain of hydrocarbon, while, the higher the duration affects the yield shifting toward long chain of hydrocarbon of methyl ester. Pedersen et al [296], studied the fatty acids chain length by lipase-catalyzed found the most from the short and medium chain of hydrocarbon chains from species of Candida Antarctica B. Besides, the chain length of the fatty acid depends on the initial reaction rates and solubility of the lipid/oil in the solution [245]. With regard to this, studies

have found majority of short and medium chain of methyl ester compound below 8 min of non-catalytic transesterification by ultra-sonication in a 7 mL system. The duration of 4 min has been selected as the choice for subsequent parameter optimization due to short and medium range of hydrocarbon methyl ester being higher in market price and its suitability as jet-fuel combustion engine while 13 to 21 carbon atoms are considered as long chain of biofuels [297]. Reaction time plays an important role for engineering applicability and economic consideration for biodiesel production. In this experiment, reaction time as showed in **Table 5-5** vary in 2 – 10 min with microalgae lipid with methanol and constant power dissipation with same wave frequency (24kHz).

5.3.2.3. Effect of pulse for ultrasound in non-catalytic transesterification

The effect for pulse in the non-catalytic transesterification by ultrasound probe have affected the yield for different methyl ester hydrocarbon chains. In **Figure 5-7(c)**, it is seen that different pulse or cycles from the ultra-sonication from quarter cycle to full cycle (continuous) to obtain highest yield of F.A.M.E. The optimized yield is selected in continuous cycles where the C4, C6 and C10 hydrocarbon chains in the weights of 8.20 mg/g, 0.33 mg/g, and 0.24 mg/g respectively. The continuous cycles product equilibrium is shifting towards medium chains of carbon content where C6 and C10 with the total of 0.57 mg/g. The lowest yield of short and medium chain of hydrocarbon at cycles 0.4 gave a total of 7.62 mg/g, which is 13.17% lower compare to continuous cycle. Full

cycles are continuously emitting wave frequency, they will be more energy intensive and have a higher tendency of polymerization for the lipid or oil compound. The advantages of utilizing non-catalytic transesterification over the base catalyst are the reduced side effects for saponification reaction [298]. Non-catalytic transesterification has reduced the need of catalysts from the catalytic transesterification reaction and further separation of the catalyst can be neglected in the process as well. Therefore, the duration of time and cost from the separation equipment can be reduced significantly in the laboratory and possibly for pilot scale. In the catalytic transesterification process, to enhance the period of methylation in the biofuel production, concentrated acids have often been used for production to separate the triglyceride compound [298]. Short chains and medium chains been found as the major methyl ester compound in *C. Sorokianiana CY-1* through rapid non-catalytic transesterification method. Usually very small amount are contained in the biomass, due to certain heterotrophic growth of microalgae that utilize short chains of fatty acids in the cell membrane for metabolite purposes [299]. Moreover, the short chains of the methyl ester by GC-FID technique showed that none of the compounds eluted prior to the procedure described. In this experiment parameter, the selection would be at one cycle or continuous as the optimum pulse yield for the F.A.M.E for rapid non-catalytic transesterification method. Hence, this non-transesterification method is applicable for any lipid compounds and potential tools for producing F.A.M.E compounds without used of catalyst. The

limitations of this experiment method of non-catalytic process is limit to short and medium chains of hydrocarbon further investigation for long chains hydrocarbon production to be conducted. The main challenges of such technique is for consistency yield of the F.A.M.E compounds where highly depend on the nature of the raw material.

5.3.3. Characterization of transesterification of microalgae oil molecule bonding

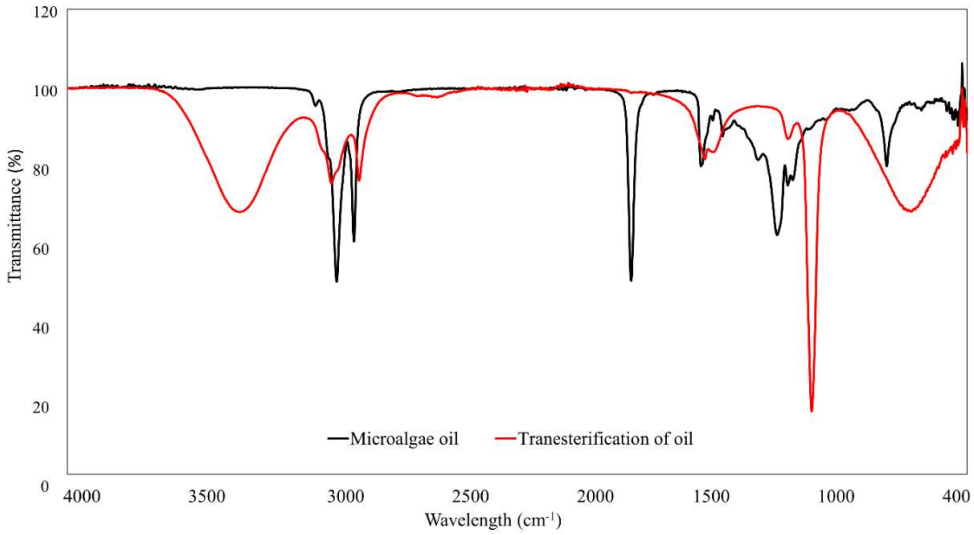


Figure 5-8: The overall absorbance spectra for microalgae oil and lipid via rapid transesterification reaction by ultrasound observed at wavelength range 400-4000 cm^{-1}

Table 5-6: Show compounds yield of saturated or polyunsaturated fatty acids from non-catalytic transesterification (HLBS/U.S.), dissolved of F.A.M.E in chloroform, catalytic transesterification (HLBS/Catalyst-sulphuric)

	HLBS/U.S.		**Dissolv. Cholo**		**HLBS/Cat(Sulp.)**	
	Hydrocarbon	mg/g	Hydrocarbon	mg/g	Hydrocarbon	mg/g
SFA	C4:0	5.713	C4:0	1.247	C4:0	0.458
	C6:0	0.236	C6:0	0.139	C6:0	0.255
	C10:0	0.030	C10:0	0.125	C10:0	1.916
	C12:0	0.013	C12:0	0.084	C12:0	0.182
PUFA	C16:1 (n-9)	0.871	C16:1 (n-9)	0.216	C16:1 (n-9)	1.278
	C18:1 (n-9)	0.436	C18:1 (n-9)	0.362	C18:1 (n-9)	1.742
	C18:2 (n-6)	0.523	C18:2 (n-6)	0.160	C18:2 (n-6)	2.178
	C18:3 (n-3)	0.566	C18:3 (n-3)	0.139	C18:3 (n-3)	1.742
[1]ΣSFA		5.992		1.595		2.811
[2]ΣPUFA		2.395		0.878		6.940

[1] Summation of polyunsaturated fatty acids
[2] Summation of saturated fatty acids

The fourier-transform infrared spectroscopy (FTIR) spectrum of samples from the oil compound and trans-esterified oil via rapid non-catalytic transesterification method was shown in **Figure 5-8**. The characteristic of transesterification of oil compound showed a broad peak at 3304.5 cm^{-1} which is an indication of the characteristic from fatty acids with hydrogen bonded O-H group. Besides, there is a saturated hydrocarbon compound with a sharp peak found at 2840.3 cm^{-1} with carbon-carbon single bond or saturated hydrocarbon chain in the analyte for microalgae oil. The wavelength absorbance for microalgae oil particularly at 1645.3 cm^{-1} also indicates the carbon-carbon

double bond or unsaturated hydrocarbon chains in the microalgae lipid meanwhile after transesterification of the oil by ultra-sonication the intensity is reduced may refer to **Table 5-6**. The dissolved of F.A.M.E in chloroform was showed less polyunsaturated of fatty acids compare to HLBS extraction method followed by catalytic transesterification. There is potential compound of cyclic alkene but more often is straight chains of the alkene hydrocarbon compounds. Wavelength at 1339.6 cm^{-1} found phenol group with O-H stretching structure where there is a potential natural antioxidant compounds in the microalgae lipids. The wavelength at 1111.5 cm^{-1} and 1013.1 cm^{-1} found in transesterification of oil in which are potential methyl ester from the sample of lipid.

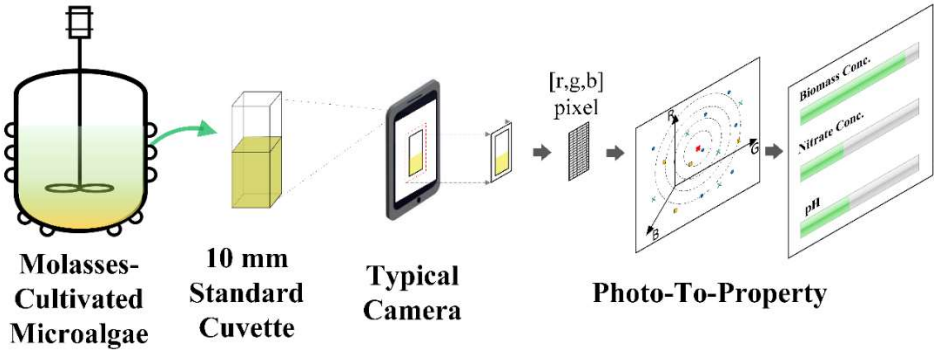
Furthermore, 2922.9 cm^{-1} and 2853.3 cm^{-1} are in the wavelength range as straight chain alkanes or saturated hydrocarbon chains. The peak at 1742.9 cm^{-1} shows the aromatic compound as ester compound from the methyl ester chains. There are aromatic rings located at frequency range of 1459.4 cm^{-1} which exist due to the polymerization from lipid compound, as a result of reactive species randomly combining into rings structure and cross-linking with other compounds [300]. The ester compound found in the peaks 1158.7 cm^{-1}, 1113.4 cm^{-1}, and 1027.7 cm^{-1} indicate more methyl ester was formed in the transesterification process through rapid non-catalytic ultrasound transesterification. The biofuels source from rapid non-catalytic transesterification of microalgae shown from the FTIR analysis have low

intensity of unsaturated hydrocarbon chain in wavelength 720.2 cm^{-1}, where it will not significantly affect the stability of the biofuels.

5.4. Conclusions

The thermal effect on Fenton reaction in a simultaneous HLBS with novel non-catalytic transesterification by ultrasonic method was studied. The thermal-assisted Fenton reaction was performed to obtain the effective lipid recovery combined with novel rapid non-catalytic reaction for transesterification through ultrasound, which has shown great potential for large scale production. Optimum lipid recovery with thermal assisted Fenton reaction in HLBS at 36.5 °C the concentration of lipid at 977.41 mg/g and lipid recovery at 53.31%. Subsequent rapid transesterification process has yielded the F.A.M.E for C4, C6, and C10 at 8.20 mg/g, 0.33 mg/g, and 0.24 mg/g respectively. The duration of the transesterification was optimized at ratio of 1:6 for lipid to methanol and duration of 4 min at 0.8 pulse for the optimum transesterification reaction for short to medium chains of hydrocarbon. This simultaneous system incorporates of pre-treatment and extraction process in a single step process with novel non-catalytic transesterification with ultra-sonication is rapid and cost effective methodology applicable for others microorganism with cellular wall membrane.

Chapter 6. *Chlorella vulgaris FSP-E* cultivation in waste molasses: Photo-to-property estimation by artificial intelligence



This chapter covers the utilization of waste molasses from the previous chapter and using artificial intelligent algorithm to estimate the medium nutrient for microalgae biomass cultivation. This experiment is potential for replacing the spectrophotometer by using photo capture and through analysis of raster image dot to evaluate the medium compound rapidly. The effect of molasses medium concentration has been optimized and through acidification pretreatment to hydrolysate the saccharides compounds. The k-nearest neighbor (KNN) algorithm is used for the prediction algorithm to justify the medium nutrient compounds. This chapter consists of the thesis-version of the manuscript published in Chemical Engineering Journal (Yew G. Y. et al., 2020, Chemical Engineering Journal, 402, 126230).

Abstract

The progress of industry revolution, which involves reutilizing waste materials and simplifying complex procedures of analysis through artificial intelligent (AI), are the motivation in this study. There are two main objectives in this work, firstly, the use of waste molasses from sugar mills as a microalgae cultivation medium for nutrients extraction. The biomass in 15% of the molasses medium without carbon dioxide aeration during cultivation have the highest dry cell weight at 1206.43 mg/L. Protein content in the biomass of 10% molasses cultivation medium is in the range of 20.60% which is higher compared to conventional cultivation mediums. Secondly, the exploitation of the deep colouration properties of molasses-cultivated microalgae, a novel photo-to-property estimation was performed by k-Nearest Neighbour (k-NN) algorithm through RGB model pixel raster in the images to rapidly determine the biomass concentration, nitrogen contraction and pH without use of tedious analytical processes. The k value at 4 was studied in normalized Root-Mean-Square-Error (RMSE) for biomass concentration at 0.10, nitrate at 0.11, and pH at 0.02 for sequence of days.

Keywords: Microalgae, Microalgae cultivation, *Chlorella sp.,* Molasses, Artificial intelligence, Image analyze algorithm

6.1 Introduction

Microalgae are eukaryote unicellular microorganism categorized as renewable, sustainable and economical sources for lipid, protein, carbohydrate and others bioactive compounds [301, 302]. The microalgae cell easily adapts to new environment by consuming only nitrogen and phosphorus as food, and can be grown in photo-bioreactors, fermenters, and open pond areas. The choice of the growth medium is independent from the cultivation system, which is based on the chosen species some can be cultivated in freshwater, wastewater and seawater. According to Wang et al.[303], through hydrothermal oxidation, converting the cyanobacterial slurry into cultivation medium to improve the biomass productivity for *Scenedesmus obliquus* improved about 1.1 times compared to BG-11. Besides, Ratanachat et al. [304], used the anaerobic digester effluent for *Nannochloropsis Salina* and *Dunaliella tertiolecta* have successfully improved the biomass productivity by 6% compared to commercial inorganic nitrogen medium. Moreover, there are several reported mediums such as food compost medium [166], aquaculture wastewater [305], dairy effluent [306], palm oil effluent POME [307] and municipal wastewater as cultivation mediums [308] for different microalgae species. The conventional cases of cultivating microalgae are with concentrated CO_2. However, due to large scale production and consideration of cost effectiveness, the cultivation without using CO_2 are being introduced from Agasteswar et al. [309], in open raceway pond with

savings of about 61% from the total operation cost. Besides, the studies from Hugo et al [310], introduced sugarcane vinasse at different concentrations to improve the biomass productivity and nutrients compound in the biomass with relative to Bold's Basal Medium (BBM).

According to Han et al. [311], the work demonstrated that banana peels can be used as the carbon source for *Oleaginous yeast* (*Cryptococcus sp*.) cell growth in the application of biodiesel product. To the author's best knowledge, our experiment has demonstrated the first application of using waste molasses from the sugar mills factory to be used as the microalgae cultivation medium without CO_2 aerated. Waste molasses from the factory can be a potential cultivation medium because cheap and rich of organic compounds such as aspartic acids, glutamic acids, lactic acids, crude protein, monosaccharides, nitrogen, phosphorus and micronutrients (K^+,Ca^{2+},Mg^{2+}) [200, 312, 313]. The presence of carbon sources in the waste molasses substitutes the requirement of CO_2 gas feed during microalgae cultivation. This mechanism is mainly caused by the existence of nutrients such as monosaccharides, disaccharides and the organic compounds to sustain the cell growth [314, 315]. A logical phenomenon for this is suspected from saccharides carbon compound in molasses have substituted carbon dioxide molecules to form for carbon sugar called glyceraldehyde-3-phosphate (G3P). Due to the nature physical properties of waste molasses are in (such high liquid viscosity and dense in color) a strenuous analytical procedure is required to properly analyzed its nutrients properties [316, 317]. Molasses

cause solution browning when diluted with deionized water, thus can provide a large spectrum of color (brown to green) with varying concentration. Due to this characteristics, it is possible to analyze the raster pixel (of microalgae images) in RGB mode to predict the color different which could lead to property estimation by a using self-learning algorithm such as k-Nearest Neighbour (k-NN). This method has reduced the requirement of laboratory procedure and provides relatively rapid properties estimations for the microalgae cultivation medium.

Artificial Intelligent (AI) algorithms have several types depending on the complexity abilities, while this work has adapted reactive machine (k-NN) algorithm. The reactive machine uses existing data with nearest neighbor data to make comparison and form a mean value. The mean value which synchronize with the images raster pixel relate to the experimental results. There are several researchers in the direction of incorporating AI algorithms with microalgae research. For example, Supriyanto, et al, [318] used an artificial neural network model to estimate growth of polyculture microalgae by using key variables of solar irradiance and temperature. According to Teng S.Y., et al, [319] a neuro-evolutionary approach is used to model and optimize the thermal conversion of microalgae during pyrolysis and gasification. The work proposed a novel Progressive Depth Swarm-Evolution (PDSE) algorithm to train evolutionary neural networks to achieve state-of-art in accuracy for microalgae conversion modelling. Furthermore, Cerbin et al [320] have discussed the potential of using

AI algorithms and image analysis to monitor microalgae production in biogas plants, however the work is preliminary, and no solid implementations were reported. In the perspective of microalgae biomass quantification through photo properties is the state-of-the-art knowledge implement in this work is the first in using multi-channel image via simple camera and AI algorithm to estimate multivariate properties (i.e. biomass content, nitrate content and pH) of waste molasses-cultivated microalgae.

In this study, the molasses medium is to be compared with the conventional BG-11 as a cultivation medium and shown to not require additional CO_2 aeration. The k-NN algorithm is incorporated to evaluate the microalgae biomass, nitrate, and pH. The manuscript will focus on two distinct novel aspects: (i) the optimization of molasses as a CO_2 non-essential cultivation medium and using their images as training data, (ii) implementation and validation of the AI algorithm in estimating microalgae properties through image recognition (photo-to-property).

6.2 Materials and Methods

6.2.1 Microalgae strain and medium compositions

A microalgae strain *Chlorella vulgaris FSP-E* was used in this study, in which the strain from southern Taiwan was isolated from freshwater. The microalgae were cultivated in various concentrations of molasses without adding any portion of chemical medium. The control parameter and pre-culture used BG-11 medium containing 1.5 mg/mL $NaNO_3$, 0.03 mg/mL K_2HPO_4, 0.075 mg/mL $MgSO_4 \cdot 7H_2O$, 0.006 mg/mL citric acid anhydrous, 2.0 mg/mL $NaCO_3$, 3.6 mg/mL $CaCl_2 \cdot 2H_2O$, 0.6 mg/mL Ammonium iron (III) citrate, 0.1 mg/mL EDTA·2Na, 2.86 mg/mL H_3BO_3, 1.81 mg/mL $MnCl_2 \cdot 4H_2O$, 0.222 mg/mL $ZnSO_4 \cdot 7H_2O$, 0.39 mg/mL $Na_2MoO_4 \cdot 2H_2O$, 0.079 mg/mL $CuSO_4 \cdot 5H_2O$, and 0.049 mg/mL $Co(NO_3)_2 \cdot 6H_2O$ in deionized water [166]. The cultivation was performed in an indoor photo-bioreactor (PBR) which consist of a 250 mL glass vessel for pre-culture with 200 mL of total volume with 1.5% of CO_2 mixed together with air continuously aerated at 200 mL/min or 0.2vvm. The batch culture of control PBR vessel was only aerated with addition of 1.5% compressed CO_2 mixed with air (0.05 vvm, volume gas per volume medium per minute) through filtered (0.45 μm) and equipped with external LED parallel lighting source surrounded by the photo-bioreactor vessels at room temperature 25 °C. The lighting intensity was adjusted to 200 μmol/m^2/s using a LI-250 light meter with LI-190SA pyrometer sensor (LI-COR, Inc., Lincoln, USA). The molasses mediums were aerated continuously by filtered air (0.45 μm) at a rate

of 50 mL/min (0.05 vvm) and without addition of any CO_2 in the PBR. All readings were performed in triplicate and average values were reported.

6.2.2 Pretreatment of waste molasses

The waste molasses was obtained from Shinko Sugar Mills Co., Ltd Japan at 83° brix polysaccharides 30.4%, inverted sugar 9.79% (disaccharides and monosaccharides) pH value is 5.83. According to Yan et al [200], convert polysaccharides and disaccharides to monosaccharides, the molasses were diluted with nitric acid (HNO_3) in a ratio of 1:1 and incubated at 60°C for 24 h to generate more molasses hydrolysate monosaccharides compounds. Subsequently, the mixture was neutralized with 5% of NaOH to pH 7.25 to meet the optimal pH range 6.50 - 7.50 for sustainable pH growth level for the C. Vulgaris FSP-E species of microalgae. The acid- hydrolysis technique will convert disaccharide compounds in the waste molasses into monosaccharides compounds. The molasses mixture percentage applied for the cultivation was 5 % molasses, 10 % molasses, 15 % molasses and 20 % molasses, while all remaining was filled with deionized water up to 1 liter.

6.2.3 Determination of microalgae cell concentration

The microalgae biomass concentration was determined by measuring the optical density at 680 nm through UV-Vis spectrophotometer (UV-1800, Shimadzu). The microalgae biomass was obtained by filtering 5 mL aliquots of the culture

through cellulose acetate membrane filter (0.45 µm pore size, 25 mm in diameter). Subsequently, each loaded filter was placed in the oven at 105 °C and weighed once the temperature cooled down. Dry weight of the blank filter was measured and subtracted from the sample loaded filter to obtain the microalgae dry cell weight (DCW). The DCW were divided by the OD_{680} values referring to optical density in wavelength 680 nm. The correlation between biomass concentration in weight, mg, and one unit of optical density of OD_{680} yielded the DCW (1 OD_{680} = 0.23 g/L DCW).

The microalgae growth in volumetric according to Krzeminska, I et al, and Junping, Lv, et al, [321, 322] for biomass productivity (P_b) and specific growth rate (µ) was calculated by the following equation.

$$P_b(\text{mg l}^{-1}\ \text{d}^{-1}) = \frac{(DW_2 - DW_1)}{(t_2 - t_1)} \qquad (6\text{-}1)$$

$$\mu(\text{d}^{-1}) = \frac{\ln(\frac{DW_2}{DW_1})}{t_2 - t_1} \qquad (6\text{-}2)$$

The equation DW_1 and DW_2 represent dry cell weight (g/L) at time t_1 and t_2, respectively.

6.2.4 Quantification of nitrate content in medium

The nitrate content was determined by using spectrophotometric method by Chew et al [166] . The microalgae samples were collected from the photo-bioreactor and centrifuged at 7000 rpm for 5 mins. Subsequently, the supernatant

was diluted with deionized water and measured at optical density of 220 nm UV-Vis spectrophotometer. Pure sodium nitrate ($NaNO_3$) was used for calibration of the standard curve.

6.2.5 Microalgae lipid extraction

The lipid content from the microalgae biomass was extracted using the method by Yew et al [204] with some modification. 30 mg of dried microalgae biomass was used, consisting of 6.50 mL of chloroform/methanol/water mixture of biomass in ratio of 1:2:0.8 (w/v). The mixture was sonicated at the frequency of 35 kHz for 5 min by ultrasound water bath (Elma, Germany). An additional 2 mL of chloroform and 0.80 mL of distilled water each were added to the mixture and further sonication for 5 min. The bottom layer of the (chloroform layer) was transferred into a petri dish and heated at 80°C for 30 minutes. The petri dish was cooled to room temperature and weighed for the total lipid content.

6.2.6 Protein extraction and quantification

For the extraction of protein from microalgae biomass, 50 mg of dry microalgae biomass was pretreated by acid and homogenized in a 10 mL water with 1 mL of 0.5 N KOH. The mixture was vortexed for 60 seconds and sonicated at the frequency of 40 kHz for 15 min. After that, the mixture was centrifuged at 7000 rpm for 5 min. The supernatant was collected for protein analysis by Bradford method. The samples with protein were pipette 0.25 mL into the vial and mixed

with 2.5 mL of Bradford reagent. The mixture followed by buffering 15 minutes for completely reaction between Bradford reagent with supernatant, was then measured at UV-Vis spectrophotometer at the wavelength of 595 nm. Bovine serum albumin (BSA) was used to construct a standard curve of protein concentration correlating with the samples in absorbance (OD_{595}).

6.2.7 Determination of carbohydrate content

The carbohydrate content from microalgae biomass was extracted according to Chew et al [166]. The microalgae weight of 50 mg of cell-disrupted microalgae biomass was hydrolyzed under acidic condition with 0.5 mL of 18 M H_2SO_4. After 30 minutes of the buffering time, 4.5 mL of deionized water was added and autoclaved at 121°C for 30 min. Once the solution reached room temperature, it was centrifuged at 7000×g for 10 min. The clear supernatant of the simple sugars was collected to conduct carbohydrate quantification by using phenol-sulphuric method Dubois, M. et al [323]. The supernatant with 10 µl, 1 mL of 18 M H_2SO_4 and 0.2 mL 4% (w/v) phenol were added, with reaction time set at 15 min, subsequently measurement using UV-Vis spectrophotometer was performed absorbance of 490 nm. Starch samples were obtained for the correlation between absorbance and carbohydrate concentration. The brix content is measured by refractometer through calibration standard using pure sucrose in 1g in 100 mL of deionized water for 1 ° brix.

6.2.8 Photo-to-Property Estimation Method

The k-NN algorithm uses Euclidean distance to determine the distance between each data point. The algorithm is implemented using Matlab 2018a for training and forecasting the data. Every sample was pipette 2 mL into a cuvette for photo imaging in a fixed position and distance for all samples captured using Qualcomm 400 series 64- Bit processor, 8 Megapixels with focus f/2.0 aperture camera. Each microalgae image is pre-processed by cropping the image to the part of cuvette with microalgae in it. The image is then converted to a 198x146 RGB array to be prepared as a numerical matrix input. When the image input is processed by the k-NN model, the distances between the multichannel RGB inputs and previous training data point available in k-NN model are evaluated based on Euclidean distance. The k number of closest neighbors to the input are obtained. The predicted result depends on the weighted average of these neighbors. In detailed, the k-NN model is implemented in this study using the steps as follow:

1. All training data are loaded. The data should be arranged in a row-major array format where the number of columns in the array represents the number of features to be studied by the k-NN model.
2. Initialize the values of k and p.
3. When test data are inputted into k-NN, iterate from 1 to total number of data points in test data, m

4. Evaluate the distance between test data and each row of training data using Euclidean distance.
5. Sort the distances, d, in an ascending order.
6. Obtain the first k rows of data points as neighbors to the test input.
7. Use weighted average on the labels of these neighbors using formula (6-3) as follow:

$$y_{test} = \frac{\sum_{i=1}^{m}\left(\frac{y_{60,i}}{d_i^p}\right)}{\sum_{i=1}^{m}\left(\frac{1}{d_i^p}\right)} \qquad (6\text{-}3)$$

This weighted average is now the output of the k-NN model.

The motivation of using weight k-NN as the driving algorithm is that conventionally microalgae properties can be identified by UV-Vis spectroscopy, which makes measurements based on light absorption and reflection. This spectral information is equivalent to image color under visible light regime, and therefore, weighted k-NN serves as the most direct and efficient algorithm to learn the similarity of color in microalgae images.

6.2.9 Preparation of Data

There are 1500 images used for data training, 300 images used for data testing and 300 images for validation, following the method by Benzmuller et al [324], using the portion 75%: 15%: 15%. All images have been cropped to rectangular shape to consist of region-of –interesting the learning phase of the algorithm.

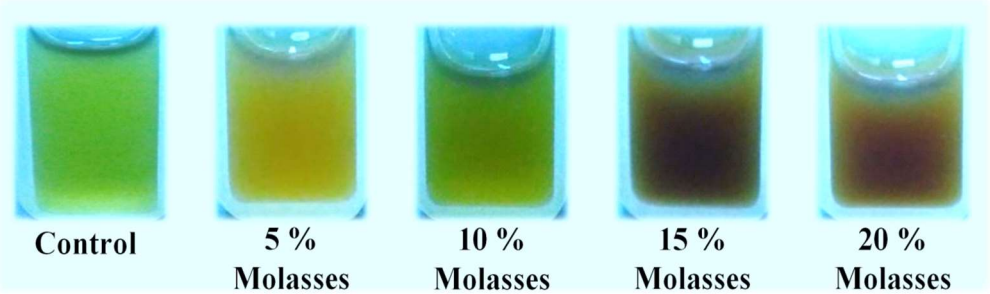


Figure 6-17: 5 selected pictures from the pool of microalgae image data for the purpose of illustration.

All the data of total lipid, protein, and carbohydrate values were subjected to ANOVA one-way with two tailed t-test with significant ($P \leq 0.05$) using Microsoft Excel. The data presented was average of three replicates.

6.3 Result and discussion

6.3.1 The effect of molasses nutrients on concentration of biomass

In this study, molasses was diluted into different concentrations for cultivation of C. vulgaris FSP-E (**Figure. 6-1**) to depict the biomass growth curve by molasses as the only nutrients source. The results, usage of 5% - 20% of molasses solution obtained higher biomass production compared to BG-11 medium as the control. The highest biomass concentration recorded at each control, 5%, 10%, 15%, and 20% of molasses was found at 212.64 mg/L, 460.80 mg/L, 728.71 mg/L, 1238.53 mg/L and 1021.51 mg/L achieved from control

BG-11 to 20% concentration of molasses medium respectively. The highest biomass was in 15% of molasses during day 14, where the biomass concentration reached 1222 mg/L and increased from 1213 mg/L during day 13th. The biomass loss observed in **Figure 6-1** was minimized due to introduction of 24 hours cycles of lighting by fluorescence light to avoid night loss effect and constant ambient temperature at 25 ºC to enhance the biomass productivity [325, 326].

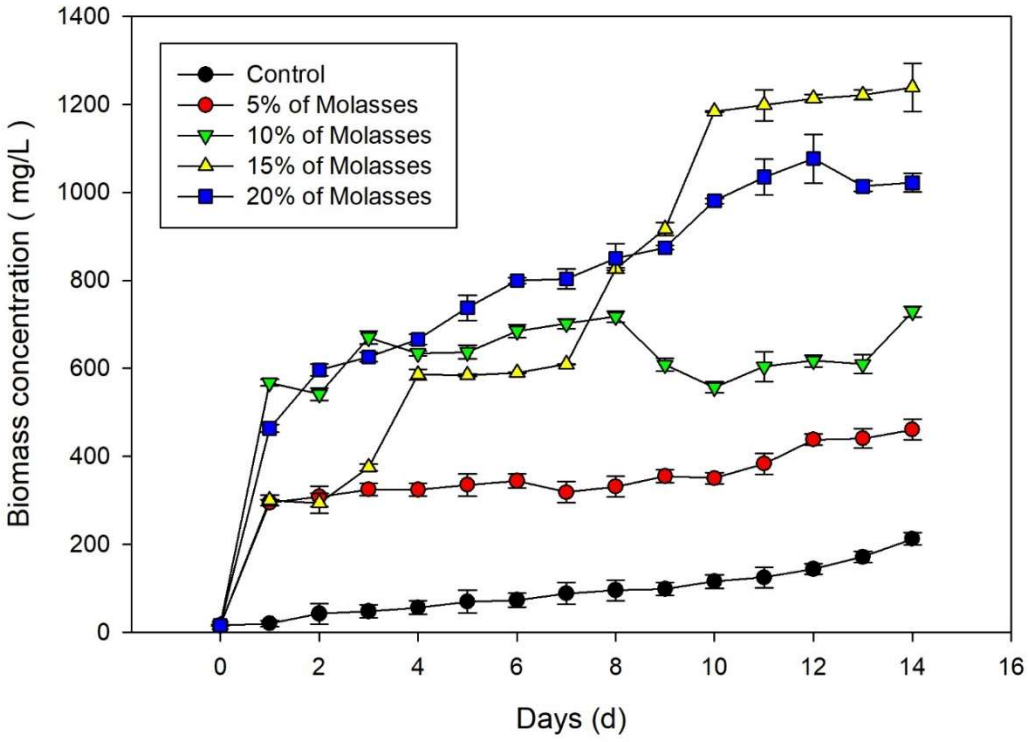


Figure 6-18: Biomass concentration shown in the growth of C. vulgaris FSP-E in BG-11 and various molasses mediums combination in without additional of CO_2 condition

For molasses mediums up to 20% including control medium (BG-11), the microalgae grew gradually for control medium along the 14 days of cultivation as shown in **Figure 6-2** while molasses medium 5% to 20% exhibited a rapid growth after day 10 period. The stress condition experienced by the microalgae due to scarcity of carbon dioxide and nutrients reduction in the PBR affected the accumulation of the biomass in such condition, have increased the metabolite within the cellular through nutrient limitation conditions [327]. The molasses contain carbohydrate, saccharides, and micro-nutrients such as sulfur, potassium and other trace minerals which can assist the microalgae growth [328]. The treated molasses carbon source which can enhance the microalgae cellular growth indirectly increased the biomass amount, as similarly reported [329]. Hence, molasses as the nutrient medium could be an alternative medium for the cultivation of microalgae in C. vulgaris FSP-E to improve the cell growth.

The 10% molasses as a medium for the microalgae growth showed high yield between day 6 to day 8, then the biomass plunged below to a value lower than 15% molasses medium, where this is subjected to statistical analysis with ($p < 0.05$). The color of the 10% medium is darker compared to 15% and 20% on the 8^{th} day which could have been affected by the light penetration. In 20% of the molasses medium, it was observed that the solution medium has been digested and agglomeration of large particles were formed around the cultivation flask. The dark color of the culture medium would promote the inhibitors such as fungus and bacteria growth that would scavenge the nutrients from the molasses

medium and compete for food with microalgae [330, 331]. Thus, it would affect the growth rate of the microalgae biomass. The biomass amount of the 15% molasses medium consist of 5.82 folds of biomass compared to control (BG-11) medium, standard deviation for the 15% biomass production in the first 7 days is 212.01 mg/L compared to the last 7 days of the biomass growth at 237.179 mg/L. In 5% molasses medium consists of lesser nutrient value, thus this may affect the biomass growth due to starvation of nitrogen in the cultivation medium [166].

Table 6-1: Comparison and indication of with and without CO_2 in biomass productivity, specific growth rate and percentage difference between both methods.

Medium	With CO_2			Without CO_2			Percentage Diff.		
	DCW (mg/L)	P_b (mg/L/d)	μ (d^{-1})	DCW (mg/L)	P_b (mg/L/d)	μ (d^{-1})	Diff. DCW (%)	Diff. P_b (%)	Diff. μ (%)
Control	501.26 ± 0.13	16.42 ± 1.10	0.19 ± 0.05	472.59 ± 0.11	16.36 ± 0.16	0.20 ± 0.08	5.72	0.37	0.25
5%	392.68 ± 1.25	34.23 ± 1.73	0.26 ± 0.24	445.81 ± 0.45	35.45 ± 1.80	0.26 ± 0.24	13.53	3.55	0.96
10%	692.87 ± 0.45	57.33 ± 0.85	0.29 ± 0.17	713.75 ± 0.42	56.05 ± 0.77	0.29 ± 0.17	3.01	2.22	0.66
15%	1186.26 ± 2.27	93.35 ± 0.10	0.33 ± 0.06	1206.4 ± 1.51	95.27 ± 0.78	0.34 ± 0.29	1.70	2.05	0.4
20%	1190.86 ± 0.21	81.47 ± 1.56	0.32 ± 0.23	1006.2 ± 0.92	78.58 ± 0.03	0.32 ± 0.02	15.36	3.54	0.93

The biomass productivity P_b (mg/L/d) and specific growth rate μ (d^{-1}) for C. vulgaris FSP-E in day 14th of the without CO_2 cultivation are showing in **Table 6-1**. The highest biomass productivity was found in 15% molasses medium at 95.27 mg/L/d, followed by 20% at 78.58 mg/L/d. The lowest biomass

productivity and specific growth rate was observed at control medium at 16.36 mg /L/d and 0.20 d^{-1}, respectively. The 15% molasses obtained the highest biomass productivity on day 14^{th} at 95.27 ± 0.01 mg/L/d with specific growth rate of 0.34 ± 0.06 d^{-1}. During the period of cultivation, the biomass fluctuated due to the insufficiency of light penetration. As shown in **Table 6-1**, the percentage of difference between with and without CO_2 for microalgae biomass productivity is less than 5% with an average of 2.35%, while specific growth rate is less than 1% with an average of 0.64%. The concentration in 5% and 15% without CO_2 is found to be higher than with CO_2 and the percentage of difference is relatively low which is supported by the finding from O' Hara et al. [332], where the saccharides may influence the signaling of metabolite within the cytoplasm during photosynthesis reaction.

However, the low light penetration may inhibit undesired microbes (e.g. Lactobacillus and streptococcus sp.) that may compete for consumption of the nutrients during the cultivation, hence enabling growth of the microalgae. However, molasses could be one of the source for protein fractions in microalgae cytoplasm which could enhance the value for albumin [333].

6.3.2 Nutrient removal from molasses by C. Vulgaris FSP-E

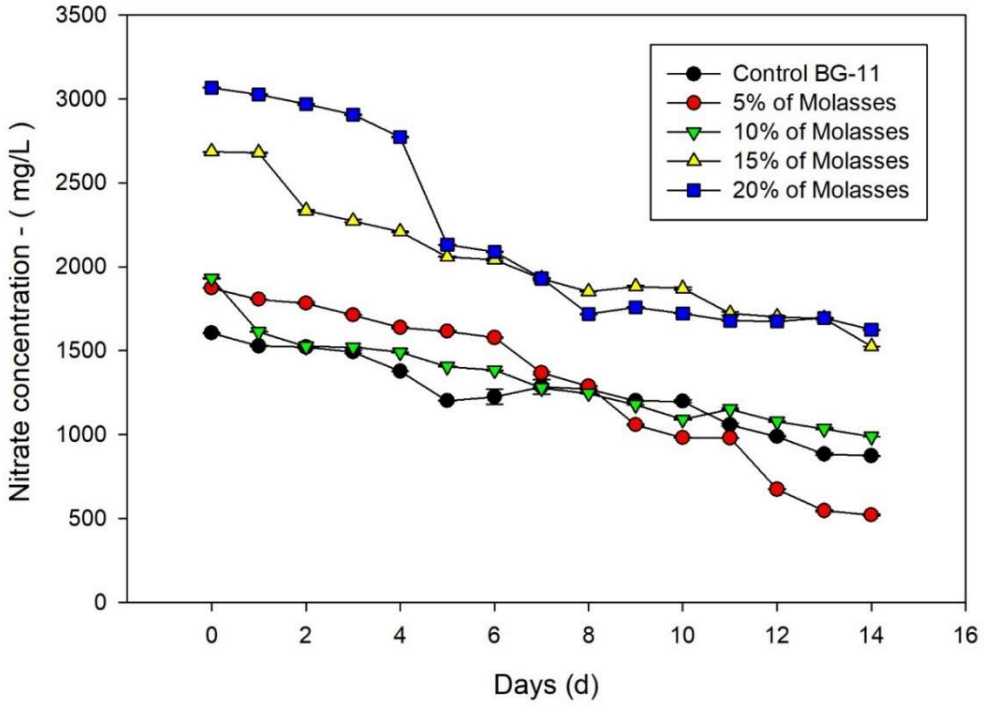


Figure 6-3: Nitrate content shown in the growth of C. vulgaris FSP-E in BG-11 and various molasses mediums combination in without additional of CO_2 condition

Microalgae require nitrite and phosphorus as important nutrients, for the purpose of metabolite cycle and biosynthesis during cell growth. Molasses consist of organic substrate and micronutrient substances, which are able to simulate the microalgae growth at the same time assist in removing organic matter in the medium during cultivation process. The major composition of the molasses waste is 17-25% of water and 75% - 95% of carbohydrate (majorly in

disaccharide) where after pre-treatment according to section 2.2, the disaccharide will be broken down to majorly monosaccharide. The waste molasses nutrients may provide nitrogen, micronutrient and organic substrate to simulate the growth of microalgae cells [334]. The molasses waste medium was able to act as the source of nutrients to be consumed by microalgae C. vulgaris FSP-E species to enhance the growth rate and produce valuable bio-products.

The nitrate concentration result for different molasses medium shows a reducing trend in the overall cultivation period in **Figure 6-3**. The reduction of 47.07% for nitrate is recorded in the medium of 20% treated molasses. The highest nitrate removal is at 5% of molasses medium with removal for 72.15% of nitrate content in the medium upon 14th day of cultivation subjected to statistical analysis with ($p < 0.05$). The presence of light source may indirectly improve the nitrate intake for the microalgae cell, as 5% of the microalgae medium in earlier stages of growth (first half of the duration) may have lighter color due to the less concentrated molasses medium [335]. The organic substrate from the molasses includes nucleic acid, sugar compound and hydrocarbon, assisting in simulating the microalgae cell growth [334]. The organic substrate especially monosaccharide in the molasses with Adenosine Monophosphate-activated Protein Kinase (AMPK) is able to simulate the signaling system for the growth of cellular of photosynthetic eukaryotic organism [336, 337]. An AMPK is an enzyme playing a role in the cellular physiology system which is able to send signal to the internal cell to activate the nitrate, disaccharide, monosaccharide

and fatty acids uptake [337, 338]. The 15% and 20% molasses concentration drop sharply of the nitrate value at the 12th day, this is related to the reduction of the nutrient content in the cultivation medium. This can also indicate the process of respiration by anaerobic organism, which requires more nitrate than oxygen to oxidize organic molecules converting to energy for the cell growth [339]. Anaerobic organisms other than microalgae present in the medium is bacteria and fungi which act as inhibiting organisms to compete for nitrate.

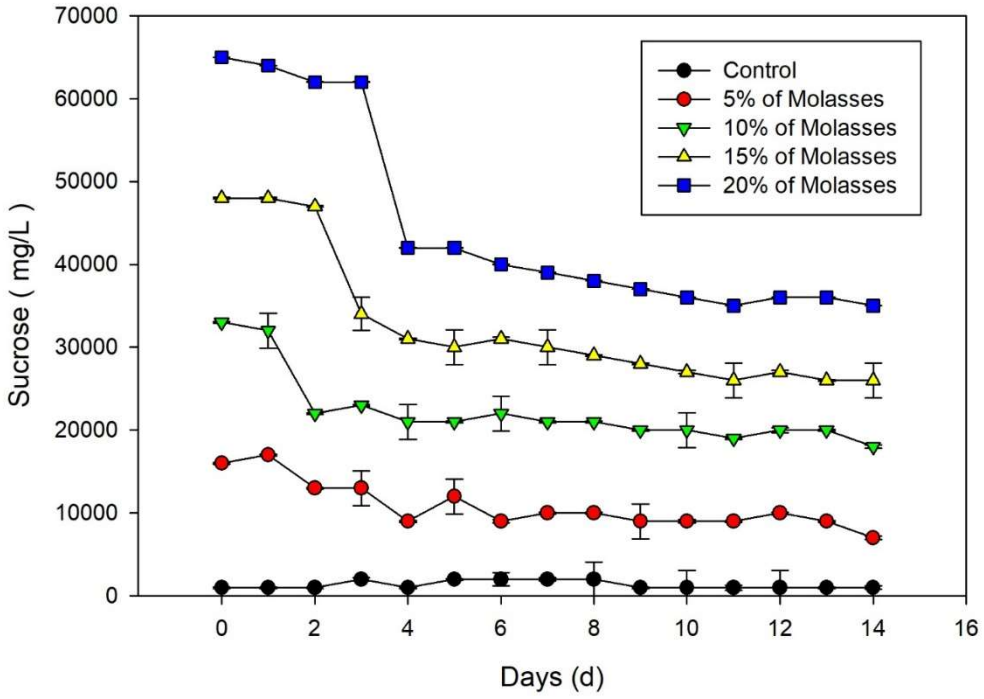


Figure 6-4: Sucrose content shown in different cultivation days for C. Vulgaris FSP-E in control BG-11 and various molasses concentration mediums without additional of CO_2 condition

The value of °brix data is collected and represent the fermentable sugars level, with calibration through the analytical standard of pure sucrose content in (mg/L) by the refractometer. The brix value indicates the sucrose amount in the medium from the refractometer, where sucrose is known as disaccharide molecule, which combines two monosaccharides by a glycosidic linkage. The sucrose content overall after pretreatment is 290,000 mg/L and is further distributed the weight in percentage of 5%, 10%, 15% and 20%, according the weight of one liter of the PBR. As in **Figure 6-4**, the initial sucrose level during day 1 for 15% and 20% is 48,000 mg/L and 65,000 mg/L respectively, which is among the highest values for the sucrose content in the cultivation medium. Amount of the molasses would directly affect the sucrose concentration level, where more molasses would introduce more sucrose into the culture medium. The sucrose reduction of 44.60% for 20% of molasses medium with initial 65,000 mg/L is reduced to 36,000 mg/L on 14th day. Control medium with BG-11 has an initial of 1000 mg/L of sucrose, resulted from the present of pre-cultured cell of polysaccharides [340]. Polysaccharides from the microalgae cell is a type of natural macromolecules found in all types of living organism, which consist of monosaccharide units through linkage of glycosidic bonds. Some of the disaccharide molecules may form during fractionating of the polysaccharides by the inhibitors and microalgae cell enzymes [341, 342]. In medium for 15% of molasses, there are 45.80% of sucrose level is been reduced, crowning the highest of the overall sucrose reduction level among 5 different mediums

including the control BG-11 subjected to statistical analysis with ($p<0.05$). However, the range of sucrose is maintained at 39%-45%, the monosaccharides is one of the prior nutrients to simulate the metabolite and as consumable substances [343]. This study has avoided the addition of CO_2 into the molasses cultivation process, and the growth of the microalgae cell was completed within the PBR with aeration source of only air injected at a rate of about 0.04% into the medium at a constant rate. According to O'Hara et al [332] the form of sucrose is an important biosynthetic pathway for the cell to regulate the photosynthetic organism growth and development of the cell. The molasses medium has abundance of monosaccharide molecules which may stimulate the production of pyruvate compounds and subsequently convert them into Acetyl-CoA for amino acid and fatty acids production.

6.3.3 The variation of pH value correlate to biomass growth

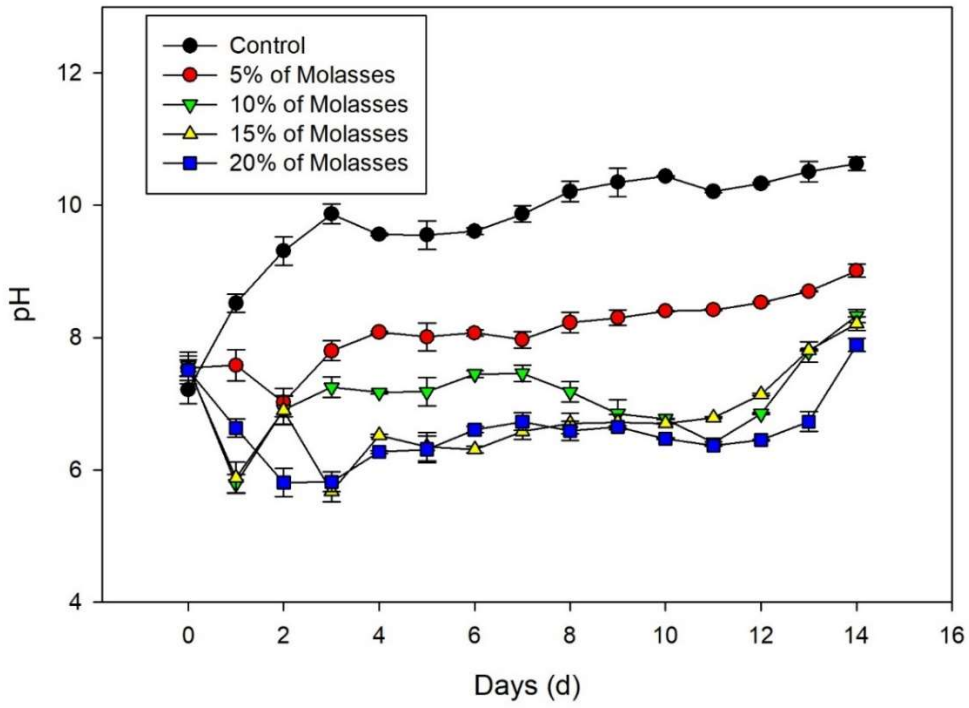


Figure 6-5: pH of the medium shown in different cultivation days for C. Vulgaris FSP-E in control BG-11 and various molasses concentration mediums without additional of CO_2 condition

The pH value is one of the key factors for the microalgae cell to initiate the growth from the internal cell. According to Vadlamani et al [344], *Chlorella sorokiniana SLA-04* is adapted in the medium where its pH is greater than 10 without additional concentrated CO_2 condition. This experiment, throughout the control and molasses cultivation medium has reached the pH of range 5.79 to 10.63, where the strain of *C. vulgaris FSP-E* has survived without additional

concentrated CO_2 to the PBR with the statistical analysis value subject to ($p < 0.05$). The treated molasses consists of lower pH value upon higher concentration of molasses added. The C. vulgaris species has widely known as strong survivability species in extreme environmental conditions by accumulating the nutrient compound under physical stress such as high temperature, dark condition and large pH variation to provide stable growth [344, 345]. The conventional marine species can tolerate of pH of around 9.31 to 10.30 where exceeding 9.41 would cause adverse cell growth rate. The treated molasses with lower pH value which is found growth in biomass and gradually raise in the pH value upon day 14. As in **Figure 6-5**, 15% and 20% of the molasses medium, consist of higher biomass productivity which is 95.26 mg/L/d and 78.58 mg/L/d respectively, where the medium is at average pH 6.78 and 6.58 respectively. *Chlorella sp.* of microalgae is highly employed as food consumption, due to high protein, lipid, and carbohydrate content production [346]. The molasses medium in different concentrations has caused variation of pH value and may affect the rate of CO_2 intake, causing higher alkalinity to promote the metabolic processes in the cell. Therefore, varying the molasses concentration may simulate the membrane transport processes and metabolic functions such as enhanced the internal cell pH regulation for optimum growth of biomass [347]. As 15% of the molasses medium showed optimum biomass production compared to others concentration, the average pH level at 6.8. While, for lowest biomass productivity at 5% of molasses concentration at pH 8.1 which

is high alkalinity value shown. The shifting of pH value by molasses concentration would affect the biomass growth rate at the same time influencing the metabolic process.

6.3.4 Biochemical composition

6.3.4.1 The total lipid content

The lipid content from the cultivation of variation waste molasses and control medium in the microalgae biomass of C. vulgaris FSP-E is shown in **Table 6-2**. The lipid content for 15% of molasses medium with deionized water was the highest at 76.53 mg/g ± 0.91, subsequently the lipid content followed by 20% and 10% of the molasses medium at 60.45 mg/g ± 0.94 and 39.52 mg/g ± 1.53 respectively. The lipid content decreased sharply from 15% to 10% of the molasses at reduced value of 48.36%. The 15% of the molasses and control medium of the lipid amount is 2.31 folds higher than the conventional BG-11 medium. The amount of lipid content in the control medium at 30.32 ± 1.10 mg/g, where 5% of the molasses medium of the lipid content is found at 38.21 ± 2.10 mg/g which is slightly higher than the control. The microalgae biomass nutrients from C. vulgaris FSP-E strain with the statistical analysis within ($p > 0.05$). The overall microalgae biomass lipid content from molasses medium is shown between 38.21 mg/g to 76.53 mg/g, which is higher compared to the reported fish lipid content investigated around 30.90 mg/g to 37.40 mg/g.

Table 6-2: The Bio-composition from different mediums of molasses and control BG-11 in without addition of CO_2 condition.

Medium	Lipid (mg/g)	Protein (mg/g)	Carbohydrate (mg/g)
Control (BG-11)	30.32 ± 1.10	234.32 ± 1.56	62.19 ± 0.15
5% of molasses	38.21 ± 2.10	294.10 ± 1.53	72.84 ± 0.64
10% of molasses	39.52 ± 1.53	254.59 ± 1.40	93.53 ± 0.15
15% of molasses	76.53 ± 0.91	286.59 ± 1.43	55.92 ± 1.22
20% of molasses	60.45 ± 0.94	284.86 ± 1.41	57.71 ± 3.10

The studies from Chew et al, mention that the accumulation of lipids under stress conditions can assist in improving the lipid content [166]. There are a variety of stress condition to improve the accumulation of lipid compounds such as varying temperature, light intensities, nitrogen source, salinity and concentration of the carbon source [348]. In this study, the color of the medium is darker as the cultivation day increases, the light penetration into the medium may strenuously spread into every microalgae cell as the biomass is getting more concentrated in the medium. Lipids are crucial energy storage molecules for plants cells, which are synthesized from acetyl CoA. Monosaccharide derived from molasses enhances the number of delivers of acetyl group to the tricarboxylic acids or

Krebs cycles for the lipogenesis of the metabolic process to convert acetyl-CoA into lipid compounds [349]. The carbon metabolism in the microalgae cell is related to environmental factors such as types of medium, temperature of the PBR, irradiance of light intensities levels, and chemical compounds for the cultivation medium. The molasses medium will create a natural inhibition of lighting conditions to signal the cell build-up the precursors to the acetyl-CoA carboxylase (ACCase) for synthesizing the triglyceride (TAG) in the cell [350]. Besides, the dark environment contributed by different concentrations of molasses medium in PBR has limited the light penetration throughout the microalgae cell in the PBR, stressing the lipid content in the cell as well. Therefore, in **Table 6-2** molasses medium lipid content is higher compared to control BG-11 medium due to the insufficient of the light that caused another environmental stress condition which would impact on the photosynthesis relative activity. It assists to shift the metabolic pathways which will affect the lipid productivity within the microalgae cell [351]. Environmental stress will reduce the growth rate and promote the cell to accumulate triglyceride (TAG) as deposited energy utilized for sustainability growth for a duration during the advantageous environment condition.

In this experiment, the waste molasses contains a large number of nitrogen and monosaccharides in the medium as nutrients for the microalgae cell as food. The light intensities and CO_2 may become the limitation for the cell growth rate. To optimize the lipid content, one of the possible approach by Tan et al [352] is

decreasing the lipid catabolism through knocking out the Acyl-CoA synthetase gene Neochloris oleoabundans species, during nitrogen deprivation condition, would accumulate optimal of lipid amount through reducing the quantity of cellular component response to external stimulus [353]. One of the direct experiments reported by Chu et al [354] starvation of nitrogen condition and its introduction to the cultivation medium will enhance the cell metabolism. In this experiment study, microalgae cells have been cultivated with stress induced through the dark medium with limited light penetration conditions. However, the cell simulates by monosaccharide for enhancing the Acyl-CoA kinase therefore, the lipid content is shown higher compared to the control medium.

6.3.4.2 The protein content

The protein extracted from C. vulgaris FSP-E microalgae biomass through various molasses medium is shown in **Table 6-2**. The highest protein content was found in 5% of molasses medium at 294.10 ± 1.53 mg/g, followed by 20% of molasses at 286.59 ± 1.41 mg/g. The lowest protein content was found in the control medium at 234.32 ± 1.56 mg/g, less 20.60% compared to 20% of molasses medium biomass. The statistical analysis was performed ($p<0.05$) by varying the molasses concentration and control medium for the cultivation. Microalgae biomass cultured with molasses medium is shown to have higher protein content compared to control BG-11 medium. According to Kim et al [355], the nitrogen source affects the protein synthesis in the cell. Molasses

contain 15% - 25% of nitrogen, consisting of different nitrogen compounds such as betaine nitrogen, alfa-amino nitrogen, ammonium and amide nitrogen [356]. Cultivation of C. vulgaris strain with molasses as the cultivation medium would assist in increasing the protein content in the biomass. Moreover, the glucose from the molasses medium will simulate the formation of macromolecules such as polysaccharides and further assisting in protein synthesis within the cellular. The building up of the polysaccharide would need energy, where the energy is derived from light, water and CO_2 through photosynthesis physiological conversion [357]. The molasses concentration as medium is beneficial to the microalgae cell growth, able to remove nutrients from waste and chemical oxygen demand COD [358, 359]. In this study, it is found that using waste molasses for microalgae cultivation would enhance the protein content compared to the BG-11 medium.

The nutrients of the cultivation medium being one of the important factors, is reported that *chlorella* species of microalgae negatively affected the growth during reduction of nitrogen below 31.50 mg/L [301]. The molasses used as the cultivation medium of nitrogen content at the range 10.57 g/L to 70.50 g/L which is viable as cultivation medium. Molasses are by-product from the industry, through microalgae cultivation it is able to remove the nutrients from waste before discharge and enhance the microalgae biomass nutrients value. During the cultivation process, by using molasses as a cultivation medium, the dark color medium reduces the light penetration directly to the microalgae cells

throughout in the PBR. According to Emerson et al [360], the light intensity is correlated to the chlorophyll concentration among the microalgae cells in the medium. The protein content from microalgae biomass, especially *Chlorella sp.* has various types of protein which is able to reduce cholesterol level [301]. All values are subjected to statistical analysis with ($p<0.05$). The high protein content in the 5% of the molasses medium of cultivation is resulted by the light medium color where higher degree of light intensity penetrates to the microalgae cell in the medium compared to others molasses medium.

6.3.4.3 The Carbohydrate content

Carbohydrate is one of the compounds derived from photosynthesis reaction in plants. The compound is contributed by the structures of the microalgae cell such as cellular wall which is made from polysaccharides. Carbohydrate is also the source for producing bioenergy such as biodiesel from the fermentation process. Different carbohydrate content could be determined from the microalgae strain, cultivation type, and cultivation conditions [166]. In **Table 6-2**, different carbohydrate amounts are obtained from different molasses concentrations in the mediums. The highest carbohydrate medium is 10% of molasses medium at 93.53 mg/g and followed by 72.84 mg/g. The carbohydrate content in 15% and 20% of the molasses medium are 57.71 ± 1.22 mg/g and 55.92 ± 1.41 mg/g respectively. Both values are low compared to the control BG-11 medium at

62.19 ± 0.15. The 10% of the molasses medium have higher carbohydrate content than control BG-11 by 33.50%.

The composition in the molasses contributes to simulation reaction of the carbohydrate production in microalgae particularly in cellular wall membrane during the cultivation periods. All nutrients data being subjected to statistical analysis with ($p<0.05$). The cellular wall from the microalgae can be affected by inhibits and distractions starting from the cell wall where the microalgae cell confers to rigidify the cellular wall to protect the internal cell. Microalgae belongs to the group of unicellular photosynthetic eukaryotes, where the cell walls are contributed by cellulose and hemicellulose [361]. The 10% of the molasses medium have the most carbohydrate content, the light penetration and nutrients are in optimum level for the production of carbohydrate. The treated molasses contains mostly monosaccharides which is part of the carbohydrate metabolite cycle to be converted into mannose, xylose and galactose as part of the polysaccharides compounds. Light intensity would increase the photosynthesis activities where enhance the metabolism within the cell to improve the structural formation of the polysaccharide for the cellular wall [19, 360, 362]. Furthermore, polysaccharide is a polymeric carbohydrate molecule chain consisting of monosaccharide units through glycosidic linkages. While cellulose from the cellular wall is a linear chain of polysaccharide of the polymer by addition of monosaccharides units, which is found in waste molasses compounds.

Moreover, the microalgae cell contains higher value of carbohydrate in 10% and 5% of the molasses medium biomass, since microalgae mainly contains cellulose with starch which is without lignin and low amount of hemicellulose [363]. The pH changing environment has caused the *Chlorella* species to change its carbon / nitrogen ratio, the alternate result from Dorling et al [364], share the same reasoning increased nitrogen content would cause reduction of lipid and carbohydrate production [364, 365]. In abundance of nitrogen conditions, the microalgae biomass would tend to increase protein content whereas in nutrient starvation environments such conditions would contribute to enhance the carbohydrate and lipid value. The cell obtains the signal to generate more lipid and carbohydrate as storage during nutrient starvation period to prolong the growth, as glycerol from the triglyceride or lipid which could be metabolized for energy which being converted into glucose or monosaccharide.

6.3.5 Predicting in K-Nearest Neighbor algorithm for biomass, nitrate content, and pH

The implementation of Artificial Intelligent (AI) for analysis of biomass maturation and biomass amount according to the physical point of the raster image pixels to analyze the biomass colors compounds. In **Figure 6-6(a), 6-6(b), and 6-6(c)**, they have shown the normalized RMSE based on different k-values from the algorithm to check the accuracy deviation from the actual experimental data. K-value in the algorithm indicates the number of data used for computation

in the algorithm model. The comparison chart for different k-values by the algorithm of k- Nearest Neighbors (k-NN) for biomass is aimed to analyze the accuracy through selecting the lowest error projected by the normalize root mean square error (nRMSE) calculation. The lowest k-value error for biomass in **Figure 6-6(a)** at k = 4 from RMSE at the average deviation 0.10 compare to the highest value at k =2 at 0.45 of error deviating from the actual experiment data compared from the total of 5 different mediums of cultivation value. Average of the error is improved 77.78% when the k-value of the algorithm reached 4. In **Figure 6-6(b)**, it is shown the lowest average for nitrate normalized RMSE is k = 4, which is 0.11 compared to the highest deviation value at k = 2 at 0.14. Theoretically, the higher the k-value, the better the forecasting performance would be due to ample amount of neighboring data points as reference to the estimation. Thus, when the k-value is low, higher deviation between actual data and predicted data is expected. Even though larger k-value increase the number of reference data points for comparison to improve the forecasting accuracy, the nRMSE scored by higher k-values in this study has suggested otherwise. The main essence of our k-NN algorithm is to deploy weighted average method to estimate unknown features of the test data based on neighboring data available. The key point here refers to the neighborhood of the test data. Though, having more neighbor is good in estimation but the size of the neighborhood (searching parameter size) could be an adverse factor. This has caused the estimation to lose locality information if the factor is too big, which is the key for k-NN to produce

an accurate estimation. According to Ma et al [366], the optimal k-value is usually obtained higher accuracy between 3 to 10 for most datasets, but not for all cases. The datasets for creating this analysis are split into training and testing randomly. In **Figure 6-6(c)**, it is shown the pH values amount for comparison of 4 different k-values 2, 3, 4, and 5 for all mediums. The lowest average nRMSE value at k=4 at 0.02, where highest average deviation at 0.21 in k-value of 2. Therefore, the k-value at 4 is the optimal value for all 3 parameters biomass weight, nitrate content, and pH value to obtain the highest accuracy value for the datasets.

There are a variety of algorithms in artificial intelligence (AI) for prediction cases where K-Nearest Neighbors is adopted here to enhance the analysis of accuracy to determine the biomass amount and maturation period in the molasses cultivation system. The k-Nearest Neighbors algorithm (k-NN) is one of the popular algorithms in which it is widely used for predictive data analysis [367]. The AI algorithm training set is served with the primary objective to observe the arbitrary microalgae cell concentration through color pixel (RGB) intensities in the overall raster image of pixels. The color changes for each microalgae cell of *Chlorella vulgaris FSP-E* will be turning from light green to dark green upon maturation as comparison data with the nearest neighbor data and formed an average as final determination. Each sample color change would indicate the nutrients and iterative to provide subsequent day's data with the number of days until the maturation period. Therefore, the experimental data generated are

determined according to the color changes especially in green by the algorithm used as a training set to improve the medium nutrient of new samples to be forecasted. As the beginning of the cultivation period color changes are more easily fluctuated. The maturation period is validated by previous experiment growth patterns as in Chen et al [368]. The implementation of AI in the microalgae cultivation is relatively faster than the conventional experiment analysis procedure.

The actual data for training and forecast data for testing shown in **Figure 6-7** is observed and found similar of growth pattern as previous experiment by Chia et al [362], the overall training data of normalized RMSE value which is without unit, k=4 shown an average at 0.10 for biomass, 0.11 for nitrate and 0.02 for pH value. It can be concluded that the artificial intelligence k-NN algorithm can be used for estimating the data of biomass, nitrate and pH value with molasses medium through images raster pixel.

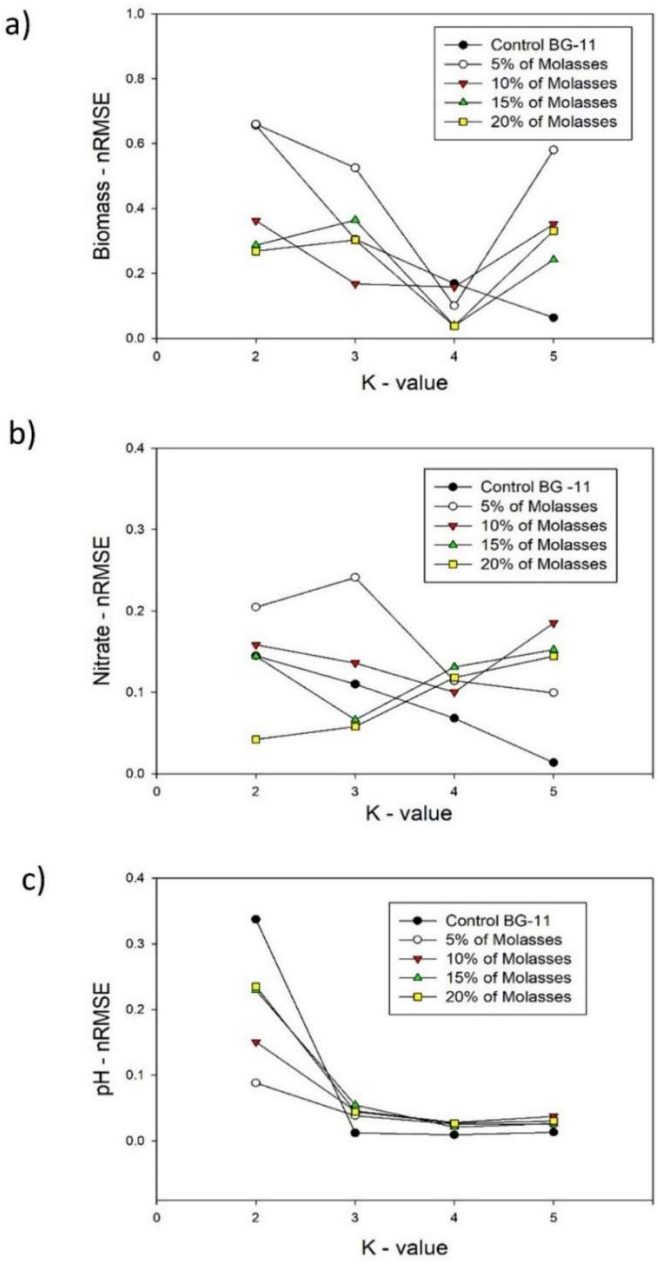


Figure 6-6: Comparison of different K-value by predicting and actual data using normalise Root Mean Square Error (nRMSE) in (a) biomass, (b) nitrate and (c) pH value.

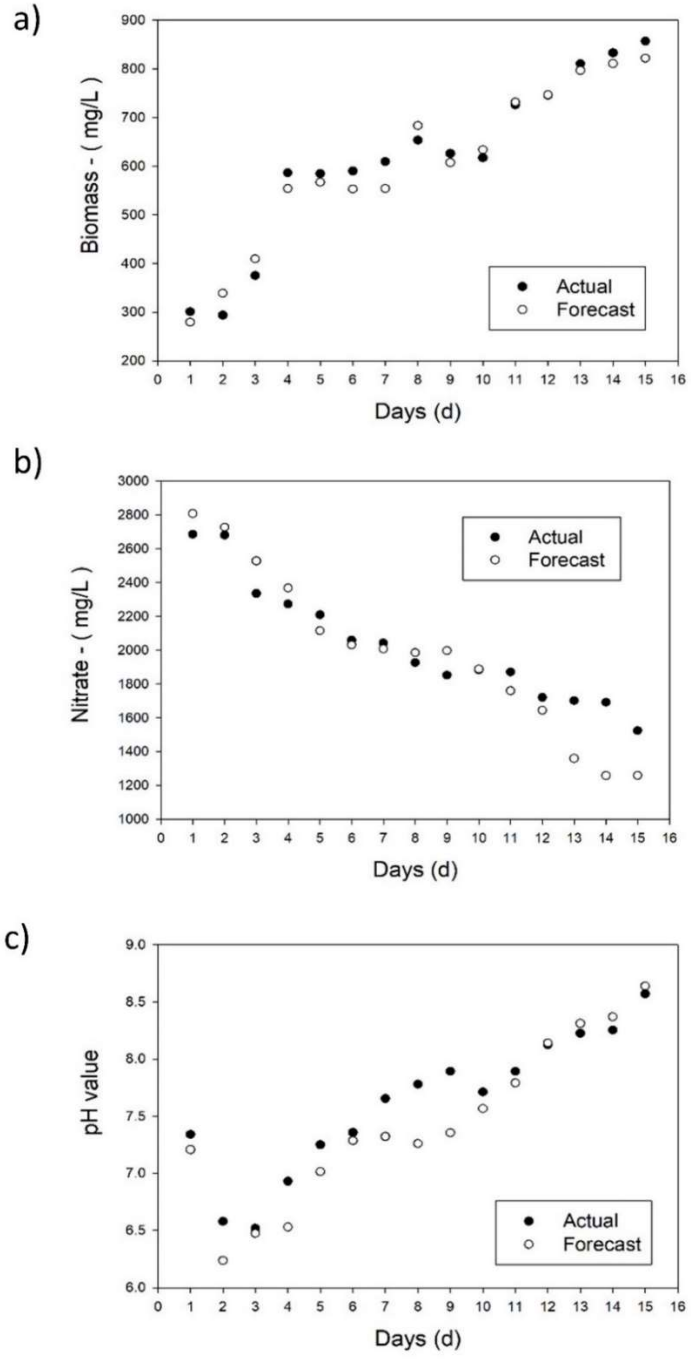
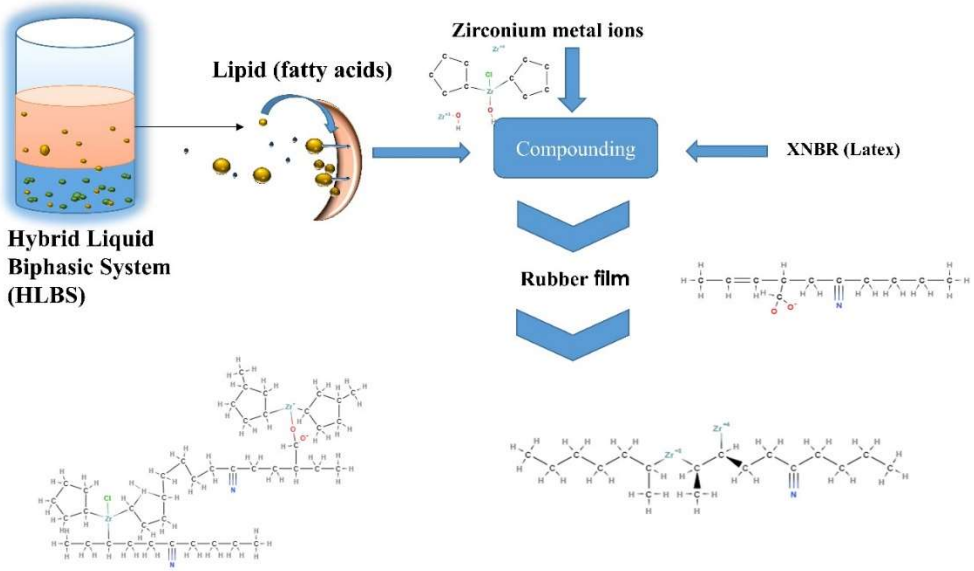


Figure 6-7: The comparison of prediction data by k=4 with actual set of biomass, nitrate, and pH value using k-NN algorithm

6.4 Conclusion

The use of waste molasses as a cultivation medium for microalgae C. vulgaris FSP-E is able to sustain the growth of the cell without addition of concentrated CO_2. The protein content from all molasses medium is found to be higher than conventional BG-11 medium. The 10% of molasses medium recorded with the protein content at 294.10 mg/g, is enhanced by 20.60% compared to BG-11. Biomass amount is found highest with 20% of the molasses medium raised 82.70% by weight, compared to conventional BG-11 medium. Besides, the k-Nearest Neighbor is viable for forecasting the biomass, nitrate and pH value with optimized at k = 4, where the average RMSE is the lowest and closest to the actual experimental data. The pretreatment with acid-alkaline method to increase the monosaccharide and disaccharide to stimulate the Acyl-CoA for higher nutrients compound generation. Molasses can be introduced to the cultivation medium for higher nutrients compound in the biomass.

Chapter 7: Stability Enhancement of Synthetic Rubber (XNBR) with Microalgae Based Fatty Acids Incorporated Zirconium Metal Ion



This chapter covers the use of lipid compound from HLBS extraction method to incorporate into (XNBR) carboxylated nitrile butadiene rubber. The introduction of Zirconium metal ions and fatty acids derived from microalgae lipid have enhanced the stability effect, where contributed in crosslinking coordination with the polymer molecules as well. The effect of tensile strength, crosslinking density, 300% and 500% specific tensile strength, elongation, aging properties, zeta potential and polydispersity index have been studied in this chapter. The experiment has supported the microalgae lipid could be applied in industrial application as positive contribution to the physical properties with synthetic rubber for lightly cross-linked products.

Abstract

Synthetic rubber derived from carboxylated nitrile butadiene rubber (XNBR) is the most demanded rubber commonly blended with a sulphur-based linkage system and used in crosslinking products. In this study, the fatty acids derived from microalgae stabilise the linker's agglomeration and compounded polymer. The rubber film's enhanced properties such as tensile strength, elongation, 300% and 500% specific elongation, crosslink density, zeta-potential, and aging were observed. Zirconium contains tetravalent charges in which the high positive charge improves the tensile strength. After binding with microalgae-derived fatty acids in Zirconium metal linker compound (L-MBL), higher stability in terms of zeta potential (-12.87 mV) with high tensile strength of 32.05 MPa and 580% elongation was noted. The compounded linker contributes to higher tensile strength and crosslink density of 32.1% and 35.7%, respectively. This investigation focuses on the prospects of XNBR polymer materials to replace accelerator and initiator components in the making of rubber film, which would otherwise trigger anaphylaxis and dermatitis allergies.

Keywords: XNBR, Synthetic rubber, Crosslinker, Microalgae, Zirconium

7.1 Introduction

The synthetic polymer of carboxylated nitrile butadiene rubber (XNBR) is mostly applied on lightly crosslinked materials (e.g. thin film, medical gloves, condom). Notably, it has a high demand in the medical gloves sector. This material is well known for its economic value and excellent physical performance [11]. The research on synthetic rubber materials, especially on XNBR, is increasing owing to their superior characteristics, such as oil-resistance, effective coating, protein-free and low permeability [120]. The molecular structure of XNBR is described as a terpolymer comprising of hydrocarbon of butadiene, acrylic acid and acrylonitrile, which is one of the several crosslinking paths for covalent or ionic bonds to establish cross-linkages [369]. The molecules of XNBR are viable for ionic binding from metal and stabilization by highly unsaturated fatty acid molecules from microalgae biomass.

The rubber materials' vulcanisation process produces a high elasticity product by forming a linkage network within the polymer compounds. The C=C double bonds from butadiene molecules are the part of the branch in the XNBR polymer molecules and act as potential sites with delocalised electron to establish bonding with other molecules. The bonding of delocalised pi bond occurs with cations during the compounding process, as the H-bond contains highly mobilized charges even in the solid-state [370]. Metal ions are the emerging components

for crosslinking which replace sulphur compounds for lightly crosslinked materials. The metal ion linkers may reduce using an accelerator, one of the causes of dermatitis issues [120]. Zirconium (Zr) is a transition metal with four ionic charges that can react with various types of metallic and non-metallic compounds at elevated temperatures [371, 372]. Studies utilised metal ions to enhance the physical properties of XNBR rubber compounds, especially by ionic bonds, and zirconium (Zr) is found as a new potential metal for this purpose. Its electron charges could be used in the formulation of XNBR rubber compounding. The XNBR polymer binds with fatty acids, particularly a high amount of unsaturated fatty acids molecules, causing electrophilic substitution during the hydrolysis reaction. The electrophile addition is between electrophile from fatty acids and nucleophile of zirconium metal ions. The electrophile substitution is through hydrolysis reaction by replacing hydrogen atom from the fatty acid chain and substituting zirconium metal. An alternative path for electrophilic addition for the bonding reaction from metal ions induces the carbon-carbon double bond.

Algae have been on the earth for 3.4 billion years and known as a promising raw material in renewable sources for various industrial applications due to the abundance of lipid. The extracted biomolecules for renewable energy and other applications are recommended due to the clean, versatile and high adaptability of different cell culture conditions [373, 374]. Therefore, this organism's versatility is always being highlighted and appears to be a good supply for a

future sustainable bio-materials source. Lipid-rich microalgae, such as *Chlorella sp.* biomass, comprises saturated and unsaturated fatty acids [19]. Most lipid-derived fatty acids as biomolecules are soluble in organic solvents but insoluble in inorganic solvents. The adaptation for the scale-up production in the glove manufacturing industry was proposed earlier through the prototype in laboratory-scale of hybrid liquid biphasic (HLBS) method as an ideal method for the rapid extraction of lipids [375]. Polar lipids, including phospholipids and glycolipids collected in the cells, fabricate membrane wall, while neutral lipid includes triglyceride, monoglyceride, and diglyceride. Unsaturated fatty acids have the potential to form covalent bonding in the XNBR polymer molecules. Functionalization of lipid is one way to reduce the unsaturated double bond or form hydrogen bonding in the fatty acid chain. The functionalized compounds bind with metal ions as an additional chain to form a linker. For example, copper ions induce electrophilic addition from fat-derived y-lactone [376], sulphonic acid-functionalization on mesoporous SBA-15 catalyst [377], and oxidation of algae oil unsaturated fatty acids via cobalt insertion of olefin internal double bond into Co-hydride [378]. The fatty acid chains may increase the covalent bonding with the pi bond from the polymer chains, particularly in butadiene branches, to establish more bonding within the molecules.

In this study, fatty acid chains-based microalgae lipid was infused with zirconium metal ions to act as the linker compounds for XNBR latex. The employed lipid microalgae species was *Chlorella sorokiniana* CY-1, while the

zirconium metal was compounded by a mixture of bis(cyclopentadienyl) zirconium (IV) dichloride and zirconium (IV) oxide. The compounded XNBR latex was tested for the effects of functionalized lipid with metal on the tensile properties, elongation, 300% and 500% specific elongation strength, zeta-potential, aging effect, and crosslink density

7.2 Materials and Methods

XNBR latex (Bangkok Synthetic) with a dry rubber content of 60 % total solid content (TSC) at pH 8.21 was obtained from B.S.T Elastomer Co. Ltd. Bis(cyclopentadienyl), zirconium (IV) dichloride ($C_{10}H_{10}Cl_2Zr$), zirconium (IV) oxide (ZrO_2), polysorbate 80 and sodium dodecyl sulfate ($NaC_{12}H_{25}SO_4$), potassium hydroxide (KOH), sulphur (S), zinc diethyldithiocarbamate (ZDEC), and zinc oxide (ZnO) were obtained from Sigma Aldrich and used without further purification.

7.2.1 Metal incorporated bio-linker (MBL) as ligand from microalgae *Chlorella sorokiniana CY-1*

The cultivation and extraction methods using the microalgae species *Chlorella sorokiniana CY-1* was according to the earlier report [18]. The conventional B&D method is time-consuming (minimum reaction time of 60 min), which depends on the solvents used along with chloroform and methanol, and it could be up to 24 h. Simultaneously, the reaction time for the tested hybrid LBS is

within minutes to obtain free fatty acid chains using microalgae. The system's conditions were: 30% hydrogen peroxide (H_2O_2), hexane (C_6H_{14}, analytical grade, 85%), contact time 3 min, room temperature (25 °C). Using evaporation, the excess organic solvent in the lipid was removed. Subsequently, 50 mL of 10% H_2O_2 and 1 µL 2% potassium permanganate ($KMnO_4$) was treated with lipid compounds at 60 °C, under atmospheric pressure for 12 h. A mixture of Bis(cyclopentadienyl) zirconium (IV) dichloride with sodium dodecyl sulfate in a ratio (1:15) was added under inert gas, followed by adding a mixture of zirconium oxide, polysorbate 80, and glycerol in a ratio (1:6:12) in deionised water and stirred for 3 h at room temperature. Both lipids and metal mixture were stirred for 12 h to form the cross-linker compounds, as shown in **Figure 7-1**, for the linker compound's potential coordination.

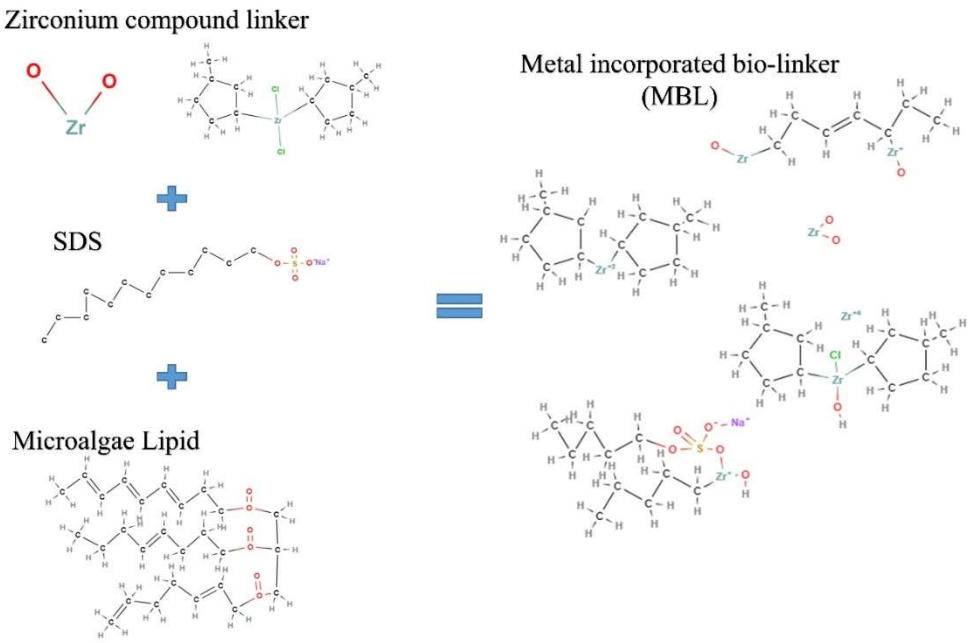


Figure 7-1: Zirconium based molecules, sodium dodecyl sulphate (SDS), and lipids that have been shown as potential linker compounds for binding.

7.2.2 Preparation of vulcanised XNBR latex film

XNBR latex was pre-vulcanised through a pH adjustment to 10.2 by adding a monovalent salt solution (KOH, 5 wt.%) as a pre-crosslink agent under stirring. Salt in latex compounding for thin-film latex is important for adjusting the pH. This allows the latex molecules with monovalent salt for pre-cross-linking. For pre-curing, salt was added for 1.5 phr for all the compounds, as shown in **Table 7-1**. The ion-based ZnO and ZrO linkers were added 1 phr for ionic crosslinking except for latex and latex-KOH samples. The conventional sulphur-based compounding formulation contains sulphur, initiator ZnO, and added accelerator of the ZDEC into latex as a compound. Thermal pre-curing was conducted for compounding samples with metal, ZnO or ZrO_2 at 55 °C for 2 h under stirring [369]. Metal incorporated bio-linker (MBL) as a linker compound includes ZrO and lipid-derived from microalgae. For maturation, stirring was conducted for 12 h at room temperature under atmospheric pressure. MBL linker is shown in **Figure 7-2**.

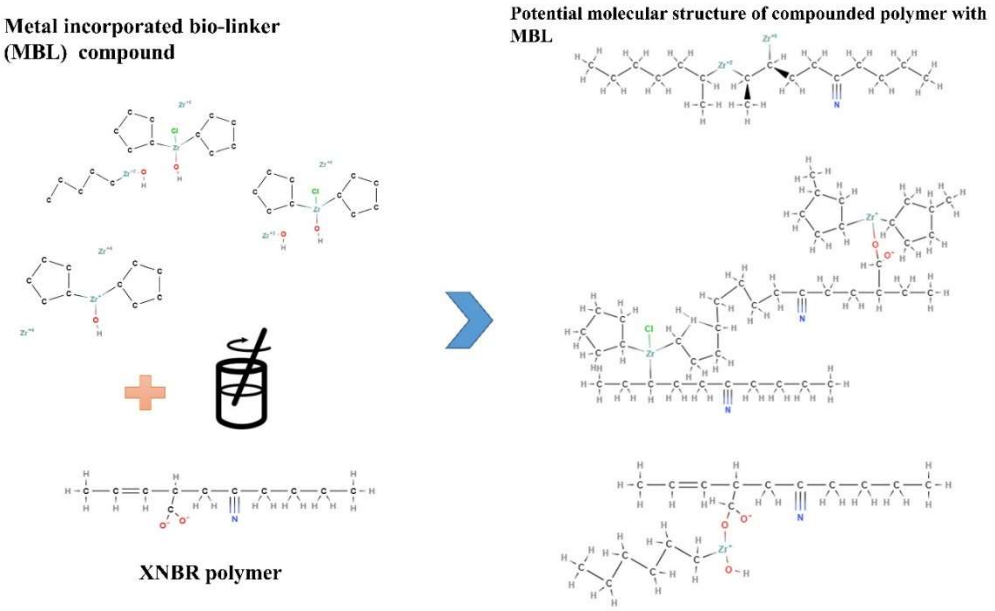


Figure 7-2: Metal incorporated bio-linker (MBL) compounded with XNBR polymer demonstrates potential coordination linking

Table 7-1: Compounding of XNBR sample formulations

Samples	**Latex (phr)**	**KOH (phr)**	**ZnO (phr)**	**Sulfur (phr)**	**ZDC (phr)**	**ZrO_2 (phr)**	**MBL (phr)**
Latex	100						
Latex - KOH	100	1.5					
Latex - Sulfur - ZnO-ZDC	100	1.5	1	1	0.5		
Latex - ZnO	100	1.5	1				
Latex - ZrO_2	100	1.5				1	
Latex - MBL	100	1.5					1

7.2.3 Preparation of latex films

The latex films were prepared through a conventional coagulant dipping procedure. The thin latex film was produced on porcelain formers which were cleaned by deionised water beforehand. Subsequently, drying was followed at 125 °C for 5 min for the latex dipping process; the formers were dipped into the calcium salt (coagulant) solution at 50-60 °C for 30 s, and the former was heated up to 100 °C for 1 min to dry the coagulant. The coagulant solution comprised calcium nitrate ($CaNO_3$), striping agent calcium carbonate ($CaCO_3$), and surfactants. Latex film was dipped into the rubber compound solution at room temperature for 30 s and placed into the oven for 1 min for drying. The latex film was then immersed into the water bath at 58-60 °C for 30 s as post leaching process, and for vulcanization, it was kept in the oven at 120 °C for 20 min. The range of film thickness ranged from 55 to 60 μm, measured using a micrometre thickness gauge.

7.2.4 Colloidal stability test

The dispersed latex liquid was collected from the latex compound solution. The concentration of latex samples was obtained using a pipette (1 of 100 part and diluted by deionised water) for determining the size and zeta potential (Malvern Zetasizer NanoZS) of the colloids. The zeta potential using M3-PALS technology and sizing measurement from a diameter range of 0.3 nm to 10 μm was conducted through a non-invasive backscatter (NIBS) technique. All the

tests were conducted at room temperature (25 °C), and triplicate reading was recorded for each sample.

7.2.5 Swelling measurement (crosslink density)

A swelling measurement test was conducted according to the Flory-Rehner method [379]. The samples from XNBR latex films were cut into a rectangular shape (surface area of 10-20 mg, 4 cm × 1 cm), and the measurement was recorded with an accuracy of ±0.1 cm and ±0.1 mg. The film samples were placed in glass vials and were filled with methanol and stored at room temperature (25 °C) for 24 h. Then, the final measurement was recorded when it reached the swollen state [380]. The samples were removed from the glass vials and dried under air for 5 min to ensure the evaporation of solvents from the film samples before taking the measurements. The crosslink density (ν) was calculated according to Eq. (7-1), where V_o is the molar volume of methanol, x = [0.487 + 0.228 × V_p], and V_p was obtained using Eq. (7-2).

$$\nu = \frac{-(\ln(1-V_p)+V_p+x(V_p^2))}{V_o(V_p^{\frac{1}{3}}-\frac{V_p}{2})} \qquad (7\text{-}1)$$

$$V_p = \frac{\rho_f \cdot V_f}{\rho_f \cdot V_f + \rho_s \cdot (1-f) V_s} \qquad (7\text{-}2)$$

Where Pf is the polymer's density, ps is the density of solvent, Vf is the volume of the polymer, Vs is the volume of solvent, and f is the polymer's volume ratio.

7.2.6 Tensile testing

The investigation on mechanical properties of rubber films was conducted by Instron IX3366 universal tensile tester (Norwood, USA). The samples were cut into dumbbell shapes according to ASTM D 412-92, Die C, and EN455 with Die D's conditions at a 500 mm/min crosshead speed. The samples were conditioned for 3 h at room temperature (23 °C). 300% and 500% of tensile strength were tested with the same equipment. Before testing, the rubber film was placed at room temperature for 24 h, and each compounding formulation sample was conducted in triplicates, and the average values were reported.

7.2.7 Aging testing

The thermal aging test was conducted in a convection oven at 120 °C for 24 h. The samples were placed at room temperature for 24 h and tested for mechanical properties (tensile strength, force at break) in dumbbell shapes according to ASTM D 412-92, Die C and EN455, Die D at a crosshead speed of 500 mm/min, and samples were conditioned at room temperature (23 °C). The samples were conducted in triplicates, and the average values were reported.

7.2.8 FTIR analysis

Infrared spectroscopy was used to obtain the chemical structure of the rubber compounds with the linker. This was based on the absorption of radiation by the molecules at a specific characteristic frequency from the emission rays using the

Perkin Elmer Fourier Transmission Infrared Radiation (FTIR). The scanning of the liquid compounded solution and solid vulcanized form of the rubber film product was in the range of 400-4000 cm^{-1}.

7.2.9 Statistical analysis

The experiment data were subjected to statistical analysis and were presented from the average of triplicate readings. Data were subjected to one-factor ANOVA using SPSS to determine the significant differences ($p \leq 0.05$).

7.3 Results and discussion

7.3.1 Characterization of the functional groups of compounded polymer

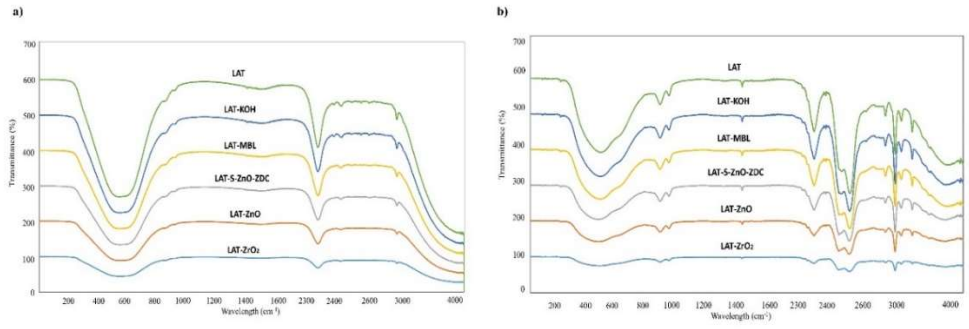


Figure 7-3: FTIR scanning in the range of 400-4000 cm^{-1} (a) compounded XNBR after 24 h of maturation (b) vulcanization of the compounded XNBR.

Figure 7-3 illustrates the compounded polymer in liquid form (**Figure 7-3a)** and vulcanised rubber film (**Figure 7-3b)**. IR spectrum for the compounded polymer in liquid form (**Figure 7-3a**) was conducted after the linker's addition and stirred

for 24 h. The spectrum shows =C-H of the alkene in the range of 1000-650 cm^{-1} and C-H methyl of alkane in long-chain from 725 to 720 cm^{-1}. As shown in Figure 8a, the transmittance intensity appears significant for the latex (LAT) sample. The carbon chain compound in the carboxylated nitrile butadiene synthetic polymer was widely dispersing mainly because no linker molecules were found. A fine peak was found between 1000 and 1300 cm^{-1} due to the C-O stretching of methyl ester. According to Xiong et al. (2015), C=O stretching leads to a narrow peak in the range of 1690-1760 cm^{-1} [381]. The C=O stretching was found in LAT and LAT-KOH samples, where there was no primary linker such as sulphur or metal ions in the polymer compound. The OH molecules establish hydrogen bonding with potassium ion with a single charge to attract the polymer compound [382]. The C≡N stretching peak of nitriles was found in the range of 2300-2200 cm^{-1}. **Figure 7-3a** also shows significant C=C-H asymmetric stretching for all the samples in the wavelength range of 3000-3100 cm^{-1}.

Figure 7-3b shows the appearance of C-O and C=O bonds in the range of 1260-1050 cm^{-1} and 1760 $cm^{-1,}$ respectively. Peaks around 2200-2300 cm^{-1} confirm the presence of nitrile group, whereas the carboxylic group was observed in the range of 2500-3300 cm^{-1}. The compounded polymer's vulcanisation process showed C-H stretching, and a weak peak arising from C≡C of alkyne was noted in the range of 3000-3100 cm^{-1} and 2190-2260 $cm^{-1,}$ respectively. A weak peak for OH stretching was found in the region of 2700-3200 cm^{-1}, indicating the

hydroxyl bonding from the addition of water molecules to the linker compound and glycerol.

7.3.2 Effect of lipid with metal on XNBR for the resultant tensile properties

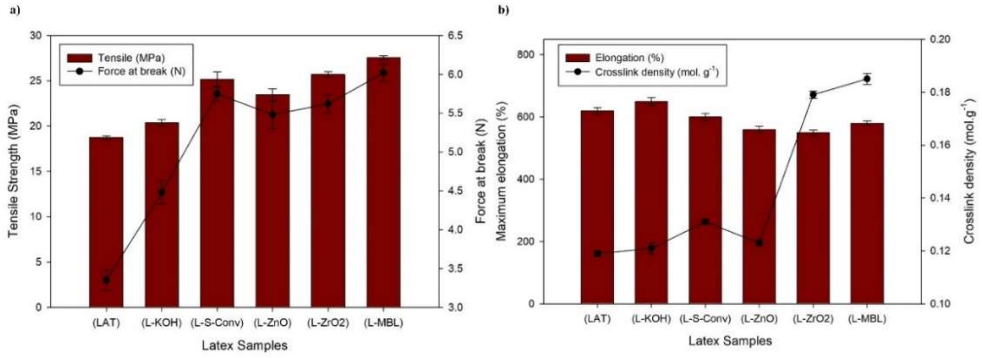


Figure 7-4: a) Comparison of the tensile strength (MPa) and force at break (N) of various latex formulation samples. b) Comparison of elongation in percentage (%) and crosslink density ($mol \cdot g^{-1}$) of various latex formulation samples.

The tensile strength measurements were conducted to study the effect of different functional linker compounds on the polymer molecules. The microalgal fatty acids ~~functionalized~~ reacted with hydrogen peroxide and potassium permanganate on the zirconium metal ions exhibited excellent tensile strength. **Figure 7-4(a)** exhibits the reduced mechanical properties in the latex (LAT) sample at 18.72 MPa, and 3.35 N, without monovalent ionic salt, sulphur or metal ion-based cross-linker. Besides, monovalent salt formed ionic bonding with polymer, which might enhance the tensile strength. LAT-KOH sample at

20.39 MPa and 4.48 N increased 8.19% and 25.22%, respectively, from the LAT compounded sample. The tetravalent and bivalent metal ions were derived from zirconium oxide (ZrO_2) and zinc oxide (ZnO), respectively, for establishing ionic bonding during vulcanization, where both form ionic bonding toward the C=C double bond and carboxylic group in the XNBR polymer [120, 383]. The tensile strength for zirconium ion samples (L-ZrO_2) was 27.19 MPa, and 5.62 N, indicating 27.19% and 40.39%, respectively higher than the control LAT sample. The tensile strength for the ionic zinc oxide sample (L-ZnO) was 20.24 MPa and 5.48 N. The distinctive mechanical strength indicates that material stiffening is contributed from higher Zr^{4+} ions, which was higher than Zn^{2+}. The incorporated metal ions and fatty acids derived from the microalgae lipid polymer (LAT-MBL) form of mixture ionic and covalent bonding with XNBR by a linker compound such as fatty acids, hydroxyl group molecules and metal ions.

The ionic compound before ionic bonding strengthens from both active metal ions of zirconium compound Bis(cyclopentadienyl) zirconium (IV) dichloride ($C_{10}H_{10}Cl_2Zr$) and zirconium (IV) oxide (ZrO_2) to increase mobilizing more metal ions for enhancing the strength of the rubber film. Therefore, the tensile strength was the highest compared to all the samples at 27.55 MPa and 6.02 N. The structure of Bis(cyclopentadienyl) zirconium (IV) dichloride consists of a zirconium central atom with two cyclopentadienyls and two chloro ligands which could be highly dissociated in the compounded linker solution. The LAT-

MBL compounded sample contains metal ions as the main curing agent during vulcanization for forming a crosslink network between XNBR macromolecules. The linker compounds may form a chain of entanglement within the rubber compound matrix through different functional groups of the compound. The covalent bonding may contribute from the fatty acid chains and hydroxyl group where elongation and dimensional stability were supported under a short period of strain. The combination of ionic and covalent compounds of the linker are the factors for obtaining soft yet high mechanical strength. The compound reduced the usage dependency on the accelerator, which triggers allergic issues of anaphylaxis and dermatitis. The L-MBL sample exceeded the tensile benchmark of ASTM 3577 for the surgical glove standard (min 24 MPa). It showed a higher tensile strength than hydrotalcite (layered magnesium aluminium) and aluminium based on the ionic liquid linker [121]. The statistical analysis showed that compounding with different linkers affect the tensile strength significantly ($p \leq 0.05$).

7.3.3 Effect of MBL on the elongation properties

The resultant elongation obtained in XNBR polymer using different linker compounds is shown in **Figure 7-4(b)**. The metal incorporated with microalgae-based fatty acids in the polymer leads to higher covalent bonding than unincorporated metal ion linker compounds. Therefore, elongation was higher as covalent bonding contributes to higher flexibility than ionic bonding. It is

challenging for the compounded polymer with the higher tensile strength to obtain higher elongation subjected to a similar tensile load for every tested sample. The XNBR latex film's elongation was measured in percentage during deformation upon the rubber film's breaking point. The highest elongation was found in the L-KOH sample (650%), followed by the LAT sample (620%), and the lowest was for L-ZrO_2 (550%). The elongation of XNBR materials was exerted on the compounded XNBR rubber film by axial force on the film's gauge length. The axial load increased on the specimen at a crosshead speed of 500 mm/min causes a proportional increase in the elongation with the exerted force until reaching the fracture point. Lower elongation was noted in the L-ZrO_2 and L-ZnO samples compared to L-KOH at 13.85% and 15.38%, respectively.

In a molecular aspect, ionic bonding contributes to enhancing tensile strength. On the other hand, the ionic strength may compromise the stretchability of the polymer chain network. As both metal-based linkers had a lower elongation where metal ion linkers contribute a major portion of ionic bonding within the polymer chains on butadiene and carboxylic groups. The compounding L-MBL sample had an elongation of 580% higher than L-ZrO_2. This may be due to the mixture of hydroxyl groups and fatty acids within the linkers, leading to covalent bonding with XNBR polymer and enhancing the elongation. The covalent bonding increases the stretchability, leading to better flexibility and mechanical properties for the compounded L-MBL polymer [384]. The MBL linker compound consists of fatty acids derived from microalgae lipid, where it was

functionalized through oxidation. The hydroxyl and metal ions bind with fatty acids as compounded linkers can stabilize the metal ions from agglomeration. Therefore, pinholes or lumped effect on the rubber film as the major defect may easily appear for any unstable compounded polymer solution [120]. The L-KOH sample exhibited the highest elongation (650%), while L-MBL showed a competitive value (580%) compared to other samples. The statistical analysis displayed that compounding with different linkers affects elongation ($p \leq 0.05$).

7.3.4 Effect of crosslink density from metal lipid linker (MBL) on XNBR

The crosslink density is defined as the important structural property for determining the density of chains connected to two polymer networks, as shown in **Figure 7-4(b)**. Metal ions and microalgae-based linker compound exhibited higher stability, preventing agglomeration and showed the lowest zeta potential during the 5th day. The physical entanglement by molecular bonding may affect the mechanical properties of the rubber film. The highest crosslink density was found in the L-MBL sample at 0.185 mol·g^{-1}, followed by L-ZrO_2 at 0.179 mol·g^{-1}. The polymer compounded with zirconium resulted in higher crosslink density compared to other samples. Crosslinking from zirconium ions contributes to higher entanglement of the molecules; hence, it may affect the vulcanized rubber film. The crosslink density indirectly correlates with the rubber film's tensile strength, as shown by L-ZrO_2 and L-MBL samples. A higher crosslink network from ionic bonding may enhance the strength of polymer

bonding. The crosslink density of L-S-ZnO-ZDC (0.131 mol·g^{-1}) samples are ranked after L-ZrO_2. The sulphur based linker initiated and accelerated the vulcanization process using ZnO and ZDC. The compounded polymer consists of the metal element, enhancing effective bridging from the polymer chains' sulphur linkage. The lowest crosslink density was found in the LAT sample (0.119 mol·g^{-1}), where the added monovalent salt improved the linking network by 1.82% in the L-KOH sample (0.121 mol·g^{-1}).

The obtained result shows that the bivalent metal ions (Zn^{2+}) compound crosslink density were lower than tetravalent metal ions as their crosslink density were 0.122 mol·g^{-1} and 0.179 mol·g^{-1}, respectively. However, both zinc oxide and zirconium oxide's crosslink density were less than the L-MBL linker compound. The linker from L-MBL has a highly mobilized compound from Bis(cyclopentadienyl) zirconium (IV) dichloride ($C_{10}H_{10}Cl_2Zr$). Zirconium atom has a centre with two delocalised compounds from cyclopentadienyl, and it can attach to two chloro ligands blended with zirconium oxide. When reacted with air and water molecules, the highly mobilized molecules will stabilise by a mixture of non-ionic surfactant with the entanglement of microalgae-based fatty acid. This causes a delay in diffusion and agglomeration from the bonding of zirconium ions with XNBR molecules. The L-MBL exhibited the highest crosslink density, and the statistical analysis showed that compounding with different linkers affects the crosslink density ($p \leq 0.05$).

7.3.5 Effect of tensile force at 300% and 500% on specific elongation

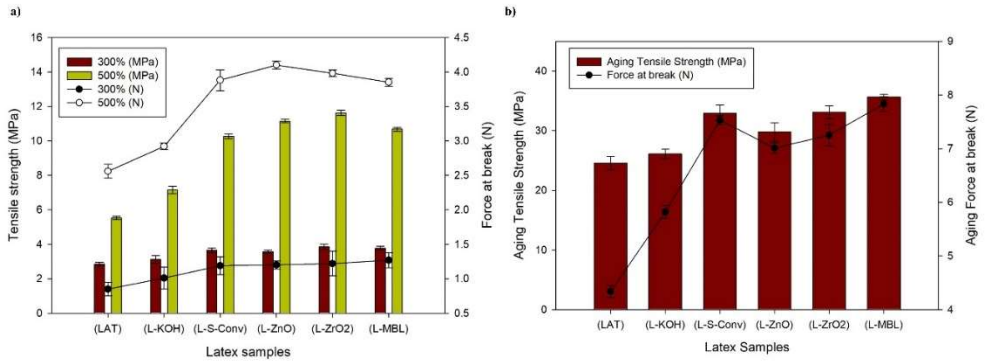


Figure 7-5: a) Comparison of specific elongation, 300% and 500% in tensile strength (MPa) and force at break (N). b) Comparison of aging profile in tensile strength (MPa) and force at break (N).

The tensile force measurements at 300% and 500% are referred to as modulus 300 (M300) and modulus 500 (M500), respectively, as shown in **Figure 7-5(a)**. Measuring the modulus of rubber film at M300 and M500 determines the rubber film's strain and elasticity. The metal ions and microalgae-based fatty acid linker compound shown before exhibited stretchability compared to the metal linker. They had higher specific tensile strength than sulphur based linker compound. Ultimate elongation may screen the overall sample's elongation at maximum to determine the changes in length from the original, while modulus was more specific for intermediate elongation with tensile strength. The highest tensile strength in specific elongation obtained from L-ZrO_2 samples for 300% and 500% elongation was 3.86 MPa (0.85 N) and 11.62 MPa (2.56 N), respectively.

The compound added into XNBR polymer contributes to different types of bonding, and each formulation affected the specific elongation tensile strength. The lowest tensile strength was obtained from the LAT sample for 300% and 500% specific elongation at 2.85 MPa (0.85 N) and 5.53 MPa (2.56 N). A lower value of specific elongation for 300% contributes to dexterity and softness upon completion for a medical glove or condom, where 500% elongation may indicate strain on the rubber film. Sulphur based linker compounds (L-S-ZnO-ZDC) showed 300% at 3.66 (1.19 N) MPa, while for L-MBL, it was a slightly higher value of 3.77 MPa (1.27 N). Besides, 500% elongation based on sulphur and metal ions linker was at 10.26 MPa (3.88 N) and 10.68 MPa (3.85 N). Based on the specific elongation results for 300% and 500%, it could be deduced that the specific tensile strength for metal-based linker is higher, and also the stretchability is larger. This could eventually affect the latex film product higher in modulus and have better elasticity. Ji Lin et al. and Zheng et al. stated that metal ions might coordinate toward higher mechanical properties in terms of strength and toughness [124, 385]. The statistical analysis showed that compounding with different linkers affects the specific elongation for 300% and 500% ($p \leq 0.05$).

7.3.6 Effect of aging for different types of linkers on XNBR film

Thermal aging involves strengthening and increased entanglement within the molecules in the rubber compound solution, which might improve the tensile

strength, as shown in **Figure 7-5(b)**. Zirconium metal ions incorporated microalgae-based fatty acids showed optimum mechanical properties after the aging test. The highest tensile strength for L-MBL by thermal aging was at 35.62 MPa (7.83 N), followed by L-ZrO_2 at 33.09 MPa (7.25 N), an improvement of 29.3% and 28.7%, respectively. A common phenomenon of lower tensile strength retention was reported for the commercial chlorinated natural rubber glove film after the aging test. Compared to the XNBR rubber film, the tensile strength of metal-based and sulphur-based linkers increased [386]. The aging test is characterized by the accelerated high temperature of rubber film obtained through the convective oven; this follows the quality control measurement based on simulated conditions for the packing compartment, which experiences increasing temperatures during shipping. The aging microstructure network was studied by Cook et al. [387]. The accelerated applied heat on the rubber film based on the transport container in the cargo shipping environment illustrated a different crosslink network structure that enabled higher tensile strength. The lowest aging tensile strength for the LAT sample was at 24.57 MPa (4.34 N), an enhancement from 18.72 (4.34 N). The actual aging condition may vary due to temperature, humidity, oxygen composition in the compartment, and rate of exposure to sunlight rays. The temperature for aging contributes to further crosslink the compound's network within the compounded formulation after the actual vulcanization process.

Furthermore, the oxygen composition and surrounding conditions may affect the oxidation of rubber film, especially for nitrile rubber film having a double bond (C=C) and sunlight with ultraviolet rays. Exposing the rubber film to radiation may affect the oxidation reaction on the polymer. The L-S-ZnO-ZDC sample was at 32.95 MPa (7.53 N) based on the conventional commercial compounding formulation in industrial glove manufacturing. It was lower compared to the L-MBL sample. The statistical analysis showed that compounding with different linker compounds affects the aging tensile strength ($p \leq 0.05$).

7.3.7 Effect on the stability of compounded polymer samples

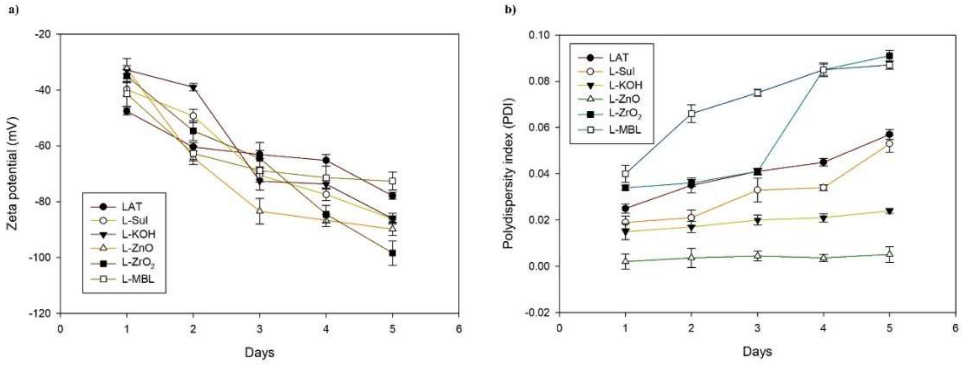


Figure 7-6: Compounded XNBR polymer (a) Zeta potential (b) Polydispersity index (PDI).

The stability of molecules is indicated by their zeta potential and polydispersity index (PDI), as shown in **Figure 7-6**, which are the vital parameters to describe the particle distribution of the compounded XNBR with different linkers. The

zirconium metal ions and microalgae-based fatty acids enhanced the stability of L-MBL samples with the addition of surfactant and fatty acids into the polymer compound. The surface charges of particles can be employed to define the stability of the molecules in the compound. **Figure 7-6(a)** shows that the standard deviation is the lowest for LAT samples, followed by L-MBL samples with -10.85 mV and -12.87 mV. The average diameter of LAT particles was 126.92 nm, while for L-MBL, it was 128.24 nm.

On the other hand, the highest standard deviation for zeta potential was found in L-ZrO_2 at -24.88 mV. All samples illustrated an increasing trend of anion character upon the 5th day. Zeta potential is a promising analytical technique for determining the electrostatic repulsion, and a zeta potential between -10 and +10 mV could be considered neutral [388]. On the first day, the highest anionic charge was found in the LAT sample (- 47.6 mV) without any linker but only water molecules with XNBR polymer. The highest zeta potential was found for the compounded L-MBL polymer sample (- 41.4 mV), while the standard deviation for L-ZrO_2 (24.88 mV) was found to be the highest. Based on the results of zeta potential, the compounded linker in L-MBL (-12.87 mV) shows higher stability in term of less deviation than L-ZnO (- 23.96 mV) and L-ZrO_2 (- 24.88 mV). On the 5th day, L-MBL consisted of metal ions and surfactant with microalgae lipid-derived fatty acids, enhancing stability [389]. The zeta potential due to charges causes agglomeration and flocculation and increases the floc size by van der Waals forces of attraction between the polymer molecules [390]. The

polydispersity index (PDI), as shown in **Figure 7-6(b),** indicates the non-uniform size distribution of the molecules. The lowest value was found in the L-KOH sample (0.015). Whereas the highest value was noted in the L-MBL sample (0.04), and both samples are considered monodisperse for the compounded polymer molecules. The highest standard deviation for PDI was found in L-ZrO_2 (0.024), and for L-MBL, it was 0.019, which is lower compared to L-ZrO_2. The overall value implies monodispersity, whereas a higher value in PDI indicates polymerization or agglomeration within the molecules. The addition of fatty acid from the microalgae-based lipid reduces the scorch time or pre-linkage before the vulcanization reaction [391]. The statistical analysis showed that the stability test data are insignificant ($p \leq 0.05$).

7.4 Conclusion

In this investigation, the microalgae lipid consists of long, medium, and short chains of unsaturated fatty acids incorporated with zirconium metal ions to form a novel linker compound for XNBR rubber. The stability of the incorporated industry-standard compounds with microalgae-based fatty acid (L-MBL) linker was found to possess 10.85%, 21.39%, and 21.06% higher stability (zeta-potential) compared to the conventional sulphur based linker (L-S-ZnO-ZDC), zirconium oxide-based linker (L-ZrO_2), and zinc oxide-based linker (L-ZnO) compounds, respectively. The tensile strength of L-MBL was 27.55 MPa which is 8.71% higher than the sulphur based linker compound. A new finding of

utilising microalgae-based fatty acids enhances the zirconium metal ions linker's stability has been exposed. The compound has shown significant improvements in XNBR rubber film's physical properties, such as tensile strength. The future application of these linkers will be in the lightly cross-linked products. This work also provides further insights into exploring potential linker combinations to be applied in heavy cross-linked products.

Chapter 8. Conclusions and Future Plans

8.1 Conclusions

The thesis objectives is explored and fulfilled involving of cultivation, extraction, transesterification and application of lipid compounds as the following i.) fulfiled the first objective from the first chapter where developed simultaneous disruption and extraction for lipid compound in a single system known as - hybrid liquid biphasic system (HLBS) ii.) achieved second objective to have optimised waste compound from waste molasses as cultivation medium with acids phase of hybrid liquid biphasic system (HLBS) for direct conversion of fatty acids iii.) fulfiled the third objective using high output system from thermal fenton reaction in HLBS with non-catalytic transesterification by sono-processes for rapid biofuel production iv.) meet second and third objectives for optimising a high output system for waste molasses cultivation medium with artificial intelligent (Ai) for photo-to-properties analysis v.) achieved third objective for making lipid compound as industry application for microalgae lipid incorporated with Zirconium metal ions as cross link agent for synthetic rubber carboxylate nitrile butadiene rubber (XNBR).

The advancement in microalgae cultivation have boost the market confident for microalgae-based products to fulfil the sustainable food and beverage demand. Moreover, the microalgae based products have notable environmental benefit with minimum negative impact for the arable land. The global microalgae based

product projected for a market value at USD 3.2 billion at the end of year 2030. Current maturity in microalgae processing and cultivation is on its path for attracting investor such as government and provide sector company for practical practise in large scale industry. Research and development is pivotal role for such technology to be continuously succeeded in innovating new equipment and scientific path for utilizing the nutrient to be used in production whether intermediate of finished products. The lipid compound from microalgae biomass is future source of raw material in biofuel and bio-molecules related products. The Hybrid Liquid Biphasic System (HLBS) which is potential mechanical pathway to be used for a rapid extraction process for lipid related application.

The third generation of biofuel is referring to microalgae derived of biofuel where able to use metabolic engineering from the cell for photosynthetic organism to produce fourth generation of biofuel directly. In this thesis, have highlighted the potential from hybrid liquid biphasic system (HLBS) for extracting fatty acids from biomass and tested on non-catalytic transesterification for the biofuel process by sono-processes through ultrasonification. The process design is disrupted by thermal Fenton reaction where optimized the lipid extract from the biomass and these reactions have increase the breakage of glycerol from the lipid (e.g. triglyceride, di-glyceride, mono-glyceride). Hence, the process of methylation is through sono-processes for the F.A.M.E production.

The microalgae lipid consists of medium to long chain of fatty acids which is suitable for enhanced the stability of metal ions charges. The polymer compounding with the emerging linker from metal ions for lightly crosslink product is a promising cross link agent for synthetic rubber. The chain of fatty acid functionalized with the oxidizing agent and binding the chain toward the Zirconium ions as a compounded linker. The fatty acids will reduce the agglomeration rate from the metal ion and act as a stabilizer which is contributing the covalent bonding to the polymer as well. Current industry is depending on sulphur crosslink compound as the primary linking agent where has reported issue for dermatitis allergic issue and anaphylaxis problem.

The application of microalgae lipid is wide and fill with various potential as the current research is primary focus on food supplement product, while this thesis has introduced the potential as industry intermediate product and alternative biofuel conversion system with enhanced properties of the existing extraction system. This innovation works has added positivity perspective for the source of renewable energy from microalgae lipid. Furthermore, this comprehensive framework has brought a new insight for the investor, environmentalist, process engineer and related stake holder for confidently adapt the knowledge and inspire for their existing project in their goal.

8.2 Limitation, recommendations and future works

The limitation of the existing experiment work is not included the analysis of risk factor for the HLBS system. The existing work of HLBS rapid disruptive extraction system is revealing the potential for simultaneous extract of lipid compound from the microalgae biomass. The limitation for HLBS using the H_2O_2 as disruptive phase may induce radicles propagation chains, where this is not recommended for nutrient extraction particularly for food products. As the nutrient have tendency for oxidized, alternate the origin of the nutrient molecular structure and contribute for the factor of mutant in some biosynthesis pathway. Hence, HLBS is towards industrial products particularly intermediate or finished substances.

Besides, the microalgae biomass cultivated from waste molasses is recommended for protein supplement as the biomass is rich in protein content. Moreover, light intensity as one of the limiting factor affecting for cultivation of the microalgae strain in waste molasses medium. The intensity of the waste molasses medium coloration would be raised as the biomass grew, suggested the source of light intensity increase the intensity as the biomass productivity raises. The acid phase of HLBS system in Chapter 4 enhanced by the conversion the F.A.M.E production through ultrasonication, where the organic solvent phase could be alternate to green solvent such as dichloromethane or ethyl lactate.

Furthermore, the non-catalytic transesterification is tested on laboratory scale and the parameter of amplitude could be further enhanced for increasing the F.A.M.E production yield. The current design of the non-catalytic system is recommended for laboratory scale while proper reactor design recommended to operate up to tones of biofuel production to sustain the market demand in future. The mechanism from the non-catalytic transesterification method can be altering for different solvent to be used such as ethanol could be generated for fatty acids ethyl ester (FAEE). A proper piping instrument diagram (PID) could be designed as control for high consistency of the biofuel production yield.

Nonetheless, the microalgae lipid extracted from the HLBS system for application in polymer cross-linking reaction have enhancing the physical properties. Besides, the fatty acids contribute for stabilization effect as the hydrocarbon chains easily binding for metal ions would assisting them from degradation and agglomeration. The limitation for current linker used on carboxylated nitrile butadiene rubber (XNBR) which is having a poor resistance to hydrocarbons, oils, and easily to oxidize in the oxygen rich environment. Besides, under sun-light consists of UV-rays have accelerate the oxidation rate for the rubber film where the physical properties of the rubber film will degrade the composition of the polymer compound.

The limitation of the works focusing on the quantity and quality from the lipid extract and applications properties. The future work is relating to up-to-date of customer needs and existing technology to visionary the applications

enhancement. The existing experiment work is based on *Chlorella sp*. of microalgae strains e.g. *Chlorella sorokiniana CY-1* and *Chlorella vulgaris FSP-E* for carrying the experiment. There should be involving of genetic modification of the strain to maximized the lipid content as the current highest lipid is found from *C. Sorokiniana CY-1* up to 60% from the biomass. The highest genetic modified strain is named *Botryococcus braunii* lipid up to 75% reported. Therefore, the recent genetic modification tools CRISPR-Cas9 which is the tools with rapid and precise modification for selected strain code.

In the case of extraction method, the developed hybrid liquid biphasic system (HLBS) can be further improvise with green solvents such as dichloromethane or ethyl lactate in the organic phase. The disruptive phase with Thermal Fenton activity could be implemented for others source of raw material with layers of cell wall. Besides, the Fenton reaction in the HLBS could be implemented with UV-rays or photovoltaic as parameters for enhancing the disruptive effect to improve the extract yield. The overall costing for HLBS is on the organic solvents where the most feasible to reduce the cost is implementing a direct methanol phase and developed as simultaneous transesterification with extractive properties. Besides, the waste molasses is rich with saccharides compounds, therefore the fermentation of bio-methane by selected strain of microalgae is one of the promising path for the bio-energy power generation.

Furthermore, the artificial intelligent for rapid analysis through photo by k-nearest neighbour (k-NN) can be upgraded to neuron network with unsupervised

learning algorithm to improvise the analysis accuracy. The current trend of deep learning can be assisted the process in the field of chemical engineering in term of lipid extraction optimization and analysis. Therefore, the different of algorithm can be exploring with feasible idea for fully automation for process control and monitoring through artificial intelligent (Ai).

Last but not least, the microalgae lipid derived of fatty acids binding with zirconium metal ions have a promising crosslink compound in the disposable rubber glove sectors. The idea for future may involve of polymerising from microalgae oil for producing bio-polymer. The integration of bio-oil with different hydrocarbon chains for polymerization is difficult as the fatty acids combine with long and short, saturated and unsaturated, polar and non-polar, therefore often agglomeration occurred before the end from the propagation step after initiated. Further refine the bio-oil with specifically butadiene is expected. However, the technology is involving precise design of reactor and refinery column.

References

[1] Sousa, I., Gouveia, L., Batista, A., Raymundo, A. & Bandarra, N., *Microalgae in novel food products*, (2008),pp

[2] Mehta, P., Singh, D., Saxena, R., Rani, R., Gupta, R., Puri, S. & Mathur, A., High-Value Coproducts from Algae—An Innovational Way to Deal with Advance Algal Industry. (2018),pp 343-363.

[3] Najafi, G., Ghobadian, B. & Yusaf, T. F., Algae as a sustainable energy source for biofuel production in Iran: A case study. *Renewable Sustainable Energy Rev.*, 15, (2011),pp. 3870-3876.

[4] Yahya, N. A., Attan, N. & Wahab, R. A., An overview of cosmeceutically relevant plant extracts and strategies for extraction of plant-based bioactive compounds. *Food Bioprod. Process.*, 112, (2018),pp. 69-85.

[5] Chew, K. W., Chia, S. R., Show, P. L., Yap, Y. J., Ling, T. C. & Chang, J.-S., Effects of water culture medium, cultivation systems and growth modes for microalgae cultivation: A review. *J. Taiwan Inst. Chem. Eng.*, 91, (2018),pp. 332-344.

[6] Kubátová, A., Koukol, O. & Novakova, A., *Geomyces destructans, phenotypic features of some Czech isolates*, 63, (2011),pp 65-75.

[7] Leong, H. Y., Ooi, C. W., Law, C. L., Julkifle, A. L., Ling, T. C. & Show, P. L., Application of liquid biphasic flotation for betacyanins extraction from peel and flesh of Hylocereus polyrhizus and antioxidant activity evaluation. *Sep. Purif. Technol.*, 201, (2018),pp. 156-166.

[8] Plaza, M. & Turner, C., Pressurized hot water extraction of bioactives. *Trend. Anal. Chem.*, 71, (2015),pp. 39-54.

[9] Murakami, S. & Aoki, N., Bio-based hydrogels prepared by cross-linking of microbial poly (γ-glutamic acid) with various saccharides. *Biomacromolecules.* 7, (2006),pp. 2122-2127.

[10] Oliva-Rodríguez, A. G., Quintero, J., Medina-Morales, M. A., Morales-Martínez, T. K., Rodríguez-De la Garza, J. A., Moreno-Dávila, M., Aroca, G. & González, L. J. R., Clostridium strain selection for co-culture with Bacillus subtilis for butanol production from agave hydrolysates. *Bioresource technology.* 275, (2019),pp. 410-415.

[11] Yew, G. Y., Tham, T. C., Law, C. L., Chu, D.-T., Ogino, C. & Show, P. L., Emerging crosslinking techniques for glove manufacturers with improved nitrile glove properties and reduced allergic risks. *Materials Today Communications.* 19, (2019),pp. 39-50.

[12] Kwiecień, I., Radecka, I., Kwiecień, M. & Adamus, G., Synthesis and structural characterization of bioactive PHA and γ-PGA oligomers for potential applications as a delivery system. *Materials.* 9, (2016),pp. 307.

[13] Manzar, M. S., Waheed, A., Qazi, I. W., Blaisi, N. I. & Ullah, N., Synthesis of a novel epibromohydrin modified crosslinked polyamine resin for highly efficient removal of methyl orange and eriochrome

black T. *Journal of the Taiwan Institute of Chemical Engineers.* (2019),pp.

[14] Tsai, W.-B., Chen, Y.-R. & Liu, H.-L., RGD-conjugated crosslinked chitosan scaffolds for culture and osteogenic differentiation of mesenchymal stem cells. *Journal of the Taiwan Institute of Chemical Engineers.* 44, (2013),pp. 1-7.

[15] Hussain, F., Shah, S. Z., Ahmad, H., Abubshait, S. A., Abubshait, H. A., Laref, A., Manikandan, A., Kusuma, H. S. & Iqbal, M., Microalgae an ecofriendly and sustainable wastewater treatment option: Biomass application in biofuel and bio-fertilizer production. A review. *Renewable and Sustainable Energy Reviews.* 137, (2021),pp. 110603.

[16] Arif, M., Wang, L., Salama, E.-S., Hussain, M. S., Li, X., Jalalah, M., Al-Assiri, M., Harraz, F. A., Ji, M.-K. & Liu, P., Microalgae isolation for nutrient removal assessment and biodiesel production. *BioEnergy Research.* 13, (2020),pp. 1247-1259.

[17] Arun, J., Gopinath, K. P., SundarRajan, P., Felix, V., JoselynMonica, M. & Malolan, R., A conceptual review on microalgae biorefinery through thermochemical and biological pathways: bio-circular approach on carbon capture and wastewater treatment. *Bioresource Technology Reports.* (2020),pp. 100477.

[18] Yew, G. Y., Chew, K. W., Malek, M. A., Ho, Y.-C., Chen, W.-H., Ling, T. C. & Show, P. L., Hybrid liquid biphasic system for cell disruption

and simultaneous lipid extraction from microalgae Chlorella sorokiniana CY-1 for biofuel production. *Biotechnology for Biofuels.* 12, (2019),pp. 252.

[19] Yew, G. Y., Lee, S. Y., Show, P. L., Tao, Y., Law, C. L., Nguyen, T. T. C. & Chang, J.-S., Recent advances in algae biodiesel production: From upstream cultivation to downstream processing. *Bioresource Technology Reports.* 7, (2019),pp. 100227.

[20] Kim, H., Kim, M., Kim, D. & Cho, M., Physicochemical Design Principles Enabling High-Energy and-Power Low-Cost Na Storage Materials. *The Journal of Physical Chemistry C.* 125, (2021),pp. 3305-3313.

[21] Shah, S. S., Qasem, M. A. A., Berni, R., Del Casino, C., Cai, G., Contal, S., Ahmad, I., Siddiqui, K. S., Gatti, E. & Predieri, S., Physico-chemical properties and toxicological effects on plant and algal models of carbon nanosheets from a nettle fibre clone. *Scientific reports.* 11, (2021),pp. 1-14.

[22] Todd, R. & Baroutian, S., A techno-economic comparison of subcritical water, supercritical CO2 and organic solvent extraction of bioactives from grape marc. *Journal of Cleaner Production.* 158, (2017),pp. 349-358.

[23] Gogate, P. R. & Joshi, S. M., Process Intensification Aspects of Extraction of Pigments from Microalgae. *Pigments from Microalgae Handbook.* Springer, (2020),pp 309-324.

[24] Oo, Y. M., Prateepchaikul, G. & Somnuk, K., Two-stage continuous production process for fatty acid methyl ester from high FFA crude palm oil using rotor-stator hydrocavitation. *Ultrasonics Sonochemistry.* 73, (2021),pp. 105529.

[25] Sun, X., You, W., Xuan, X., Ji, L., Xu, X., Wang, G., Zhao, S., Boczkaj, G., Yoon, J. Y. & Chen, S., Effect of the cavitation generation unit structure on the performance of an advanced hydrodynamic cavitation reactor for process intensifications. *Chemical Engineering Journal.* 412, (2021),pp. 128600.

[26] Zhao, C., Qiao, X., Shao, Q., Hassan, M., Ma, Z. & Yao, L., Synergistic effect of hydrogen peroxide and ammonia on lignin. *Industrial Crops and Products.* 146, (2020),pp. 112177.

[27] Baizura, B. N., Noor'ain, S., Zhariff, M. M., Hajar, Z. S., Shahrizan, S. M., Vinomalar, G., Norleen, M. A., Khoon, K. Y. S. & Abdul, G. Z., Enhancing Post-market Surveillance Through Laboratory Testing on Blue-green Algae Products in Malaysia. (2018),pp.

[28] Council, N. R., *America's energy future: technology and transformation*, National Academies Press, (2010),pp

[29] Rogelj, J., Den Elzen, M., Höhne, N., Fransen, T., Fekete, H., Winkler, H., Schaeffer, R., Sha, F., Riahi, K. & Meinshausen, M., Paris Agreement climate proposals need a boost to keep warming well below 2 C. *Nature.* 534, (2016),pp. 631.

[30] Saladini, F., Patrizi, N., Pulselli, F. M., Marchettini, N. & Bastianoni, S., Guidelines for emergy evaluation of first, second and third generation biofuels. *Renewable Sustainable Energy Rev.*, 66, (2016),pp. 221-227.

[31] Naik, S. N., Goud, V. V., Rout, P. K. & Dalai, A. K., Production of first and second generation biofuels: a comprehensive review. *Renewable and sustainable energy reviews.* 14, (2010),pp. 578-597.

[32] Sun, Y. & Cheng, J., Hydrolysis of lignocellulosic materials for ethanol production: a review. *Bioresour. Technol.*, 83, (2002),pp. 1-11.

[33] Binod, P., Gnansounou, E., Sindhu, R. & Pandey, A., Enzymes for second generation biofuels: recent developments and future perspectives. *Bioresour. Technol. Rep.*, (2018),pp.

[34] Ranjith Kumar, R., Hanumantha Rao, P. & Arumugam, M., Lipid extraction methods from microalgae: a comprehensive review. *Frontiers in Energy Research.* 2, (2015),pp. 61.

[35] Ahmad, F., Khan, A. U. & Yasar, A., Transesterification of oil extracted from different species of algae for biodiesel production. *Afr. J. Environ. Sci. Technol.*, 7, (2013),pp. 358-364.

[36] Satputaley, S. S., Zodpe, D. B. & Deshpande, N. V., Performance, Combustion and Exhaust Emissions Analysis of a Diesel Engine Fuelled with Algae Oil and Algae Biodiesel. *Mater. Today: Proc.*, 5, (2018),pp. 23022-23032.

[37] Natarajan, S., Trasy, K. A., Srihari, N. & Raja, S., Effects of Injection Timing on CI Engine Fuelled with Algae Oil Blend with Taguchi Technique. *Energy Procedia.* 105, (2017),pp. 1043-1050.

[38] Vo, P., Ngo, H. H., Guo, W. S., Chang, S. W., Nguyen, D. D., Nguyen, P. D., Bui, X.-T., Zhang, X. B. & Guo, J. B., *Can algae-based technologies be an affordable green process for biofuel production and wastewater remediation?*, 256, (2018),pp

[39] Chisti, Y., Biodiesel from microalgae. *Biotechnology advances.* 25, (2007),pp. 294-306.

[40] Berberi, V., Turcotte, F., Lantagne, G., Chornet, M. & Lavoie, J.-M., High yields of sugars via the non-enzymatic hydrolysis of cellulose. *Algal ResearchAfrican Journal of Environmental Science and Technology*

143, (2011),pp. 87-96.

[41] Fargione, J., Hill, J., Tilman, D., Polasky, S. & Hawthorne, P., Land clearing and the biofuel carbon debt. *Science.* 319, (2008),pp. 1235-1238.

[42] Demirbas, A. & Demirbas, M. F., Importance of algae oil as a source of biodiesel. *Energy Convers. Manage.*, 52, (2011),pp. 163-170.

[43] Janaun, J. & Ellis, N., Perspectives on biodiesel as a sustainable fuel. *Renewable Sustainable Energy Rev.*, 14, (2010),pp. 1312-1320.

[44] Cornejo-Corona, I., Thapa, H. R., Browne, D. R., Devarenne, T. P. & Lozoya-Gloria, E., Stress responses of the oil-producing green microalga Botryococcus braunii Race B. *PeerJ.* 4, (2016),pp. e2748.

[45] Fried, S., Mackie, B. & Nothwehr, E., Nitrate and phosphate levels positively affect the growth of algae species found in Perry Pond. *Tillers.* 4, (2003),pp. 21-24.

[46] Lowrey, J., Brooks, M. S. & McGinn, P. J., Heterotrophic and mixotrophic cultivation of microalgae for biodiesel production in agricultural wastewaters and associated challenges—a critical review. *J. Appl. Phycol.*, 27, (2015),pp. 1485-1498.

[47] Lam, M. K., Lee, K. T. & Mohamed, A. R., Current status and challenges on microalgae-based carbon capture. *Int. J. Greenhouse Gas Control.* 10, (2012),pp. 456-469.

[48] Ras, M., Steyer, J.-P. & Bernard, O., Temperature effect on microalgae: a crucial factor for outdoor production. *Rev. Environ. Sci. Biotechnol.*, 12, (2013),pp. 153-164.

[49] Ahlgren, G., Temperature functions in biology and their application to algal growth constants. *Oikos.* (1987),pp. 177-190.

[50] Chia, S. R., Ong, H. C., Chew, K. W., Show, P. L., Phang, S.-M., Ling, T. C., Nagarajan, D., Lee, D.-J. & Chang, J.-S., Sustainable approaches for algae utilisation in bioenergy production. *Renewable energy.* 129, (2018),pp. 838-852.

[51] Converti, A., Casazza, A. A., Ortiz, E. Y., Perego, P. & Del Borghi, M., Effect of temperature and nitrogen concentration on the growth and lipid content of Nannochloropsis oculata and Chlorella vulgaris for biodiesel production. *Chem. Eng. Process. Process Intensif.*, 48, (2009),pp. 1146-1151.

[52] Chen, C. Y. & Durbin, E. G., Effects of pH on the growth and carbon uptake of marine phytoplankton. *Mar. Ecol. Prog. Ser.*, 109, (1994),pp. 83-83.

[53] Hires, R., Stroup, E. D. & Seitz, R. C. ATLAS OF THE DISTRIBUTION OF DISSOLVED OXYGEN AND PH IN CHESAPEAKE BAY 1949-1961. JOHNS HOPKINS UNIV BALTIMORE MD CHESAPEAKE BAY INST, (1963),pp.

[54] James, S. C., Janardhanam, V. & Hanson, D. T., Simulating pH effects in an algal-growth hydrodynamics model1. *J. Phycol.*, 49, (2013),pp. 608-615.

[55] Takagi, M. & Yoshida, T., Effect of salt concentration on intracellular accumulation of lipids and triacylglyceride in marine microalgae Dunaliella cells. *J. Biosci. Bioeng.*, 101, (2006),pp. 223-226.

[56] Ho, S.-H., Nakanishi, A., Ye, X., Chang, J.-S., Hara, K., Hasunuma, T. & Kondo, A., *Optimizing biodiesel production in marine Chlamydomonas sp. JSC4 through metabolic profiling and an innovative salinity-gradient strategy*, 7, (2014),pp 97.

[57] Goldman, J. C., Azov, Y., Riley, C. B. & Dennett, M. R., The effect of pH in intensive microalgal cultures. I. Biomass regulation. *Journal of Experimental Marine Biology and Ecology.* 57, (1982),pp. 1-13.

[58] Dayananda, C., Sarada, R., Usha Rani, M., Shamala, T. R. & Ravishankar, G. A., Autotrophic cultivation of Botryococcus braunii for the production of hydrocarbons and exopolysaccharides in various media. *Biomass Bioenergy.* 31, (2007),pp. 87-93.

[59] Dayananda, C., Kumudha, A. & Gokare, R., *Isolation, characterization and outdoor cultivation of green microalgae Botryococcus sp*, 5, (2010),pp 2497–2505.

[60] Church, J., Hwang, J.-H., Kim, K.-T., McLean, R., Oh, Y.-K., Nam, B., Joo, J. C. & Lee, W. H., Effect of salt type and concentration on the growth and lipid content of Chlorella vulgaris in synthetic saline wastewater for biofuel production. *Bioresour. Technol.*, 243, (2017),pp. 147-153.

[61] Rachlin, J. & Grosso, A., *The effects of pH on the growth of Chlorella vulgaris and its interactions with cadmium toxicity*, 20, (1991),pp 505-8.

[62] Ota, M., Takenaka, M., Sato, Y., Smith Jr, R. L. & Inomata, H., Effects of light intensity and temperature on photoautotrophic growth of a green microalga, Chlorococcum littorale. *Biotechnol. Rep.*, 7, (2015),pp. 24-29.

[63] Xu, Y., Ibrahim, I. M. & Harvey, P. J., The influence of photoperiod and light intensity on the growth and photosynthesis of Dunaliella salina (chlorophyta) CCAP 19/30. *Plant Physiol. Biochem.*, 106, (2016),pp. 305-315.

[64] Benckiser. 2014. *Rate of photosynthesis : limiting factors* [Online]. Available: http://www.rsc.org/learn-chemistry/content/filerepository/CMP/00/001/068/Rate of photosynthesis limiting factors.pdf.

[65] Singh, S. P. & Singh, P., Effect of temperature and light on the growth of algae species: A review. *Renewable Sustainable Energy Rev.*, 50, (2015),pp. 431-444.

[66] Edmundson, S. J. & Huesemann, M. H., The dark side of algae cultivation: Characterizing night biomass loss in three photosynthetic algae, Chlorella sorokiniana, Nannochloropsis salina and Picochlorum sp. *ALGAL Res.*, 12, (2015),pp. 470-476.

[67] Chen, C.-Y., Yeh, K.-L., Aisyah, R., Lee, D.-J. & Chang, J.-S., Cultivation, photobioreactor design and harvesting of microalgae for

biodiesel production: a critical review. *Bioresource technology.* 102, (2011),pp. 71-81.

[68] Baba, M. & Shiraiwa, Y., *Biosynthesis of Lipids and Hydrocarbons in Algae*, (2013),pp 331-356.

[69] Thangamani, P., Chellappan, A., Citarasu, T., Thangaswamy, S., S, A., Gopal, P. & Babu, M., *EFFECT OF DIFFERENT CULTURE MEDIA FOR THE GROWTH AND OIL YIELD IN SELECTED MARINE MICROALGAE*, Vol. 31, No. (3-4), (2016),pp 165-177.

[70] Ambati, D. R. R., Sarada, R. & Gokare, R., *Enhancement of carotenoids in green alga Botyrocccus braunii in various autotrophic media under stress conditions*, 5, (2010),pp 87-92.

[71] Lucker, B. F., Hall, C. C., Zegarac, R. & Kramer, D. M., The environmental photobioreactor (ePBR): An algal culturing platform for simulating dynamic natural environments. *ALGAL Res.*, 6, (2014),pp. 242-249.

[72] Dayananda, C., Sarada, R., Rani, M. U., Shamala, T. & Ravishankar, G., Autotrophic cultivation of Botryococcus braunii for the production of hydrocarbons and exopolysaccharides in various media. *Biomass and Bioenergy.* 31, (2007),pp. 87-93.

[73] Kim, J., Yoo, G., Lee, H., Lim, J., Kim, K., Woong Kim, C., S Park, M. & W. Ji-Won Yang, J., *Methods of downstream processing for the production of biodiesel from microalgae*, 31, (2013),pp

[74] Popper, Z., Ralet, M.-C. & Domozych, D., *Plant and algal cell walls: diversity and functionality PREFACE*, 114, (2014),pp 1043-8.

[75] Hanikenne, M., Merchant, S. & Hamel, P. P., *Transition Metal Nutrition: A Balance Between Deficiency and Toxicity*, 2, (2009),pp 333-399.

[76] Hoover, L. A., Phillip, W. A., Tiraferri, A., Yip, N. Y. & Elimelech, M. Forward with osmosis: emerging applications for greater sustainability. ACS Publications, (2011),pp.

[77] Munshi, F. M., Church, J., McLean, R., Maier, N., Sadmani, A. A., Duranceau, S. J. & Lee, W. H., Dewatering algae using an aquaporin-based polyethersulfone forward osmosis membrane. *Sep. Purif. Technol.*, 204, (2018),pp. 154-161.

[78] Kerr, W. L., Chapter 12 - Food Drying and Evaporation Processing Operations. *In:* KUTZ, M. (ed.) *Handbook of Farm, Dairy and Food Machinery Engineering (Second Edition).* San Diego: Academic Press, (2013),pp 317-354.

[79] Nguyen, T. K. & Ratti, C., Air-Drying and Non-Equilibrium States/Glass Transition. *Non-Equilibrium States and Glass Transitions in Foods.* Elsevier, (2017),pp 89-109.

[80] Desmorieux, H. & Decaen, N., Convective drying of spirulina in thin layer. *J. Food Eng.*, 66, (2005),pp. 497-503.

[81] Chen, C.-L., Chang, J.-S. & Lee, D.-J., Dewatering and drying methods for microalgae. *Drying Technol.*, 33, (2015),pp. 443-454.

[82] Desmorieux, H. & Hernandez, F., *BIOCHEMICAL AND PHYSICAL CRITERIA OF SPIRULINA AFTER DIFFERENT DRYING PROCESSES*, (2004),pp 900-907.

[83] Passos, F., Uggetti, E., Carrère, H. & Ferrer, I., Pretreatment of microalgae to improve biogas production: a review. *Bioresour. Technol.*, 172, (2014),pp. 403-412.

[84] González-Fernández, C., Sialve, B., Bernet, N. & Steyer, J. P., Impact of microalgae characteristics on their conversion to biofuel. Part II: Focus on biomethane production. *Biofuels, Bioprod. Biorefin.*, 6, (2012),pp. 205-218.

[85] Dunker, S. & Wilhelm, C., Cell wall structure of coccoid green algae as an important trade-off between biotic interference mechanisms and multidimensional cell growth. *Front. Microbiol.*, 9, (2018),pp. 719.

[86] McMillan, J. R., Watson, I. A., Ali, M. & Jaafar, W., Evaluation and comparison of algal cell disruption methods: microwave, waterbath, blender, ultrasonic and laser treatment. *Appl. Energy.* 103, (2013),pp. 128-134.

[87] Tsapekos, P., Kougias, P. G., Frison, A., Raga, R. & Angelidaki, I., Improving methane production from digested manure biofibers by mechanical and thermal alkaline pretreatment. *Bioresour. Technol.*, 216, (2016),pp. 545-552.

[88] Lee, A. K., Lewis, D. M. & Ashman, P. J., Disruption of microalgal cells for the extraction of lipids for biofuels: processes and specific energy requirements. *Biomass and bioenergy.* 46, (2012),pp. 89-101.

[89] Folch, J., Lees, M. & Sloane Stanley, G., A simple method for the isolation and purification of total lipides from animal tissues. *J biol Chem.* 226, (1957),pp. 497-509.

[90] Bligh, E. G. & Dyer, W. J., A rapid method of total lipid extraction and purification. *Canadian journal of biochemistry and physiology.* 37, (1959),pp. 911-917.

[91] Breil, C., Abert Vian, M., Zemb, T., Kunz, W. & Chemat, F., "Bligh and Dyer" and Folch methods for solid–liquid–liquid extraction of lipids from microorganisms. Comprehension of solvatation mechanisms and towards substitution with alternative solvents. *Int. J. Mol. Sci.*, 18, (2017),pp. 708.

[92] Cequier-Sánchez, E., Rodríguez, C., G Ravelo, A. & Zárate, R., *Dichloromethane as a Solvent for Lipid Extraction and Assessment of Lipid Classes and Fatty Acids from Samples of Different Natures*, 56, (2008),pp 4297-303.

[93] Schlechtriem, C., Focken, U. & Becker, K., *Effect of different lipid extraction methods on ??13C of lipid and lipid-free fractions of fish and different fish feeds*, 39, (2003),pp 135-40.

[94] M Burja, A., E Armenta, R., Radianingtyas, H. & J Barrow, C., *Evaluation of Fatty Acid Extraction Methods for Thraustochytrium sp. ONC-T18*, 55, (2007),pp 4795-801.

[95] Lee, S. Y., Khoiroh, I., Ling, T. C. & Show, P. L., Enhanced recovery of lipase derived from Burkholderia cepacia from fermentation broth using recyclable ionic liquid/polymer-based aqueous two-phase systems. *Sep. Purif. Technol.*, 179, (2017),pp. 152-160.

[96] Show, P. L., Tan, C. P., Anuar, M. S., Ariff, A., Yusof, Y. A., Chen, S. K. & Ling, T. C., Direct recovery of lipase derived from Burkholderia cepacia in recycling aqueous two-phase flotation. *Sep. Purif. Technol.*, 80, (2011),pp. 577-584.

[97] Li, Z., Fan, Y. & Xi, J., Recent advances in high voltage electric discharge extraction of bioactive ingredients from plant materials. *Food Chem.*, 277, (2019),pp. 246-260.

[98] Zaaboul, F., Raza, H., Cao, C. & Yuanfa, L., The impact of roasting, high pressure homogenization and sterilization on peanut milk and its oil bodies. *Food Chem.*, 280, (2019),pp. 270-277.

[99] Larach, M. C. 2012. *HYDRODYNAMIC EXTRACTION OF OILS FROM PHOTOSYNTHETIC CULTURES*. USA patent application.

[100] Rezzoug, S.-A., W. Baghdadi, M., Louka, N., Boutekedjiret, C. & Allaf, K., *Study of a new extraction process: Controlled instantaneous*

decompression. Application to the extraction of essential oil from rosemary leaves, 13, (1998),pp 251-258.

[101] Wajda, T. & Gabriel, K., Thermolysis reactor scale-up for pilot scale CuCl hybrid hydrogen production. *Int. J. Hydrogen Energy.* 44, (2019),pp. 9779-9790.

[102] Prado, J. M., Vardanega, R., Debien, I. C., de Almeida Meireles, M. A., Gerschenson, L. N., Sowbhagya, H. B. & Chemat, S., Conventional extraction. *Food Waste Recovery.* Elsevier, (2015),pp 127-148.

[103] Adetunji, A. I., Du Clou, H., Walford, S. N. & Taylor, J. R., Complementary effects of cell wall degrading enzymes together with lactic acid fermentation on cassava tuber cell wall breakdown. *Ind. Crops Prod.*, 90, (2016),pp. 110-117.

[104] Marathe, S. J., Jadhav, S. B., Bankar, S. B., Dubey, K. K. & Singhal, R. S., Improvements in the extraction of bioactive compounds by enzymes. *Curr. Opin. Food Sci.*, (2019),pp.

[105] Suarez Garcia, E., Suarez Ruiz, C. A., Tilaye, T., Eppink, M. H. M., Wijffels, R. H. & van den Berg, C., Fractionation of proteins and carbohydrates from crude microalgae extracts using an ionic liquid based-aqueous two phase system. *Sep. Purif. Technol.*, 204, (2018),pp. 56-65.

[106] Barbarino, E. & Lourenço, S. O., An evaluation of methods for extraction and quantification of protein from marine macro-and microalgae. *J. Appl. Phycol.*, 17, (2005),pp. 447-460.

[107] Sankaran, R., Manickam, S., Yap, Y. J., Ling, T. C., Chang, J.-S. & Show, P. L., Extraction of proteins from microalgae using integrated method of sugaring-out assisted liquid biphasic flotation (LBF) and ultrasound. *Ultrason. Sonochem.*, 48, (2018),pp. 231-239.

[108] Sati, H., Mitra, M., Mishra, S. & Baredar, P., Microalgal lipid extraction strategies for biodiesel production: A review. *ALGAL Res.*, 38, (2019),pp. 101413.

[109] Singh, R., Chapter 1 - Introduction to Membrane Technology. *In:* SINGH, R. (ed.) *Membrane Technology and Engineering for Water Purification (Second Edition).* Oxford: Butterworth-Heinemann, (2015),pp 1-80.

[110] Bhatia, S., *Advanced renewable energy systems,(Part 1 and 2)*, WPI Publishing, (2014),pp

[111] Zhang, X., Yan, S., Tyagi, R. D., Drogui, P. & Surampalli, R. Y., Ultrasonication aided biodiesel production from one-step and two-step transesterification of sludge derived lipid. *Energy.* 94, (2016),pp. 401-408.

[112] Patel, N. K. & Shah, S. N., 11 - Biodiesel from Plant Oils. *In:* AHUJA, S. (ed.) *Food, Energy, and Water.* Boston: Elsevier, (2015),pp 277-307.

[113] Brailo, M., Schreier, H. J., McDonald, R., Maršić-Lučić, J., Gavrilović, A., Pećarević, M. & Jug-Dujaković, J., Bacterial community analysis of marine recirculating aquaculture system bioreactors for complete nitrogen removal established from a commercial inoculum. *Aquaculture.* 503, (2019),pp. 198-206.

[114] Kshirsagar, A. D., Bioremediation of wastewater by using microalgae: an experimental study. *Int. J. Life Sci. Biotechnol. Pharm. Res.*, 2, (2013),pp. 339-346.

[115] Mata, T. M., Martins, A. A. & Caetano, N. S., Microalgae for biodiesel production and other applications: a review. *Renewable Sustainable Energy Rev.*, 14, (2010),pp. 217-232.

[116] Gupta, S. K., Ansari, F. A., Shriwastav, A., Sahoo, N. K., Rawat, I. & Bux, F., Dual role of Chlorella sorokiniana and Scenedesmus obliquus for comprehensive wastewater treatment and biomass production for bio-fuels. *J. Clean. Prod.*, 115, (2016),pp. 255-264.

[117] J Craggs, R., Davies-Colley, R., Tanner, C. & Sukias, J., *Advanced pond system: Performance with high rate ponds of different depths and areas*, 48, (2003),pp 259-67.

[118] J Craggs, R., Heubeck, S., J Lundquist, T. & Benemann, J., *Algal biofuels from wastewater treatment high rate algal ponds*, 63, (2011),pp 660-5.

[119] Wemyss, A. M., Bowen, C., Plesse, C., Vancaeyzeele, C., Nguyen, G. T., Vidal, F. & Wan, C., Dynamic crosslinked rubbers for a green future: A material perspective. *Materials Science and Engineering: R: Reports.* 141, (2020),pp. 100561.

[120] Yew, G. Y., Tham, T. C., Show, P.-L., Ho, Y.-C., Ong, S. K., Law, C. L., Song, C. & Chang, J.-S., Unlocking the Secret of Bio-additive Components in Rubber Compounding in Processing Quality Nitrile Glove. *Applied biochemistry and biotechnology.* 191, (2020),pp. 1-28.

[121] Marzec, A., Laskowska, A., Boiteux, G., Zaborski, M., Gain, O. & Serghei, A. Published. Properties of carboxylated nitrile rubber/hydrotalcite composites containing imidazolium ionic liquids. Macromolecular Symposia, 2014. Wiley Online Library, 341, (2014),pp 7-17.

[122] Fleischmann, D. D., Ayalur-Karunakaran, S., Arbeiter, F., Schaller, R., Holzner, A., Kern, W. & Schlögl, S., Influence of crosslinker and water on mechanical properties of carboxylated nitrile butadiene rubber (XNBR). *Polymer Testing.* 66, (2018),pp. 24-31.

[123] Zeng, D., Dong, B., Qi, Y., Yu, Z., Wang, J., Huang, X., Liu, X. & Liu, Y., On how CO2 partial pressure on corrosion of HNBR rubber O-ring in CO2–H2S–CH4 environment. *International Journal of Hydrogen Energy.* 46, (2021),pp. 8300-8316.

[124] Zheng, N., Qiu, Z. M., Liu, J., Wang, X. M., He, W. J. & Xiao, J. J., Effect of different curing systems on cell structure, mechanical properties and aging resistance of nitrile butadiene rubber foam coating with liquid compounds. *Materials Research Innovations.* 18, (2014),pp. 152-159.

[125] Chen, B.-Y., Shiau, T.-J., Hung, J.-Y., Wei, Y.-H. & Lan, C.-W., Feasibility study on production of biodegradable polymer and wastewater treatment using Aeromonas strains for materials recycling. *Journal of the Taiwan Institute of Chemical Engineers.* 45, (2014),pp. 648-652.

[126] Chen, Y.-A., Tsai, G.-S., Chen, E.-C. & Wu, T.-M., Thermal degradation behaviors and biodegradability of novel nanocomposites based on various poly [(butylene succinate)-co-adipate] and modified layered double hydroxides. *Journal of the Taiwan Institute of Chemical Engineers.* 77, (2017),pp. 263-270.

[127] Kim, J.-Y., Lee, H. W., Lee, S. M., Jae, J. & Park, Y.-K., Overview of the recent advances in lignocellulose liquefaction for producing biofuels, bio-based materials and chemicals. *Bioresource technology.* (2019),pp.

[128] Balakrishnan, P., Sreekala, M., Geethamma, V., Kalarikkal, N., Kokol, V., Volova, T. & Thomas, S., Physicochemical, mechanical, barrier and antibacterial properties of starch nanocomposites crosslinked with pre-

oxidised sucrose. *Industrial Crops and Products.* 130, (2019),pp. 398-408.

[129] Zhang, L. & Sun, X., Effects of bean dregs and crab shell powder additives on the composting of green waste. *Bioresource technology.* 260, (2018),pp. 283-293.

[130] Pan, J., Cai, H., Zhang, Z., Liu, H., Li, R., Mao, H., Awasthi, M. K., Wang, Q. & Zhai, L., Comparative evaluation of the use of acidic additives on sewage sludge composting quality improvement, nitrogen conservation, and greenhouse gas reduction. *Bioresource technology.* 270, (2018),pp. 467-475.

[131] Badhan, A., Ribeiro Jr, G. O., Jones, D. R., Wang, Y., Abbott, D. W., Di Falco, M., Tsang, A. & McAllister, T. A., Identification of novel enzymes to enhance the ruminal digestion of barley straw. *Bioresource technology.* 260, (2018),pp. 76-84.

[132] Proenca, B. C., Blaga, L., Santos, J., Canto, L. B., Amancio-Filho, S. T. & Engineers, S. o. P. Published. Force controlled friction riveting of glass fiber reinforced polyamide 6 and aluminum alloy 6056 hybrid joints. Proceedings of the Annual Technical Conference of Society of Plastics Engineers (ANTEC 2015), 2015. Society of Plastics Engineers USA, (2015),pp

[133] Li, F. & Larock, R. C., Synthesis, structure and properties of new tung oil− styrene− divinylbenzene copolymers prepared by thermal polymerization. *Biomacromolecules.* 4, (2003),pp. 1018-1025.

[134] Mosiewicki, M. A. & Aranguren, M. I., A short review on novel biocomposites based on plant oil precursors. *European Polymer Journal.* 49, (2013),pp. 1243-1256.

[135] Kong, X. & Narine, S. S., Physical properties of polyurethane plastic sheets produced from polyols from canola oil. *Biomacromolecules.* 8, (2007),pp. 2203-2209.

[136] Kaewcharoensombat, U., Prommetta, K. & Srinophakun, T., Life cycle assessment of biodiesel production from jatropha. *Journal of the Taiwan Institute of Chemical Engineers.* 42, (2011),pp. 454-462.

[137] Hottle, T. A., Bilec, M. M. & Landis, A. E., Sustainability assessments of bio-based polymers. *Polymer Degradation and Stability.* 98, (2013),pp. 1898-1907.

[138] Lim, L. Y., Lee, C. T., Bong, C. P. C., Lim, J. S., Sarmidi, M. R. & Klemes, J. J., A Review on the Impacts of Compost on Soil Nitrogen Dynamics. *Chemical Engineering Transactions.* 63, (2018),pp. 349-354.

[139] Pervaiz, M. & Sain, M., Biorefinery: opportunities and barriers for petro-chemical industries. *Pulp and Paper Canada.* 107, (2006),pp. 31-33.

[140] Pfister, D. P. & Larock, R. C., Thermophysical properties of conjugated soybean oil/corn stover biocomposites. *Bioresource technology.* 101, (2010),pp. 6200-6206.

[141] Vink, E. T., Davies, S. & Kolstad, J. J., The eco-profile for current Ingeo® polylactide production. *Industrial Biotechnology.* 6, (2010),pp. 212-224.

[142] Roy, R. V., Das, M., Banerjee, R. & Bhowmick, A. K., Comparative studies on crosslinked and uncrosslinked natural rubber biodegradation by Pseudomonas sp. *Bioresource technology.* 97, (2006),pp. 2485-2488.

[143] Bhatt, R., Shah, D., Patel, K. & Trivedi, U., PHA–rubber blends: Synthesis, characterization and biodegradation. *Bioresource technology.* 99, (2008),pp. 4615-4620.

[144] Chew, K. W., Yap, J. Y., Show, P. L., Suan, N. H., Juan, J. C., Ling, T. C., Lee, D.-J. & Chang, J.-S., Microalgae biorefinery: High value products perspectives. *Bioresource Technology.* 229, (2017),pp. 53-62.

[145] Paul Abishek, M., Patel, J. & Prem Rajan, A., Algae oil: a sustainable renewable fuel of future. *Biotechnology research international.* 2014, (2014),pp.

[146] Subramanian, S., Barry, A. N., Pieris, S. & Sayre, R. T., Comparative energetics and kinetics of autotrophic lipid and starch metabolism in

chlorophytic microalgae: implications for biomass and biofuel production. *Biotechnology for biofuels.* 6, (2013),pp. 150.

[147] Hossain, N., Mahlia, T. & Saidur, R., Latest development in microalgae-biofuel production with nano-additives. *Biotechnology for Biofuels.* 12, (2019),pp. 125.

[148] Borowitzka, M. A. & Moheimani, N. R., *Algae for biofuels and energy*, Springer, 5, (2013),pp

[149] Tester, C. C. & Joester, D., Chapter Twelve - Precipitation in Liposomes as a Model for Intracellular Biomineralization. *In:* DE YOREO, J. J. (ed.) *Methods in Enzymology.* Academic Press, 532, (2013),pp 257-276.

[150] Ariede, M. B., Candido, T. M., Jacome, A. L. M., Velasco, M. V. R., de Carvalho, J. C. M. & Baby, A. R., Cosmetic attributes of algae - A review. *Algal Research.* 25, (2017),pp. 483-487.

[151] Demirbas, A. & Fatih Demirbas, M., Importance of algae oil as a source of biodiesel. *Energy Conversion and Management.* 52, (2011),pp. 163-170.

[152] Stefan Mecking, P. K. 2014. *Production of synthetic polymer from algae oil* [Online]. Germany: Biopro Baden-Wurttemberg GmbH. Available: https://www.biooekonomie-bw.de/en/articles/news/production-of-synthetic-polymers-from-algae-oil/ [Accessed 24/04/2019 2019].

[153] Lawrence, C., Chapter 10 - Fibre to Yarn: Filament Yarn Spinning. *In:* SINCLAIR, R. (ed.) *Textiles and Fashion.* Woodhead Publishing, (2015),pp 213-253.

[154] Rerek, M. E., 27 - ProLipid® Skin-Mimetic Lamellar Gel Carrier and Delivery Systems. *In:* ROSEN, M. R. (ed.) *Delivery System Handbook for Personal Care and Cosmetic Products.* Norwich, NY: William Andrew Publishing, (2005),pp 569-586.

[155] Vovers, J., Smith, K. H. & Stevens, G. W., Chapter 4 - Bio-Based Molecular Solvents. *In:* PENA-PEREIRA, F. & TOBISZEWSKI, M. (eds.) *The Application of Green Solvents in Separation Processes.* Elsevier, (2017),pp 91-110.

[156] Patel, A., Mikes, F. & Matsakas, L., An Overview of Current Pretreatment Methods Used to Improve Lipid Extraction from Oleaginous Micro-Organisms. *Molecules (Basel, Switzerland).* 23, (2018),pp. 1562.

[157] D'Hondt, E., Martín-Juárez, J., Bolado, S., Kasperoviciene, J., Koreiviene, J., Sulcius, S., Elst, K. & Bastiaens, L., 6 - Cell disruption technologies. *In:* GONZALEZ-FERNANDEZ, C. & MUÑOZ, R. (eds.) *Microalgae-Based Biofuels and Bioproducts.* Woodhead Publishing, (2017),pp 133-154.

[158] Munir, N., Sharif, N., Shagufta, N., Saleem, F. & Manzoor, F., Harvesting and processing of microalgae biomass fractions for biodiesel production (a review). *Sci Tech Dev.* 32, (2013),pp. 235-243.

[159] Show, K.-Y., Lee, D.-J., Tay, J.-H., Lee, T.-M. & Chang, J.-S., Microalgal drying and cell disruption–recent advances. *Bioresource technology.* 184, (2015),pp. 258-266.

[160] Hayes, M., Skomedal, H., Skjånes, K., Mazur-Marzec, H., Toruńska-Sitarz, A., Catala, M., Isleten Hosoglu, M. & García-Vaquero, M., 15 - Microalgal proteins for feed, food and health. *In:* GONZALEZ-FERNANDEZ, C. & MUÑOZ, R. (eds.) *Microalgae-Based Biofuels and Bioproducts.* Woodhead Publishing, (2017),pp 347-368.

[161] Concas, A., Pisua, M. & Caoa, G., Microalgal cell disruption through Fenton reaction: experiments, modeling and remarks on its effect on the extracted lipids composition. *CHEMICAL ENGINEERING.* 43, (2015),pp.

[162] Nic, M., Jirat, J. & Kosata, B., Compendium of Chemical Terminology Gold Book. *IUPAC Compendium of Chemical Terminology.* (2014),pp. 1132.

[163] Lymar, S. V., Khairutdinov, R. F. & Hurst, J. K., Hydroxyl radical formation by O− O bond homolysis in peroxynitrous acid. *Inorganic chemistry.* 42, (2003),pp. 5259-5266.

[164] Liu, W., Ma, D., Guo, H. & Gu, G., UV-induced catalyst-free intramolecular formal Heck reaction. *Journal of Saudi Chemical Society.* (2018),pp.

[165] Chen, C.-Y., Yeh, K.-L., Chang, H.-Y. & Chang, J.-S., Strategies to Improve Oil/Lipid Production of Microalgae in Outdoor Cultivation Using Vertical Tubular-type Photobioreactors. *Energy Procedia.* 61, (2014),pp. 2755-2758.

[166] Chew, K. W., Chia, S. R., Show, P. L., Ling, T. C., Arya, S. S. & Chang, J.-S., Food waste compost as an organic nutrient source for the cultivation of Chlorella vulgaris. *Bioresource Technology.* 267, (2018),pp. 356-362.

[167] Mitra, S., *Protective role of native bovine serum albumin and alpha-unsaturated fatty acids on catechin oxidation*, 51, (2012),pp 1131-1144.

[168] Dzomba, P., Togarepi, E., Musekiwa, C. & Chagwiza, C., Improving oxidative stability of soya and sunflower oil using Temnocalyx obovatus extracts. *African Journal of Biotechnology.* 11, (2012),pp. 11099-11103.

[169] Gomez, N. A., Abonia, R., Cadavid, H. & Vargas, I. H., Chemical and spectroscopic characterization of a vegetable oil used as dielectric coolant in distribution transformers. *Journal of the Brazilian Chemical Society.* 22, (2011),pp. 2292-2303.

[170] Gosch, B. J., Magnusson, M., Paul, N. A. & de Nys, R., Total lipid and fatty acid composition of seaweeds for the selection of species for oil-based biofuel and bioproducts. *GCB Bioenergy.* 4, (2012),pp. 919-930.

[171] Carpio, R. B., De Leon, R. L. & Martinez-Goss, M. R., Growth, lipid content, and lipid profile of the green Alga, Chlorella Vulgaris Beij., under different concentrations of Fe and CO2. *J Eng Sci Technol.* 6, (2015),pp. 19-30.

[172] Fry, R., *Systems Biology in Toxicology and Environmental Health*, Academic Press, (2015),pp

[173] Mujtaba, G., Choi, W., Lee, C.-G. & Lee, K., Lipid production by Chlorella vulgaris after a shift from nutrient-rich to nitrogen starvation conditions. *Bioresource technology.* 123, (2012),pp. 279-283.

[174] Kang, N., Lee, D. S. & Yoon, J., Kinetic modeling of Fenton oxidation of phenol and monochlorophenols. *Chemosphere.* 47, (2002),pp. 915-924.

[175] Buxton, G. V., Greenstock, C. L., Helman, W. P. & Ross, A. B., Critical review of rate constants for reactions of hydrated electrons, hydrogen atoms and hydroxyl radicals (· OH/· O− in aqueous solution. *Journal of physical and chemical reference data.* 17, (1988),pp. 513-886.

[176] Yu, X.-Y., Critical evaluation of rate constants and equilibrium constants of hydrogen peroxide photolysis in acidic aqueous solutions

containing chloride ions. *Journal of physical and chemical reference data.* 33, (2004),pp. 747-763.

[177] Hey, D. H. & Waters, W. A., 11 - Free Radicals and Homolytic Reactions. *In:* COFFEY, S. (ed.) *Rodd's Chemistry of Carbon Compounds (Second Edition).* Amsterdam: Elsevier, (1964),pp 306-333.

[178] Ayala, A., Muñoz, M. F. & Argüelles, S., Lipid peroxidation: production, metabolism, and signaling mechanisms of malondialdehyde and 4-hydroxy-2-nonenal. *Oxidative medicine and cellular longevity.* 2014, (2014),pp.

[179] Sultana, R., Perluigi, M. & Butterfield, D. A., Lipid peroxidation triggers neurodegeneration: a redox proteomics view into the Alzheimer disease brain. *Free Radic Biol Med.* 62, (2013),pp. 157-169.

[180] Rarata, G., Florczuk, W. & Smetek, J., Research on preparation and propulsive applications of highly concentrated hydrogen peroxide. *J Aerosp Sci Technol.* 1, (2016),pp. 42-47.

[181] Hutchins, P. M., Barkley, R. M. & Murphy, R. C., Separation of cellular nonpolar neutral lipids by normal-phase chromatography and analysis by electrospray ionization mass spectrometry. *Journal of lipid research.* 49, (2008),pp. 804-813.

[182] Navarro López, E., Robles Medina, A., González Moreno, P. A., Esteban Cerdán, L. & Molina Grima, E., Extraction of microalgal lipids

and the influence of polar lipids on biodiesel production by lipase-catalyzed transesterification. *Bioresource Technology.* 216, (2016),pp. 904-913.

[183] Alex, S., Thanh, H. L. & Vocelle, D., Studies of the effect of hydrogen bonding on the absorption and fluorescence spectra of all-trans-retinal at room temperature. *Canadian Journal of Chemistry.* 70, (1992),pp. 880-887.

[184] Morris, J. B., Chapter 28 - Deposition of Inhaled Gases and Vapors. *In:* PARENT, R. A. (ed.) *Comparative Biology of the Normal Lung (Second Edition).* San Diego: Academic Press, (2015),pp 537-560.

[185] Andersson, H., Carlsson, A.-C. C., Nekoueishahraki, B., Brath, U. & Erdélyi, M., Chapter Two - Solvent Effects on Nitrogen Chemical Shifts. *In:* WEBB, G. A. (ed.) *Annual Reports on NMR Spectroscopy.* Academic Press, 86, (2015),pp 73-210.

[186] Snyder, L. High-Performance Liquid Chromatography (C. Horváth, ed.), Vol. 3. New York: Academic Press, (1983),pp.

[187] Guide, H. P. S., Burdick and Jackson Laboratories. *Inc., Muskegon, MI.* (1980),pp.

[188] Li, Y., Naghdi, F. G., Garg, S., Adarme-Vega, T. C., Thurecht, K. J., Ghafor, W. A., Tannock, S. & Schenk, P. M., A comparative study: the impact of different lipid extraction methods on current microalgal lipid research. *Microbial cell factories.* 13, (2014),pp. 14.

[189] Cao, Y., Liu, W., Xu, X., Zhang, H., Wang, J. & Xian, M., Production of free monounsaturated fatty acids by metabolically engineered Escherichia coli. *Biotechnology for biofuels.* 7, (2014),pp. 59-59.

[190] Rice-Evans, C. A., Chapter 5 - Formation of free radicals and mechanisms of action in normal biochemical processes and pathological states. *In:* RICE-EVANS, C. A. & BURDON, R. H. (eds.) *New Comprehensive Biochemistry.* Elsevier, 28, (1994),pp 131-153.

[191] Wu, M.-L., Tsai, K.-L., Wang, S.-M., Wu, J.-C., Wang, B.-S. & Lee, Y.-T., Mechanism of hydrogen peroxide and hydroxyl free radical–induced intracellular acidification in cultured rat cardiac myoblasts. *Circulation research.* 78, (1996),pp. 564-572.

[192] Hansen, C. M., *Hansen solubility parameters: a user's handbook*, CRC press, (2002),pp

[193] Steriti, A., Rossi, R., Concas, A. & Cao, G., A novel cell disruption technique to enhance lipid extraction from microalgae. *Bioresource technology.* 164, (2014),pp. 70-77.

[194] Alaswad, A., Dassisti, M., Prescott, T., Olabi, A. G. J. R. & Reviews, S. E., Technologies and developments of third generation biofuel production. *Renewable and Sustainable Energy Reviews.* 51, (2015),pp. 1446-1460.

[195] Leonard, M. D., Michaelides, E. E. & Michaelides, D. N., Energy storage needs for the substitution of fossil fuel power plants with renewables. *Renewable Energy.* 145, (2020),pp. 951-962.

[196] Feron, P., Cousins, A., Jiang, K., Zhai, R., Shwe Hla, S., Thiruvenkatachari, R. & Burnard, K., Towards Zero Emissions from Fossil Fuel Power Stations. *International Journal of Greenhouse Gas Control.* 87, (2019),pp. 188-202.

[197] Chew, K. W., Chia, S. R., Lee, S. Y., Zhu, L. & Show, P. L., Enhanced microalgal protein extraction and purification using sustainable microwave-assisted multiphase partitioning technique. *Chemical Engineering Journal.* 367, (2019),pp. 1-8.

[198] Poblete, R., Oller, I., Maldonado, M. I., Luna, Y. & Cortes, E., Cost estimation of COD and color removal from landfill leachate using combined coffee-waste based activated carbon with advanced oxidation processes. *Journal of environmental chemical engineering.* 5, (2017),pp. 114-121.

[199] Yu, M., Chang, S., Li, D., Zhang, C., Jiang, L., Han, Y., Qi, L., Li, J. & Li, S., A Comparison of NaOH, Fenton, and Their Combined Pretreatments for Improving Saccharification of Corn Stalks. *Energy & Fuels.* 31, (2017),pp. 10983-10989.

[200] Yan, D., Lu, Y., Chen, Y.-F. & Wu, Q., Waste molasses alone displaces glucose-based medium for microalgal fermentation towards cost-saving

biodiesel production. *Bioresource Technology.* 102, (2011),pp. 6487-6493.

[201] Lunsin, R., Duanyai, S., Pilajun, R., Duanyai, S. & Sombatsri, P., Effect of urea- and molasses-treated sugarcane bagasse on nutrient composition and in vitro rumen fermentation in dairy cows. *Agriculture and Natural Resources.* 52, (2018),pp. 622-627.

[202] Satyawali, Y. & Balakrishnan, M., Wastewater treatment in molasses-based alcohol distilleries for COD and color removal: A review. *Journal of Environmental Management.* 86, (2008),pp. 481-497.

[203] Ferreira, A. M., Esteves, P. D. O., Boal-Palheiros, I., Pereiro, A. B., Rebelo, L. P. N. & Freire, M. G., Enhanced tunability afforded by aqueous biphasic systems formed by fluorinated ionic liquids and carbohydrates. *Green Chem.* 18, (2016),pp. 1070-1079.

[204] Yew, G. Y., Chew, K. W., Malek, M. A., Ho, Y.-C., Chen, W.-H., Ling, T. C. & Show, P. L., Hybrid liquid biphasic system for cell disruption and simultaneous lipid extraction from microalgae Chlorella sorokiniana CY-1 for biofuel production. *Biotechnology for biofuels.* 12, (2019),pp. 1-12.

[205] Phwan, C. K., Chew, K. W., Sebayang, A. H., Ong, H. C., Ling, T. C., Malek, M. A., Ho, Y.-C. & Show, P. L., Effects of acids pre-treatment on the microbial fermentation process for bioethanol production from microalgae. *Biotechnology for biofuels.* 12, (2019),pp. 191.

[206] Ahmadian, M., Duncan, R. E., Jaworski, K., Sarkadi-Nagy, E. & Sul, H. S., Triacylglycerol metabolism in adipose tissue. *Future Lipidol.* 2, (2007),pp. 229-237.

[207] Gilham, D. & Lehner, R., The physiological role of triacylglycerol hydrolase in lipid metabolism. *Reviews in Endocrine and Metabolic Disorders.* 5, (2004),pp. 303-309.

[208] Delrue, F., Setier, P.-A., Sahut, C., Cournac, L., Roubaud, A., Peltier, G. & Froment, A.-K., An economic, sustainability, and energetic model of biodiesel production from microalgae. *Bioresource technology.* 111, (2012),pp. 191-200.

[209] Sanz-Luque, E., Chamizo-Ampudia, A., Llamas, A., Galvan, A. & Fernandez, E., Understanding nitrate assimilation and its regulation in microalgae. *Frontiers in plant science.* 6, (2015),pp. 899.

[210] Le Costaouëc, T., Unamunzaga, C., Mantecon, L. & Helbert, W., New structural insights into the cell-wall polysaccharide of the diatom Phaeodactylum tricornutum. *Algal Research.* 26, (2017),pp. 172-179.

[211] El-Naggar, N. E.-A., Hussein, M. H., Shaaban-Dessuuki, S. A. & Dalal, S. R., Production, extraction and characterization of Chlorella vulgaris soluble polysaccharides and their applications in AgNPs biosynthesis and biostimulation of plant growth. *Scientific Reports.* 10, (2020),pp. 1-19.

[212] Wang, D., Li, Y., Hu, X., Su, W. & Zhong, M., Combined enzymatic and mechanical cell disruption and lipid extraction of green alga Neochloris oleoabundans. *International journal of molecular sciences.* 16, (2015),pp. 7707-7722.

[213] Rezaei, M., Fani, A., Moini, A. L., Mirzajani, P., Malekirad, A. A. & Rafiei, M., Determining Nitrate and Nitrite Content in Beverages, Fruits, Vegetables, and Stews Marketed in Arak, Iran. *International Scholarly Research Notices.* 2014, (2014),pp. 439702.

[214] Bhange, V. P., William, S. P., Sharma, A., Gabhane, J., Vaidya, A. N. & Wate, S. R., Pretreatment of garden biomass using Fenton's reagent: influence of Fe(2+) and H2O2 concentrations on lignocellulose degradation. *J Environ Health Sci Eng.* 13, (2015),pp. 12-12.

[215] Jung, Y. S., Lim, W. T., Park, J. Y. & Kim, Y. H., Effect of pH on Fenton and Fenton-like oxidation. *Environmental technology.* 30, (2009),pp. 183-190.

[216] Nair, A. T., Senthilnathan, J. & Nagendra, S. M. S., Application of the phycoremediation process for tertiary treatment of landfill leachate and carbon dioxide mitigation. *Journal of Water Process Engineering.* 28, (2019),pp. 322-330.

[217] Ferraz, F. M. & Yuan, Q., Performance of oat hulls activated carbon for COD and color removal from landfill leachate. *Journal of Water Process Engineering.* 33, (2020),pp. 101040.

[218] Indarti, E., Majid, M. I. A., Hashim, R. & Chong, A., Direct FAME synthesis for rapid total lipid analysis from fish oil and cod liver oil. *Journal of Food Composition and Analysis.* 18, (2005),pp. 161-170.

[219] Gosch, B. J., Magnusson, M., Paul, N. A. & de Nys, R., Total lipid and fatty acid composition of seaweeds for the selection of species for oil-based biofuel and bioproducts. *Gcb Bioenergy.* 4, (2012),pp. 919-930.

[220] Jung, Y. H., Kim, H. K., Park, H. M., Park, Y.-C., Park, K., Seo, J.-H. & Kim, K. H., Mimicking the Fenton reaction-induced wood decay by fungi for pretreatment of lignocellulose. *Bioresource technology.* 179, (2015),pp. 467-472.

[221] Yew, G. Y., Puah, B. K., Chew, K. W., Teng, S. Y., Show, P. L. & Nguyen, T. H. P., Chlorella vulgaris FSP-E cultivation in waste molasses: Photo-to-property estimation by artificial intelligence. *Chemical Engineering Journal.* (2020),pp. 126230.

[222] Iris, K. & Tsang, D. C., Conversion of biomass to hydroxymethylfurfural: A review of catalytic systems and underlying mechanisms. *Bioresource technology.* 238, (2017),pp. 716-732.

[223] Cheng, J., Sun, J., Huang, Y., Feng, J., Zhou, J. & Cen, K., Dynamic microstructures and fractal characterization of cell wall disruption for microwave irradiation-assisted lipid extraction from wet microalgae. *Bioresource Technology.* 150, (2013),pp. 67-72.

[224] Harun, R. & Danquah, M. K., Influence of acid pre-treatment on microalgal biomass for bioethanol production. *Process Biochemistry.* 46, (2011),pp. 304-309.

[225] Chen, Y., Teng, J., Shen, L., Yu, G., Li, R., Xu, Y., Wang, F., Liao, B.-Q. & Lin, H., Novel insights into membrane fouling caused by gel layer in a membrane bioreactor: effects of hydrogen bonding. *Bioresource technology.* 276, (2019),pp. 219-225.

[226] Anastopoulos, G., Lois, E., Karonis, D., Kalligeros, S. & Zannikos, F., Impact of oxygen and nitrogen compounds on the lubrication properties of low sulfur diesel fuels. *Energy.* 30, (2005),pp. 415-426.

[227] Romera, E., González, F., Ballester, A., Blázquez, M. L. & Muñoz, J. A., Comparative study of biosorption of heavy metals using different types of algae. *Bioresource Technology.* 98, (2007),pp. 3344-3353.

[228] Zhang, X., Zhou, X., Xi, H., Sun, J., Liang, X., Wei, J., Xiao, X., Liu, Z., Li, S. & Liang, Z., Interpretation of adhesion behaviors between bacteria and modified basalt fiber by surface thermodynamics and extended DLVO theory. *Colloids and Surfaces B: Biointerfaces.* 177, (2019),pp. 454-461.

[229] Karimi, K. & Taherzadeh, M. J., A critical review of analytical methods in pretreatment of lignocelluloses: composition, imaging, and crystallinity. *Bioresource technology.* 200, (2016),pp. 1008-1018.

[230] González-Fernández, C., Sialve, B., Bernet, N. & Steyer, J. P., Thermal pretreatment to improve methane production of Scenedesmus biomass. *Biomass and Bioenergy.* 40, (2012),pp. 105-111.

[231] Brandt, M. J., Johnson, K. M., Elphinston, A. J. & Ratnayaka, D. D., Chapter 7 - Chemistry, Microbiology and Biology of Water. *In:* BRANDT, M. J., JOHNSON, K. M., ELPHINSTON, A. J. & RATNAYAKA, D. D. (eds.) *Twort's Water Supply (Seventh Edition).* Boston: Butterworth-Heinemann, (2017),pp 235-321.

[232] Corey, H. E., Stewart and beyond: New models of acid-base balance. *Kidney International.* 64, (2003),pp. 777-787.

[233] Padró, J. M., Acquaviva, A., Tascon, M., Gagliardi, L. G. & Castells, C. B., Effect of temperature and solvent composition on acid dissociation equilibria, I: Sequenced pssKa determination of compounds commonly used as buffers in high performance liquid chromatography coupled to mass spectroscopy detection. *Analytica Chimica Acta.* 725, (2012),pp. 87-94.

[234] Phyo, P., Gu, Y. & Hong, M., Impact of acidic pH on plant cell wall polysaccharide structure and dynamics: insights into the mechanism of acid growth in plants from solid-state NMR. *Cellulose.* 26, (2019),pp. 291-304.

[235] Templeton, D. W., Quinn, M., Van Wychen, S., Hyman, D. & Laurens, L. M., Separation and quantification of microalgal carbohydrates. *Journal of Chromatography A.* 1270, (2012),pp. 225-234.

[236] Knothe, G., Dependence of biodiesel fuel properties on the structure of fatty acid alkyl esters. *Fuel Processing Technology.* 86, (2005),pp. 1059-1070.

[237] Kumar, N., Oxidative stability of biodiesel: Causes, effects and prevention. *Fuel.* 190, (2017),pp. 328-350.

[238] Leung, D. Y. C., Koo, B. C. P. & Guo, Y., Degradation of biodiesel under different storage conditions. *Bioresource Technology.* 97, (2006),pp. 250-256.

[239] Schönborn, A., Ladommatos, N., Williams, J., Allan, R. & Rogerson, J., The influence of molecular structure of fatty acid monoalkyl esters on diesel combustion. *Combustion and Flame.* 156, (2009),pp. 1396-1412.

[240] Kalam, M. A., Husnawan, M. & Masjuki, H. H., Exhaust emission and combustion evaluation of coconut oil-powered indirect injection diesel engine. *Renewable Energy.* 28, (2003),pp. 2405-2415.

[241] Concas, A., Pisua, M. & Caoa, G., Microalgal cell disruption through Fenton reaction: experiments, modeling and remarks on its effect on the extracted lipids composition. *Chemical Engineering.* 43, (2015),pp. 392-401.

[242] Gligorovski, S., Strekowski, R., Barbati, S. & Vione, D., Environmental implications of hydroxyl radicals (• OH). *Chemical Reviews.* 115, (2015),pp. 13051-13092.

[243] Olczyk, P., Ramos, P., Komosinska-Vassev, K., Mencner, L., Olczyk, K. & Pilawa, B., Influence of Temperature on Free Radical Generation in Propolis-Containing Ointments. *Evidence-Based Complementary and Alternative Medicine.* 2016, (2016),pp. 1-8.

[244] Bahadar, A., Khan, M. B., Asim, M. & Jalwana, K., Supercritical fluid extraction of microalgae (Chlorella vulagaris) biomass. *Handbook of Marine Microalgae.* Elsevier, (2015),pp 317-330.

[245] Wang, S., A Comparative study of Fenton and Fenton-like reaction kinetics in decolourisation of wastewater. *Dyes and Pigments.* 76, (2008),pp. 714-720.

[246] Li, J., Xiao, C., Wang, K., Li, Y. & Zhang, G., Enhanced Generation of Reactive Oxygen Species under Visible Light Irradiation by Adjusting the Exposed Facet of FeWO4 Nanosheets To Activate Oxalic Acid for Organic Pollutant Removal and Cr(VI) Reduction. *Environmental Science & Technology.* 53, (2019),pp. 11023-11030.

[247] Nasreen, S., Nafees, M., Qureshi, L. A., Asad, M. S., Sadiq, A. & Ali, S. D., Review of Catalytic Transesterification Methods for Biodiesel Production. *Biofuels: State of Development.* (2018),pp. 93.

[248] Guo, T., Wang, K., Zhang, G. & Wu, X., A novel α-Fe2O3@g-C3N4 catalyst: Synthesis derived from Fe-based MOF and its superior photo-Fenton performance. *Applied Surface Science.* 469, (2019),pp. 331-339.

[249] Cheirsilp, B., Srinuanpan, S. & Mandik, Y. I., Chapter 6 - Efficient Harvesting of Microalgal biomass and Direct Conversion of Microalgal Lipids into Biodiesel. *In:* YOUSUF, A. (ed.) *Microalgae Cultivation for Biofuels Production.* Academic Press, (2020),pp 83-96.

[250] Kayode, B. & Hart, A., An overview of transesterification methods for producing biodiesel from waste vegetable oils. *Biofuels.* 10, (2019),pp. 419-437.

[251] Maeda, H., Hagiwara, S., Nabetani, H., Sagara, Y., Soerawidjaya, T. H., Tambunan, A. H. & Abdullah, K., Biodiesel fuels from palm oil via the non-catalytic transesterification in a bubble column reactor at atmospheric pressure: a kinetic study. *Renewable Energy.* 33, (2008),pp. 1629-1636.

[252] Liang, K., Zhang, Q. & Cong, W., Enzyme-assisted aqueous extraction of lipid from microalgae. *Journal of agricultural and food chemistry.* 60, (2012),pp. 11771-11776.

[253] Ma, Y., Gao, Z., Wang, Q. & Liu, Y., Biodiesels from microbial oils: Opportunity and challenges. *Bioresource Technology.* 263, (2018),pp. 631-641.

[254] Ong, M. Y., Chew, K. W., Show, P. L. & Nomanbhay, S., Optimization and kinetic study of non-catalytic transesterification of palm oil under subcritical condition using microwave technology. *Energy Conversion and Management.* 196, (2019),pp. 1126-1137.

[255] Liu, J., Huang, J., Sun, Z., Zhong, Y., Jiang, Y. & Chen, F., Differential lipid and fatty acid profiles of photoautotrophic and heterotrophic Chlorella zofingiensis: Assessment of algal oils for biodiesel production. *Bioresource Technology.* 102, (2011),pp. 106-110.

[256] Baümler, E. R., Carrín, M. E. & Carelli, A. A., Diffusion of tocopherols, phospholipids and sugars during oil extraction from sunflower collets using ethanol as solvent. *Journal of Food Engineering.* 194, (2017),pp. 1-8.

[257] Kumar, G., Shobana, S., Chen, W.-H., Bach, Q.-V., Kim, S.-H., Atabani, A. & Chang, J.-S., A review of thermochemical conversion of microalgal biomass for biofuels: chemistry and processes. *Green Chemistry.* 19, (2017),pp. 44-67.

[258] Chia, S. R., Chew, K. W., Show, P. L., Yap, Y. J., Ong, H. C., Ling, T. C. & Chang, J. S., Analysis of economic and environmental aspects of microalgae biorefinery for biofuels production: a review. *Biotechnology journal.* 13, (2018),pp. 1700618.

[259] Folch, J., Lees, M. & Stanley, G. S., A simple method for the isolation and purification of total lipides from animal tissues. *J. of Biol. Chem.*, 226, (1957),pp. 497-509.

[260] Tao, Y., Wang, Y., Pan, M., Zhong, S., Wu, Y., Yang, R., Han, Y. & Zhou, J., Combined ANFIS and numerical methods to simulate ultrasound-assisted extraction of phenolics from chokeberry cultivated in China and analysis of phenolic composition. *Separation and Purification Technology.* 178, (2017),pp. 178-188.

[261] Tao, Y., Han, Y., Liu, W., Peng, L., Wang, Y., Kadam, S., Show, P. L. & Ye, X., Parametric and phenomenological studies about ultrasound-enhanced biosorption of phenolics from fruit pomace extract by waste yeast. *Ultrasonics sonochemistry.* 52, (2019),pp. 193-204.

[262] Nikitenko, S., Plasma Formation during Acoustic Cavitation: Toward a New Paradigm for Sonochemistry. *Advances in Physical Chemistry.* 2014, (2014),pp. ID 173878.

[263] Gao, L., Li, D., Gao, F., Liu, Z., Hou, Y., Chen, S. & Zhang, D., Hydroxyl radical-aided thermal pretreatment of algal biomass for enhanced biodegradability. *Biotechnology for biofuels.* 8, (2015),pp. 194.

[264] Bitzer, Z. T., Goel, R., Reilly, S. M., Foulds, J., Muscat, J., Elias, R. J. & Richie Jr, J. P., Effects of solvent and temperature on free radical

formation in electronic cigarette aerosols. *Chemical research in toxicology.* 31, (2017),pp. 4-12.

[265] Concas, A., Pisu, M. & Cao, G., Disruption of microalgal cells for lipid extraction through Fenton reaction: modeling of experiments and remarks on its effect on lipids composition. *Chemical Engineering Journal.* 263, (2015),pp. 392-401.

[266] Wu, Y., Zhou, S., Qin, F., Zheng, K. & Ye, X., Modeling the oxidation kinetics of Fenton's process on the degradation of humic acid. *Journal of Hazardous Materials.* 179, (2010),pp. 533-539.

[267] Farré, M. J., Doménech, X. & Peral, J., Combined photo-Fenton and biological treatment for Diuron and Linuron removal from water containing humic acid. *Journal of hazardous materials.* 147, (2007),pp. 167-174.

[268] Neyens, E. & Baeyens, J., A review of classic Fenton's peroxidation as an advanced oxidation technique. *Journal of Hazardous materials.* 98, (2003),pp. 33-50.

[269] Gómez Millán, G., Hellsten, S., King, A. W. T., Pokki, J.-P., Llorca, J. & Sixta, H., A comparative study of water-immiscible organic solvents in the production of furfural from xylose and birch hydrolysate. *Journal of Industrial and Engineering Chemistry.* 72, (2019),pp. 354-363.

[270] Schweikert, C., Liszkay, A. & Schopfer, P., Polysaccharide degradation by Fenton reaction- or peroxidase-generated hydroxyl radicals in isolated plant cell walls. *Phytochemistry.* 61, (2002),pp. 31-35.

[271] Shin, H.-Y., Shim, S.-H., Ryu, Y.-J., Yang, J.-H., Lim, S.-M. & Lee, C.-G., Lipid Extraction from Tetraselmis sp. Microalgae for Biodiesel Production Using Hexane-based Solvent Mixtures. *Biotechnology and bioprocess engineering.* 23, (2018),pp. 16-22.

[272] Sousa, H. & Crespo, J., Enzymatic biphasic membrane reactors for the synthesis of chiral products. *Progr. in Biotechnol.*, 15, (1998),pp 673-678.

[273] Kim, D.-Y., Park, J.-Y., Choi, S.-A., Oh, Y.-K., Lee, I.-G., Seo, Y.-W. & Han, J.-I., The effects of microalgal cell disruption via FeCl3-based synergistic effect between Fenton-like and Lewis acid reaction for lipid extraction. *Algal Research.* 6, (2014),pp. 86-90.

[274] Phaniendra, A., Jestadi, D. B. & Periyasamy, L., Free radicals: properties, sources, targets, and their implication in various diseases. *Ind. J. of Clin. Biochem.*, 30, (2015),pp. 11-26.

[275] Vijay Kumar, M., Veeresh Babu, A. & Ravi Kumar, P., The impacts on combustion, performance and emissions of biodiesel by using additives in direct injection diesel engine. *Alexandria Engineering Journal.* 57, (2018),pp. 509-516.

[276] Hussain, J., Liu, Y., Lopes, W. A., Druzian, J. I., Souza, C. O., Carvalho, G. C., Nascimento, I. A. & Liao, W., Effects of different biomass drying and lipid extraction methods on algal lipid yield, fatty acid profile, and biodiesel quality. *Applied biochemistry and biotechnology.* 175, (2015),pp. 3048-3057.

[277] Efthymiopoulos, I., Hellier, P., Ladommatos, N., Kay, A. & Mills-Lamptey, B., Effect of solvent extraction parameters on the recovery of oil from spent coffee grounds for biofuel production. *Waste and biomass valorization.* 10, (2019),pp. 253-264.

[278] Rodolfi, L., Chini Zittelli, G., Bassi, N., Padovani, G., Biondi, N., Bonini, G. & Tredici, M. R., Microalgae for oil: Strain selection, induction of lipid synthesis and outdoor mass cultivation in a low-cost photobioreactor. *Biotechnology and bioengineering.* 102, (2009),pp. 100-112.

[279] Loganathan, S., Biohydro-fined diesel (BHD) and biodiesel (BOD) production process and property review. *Innovations in Fuel Economy and Sustainable Road Transport.* Woodhead Publishing, (2011),pp 97-107.

[280] Zahan, K. & Kano, M., Biodiesel production from palm oil, its by-products, and mill effluent: A review. *Energies.* 11, (2018),pp. 2132.

[281] Beuermann, S., Buback, M., Isemer, C., Lacík, I. & Wahl, A., Pressure and Temperature Dependence of the Propagation Rate Coefficient of

Free-Radical Styrene Polymerization in Supercritical Carbon Dioxide. *Macromolecules.* 35, (2002),pp. 3866-3869.

[282] Jubsilp, C., Takeichi, T. & Rimdusit, S., Chapter 7 - Polymerization Kinetics. *In:* ISHIDA, H. & AGAG, T. (eds.) *Handbook of Benzoxazine Resins.* Amsterdam: Elsevier, (2011),pp 157-174.

[283] Aksoy, L., Kolay, E., Ağılönü, Y., Aslan, Z. & Kargıoğlu, M., Free radical scavenging activity, total phenolic content, total antioxidant status, and total oxidant status of endemic Thermopsis turcica. *Saudi journal of biological sciences.* 20, (2013),pp. 235-239.

[284] Lee, J.-Y., Yoo, C., Jun, S.-Y., Ahn, C.-Y. & Oh, H.-M., Comparison of several methods for effective lipid extraction from microalgae. *Bioresource Technology.* 101, (2010),pp. S75-S77.

[285] Furuta, S., Matsuhashi, H. & Arata, K., Biodiesel fuel production with solid superacid catalysis in fixed bed reactor under atmospheric pressure. *Catalysis communications.* 5, (2004),pp. 721-723.

[286] Helwani, Z., Othman, M. R., Aziz, N., Kim, J. & Fernando, W. J. N., Solid heterogeneous catalysts for transesterification of triglycerides with methanol: A review. *Applied Catalysis A: General.* 363, (2009),pp. 1-10.

[287] Shumaker, J. L., Crofcheck, C., Tackett, S. A., Santillan-Jimenez, E., Morgan, T., Ji, Y., Crocker, M. & Toops, T. J., Biodiesel synthesis

using calcined layered double hydroxide catalysts. *Applied Catalysis B: Environmental.* 82, (2008),pp. 120-130.

[288] Shah, S. & Gupta, M. N., Lipase catalyzed preparation of biodiesel from Jatropha oil in a solvent free system. *Process Biochemistry.* 42, (2007),pp. 409-414.

[289] Saka, S. & Kusdiana, D., Biodiesel fuel from rapeseed oil as prepared in supercritical methanol. *Fuel.* 80, (2001),pp. 225-231.

[290] Nayak, S. N., Bhasin, C. P. & Nayak, M. G., A review on microwave-assisted transesterification processes using various catalytic and non-catalytic systems. *Renewable Energy.* 143, (2019),pp. 1366-1387.

[291] Musa, I. A., The effects of alcohol to oil molar ratios and the type of alcohol on biodiesel production using transesterification process. *Egyptian Journal of Petroleum.* 25, (2016),pp. 21-31.

[292] Barakos, N., Pasias, S. & Papayannakos, N., Transesterification of triglycerides in high and low quality oil feeds over an HT2 hydrotalcite catalyst. *Bioresource Technology.* 99, (2008),pp. 5037-5042.

[293] Lee, J.-S. & Saka, S., Biodiesel production by heterogeneous catalysts and supercritical technologies. *Bioresource Technology.* 101, (2010),pp. 7191-7200.

[294] Mohanty, A. D. & Bae, C., Chapter One - Transition Metal-Catalyzed Functionalization of Polyolefins Containing CC, CC, and CH Bonds.

In: PÉREZ, P. J. (ed.) *Advances in Organometallic Chemistry.* Academic Press, 64, (2015),pp 1-39.

[295] Guengerich, F. P. & Yoshimoto, F. K., Formation and cleavage of C–C bonds by enzymatic oxidation–reduction reactions. *Chemical reviews.* 118, (2018),pp. 6573-6655.

[296] Pedersen, N. R., Wimmer, R., Emmersen, J., Degn, P. & Pedersen, L. H., Effect of fatty acid chain length on initial reaction rates and regioselectivity of lipase-catalysed esterification of disaccharides. *Carbohydrate research.* 337, (2002),pp. 1179-1184.

[297] Labatut, R. A. & Pronto, J. L., Sustainable Waste-to-Energy Technologies: Anaerobic Digestion. *Sustainable Food Waste-To-energy Systems.* Elsevier, (2018),pp 47-67.

[298] Goff, M. J., Bauer, N. S., Lopes, S., Sutterlin, W. R. & Suppes, G. J., Acid-catalyzed alcoholysis of soybean oil. *Journal of the American Oil Chemists' Society.* 81, (2004),pp. 415-420.

[299] Chalima, A., Oliver, L., Fernández de Castro, L., Karnaouri, A., Dietrich, T. & Topakas, E., Utilization of volatile fatty acids from microalgae for the production of high added value compounds. *Fermentation.* 3, (2017),pp. 54.

[300] Asandulesa, M., Topala, I., Pohoata, V. & Dumitrascu, N., Influence of operational parameters on plasma polymerization process at

atmospheric pressure. *Journal of Applied Physics.* 108, (2010),pp. 093310.

[301] Khan, M. I., Shin, J. H. & Kim, J. D., The promising future of microalgae: current status, challenges, and optimization of a sustainable and renewable industry for biofuels, feed, and other products. *Microbial cell factories.* 17, (2018),pp. 36.

[302] Zhu, L. D., Hiltunen, E., Antila, E., Zhong, J. J., Yuan, Z. H. & Wang, Z. M., Microalgal biofuels: Flexible bioenergies for sustainable development. *Renewable and Sustainable Energy Reviews.* 30, (2014),pp. 1035-1046.

[303] Wang, R., Zhu, W., Hu, S., Feng, G., Xue, Z. & Chen, H., Hydrothermal pretreatment of salvaged cyanobacteria and use of pretreated medium for cultivating Scenedesmus obliquus. *Bioresource Technology.* 294, (2019),pp. 122120.

[304] Racharaks, R., Ge, X. & Li, Y., Cultivation of marine microalgae using shale gas flowback water and anaerobic digestion effluent as the cultivation medium. *Bioresource Technology.* 191, (2015),pp. 146-156.

[305] Guo, Z., Liu, Y., Guo, H., Yan, S. & Mu, J., Microalgae cultivation using an aquaculture wastewater as growth medium for biomass and biofuel production. *Journal of Environmental Sciences.* 25, (2013),pp. S85-S88.

[306] Pandey, A., Srivastava, S. & Kumar, S., Isolation, screening and comprehensive characterization of candidate microalgae for biofuel feedstock production and dairy effluent treatment: A sustainable approach. *Bioresource Technology.* 293, (2019),pp. 121998.

[307] Nur, M. M. A. & Buma, A. G. J., Opportunities and Challenges of Microalgal Cultivation on Wastewater, with Special Focus on Palm Oil Mill Effluent and the Production of High Value Compounds. *Waste and Biomass Valorization.* 10, (2019),pp. 2079-2097.

[308] Olsson, J., Feng, X. M., Ascue, J., Gentili, F. G., Shabiimam, M. A., Nehrenheim, E. & Thorin, E., Co-digestion of cultivated microalgae and sewage sludge from municipal waste water treatment. *Bioresource Technology.* 171, (2014),pp. 203-210.

[309] Vadlamani, A., Pendyala, B., Viamajala, S. & Varanasi, S., High Productivity Cultivation of Microalgae without Concentrated CO2 Input. *ACS Sustainable Chemistry & Engineering.* 7, (2019),pp. 1933-1943.

[310] Santana, H., Cereijo, C. R., Teles, V. C., Nascimento, R. C., Fernandes, M. S., Brunale, P., Campanha, R. C., Soares, I. P., Silva, F. C. P., Sabaini, P. S., Siqueira, F. G. & Brasil, B. S. A. F., Microalgae cultivation in sugarcane vinasse: Selection, growth and biochemical characterization. *Bioresource Technology.* 228, (2017),pp. 133-140.

[311] Han, S., Kim, G.-Y. & Han, J.-I., Biodiesel production from oleaginous yeast, Cryptococcus sp. by using banana peel as carbon source. *Energy Reports.* 5, (2019),pp. 1077-1081.

[312] Ortegón, G. P., Arboleda, F. M., Candela, L., Tamoh, K. & Valdes-Abellan, J., Vinasse application to sugar cane fields. Effect on the unsaturated zone and groundwater at Valle del Cauca (Colombia). *Science of The Total Environment.* 539, (2016),pp. 410-419.

[313] Ikegami, K., Hirose, Y., Sakashita, H., Maruyama, R. & Sugiyama, T., Role of polyphenol in sugarcane molasses as a nutrient for hexavalent chromium bioremediation using bacteria. *Chemosphere.* 250, (2020),pp. 126267.

[314] Tsigie, Y. A., Wang, C.-Y., Truong, C.-T. & Ju, Y.-H., Lipid production from Yarrowia lipolytica Po1g grown in sugarcane bagasse hydrolysate. *Bioresource Technology.* 102, (2011),pp. 9216-9222.

[315] Anhwange, B., Ugye, T. & Nyiaatagher, T., Chemical composition of Musa sapientum (banana) peels. *Journal of Food Technology.* 6, (2008),pp. 263-266.

[316] Wang, B.-S., Chang, L.-W., Kang, Z.-C., Chu, H.-L., Tai, H.-M. & Huang, M.-H., Inhibitory effects of molasses on mutation and nitric oxide production. *Food chemistry.* 126, (2011),pp. 1102-1107.

[317] Wrolstad, R. E. Color and pigment analyses in fruit products. *Station bulletin (Oregon State University, Agriculture Experiment Station)* Oregon State University, 624, (1993),pp.

[318] Supriyanto, Noguchi, R., Ahamed, T., Rani, D. S., Sakurai, K., Nasution, M. A., Wibawa, D. S., Demura, M. & Watanabe, M. M., Artificial neural networks model for estimating growth of polyculture microalgae in an open raceway pond. *Biosystems Engineering.* 177, (2019),pp. 122-129.

[319] Teng, S. Y., Loy, A. C. M., Leong, W. D., How, B. S., Chin, B. L. F. & Máša, V., Catalytic thermal degradation of Chlorella vulgaris: Evolving deep neural networks for optimization. *Bioresource Technology.* 292, (2019),pp. 121971.

[320] Cerbin, S., Nowakowski, K., Dach, J., Pilarski, K., Boniecki, P., Przybyl, J. & Lewicki, A., *Possibilities of neural image analysis implementation in monitoring of microalgae production as a substrate for biogas plant*, SPIE, 8334, (2012),pp

[321] Lv, J., Wang, X., Liu, W., Feng, J., Liu, Q., Nan, F., Jiao, X. & Xie, S., The Performance of a Self-Flocculating Microalga Chlorococcum sp. GD in Wastewater with Different Ammonia Concentrations. *International journal of environmental research and public health.* 15, (2018),pp. 434.

[322] Krzemińska, I., Pawlik-Skowrońska, B., Trzcińska, M. & Tys, J., Influence of photoperiods on the growth rate and biomass productivity of green microalgae. *Bioprocess and biosystems engineering.* 37, (2014),pp. 735-741.

[323] Dubois, M., Gilles, K., Hamilton, J., Rebers, P. & Smith, F., A colorimetric method for the determination of sugars. *Nature.* 168, (1951),pp. 167-167.

[324] Benzmüller, C. & Stuckenschmidt, H., *KI 2019: Advances in Artificial Intelligence: ,* Kassel, Germany, Springer Nature, 11793, (2019),pp 321-322.

[325] Ogbonna, J. C. & Tanaka, H., Night biomass loss and changes in biochemical composition of cells during light/dark cyclic culture of Chlorella pyrenoidosa. *Journal of Fermentation and Bioengineering.* 82, (1996),pp. 558-564.

[326] Torzillo, G., Sacchi, A. & Materassi, R., Temperature as an important factor affecting productivity and night biomass loss in Spirulina platensis grown outdoors in tubular photobioreactors. *Bioresource technology.* 38, (1991),pp. 95-100.

[327] Sun, X.-M., Ren, L.-J., Zhao, Q.-Y., Ji, X.-J. & Huang, H., Microalgae for the production of lipid and carotenoids: a review with focus on stress regulation and adaptation. *Biotechnology for biofuels.* 11, (2018),pp. 272.

[328] Radzun, K. A., Wolf, J., Jakob, G., Zhang, E., Stephens, E., Ross, I. & Hankamer, B., Automated nutrient screening system enables high-throughput optimisation of microalgae production conditions. *Biotechnology for biofuels.* 8, (2015),pp. 65.

[329] Gaurav, K., Srivastava, R., Sharma, J. G., Singh, R. & Singh, V., Molasses-based growth and lipid production by Chlorella pyrenoidosa: A potential feedstock for biodiesel. *International Journal of Green Energy.* 13, (2016),pp. 320-327.

[330] Fukami, K., Nishijima, T. & Ishida, Y., Stimulative and inhibitory effects of bacteria on the growth of microalgae. *Hydrobiologia.* 358, (1997),pp. 185-191.

[331] Lian, J., Wijffels, R. H., Smidt, H. & Sipkema, D., The effect of the algal microbiome on industrial production of microalgae. *Microbial Biotechnology.* 11, (2018),pp. 806-818.

[332] O'Hara, L. E., Paul, M. J. & Wingler, A., How do sugars regulate plant growth and development? New insight into the role of trehalose-6-phosphate. *Molecular plant.* 6, (2013),pp. 261-274.

[333] Egesten, A., Frick, I.-M., Mörgelin, M., Olin, A. I. & Björck, L., Binding of albumin promotes bacterial survival at the epithelial surface. *Journal of Biological Chemistry.* 286, (2011),pp. 2469-2476.

[334] Andrade, M. R. & Costa, J. A. V., Mixotrophic cultivation of microalga Spirulina platensis using molasses as organic substrate. *Aquaculture.* 264, (2007),pp. 130-134.

[335] Delgadillo-Mirquez, L., Lopes, F., Taidi, B. & Pareau, D., Nitrogen and phosphate removal from wastewater with a mixed microalgae and bacteria culture. *Biotechnology Reports.* 11, (2016),pp. 18-26.

[336] Shaw, R. J., LKB1 and AMP-activated protein kinase control of mTOR signalling and growth. *Acta physiologica.* 196, (2009),pp. 65-80.

[337] Gimpel, J. A., Henríquez, V. & Mayfield, S. P., In metabolic engineering of eukaryotic microalgae: potential and challenges come with great diversity. *Frontiers in microbiology.* 6, (2015),pp. 1376.

[338] Wan, L., Han, J., Sang, M., Li, A., Wu, H., Yin, S. & Zhang, C., De novo transcriptomic analysis of an oleaginous microalga: pathway description and gene discovery for production of next-generation biofuels. *PloS one.* 7, (2012),pp. e35142.

[339] Spangler, W. & Gilmour, C., Biochemistry of Nitrate Respiration in Pseudomonas stutzeri I. Aerobic and Nitrate Respiration Routes of Carbohydrate Catabolism. *Journal of bacteriology.* 91, (1966),pp. 245-250.

[340] Park, J. C., Park, T. Y., Kim, D. H., Cha, H. J. & Seo, J. H., Multifunctional nanocomposite clusters enabled by

amphiphilic/bioactive natural polysaccharides. *Chemical Engineering Journal.* 379, (2020),pp. 122406.

[341] Brasil, B. d. S. A. F., de Siqueira, F. G., Salum, T. F. C., Zanette, C. M. & Spier, M. R., Microalgae and cyanobacteria as enzyme biofactories. *Algal Research.* 25, (2017),pp. 76-89.

[342] Gerken, H. G., Donohoe, B. & Knoshaug, E. P., Enzymatic cell wall degradation of Chlorellavulgaris and other microalgae for biofuels production. *Planta.* 237, (2013),pp. 239-253.

[343] Ren, X., Deschênes, J.-S., Tremblay, R., Peres, S. & Jolicoeur, M., A kinetic metabolic study of lipid production in Chlorella protothecoides under heterotrophic condition. *Microbial cell factories.* 18, (2019),pp. 113.

[344] Vadlamani, A., Viamajala, S., Pendyala, B. & Varanasi, S., Cultivation of microalgae at extreme alkaline pH conditions: a novel approach for biofuel production. *ACS Sustainable Chemistry & Engineering.* 5, (2017),pp. 7284-7294.

[345] Chou, H.-H., Su, H.-Y., Song, X.-D., Chow, T.-J., Chen, C.-Y., Chang, J.-S. & Lee, T.-M., Isolation and characterization of Chlorella sp. mutants with enhanced thermo-and CO 2 tolerances for CO 2 sequestration and utilization of flue gases. *Biotechnology for biofuels.* 12, (2019),pp. 251.

[346] Guccione, A., Biondi, N., Sampietro, G., Rodolfi, L., Bassi, N. & Tredici, M. R., Chlorella for protein and biofuels: from strain selection to outdoor cultivation in a Green Wall Panel photobioreactor. *Biotechnology for biofuels.* 7, (2014),pp. 84.

[347] Raven, J., Short-and long-distance transport of boric acid in plants. *New Phytologist.* 84, (1980),pp. 231-249.

[348] López, G., Yate, C., Ramos, F. A., Cala, M. P., Restrepo, S. & Baena, S., Production of Polyunsaturated Fatty Acids and Lipids from Autotrophic, Mixotrophic and Heterotrophic cultivation of Galdieria sp. strain USBA-GBX-832. *Scientific reports.* 9, (2019),pp. 1-13.

[349] Kornberg, H. & Gotto, A., Biosynthesis of Cell Constituents from C2-Compounds: Formation of Malate from Glycollate by Pseudomonas ovalis Chester. *Nature.* 183, (1959),pp. 1791-1793.

[350] Valenzuela, J., Mazurie, A., Carlson, R. P., Gerlach, R., Cooksey, K. E., Peyton, B. M. & Fields, M. W., Potential role of multiple carbon fixation pathways during lipid accumulation in Phaeodactylum tricornutum. *Biotechnology for biofuels.* 5, (2012),pp. 40.

[351] Heydarizadeh, P., Poirier, I., Loizeau, D., Ulmann, L., Mimouni, V., Schoefs, B. & Bertrand, M., Plastids of marine phytoplankton produce bioactive pigments and lipids. *Marine drugs.* 11, (2013),pp. 3425-3471.

[352] Tan, K. W. M. & Lee, Y. K., The dilemma for lipid productivity in green microalgae: importance of substrate provision in improving oil

yield without sacrificing growth. *Biotechnology for biofuels.* 9, (2016),pp. 255.

[353] Rismani-Yazdi, H., Haznedaroglu, B. Z., Hsin, C. & Peccia, J., Transcriptomic analysis of the oleaginous microalga Neochloris oleoabundans reveals metabolic insights into triacylglyceride accumulation. *Biotechnology for Biofuels.* 5, (2012),pp. 74.

[354] Chu, F., Cheng, J., Zhang, X., Ye, Q. & Zhou, J., Enhancing lipid production in microalgae Chlorella PY-ZU1 with phosphorus excess and nitrogen starvation under 15% CO2 in a continuous two-step cultivation process. *Chemical Engineering Journal.* 375, (2019),pp. 121912.

[355] Kim, G., Mujtaba, G. & Lee, K., Effects of nitrogen sources on cell growth and biochemical composition of marine chlorophyte Tetraselmis sp. for lipid production. *Algae.* 31, (2016),pp. 257-266.

[356] Jevtić-Mučibabić, R., Grbić, J., Mišljenović, N., Koprivica, G., Kuljanin, T. & Radivojević, S., Nitrogen compounds in the molasses. *Journal on Processing and Energy in Agriculture.* 15, (2011),pp. 169-172.

[357] Janoska, A., Lamers, P. P., Hamhuis, A., van Eimeren, Y., Wijffels, R. H. & Janssen, M., A liquid foam-bed photobioreactor for microalgae production. *Chemical Engineering Journal.* 313, (2017),pp. 1206-1214.

[358] Ma, C., Wen, H., Xing, D., Pei, X., Zhu, J., Ren, N. & Liu, B., Molasses wastewater treatment and lipid production at low temperature conditions by a microalgal mutant Scenedesmus sp. Z-4. *Biotechnology for biofuels.* 10, (2017),pp. 111.

[359] Di Caprio, F., Altimari, P. & Pagnanelli, F., Integrated microalgae biomass production and olive mill wastewater biodegradation: Optimization of the wastewater supply strategy. *Chemical Engineering Journal.* 349, (2018),pp. 539-546.

[360] Emerson, R., Photosynthesis as a function of light intensity and of temperature with different concentrations of chlorophyll. *The Journal of general physiology.* 12, (1929),pp. 623.

[361] Al Abdallah, Q., Nixon, B. T. & Fortwendel, J. R., The enzymatic conversion of major algal and cyanobacterial carbohydrates to bioethanol. *Frontiers in energy research.* 4, (2016),pp. 36.

[362] Chia, S. R., Chew, K. W., Zaid, H. F. M., Chu, D.-T., Tao, Y. & Show, P. L., Microalgal Protein Extraction From Chlorella vulgaris FSP-E Using Triphasic Partitioning Technique With Sonication. *Frontiers in Bioengineering and Biotechnology.* 7, (2019),pp.

[363] Chen, C.-Y., Zhao, X.-Q., Yen, H.-W., Ho, S.-H., Cheng, C.-L., Lee, D.-J., Bai, F.-W. & Chang, J.-S., Microalgae-based carbohydrates for biofuel production. *Biochemical Engineering Journal.* 78, (2013),pp. 1-10.

[364] Dorling, M., McAuley, P. & Hodge, H., Effect of pH on growth and carbon metabolism of maltose-releasing Chlorella (Chlorophyta). *European Journal of Phycology.* 32, (1997),pp. 19-24.

[365] Rehman, Z. U. & Anal, A. K., Enhanced lipid and starch productivity of microalga (Chlorococcum sp. TISTR 8583) with nitrogen limitation following effective pretreatments for biofuel production. *Biotechnology Reports.* 21, (2019),pp. e00298.

[366] Ma, C.-M., Yang, W.-S. & Cheng, B.-W., How the parameters of k-nearest neighbor algorithm impact on the best classification accuracy: In case of parkinson dataset. *Journal of Applied Sciences.* 14, (2014),pp. 171-176.

[367] Cherif, W., Optimization of K-NN algorithm by clustering and reliability coefficients: application to breast-cancer diagnosis. *Procedia Computer Science.* 127, (2018),pp. 293-299.

[368] Chen, C. Y., Lee, P. J., Tan, C. H., Lo, Y. C., Huang, C. C., Show, P. L., Lin, C. H. & Chang, J. S., Improving protein production of indigenous microalga Chlorella vulgaris FSP-E by photobioreactor design and cultivation strategies. *Biotechnology journal.* 10, (2015),pp. 905-914.

[369] Lenko, D., Schlögl, S., Temel, A., Schaller, R., Holzner, A. & Kern, W., Dual crosslinking of carboxylated nitrile butadiene rubber latex employing the thiol-ene photoreaction. *Journal of Applied Polymer Science.* 129, (2013),pp. 2735-2743.

[370] Sobczyk, L., Grabowski, S. J. & Krygowski, T. M., Interrelation between H-Bond and Pi-Electron Delocalization. *Chemical Reviews.* 105, (2005),pp. 3513-3560.

[371] Pourmortazavi, S., Hosseini, S., Hajimirsadeghi, S. & Alamdari, R. F., Investigation on thermal analysis of binary zirconium/oxidant pyrotechnic systems. *Combustion science and technology.* 180, (2008),pp. 2093-2102.

[372] Yau, T. L. & Annamalai, V. E., Corrosion of Zirconium and its Alloys. *Reference Module in Materials Science and Materials Engineering.* Elsevier, 3, (2016),pp 2094-2134.

[373] Ling, T. C., Phang, S.-M., Nagarajan, D., Lee, D.-J., Ong, H. C., Show, P. L., Chew, K. W., Chang, J.-S. & Chia, S. R., Sustainable approaches for algae utilisation in bioenergy production. *Renewable Energy.* 129, (2017),pp. 838-852.

[374] Safi, C., Zebib, B., Merah, O., Pontalier, P. Y. & Vaca-Garcia, C., Morphology, composition, production, processing and applications of Chlorella vulgaris: A review. *Renewable and Sustainable Energy Reviews.* 35, (2014),pp. 265-278.

[375] Sati, H., Mitra, M., Mishra, S. & Baredar, P., Microalgal lipid extraction strategies for biodiesel production: A review. *Algal Research.* 38, (2019),pp. 101413-101413.

[376] Biermann, U. & Metzger, J. O., Catalytic C, C-bond forming additions to unsaturated fatty compounds. *Topics in catalysis.* 27, (2004),pp. 119-130.

[377] Zuo, D., Lane, J., Culy, D., Schultz, M., Pullar, A. & Waxman, M., Sulfonic acid functionalized mesoporous SBA-15 catalysts for biodiesel production. *Applied Catalysis B: Environmental.* 129, (2013),pp. 342-350.

[378] Goldbach, V., Roesle, P. & Mecking, S., Catalytic isomerizing ω-functionalization of fatty acids. *ACS Catalysis.* 5, (2015),pp. 5951-5972.

[379] Flory, P. J., Principles of polymer chemistry. *Macromolecular Science.* 1, (1953),pp. 69-98.

[380] Ain, Z. & Azura, A., Effect of different types of filler and filler loadings on the properties of carboxylated acrylonitrile–butadiene rubber latex films. *Journal of Applied Polymer Science.* 119, (2011),pp. 2815-2823.

[381] Xiong, G., Li, Y., Jin, L. & Hu, H., In situ FT-IR spectroscopic studies on thermal decomposition of the weak covalent bonds of brown coal. *Journal of analytical and applied pyrolysis.* 115, (2015),pp. 262-267.

[382] Obrezkov, F. A., Ramezankhani, V., Zhidkov, I., Traven, V. F., Kurmaev, E. Z., Stevenson, K. J. & Troshin, P. A., High-Energy and High-Power-Density Potassium Ion Batteries Using Dihydrophenazine-

Based Polymer as Active Cathode Material. *The journal of physical chemistry letters.* 10, (2019),pp. 5440-5445.

[383] Krzemińska, S. M., Smejda-Krzewicka, A. A., Leniart, A., Lipińska, L. & Woluntarski, M., Effects of curing agents and modified graphene oxide on the properties of XNBR composites. *Polymer Testing.* 83, (2020),pp. 106368.

[384] Cheng, H., Zhao, K., Gong, Y., Wang, X., Wang, R., Wang, F., Hu, R., Wang, F., Zhang, X., He, J. & Tian, X., Covalent coupling regulated thermal conductivity of poly(vinyl alcohol)/boron nitride composite film based on silane molecular structure. *Composites Part A: Applied Science and Manufacturing.* 137, (2020),pp. 106026.

[385] Lin, J., Zheng, S. Y., Xiao, R., Yin, J., Wu, Z. L., Zheng, Q. & Qian, J., Constitutive behaviors of tough physical hydrogels with dynamic metal-coordinated bonds. *Journal of the Mechanics and Physics of Solids.* 139, (2020),pp. 103935.

[386] Mustafa, A., Davies, R. & Cook, S., Ageing resistance and network structures of some commercial natural rubber gloves. *Journal of Rubber Research.* 6(4), (2003),pp. 207-220.

[387] Cook, S., Cudby, P., Davies, R. & Morris, M., The microstructure of natural rubber latex films. *Rubber chemistry and technology.* 70, (1997),pp. 549-559.

[388] Clogston, J. D. & Patri, A. K., Zeta Potential Measurement. *In:* MCNEIL, S. E. (ed.) *Characterization of Nanoparticles Intended for Drug Delivery.* Totowa, NJ: Humana Press, (2011),pp 63-70.

[389] Rao, C. R. & Trivedi, D., Biphasic synthesis of fatty acids stabilized silver nanoparticles: Role of experimental conditions on particle size. *Materials Chemistry and Physics.* 99, (2006),pp. 354-360.

[390] Sharp, E. L., Jarvis, P., Parsons, S. A. & Jefferson, B., The impact of zeta potential on the physical properties of ferric− NOM flocs. *Environmental science & technology.* 40, (2006),pp. 3934-3940.

[391] Ismail, H. & Ruhaizat, T. A., Effect of palm oil fatty acid on curing characteristics and mechanical properties of CaCO3 filled natural rubber compounds. *Iranian Polymer Journal.* 6, (1997),pp. 97-104.